Sandia National Laboratories
Waste Isolation Pilot Plant

2004 Compliance Recertification Application
Performance Assessment Baseline Calculation

Author:	Christi Leigh (6821)		9/20/05
	Print	Signature	Date
Author:	Joe Kanney (6821)		10/19/05
	Print	Signature	Date
Author:	Larry Brush (6822)		9/20/05
	Print	Signature	Date
Author:	Jim Garner (6821)		9-20-05
	Print	Signature	Date
Author:	Ross Kirkes (6821)		9-20-05
	Print	Signature	Date
Author:	Tom Lowry (6115)		10/19/05
	Print	Signature	Date
Author:	Martin Nemer (6821)		9-20-05
	Print	Signature	Date
Author:	Josh Stein (6852)		9-20-05
	Print	Signature	Date
Author:	Eric Vugrin (6821)		9/20/05
	Print	Signature	Date
Author:	Steve Wagner (6821)		9/20/05
	Print	Signature	Date
Author:	Tom Kirchner (6821)		9/20/05
	Print	Signature	Date
Technical Review:	Jon Helton (1533)		10/19/05
	Print	Signature	Date
Management Review:	David Kessel (6821)		9/20/05
	Print	Signature	Date
Management Review:	Mark Rigali (6822)		9/20/05
	Print	Signature	Date
QA Review	Mario Chavez (6820)		10/19/05
	Print	Signature	Date

WIPP: 1.4.1.1.:PA:QA-L:540232

CONTENTS

Information Only

Information Only

TABLES

Information Only

FIGURES

Information Only

Information Only

Information Only

ACRONYMS

AP	Analysis Plan
BNL	Brookhaven National Laboratory
CAMDAT	Compliance Assessment Methodology Database
CCA	Compliance Certification Application
CCDF	Complementary Cumulative Distribution Function
CFR	Code of Federal Regulations
CH	Contact Handled
CMS	Code Management System
CPR	Cellulose, Plastic, and Rubber
CRA	Compliance Recertification Application
DBR	Direct Brine Release
DCL	Digital Command Language
DOE	U.S. Department of Energy
DRZ	Disturbed Rock Zone
EPA	U.S. Environmental Protection Agency
ERDA	Energy Research and Development Administration
FEP	Features, Events, and Processes
FGE	Fissile Gram Equivalent
FMT	Fracture-Matrix Transport
GWB	Generic Weep Brine
Handford-RL	Hanford Office of Richland Operations
INEEL	Idaho National Engineering and Environmental Laboratory
LANL	Los Alamos National Laboratory
LWB	Land Withdrawal Boundary
MB	Marker Bed
NP	Nuclear Waste Management Procedure
PA	Performance Assessment
PABC	Performance Assessment Baseline Calculation
PAPDB	Performance Assessment Parameter Database
PAVT	Performance Assessment Verification Test
PRCC	Partial Rank Correlation Coefficient
QA	Quality Assurance
RH	Remote Handled
RoR	Rest of Repository
SNL	Sandia National Laboratories
SPR	Software Problem Report
TRU	Transuranic Waste
WIPP	Waste Isolation Pilot Plant

Information Only

EXECUTIVE SUMMARY

The U.S. Environmental Protection Agency (EPA) determined that the Waste Isolation Pilot Plant (WIPP) was in compliance with the Containment Requirements of Title 40 Code of Federal Regulations (CFR) 191.13 in 1998 (U. S. EPA, 1998). The WIPP Land Withdrawal Act (LWA), Public Law 02-579 as amended by Pubic Law No. 104-201, requires the U.S. Department of Energy (DOE) to provide the EPA with documentation of continued compliance with the disposal standards within five years of first waste receipt and every five years thereafter. Therefore, the DOE conducted a new performance assessment (PA) for the WIPP which is called the CRA-2004 PA and is documented in the DOE's Compliance Recertification Application (CRA) (U. S. DOE, 2004). During review of the CRA, the EPA required several changes to the PA. These changes have been included in a new PA, the CRA-2004 Performance Assessment Baseline Calculation (PABC).

The CRA-2004 PABC demonstrates that the WIPP continues to comply with the Containment Requirements of 40 CFR 191.13. Containment Requirements are stringent and state that the DOE must demonstrate a reasonable expectation that the probabilities of cumulative radionuclide releases from the disposal system during the 10,000 years following closure will fall below specified limits. The PA analyses supporting this determination must be quantitative and consider uncertainties caused by all significant processes and events that may affect the disposal system, including future inadvertent human intrusion into the repository. This quantitative PA is conducted using a series of linked computer models in which uncertainties are addressed by a Monte Carlo procedure for sampling selected input parameters.

As required by regulation, results of the PA are displayed as complementary cumulative distribution functions (CCDFs) that display the probability and magnitude of predicted releases from the disposal system over the regulatory period compared to acceptable limits as specified by the EPA. These CCDFs are calculated using reasonable and, in many cases conservative conceptual models based on the scientific understanding of the disposal system's behavior. Parameters used in these models are derived from experimental data, field observations, and relevant technical literature.

In a broad sense, the CRA-2004 PABC closely resembles the PA conducted and presented in the CRA (U. S. DOE, 2004), however the changes requested by the EPA result in some subtle differences in the results. Notable changes included in the PABC are: 1) updated waste information; 2) revision of microbial degradation rates and probability; 3) changes to the gas generation reaction pathway; 4) updated actinide solubility values and uncertainty ranges; 5) modification to transmissivities in the mining scenario; and 6) minor revisions in the calculations of spallings. Other minor corrections or revisions are noted in applicable sections throughout this report.

As anticipated, the overall mean CCDF continues to lie entirely below the specified limits, and the WIPP therefore continues to be in compliance with the containment requirements of 40 CFR Part 191, Subpart B. Sensitivity analysis of results shows that the location of the mean CCDF is dominated by radionuclide releases that could occur on the surface during an inadvertent penetration of the repository by a future drilling operation. Releases of radionuclides to the accessible environment resulting from transport in groundwater through the shaft seal systems

and the subsurface geology are negligible, with or without human intrusion, and make no contribution to the location of the mean CCDF. No releases are predicted to occur at the ground surface in the absence of human intrusion. The natural and engineered barrier systems of the WIPP provide robust and effective containment of transuranic (TRU) waste even if the repository is penetrated by multiple boreholes.

Information Only

1. INTRODUCTION

1.1   BACKGROUND

The Waste Isolation Pilot Plant (WIPP) is located in southeastern New Mexico and has been developed by the U.S. Department of Energy (DOE) for the geologic (deep underground) disposal of transuranic (TRU) waste (U. S. DOE, 1980), (U. S. DOE, 1990), (U. S. DOE, 1993). In 1992, Congress designated the U.S. Environmental Protection Agency (EPA) as the regulator for the WIPP site, and mandated that once DOE demonstrated to EPA's satisfaction that WIPP complied with Title 40 of the Code of Federal Regulations (CFR), Part 191 (U. S. DOE, 1996), (U. S. EPA, 1996), EPA would certify the repository. To show compliance with the containment regulations, the DOE had their scientific advisor, Sandia National Laboratories (SNL) develop a computational modeling system to predict the future performance of the repository for 10,000 years after closure. SNL has developed a system, called WIPP Performance Assessment (PA), which examines potential release scenarios, quantifies their likelihoods, estimates potential releases to the surface or the site boundary, and evaluates the potential consequences. The regulations also require that these models be maintained and updated with new information to be part of a recertification process that occurs at five-year intervals after the first waste is received at the site.

1.2   COMPLIANCE CERTIFICATION APPLICATION

To demonstrate compliance with the disposal regulation, DOE submitted the Compliance Certification Application (CCA) to the EPA, in October 1996, which included the results of the WIPP PA system. During the review of the CCA, EPA requested an additional Performance Assessment Verification Test (PAVT), which revised selected CCA inputs to the PA (Sandia National Laboratories, 1997). The PAVT analysis ran the full suite of WIPP PA codes and confirmed the conclusions of the CCA analysis that the repository design met the regulations. Following the receipt of the PAVT analysis, EPA ruled in May 1998 that WIPP had met the regulations for permanent disposal of transuranic waste. The first shipment of radioactive waste from the nation's nuclear weapons complex arrived at the WIPP site in late March 1999, starting the five-year clock for the site's required recertification. The results of CCA PA analyses were subsequently summarized in a SNL report (Helton et al., 1998).

1.3   2004 COMPLIANCE RECERTIFICATION APPLICATION

The first Compliance Recertification Application (CRA-2004) was submitted to the EPA by the DOE in March 2004 (U. S. DOE, 2004). During its review of CRA-2004, the EPA requested additional information (Cotsworth, 2004b; Cotsworth, 2004c; Cotsworth, 2004a; Cotsworth, 2004d; Gitlin, 2005). The DOE and SNL responded to EPA in writing (Detwiler, 2004a; Detwiler, 2004b; Detwiler, 2004c; Detwiler, 2004d; Detwiler, 2004e; Detwiler, 2004f) (Piper, 2004), (Triay, 2005), (Patterson, 2005) and by engaging in technical meetings with EPA staff. As a result of these technical interactions, the EPA instructed DOE to revise the CRA-2004 PA analysis and run a new PA analysis, which would be considered the new PA baseline if the EPA recertifies the WIPP site for continued operation [referred to in this document as the CRA-2004 Performance Assessment Baseline Calculation (PABC)].

1.4   OBJECTIVES FOR THE CRA-2004 PABC ANALYSIS

The EPA required that DOE revise the CRA-2004 analysis and present results for evaluation by the EPA (Cotsworth, 2005). The EPA noted a number of technical changes and corrections to the CRA-2004 PA that it deemed necessary. Additionally, the EPA stated that a number of modeling assumptions used in CRA-2004 have not been sufficiently justified and that alternative modeling assumptions must be used. These changes directed by the EPA are discussed below in Section 2. The objective of this report is to summarize the CRA-2004 PABC results and how they were obtained.

2.   UPDATES FROM CRA-2004 TO CRA-2004 PABC

A PA very similar to that conducted for CRA-2004 was performed in support of the CRA-2004 PABC. PA begins with an analysis of the features, events, and processes (FEPs) that may have bearing on the performance of the repository. The FEPs are screened to determine which FEPs will be retained in PA; these screened-in FEPs are combined into scenarios for the PA calculations.

A FEPs impact assessment was conducted according to SP 9-4 (Kirkes, 2005c) in support of the CRA-2004 PABC. The impact assessment determined if the changes associated with the CRA-2004 PABC created any inconsistencies or conflicts with the current FEPs baseline. The FEPs impact assessment did not identify any inconsistencies, omissions, or other problems with the current baseline in consideration of the proposed changes for the CRA-2004 PABC. The assessment concluded that no revision to the baseline FEPs list (Kirkes, 2005a) or the baseline FEPs screening document [(U. S. DOE, 2004) Appendix PA, Attachment SCR] was warranted due to the changes associated with the CRA-2004 PABC (Kirkes, 2005b).

Scenarios are formulated from FEPs. The scenarios are modeled using conceptual models that represent the physical and chemical processes of the repository. The scenarios for the CRA-2004 PA and the CRA-2004 PABC are identical. The conceptual models are implemented through a series of computer simulations and associated parameters that describe the natural and engineered components of the disposal system (e.g., site characteristics, waste forms, waste quantities, and engineered features). In general, the modeling and the parameters in the CRA-2004 PABC are the same as the CRA-2004 PA, except as noted below:

1. Inventory information was updated.
2. Changes to the parameter describing the probability of microbial gas generation in the repository were made.
3. Microbial gas generation rates were revised.
4. The methanogenesis assumption was changed.
5. Actinide solubilities were updated.
6. Implementation of uncertainty for the actinide solubilities was updated.
7. The mining modification to the Culebra T-fields was modified.
8. A full set of 300 spallings calculations were performed.
9. Other minor parameter changes were made.

In addition, revisions to some of the WIPP PA codes were made to support the CRA-2004 PABC. Software revisions are discussed in Section 3.0.

2.1   REVISED INVENTORY

Leigh et al. (Leigh et al., 2005) summarizes the changes that were made to the inventory for the CRA-2004 PABC and provides an analysis of the CRA-2004 PABC inventory as it compares to the CRA-2004 inventory and the inventory already emplaced in the repository. There were three primary changes in the inventory.

First, the Hanford Office of Richland Operations (Hanford-RL) waste streams were corrected for an error in reporting made by Hanford-RL during the data call for the CRA-2004. The site over-reported their waste. As a result, the volumes, both Contact Handled (CH-TRU) and Remote Handled (RH-TRU), from Hanford-RL in the CRA-2004 PABC inventory are smaller than the volumes from Hanford-RL in the CRA-2004 inventory.

Second, the pre-1970 buried waste at Idaho National Engineering and Environmental Laboratory (INEEL[1]) was added to the TRU waste inventory that is possibly coming to WIPP. As a result, the volumes from INEEL (particularly in the "projected" category) in the CRA-2004 PABC inventory are larger than the volumes from INEEL in the CRA-2004 inventory.

Third, and most significant for PA, the Los Alamos National Laboratory (LANL) waste stream LA-TA-55-48 was updated. In the inventory for CRA-2004, LA-TA-55-48 was reported as 2.11 m^3 in storage and 13.7 m^3 projected for a total disposal inventory of 31 m^3 (the scaling factor for CH-TRU waste in the CRA-2004 was 2.11). With this volume and concentration, LA-TA-55-48 caused a shift in the complimentary cumulative distribution function (CCDF) for compliance. However, given the radionuclide concentrations reported for this volume of waste, the fissile gram equivalents (FGE) per container were approximately ten times that allowed for shipment to WIPP. During the inventory update for the CRA-2004 PABC, this abnormality was noted. As a result, the LANL site was contacted and asked to re-examine their reporting of this waste stream. LANL provided new data for LA-TA-55-48 for the CRA-2004 PABC. The stored volume was changed to 2.72 m^3 while the projected volume remained as 13.7 m^3 for a disposal volume of 23 m^3 (the scaling factor for CRA-2004 PABC is 1.48). The new data for LA-TA-55-48 also had reduced radionuclide concentrations so that the FGE for LA-TA-55-48 reported by the LANL site for CRA-2004 PABC are within the FGE limits for waste that is shippable to WIPP.

Figure 2-1 and Figure 2-2 show the CH-TRU and RH-TRU disposal inventory volumes for the CRA-2004 PABC and CRA-2004. There are no differences in the values used for emplaced volumes between CRA-2004 and CRA-2004 PABC. The stored inventory values for CH-TRU and RH-TRU waste did not change significantly as a result of the inventory update for the CRA-2004 PABC. For the CRA-2004 PABC, in the projected category, the DOE estimates 3.5×10^4 m^3 (a 10,000 m^3 increase over the CRA-2004) of CH-TRU waste and 2.1×10^3 m^3 (a 8,300 m^3 decrease from CRA-2004) of RH-TRU waste. The increase in projected CH-TRU waste is a direct result of adding the pre-1970 buried waste from INEEL. This is offset by a decrease in the

---

[1] For the purposes of this document, the acronym INEEL is used for consistency with all supporting documentation. The INEEL acronym has recently been changed to Idaho National Laboratory (INL).

projected CH-TRU waste volume from Hanford-RL due to corrections made to their waste streams. The decrease in projected RH-TRU waste is a result of corrections made to the Hanford-RL waste streams.

Figure 2-3 and Figure 2-4 show the CH-TRU and RH-TRU waste material concentrations for the CRA-2004 PABC, CRA-2004, and CCA. A comparison of the CCA inventory and CRA-2004 inventory was made in Chapter 4 of CRA-2004 (U. S. DOE, 2004). There are only slight differences in the overall cellulose, plastic, and rubber (CPR) concentrations and metal concentrations in CH-TRU between the CRA-2004 PABC and CRA-2004. The biggest difference is in the "other" category for CH-TRU waste. This is due to the addition of the pre-1970 buried waste from INEEL. Differences between the CRA-2004 and CRA-2004 PABC waste material concentrations in RH-TRU are a direct result of corrections made to the Hanford-RL waste streams. There are only minor differences in the packaging material densities between the CRA-2004 and the CRA-2004 PABC inventories.

Unique to the CRA-2004 PABC is the fact that emplacement materials have been accounted for in the CRA-2004 PABC inventory. Emplacement materials include but are not limited to plastic that is wrapped around 7-packs of drums, plastic and cardboard slipsheets placed between waste packages stacked on top of one another in the repository, and the plastic supersacks used to emplace MgO. Emplacement materials added 1.48×10^6 kg to the plastics inventory and 2.07×10^5 kg to the cellulose inventory for CRA-2004 PABC.

Finally, radionuclide activities in the CRA-2004 PABC inventory are generally less than those in the CRA-2004 inventory as evidenced by the fact that the waste unit factor changed from 2.48 in CRA-2004 to 2.32 in the CRA-2004 PABC. This is shown for a few radionuclides in Figure 2-5. The overall decrease in radionuclide activity in the disposal volume for WIPP is a result of adding the pre-1970 buried waste from INEEL to the inventory. This waste is a fairly low activity waste.

CRA-2004 PABC
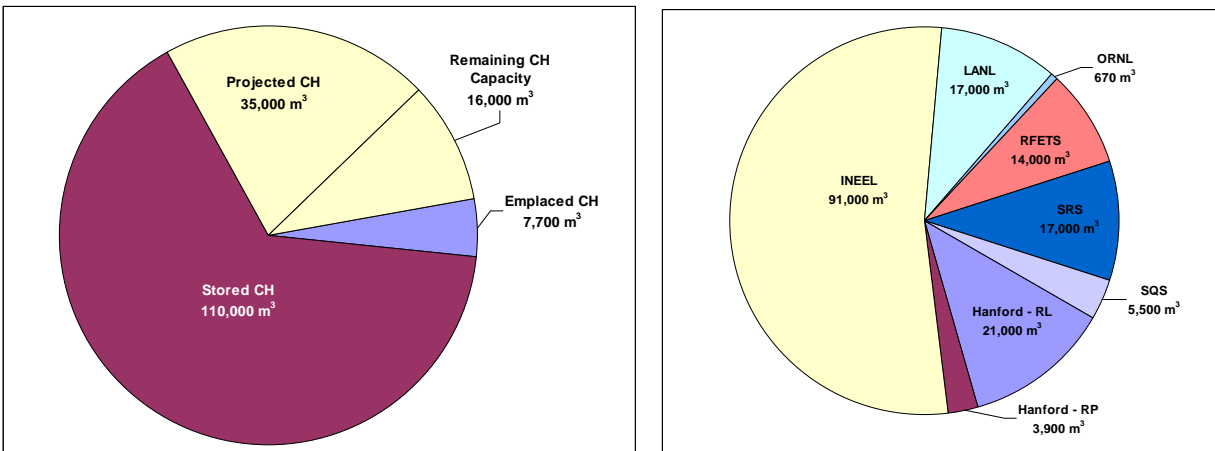
CRA-2004
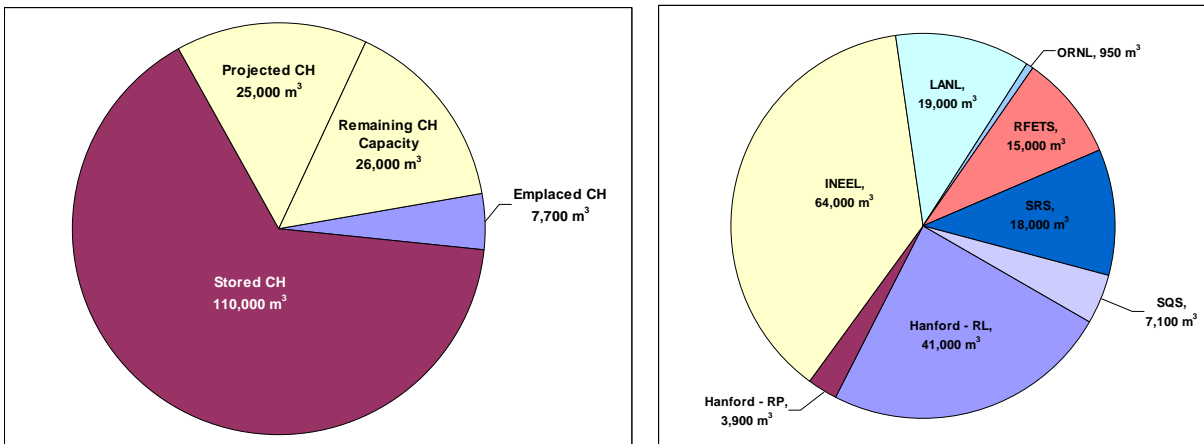
Figure 2-1. CH-TRU Waste Disposal Inventory for WIPP for the CRA-2004 PABC (above) and the CRA-2004 (below).
The disposal volume is the sum of the emplaced, stored and scaled projected volume.

Information Only
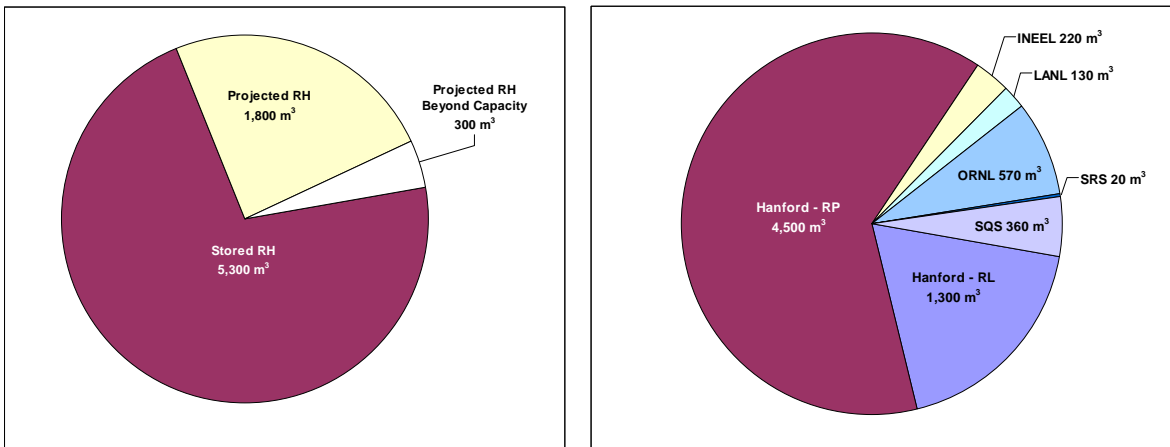
CRA-2004 PABC
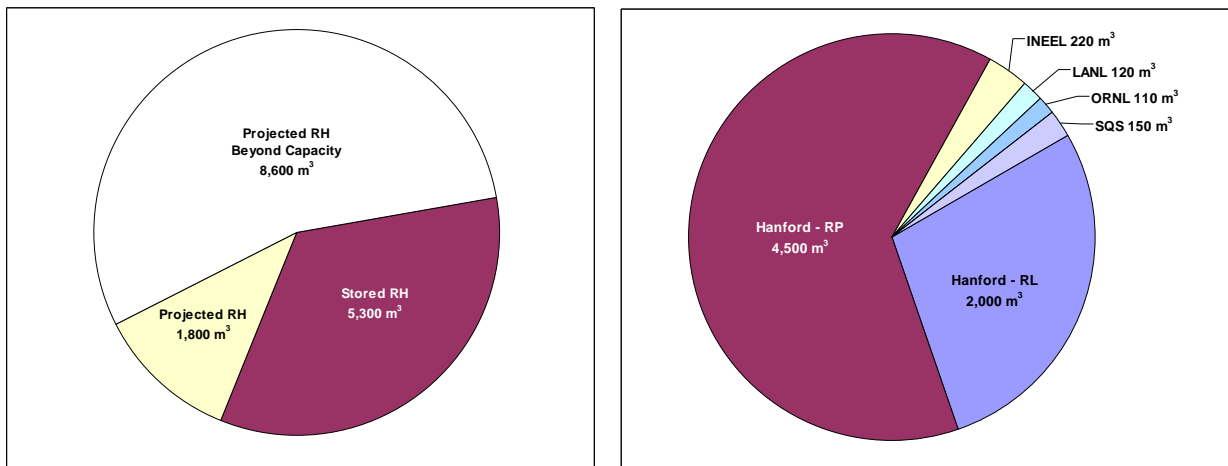
CRA-2004

Figure 2-2. RH-TRU Waste Disposal Inventory for WIPP for the CRA-2004 PABC (above) and the CRA-2004 (below).
The disposal volume is the sum of the stored and scaled projected volume.
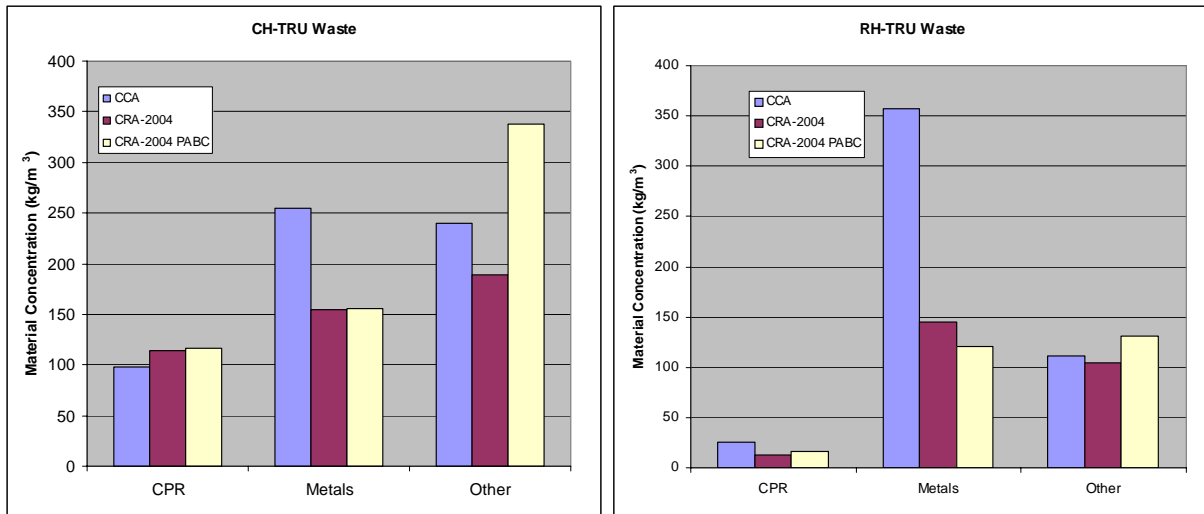
Figure 2-3. CH-TRU and RH-TRU Waste Material Densities for the CRA-2004 PABC Compared to the CRA-2004 PA and TWBIR Revision 3.
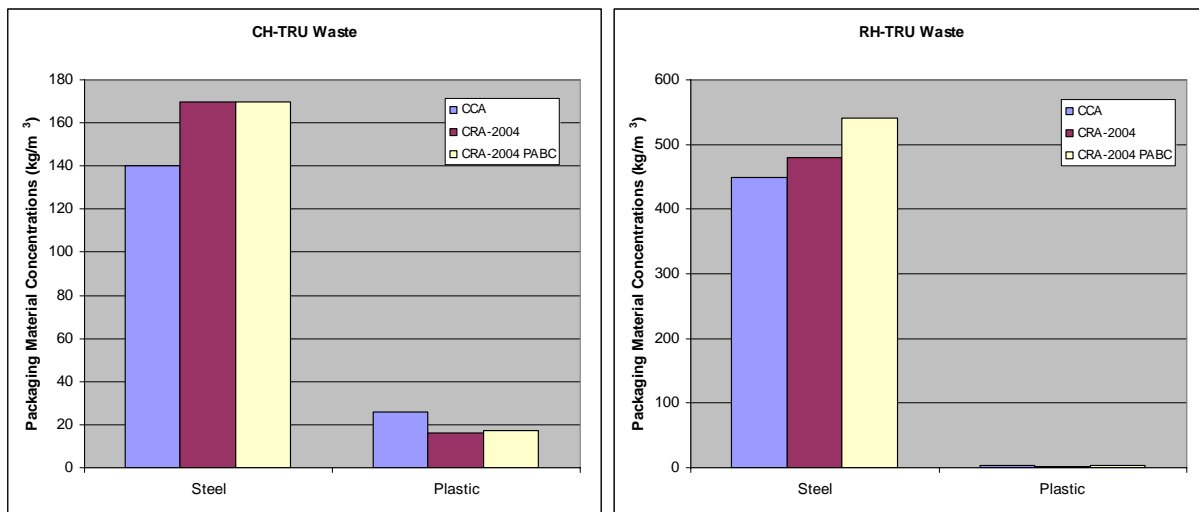
Figure 2-4. CH-TRU and RH-TRU Package Material Densities for the CRA-2004 PABC Compared to the CRA-2004 PA and TWBIR Revision 3.

21 of 153   Information Only

Radionuclide Activities at Closure
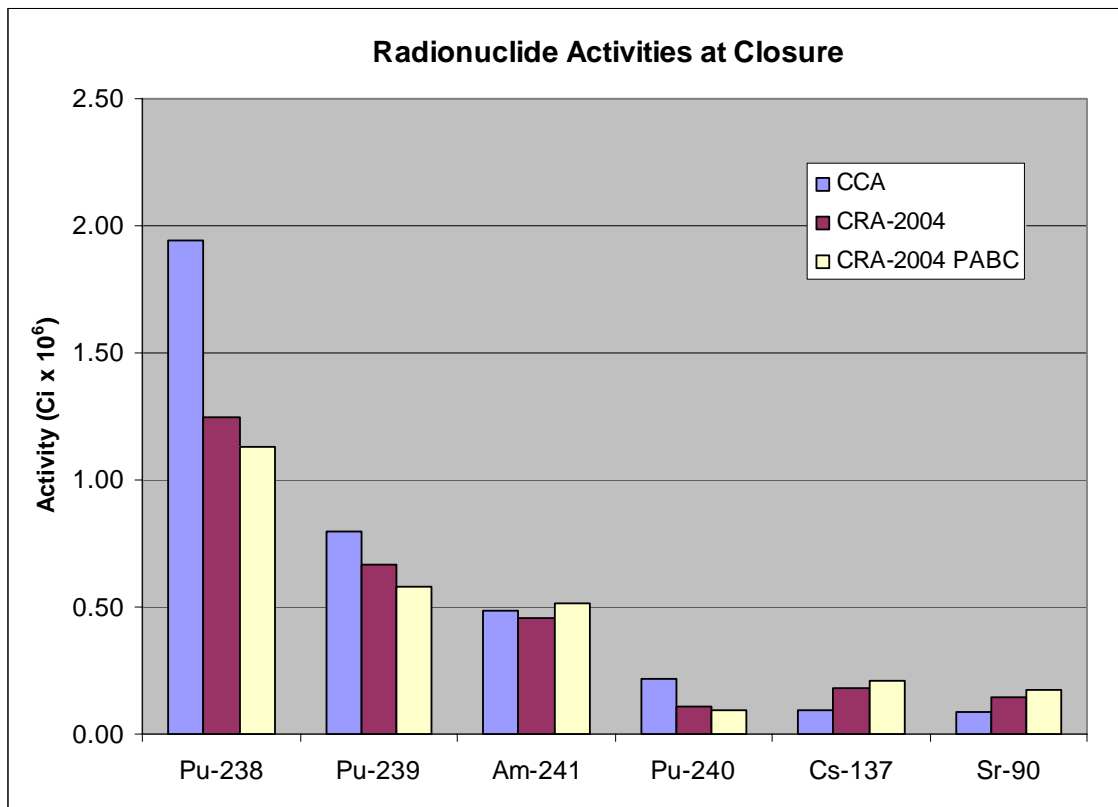
Figure 2-5. TRU Waste Radionuclide Activity Values for the CRA-2004 PABC Compared to the CRA-2004 PA and TWBIR Revision 3.

2.2   REVISION OF PROBABILITY OF MICROBIAL DEGRADATION

During a technical exchange with EPA in January 2005, EPA requested a change to the parameter that defines the probability that microbial gas generation will occur in the WIPP. Advances in microbiology have found microbes existing in a wide variety of so-called "extreme" environments that were previously not considered to be conducive to supporting microbes. Based on these scientific advances, the EPA stated that the probability that microbial activity and resulting microbial gas generation would occur in the WIPP should be changed from 0.5, which corresponds to microbial activity in 50% of vectors, to 1.0. The DOE requested that microbial gas generation rates be changed to reflect data from long-term microbial gas-generation experiments performed at Brookhaven National Laboratory (BNL) (Francis et al., 1997; U. S. DOE, 2002). Microbial gas-generation rates used in PA for the CCA, the PAVT and the CRA-2004 were based upon the first one to three years of data from these experiments, but approximately 10 years of data are now available. The full range of data from the experiments shows that rates of microbial gas generation decrease rapidly with time, slowing significantly after the first few years. The implementation of a new probability for microbial gas generation (a probability of 1) for the CRA-2004 PABC is discussed in Nemer and Stein (2005).

2.3   REVISION OF MICROBIAL GAS GENERATION RATES

The microbial-generation rates used in the CCA, the PAVT and the CRA-2004 were based upon the first one to three years of data from experiments performed at BNL (Francis et al., 1997). Looking over the entire 10 years of experimental data, the rates of microbial gas generation decrease significantly with time. An example of this behavior is shown in Figure 2-6, where the accumulation of carbon dioxide is plotted versus time. As seen in the figure, the accumulation rate decreases significantly after about 500 days. Such decreases in the rates of microbial activity are commonly observed in many microbial systems and are generally attributed to the sequential use of different electron acceptors, different substrates, and the build-up of microbial metabolites (Monod, 1949).   For the CRA-2004 PABC calculations, the following three modifications were made in the implementation of microbial gas generation rates:

1. Gas generation rate distributions were modified to reflect rates observed in long-term experiments run at BNL.

2. The brief initial period of faster gas generation rates was accounted for by adding additional gas to the repository as an initial condition.

3. An additional uncertainty factor was added to the calculation of the microbial gas generation rates for the WIPP to account for differences in conditions between the experiments and the WIPP underground.

The implementation of new gas generation rates for the CRA-2004 PABC is discussed in Nemer and Stein (2005).
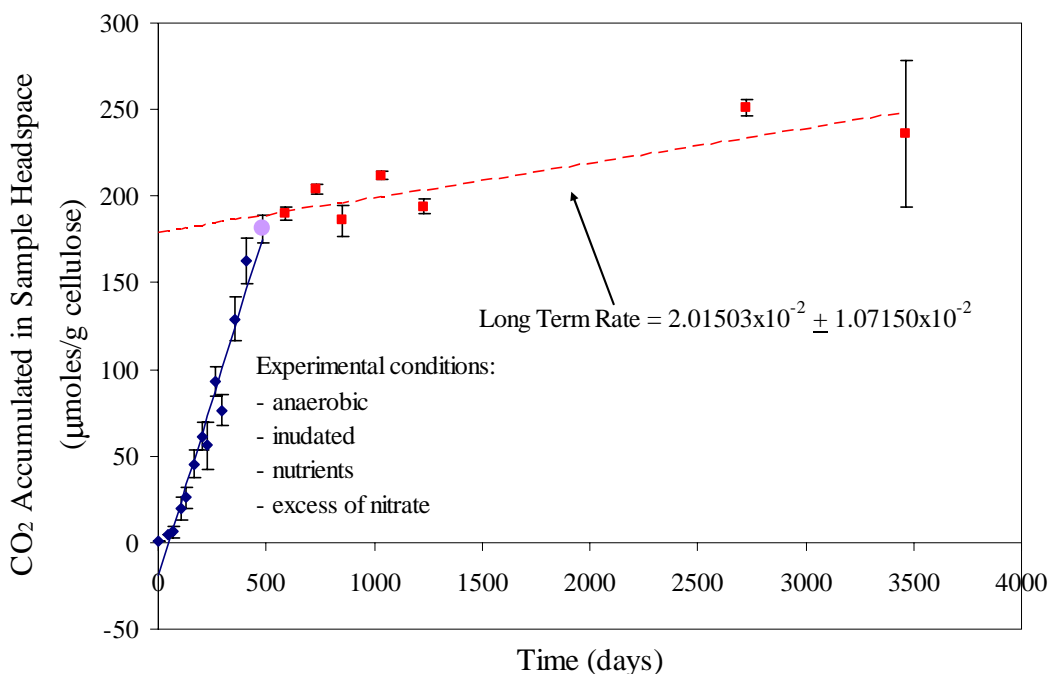
Figure 2-6. Carbon Dioxide Accumulated in Experiments that were Inundated, Inoculated, Amended, and with Excess Nitrate. (Nemer et al., 2005).

2.4   REMOVAL OF METHANOGENESIS FROM THE MICROBIAL GAS GENERATION MODEL

As a consequence of its completeness review of the CRA-2004, the EPA stated in comment G-14 of the Third Completeness Letter (Cotsworth, 2004c) if DOE cannot provide EPA with new and convincing evidence that methanogenesis will be the dominant pathway for microbial gas generation, the WIPP PA simulations must assume that microbial gas generation occurs only by denitrification and sulfate reduction and not by methanogenesis. It is commonly accepted that methanogenesis only occurs when the availability of NO_3^- and SO_4^{2-} limits denitrification and sulfate reduction. The amount of nitrate available is limited to that initially in the waste. Thus, DOE removed methanogenesis from the gas generation model for the CRA-2004 PABC.

The WIPP PA calculations consider three reaction pathways (Wang and Brush, 1996):

$$C_6H_{10}O_5 + 4.8\ H^+ + 4.8\ NO_3^- \rightarrow 7.4\ H_2O + 6\ CO_2 + 2.4\ N_2 \quad [\text{denitrification}] \quad (1)$$

$$C_6H_{10}O_5 + 6\ H^+ + 3\ SO_4^{2-} \rightarrow 5\ H_2O + 6\ CO_2 + 3\ H_2S \quad [\text{sulfate reduction}] \quad (2)$$

$$C_6H_{10}O_5 + H_2O \rightarrow 3\ CH_4 + 3\ CO_2 \quad [\text{methanogenesis}] \quad (3)$$
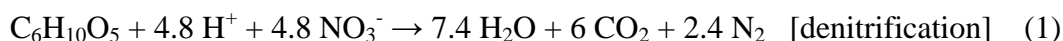
Reactions (1)-(3) are assumed to proceed sequentially according to the energy yield of each reaction. The reactions occur sequentially after concentrations of electron acceptors become depleted. In the CRA-2004, NO_3^- availability was limited such that approximately 2.5% of gas was produced through denitrification; SO_4^{2-} availability limited gas produced by sulfate reduction to approximately 1.2%; approximately 96.3% of microbial gas generation occurred by methanogenesis.

In contrast, the calculations for the CRA-2004 PABC assume that an excess of SO_4^{2-} is always present in the repository. As such, the methanogenesis mechanism has been removed from WIPP PA models. Given the new inventory for nitrate and the new inventory of CPR, 4% (of total moles) of gas generation now occurs by denitrification and 96% of gas generation occurs by sulfate reduction (Nemer and Stein, 2005). Implementation of the gas generation model without methanogenesis is discussed in Nemer and Stein (2005).

2.5   ACTINIDE SOLUBILITY UPDATE

The Fracture-Matrix Transport (FMT) code (Babb and Novak, 1997; Wang, 1998); is used to calculate actinide solubilities in WIPP brines. The EPA requested (Cotsworth, 2005) parameter changes related to the FMT calculations for actinide solubility in the CRA-2004 PABC. In particular, organic-ligand concentrations for the CRA-2004 PABC were recalculated by Brush and Xiong [(2005), Table 4] based on revised organic ligand masses in the inventory and on a revised volume of brine. The other chemical conditions for the CRA-2004 PABC solubility calculations include: (1) use of Generic Weep Brine (GWB) (Snider, 2003) and Energy Research and Development Administration (WIPP Well) 6 (ERDA-6) (Popielak et al., 1983) to simulate Salado and Castile brines, respectively; (2) the assumption that instantaneous, reversible

equilibria among GWB or ERDA-6, major Salado minerals such as halite (NaCl) and anhydrite ($CaSO_4$), and the MgO hydration and carbonation products brucite ($Mg(OH)_2$) and hydromagnesite ($Mg_5(CO_3)_4(OH)_2 \cdot 4H_2O$) will control chemical conditions, such as f_{CO_2}, pH, and brine composition; and (3) elimination of separate, slightly different chemical conditions characteristic of the absence of microbial activity from the calculations (since all vectors are assumed to have microbial degradation for CRA-2004 PABC).

The EPA also specified that a revised estimate of 1×10^{-3} M be used for the solubility of U(VI) in WIPP brines for the CRA-2004 PABC source term. The EPA specified this value during a DOE-EPA teleconference on March 2, 2005 (Brush, 2005).

Implementation of the new actinide solubility values is discussed in Garner and Leigh (2005).

2.6   SOLUBILITY UNCERTAINTY UPDATE

Xiong et al. (2004) re-established the uncertainty range and probability distribution for An(III), An(IV), and An(V)[2] solubility predictions in response to EPA requests (Cotsworth, 2004b; Cotsworth, 2004a) to update the ranges and distributions established by Bynum (1996a, 1996b, 1996c) for the PA calculations for the CCA. Xiong et al. (2004) concluded that (1) the An(III) thermodynamic speciation and solubility model implemented in FMT slightly overpredicted the measured An(III) solubilities; (2) the An(IV) model in FMT significantly underpredicted the measured An(IV) solubilities; (3) the An(V) model in FMT slightly overpredicted the measured An(V) solubilities; and (4) overall, the An(III), An(IV), and An(V) models in FMT together significantly underpredicted the measured An(III), An(IV), and An(V) solubilities. Xiong et al. (2004) used the thermodynamic database FMT_040628.CHEMDAT for their analysis. Because the An(IV) model in FMT significantly underpredicted the measured An(IV) solubilities, Nowak and Xiong (2005) identified the value of the dimensionless standard chemical potential (μ^0/RT) for $Th(OH)_4(aq)$ in FMT_040628.CHEMDAT, -622.4700, as the cause of this problem; and recommended that μ^0/RT for $Th(OH)_4(aq)$ be changed from -622.4700 to -626.5853. Xiong (2005) made this change and released the corrected version of the database, FMT_050405.CHEMDAT.

Xiong et al. (Xiong et al., 2005) used FMT_050405.CHEMDAT to establish a revised uncertainty range and probability distribution for An(IV) solubility predictions. Xiong et al. (2005) did not revise the ranges and distributions for An(III) and An(V) solubility predictions established by Xiong et al. (2004).

The EPA specified that a fixed value be used for U(VI). In the CCA PA, the PAVT, and the CRA-2004 PA, the uncertainty range of -2.0 to +1.4 orders of magnitude was applied to the U(VI) solubility estimate of Hobart and Moore (1996). For the CRA-2004 PABC the U(VI) solubility is fixed at 1×10^{-3} M.

Implementation of the new actinide solubility variabilities is discussed in Garner and Leigh (2005).

---

[2] An(III), An(IV) and An(V) are actinides in the +III, +IV and +V oxidation states.

2.7   REVISION OF THE MINING MODIFICATION TO THE CULEBRA T-FIELDS

During the review of CRA-2004 [(Cotsworth, 2004d), Comment G-11], the EPA did not agree with the approach used to account for the potential effect of potash mining on Culebra T-fields, which included a 0.5-mile-diameter exclusion zone around existing oil and gas wells for potash resources outside the Land Withdrawal Boundary (LWB). In response to comment G-11, the potash mining areas were redefined to consist of all mined and unmined potash resources including where they fall within 0.5-mile-diameter exclusion zones around oil and gas wells. Based upon the new mining areas, the mining modifications to the Culebra T-fields and the Culebra flow fields were re-calculated in (Lowry, 2004) and presented to the EPA in Piper (2004). This formulation of the mining modifications is the basis for new Culebra flow and transport calculations for the CRA-2004 PABC as discussed in Lowry and Kanney (2005).

2.8   REVISIONS TO THE CALCULATION OF SPALLINGS

Calculation of spallings releases followed the same procedure used for CRA-2004 and outlined in Lord (2002) with four significant procedural changes. First, the sampling of uncertain DRSPALL parameters was done in the same Latin hypercube sample as the uncertain parameters for other WIPP PA codes (Kirchner, 2005a). This change ensured that no spurious correlations exist between the DRSPALL parameters and the other sampled parameters because the Latin hypercube sampling code LHS enforces zero correlations between parameters unless a correlation is specified (Vugrin, 2005f; Vugrin, 2005j).

Secondly, whereas the CRA-2004 consisted of one replicate of fifty DRSPALL vectors and four DRSPALL pressure scenarios per vector, a larger set of DRSPALL calculations were performed for the CRA-2004 PABC: three replicates consisting of 100 vectors each and four DRSPALL pressure scenarios were calculated for each vector. The end result was a set of 1,200 DRSPALL calculations. The EPA stated that the DOE must run a full set of vectors for each replicate for the CRA-2004 PABC (Cotsworth, 2005).

Third, a new procedure was established to create the file containing the DRSPALL calculation data for the code CUTTINGS_S (Vugrin, 2005k).

Finally, since CRA-2004 used only 50 DRSPALL vectors for all three replicates of the CRA-2004 PA, the parameter SPALLMOD:RNDSPALL was used by CUTTINGS_S Version 5.10 (Hansen, 2003) to map the 50 DRSPALL vectors to the 300 PA vectors (Lord et al., 2005). Use of this parameter was unnecessary for the CRA-2004 PABC since this analysis consisted of 300 DRSPALL vectors.   The parameter SPALLMOD:RNDSPALL was not sampled (Kirchner, 2005a), and DRSPALL Vector 1 of Replicate R1 was mapped to PA Vector 1 of Replicate R1, Vector 2 was mapped to Vector 2, and so forth.

2.9   INPUT PARAMETER CHANGES

Table 2-1 provides a list of all of the parameters that were updated for the CRA-2004 PABC. References that discuss the justification for parameter changes are given in the table.

Information Only

Table 2-1. Parameters that Were Updated for the CRA-2004 PABC.

Description	Name	Justification
WIPP-Scale Initial Radionuclide Inventory In Curies see: (Garner and Leigh, 2005)	INVCHD and INVRHD for the following materials: AM 241; AM 243; CF 252; CM 243; CM 244; CM 245; CM248; CS 137; NP 237; PA 231; PB 210; PM 147; PU 238; PU 239; PU 240; PU 241; PU 242; PU 244; RA 226; RA 228; SR 90; TH 229; TH 230; TH 232; U 233; U 234; U 235; U 236; U 238	(Leigh, 2005b)
WIPP-Scale Initial Radionuclide Inventory In Curies see: (Garner and Leigh, 2005)	INVCHD and INVRHD for the following materials: AM241L, TH230L, PU238L, U234L, PU239L	(Leigh and Trone, 2005a)
Waste Unit Factord see: (Fox, 2005; Garner and Leigh, 2005)	WUF for the material: BOREHOLE	(Leigh and Trone, 2005b)
WIPP-Scale Masses of nitrate and sulfate see: (Nemer and Stein, 2005)	QINIT for the following materials: NITRATE and SULFATE	(Leigh, 2005a; Trone, 2005)
Residual saturation and rock compressibility for MB 138, MB 139 and Anhydrite A & B see: Vugrin et al. (2005)	COMP_RCK and SAT_RGAS for the following materials: S_MB139, S_MB138, and S_ANH_AB	(Vugrin et al., 2005)
Waste Material Parameters see: (Nemer and Stein, 2005)	DCELLCHW, DCELLRHW, DIRONCHW ,DIRONRHW, DIRNCCHW ,DIRNCRHW, DPLASCHW, DPLASRHW, DPLSCCHW, DPLSCRHW, DRUBBCHW, DRUBBRHW for the following material: WAS_AREA	(Crawford, 2005)
Inundated Rate Of Cellulose Biodegradation In The Waste Area see: (Nemer and Stein, 2005)	GRATMICI for the following materials: WAS_AREA	(Nemer et al., 2005)
Humid Rate Of Cellulose Biodegradation In The Waste Area see: (Nemer and Stein, 2005)	GRATMICH for the following materials: WAS_AREA	(Nemer et al., 2005)
Actinide Solubilities in Castile and Salado Brines see: (Garner and Leigh, 2005)	SOLCOH and SOLSOH for the following properties: SOLMOD3, SOLMOD4, SOLMOD5 and SOLMOD6.	(Brush, 2005)
Probability of microbial degradation In The Waste Area see: (Nemer and Stein, 2005)	PROBDEG for the following materials: WAS_AREA	(Nemer, 2005)
Parameters Added for the CRA-2004 PABC		

Description	Name	Justification
Probability of attaining sampled microbial gas generation rate see: (Nemer and Stein, 2005)	BIOGENFC for the following materials: WAS_AREA	(Nemer et al., 2005)
Shear rate and flow rate for the drilling fluid for the Cuttings model. see: (Vugrin, 2005a)	DRILLMUD for the following properties: MUDFLWRT and SHEARRT	(Vugrin, 2005g)
Actinide solubility variability see: (Garner and Leigh, 2005)	SOLVAR for the following materials: SOLMOD4 and SOLMOD3	(Xiong et al., 2005)
Parameters Used in CRA-2004 that were not used in the CRA-2004 PABC		
Multiplication factors for actinide solubilities in Salado brine see: (Garner and Leigh, 2005)	SOLSIM for the following materials: SOLAM3, SOLPU3, SOLPU4,SOLU4, SOLTH4, SOLU6	NA
Multiplication factors for actinide solubilities in Castile brine see: (Garner and Leigh, 2005)	SOLCIM for the following materials SOLAM3, SOLPU3, SOLPU4,SOLU4, SOLTH4, SOLU6	NA
Actinide solubilities in Salado brine see: (Garner and Leigh, 2005)	SOLSOC for the following materials: SOLMOD3, SOLMOD4, SOLMOD5, SOLMOD6	NA
Actinide solubilities in Castile brine see: (Garner and Leigh, 2005)	SOLCOC for the following materials: SOLMOD3, SOLMOD4, SOLMOD5, SOLMOD6	NA
Index for selecting realizations of the SPALL model see: (Vugrin, 2005b)	RNDSPALL for the material SPALLMOD	NA

During the process of revising the code CUTTINGS_S Version 5.10, it was identified that two parameter values affected by current drilling practices were hardcoded into the source code of CUTTINGS_S Version 5.10. The decision was made to remove these parameters from the source code and to place them into the input control file of CUTTINGS_S Version 6.00 (Vugrin, 2005k). The two parameters are a shear rate and the drilling mud flow rate per unit length of the drillbit diameter, referred to in the *User's Manual for CUTTINGS_S Version 6.00* (Vugrin, 2005k) by the variable names SHEARRT and MUDFLWRT, respectively. The values have not changed; they have only moved from the source code to the input file to improve the transparency of the calculations and the maintainability of the code.

As a part of the quality assurance (QA) review of *Analysis Package for CUTTINGS_S: CRA-2004 Performance Assessment Baseline Calculation* (Vugrin, 2005a), Chavez requested that these parameters be added to the WIPP PA Parameter Database (PAPDB) (Chavez, 2005). The

two parameters DRILLMUD: SHEARRT and DRILLMUD:MUDFLWRT were added to the PAPDB (Vugrin, 2005g). The parameter values were manually entered into the CUTTINGS_S input file for the CRA-2004 PABC, but the intent is to have these pulled by MATSET in the future. These were the two most recent changes to the parameters for WIPP PA in support of the CRA-2004 PABC. Other parameter changes have been made and documented according to Nuclear Waste Management Procedure (NP) 9-2, Parameters (Chavez, 2002).

3. SUMMARY OF PERFORMANCE ASSESSMENT CALCULATIONS FOR THE CRA-2004 PABC

The WIPP PA quantifies the potential releases of radioactive materials from the disposal system to the accessible environment over the 10,000-year regulatory period using a suite of numerical models. These numerical models are included in various computer codes as shown in Figure 3-1. There is a significant amount of uncertainty associated with characterizing the physical properties of geologic materials that influence potential releases. WIPP PA considers both subjective (epistemic) uncertainty and stochastic (aleatory) uncertainty. Properties such as permeability and porosity are usually measured indirectly and can vary significantly depending upon location. This uncertainty assigning the appropriate value to certain physical properties is termed subjective uncertainty. Subjective uncertainty can, in theory, be reduced by further study of the system. Subjective uncertainty is dealt with in WIPP PA by running multiple realizations in which the values of uncertain parameters are varied. To ensure that low probability (and possibly high consequence) combinations are represented, Latin hypercube sampling is used to create the realizations. For the WIPP PA, the LHS code (Vugrin, 2005h) is used to create a "replicate" of 100 distinct parameter sets ("vectors") that span a wide range of parameter uncertainty. Three replicates are run for a total of 300 separate vectors to ensure that the Latin hypercube replicates are representative. This is the start of the WIPP PA calculation.

For each of the 300 vectors, the other codes are run. The PANEL (Garner, 2003b) code quantifies the mobilization of actinides by brine. BRAGFLO (Stein, 2003a) is used to calculate Salado brine and gas flow. NUTS (Leigh, 2003) is used to calculate Salado transport. The CUTTINGS_S (Gilkey and Vugrin, 2005) code is used to calculate single intrusion direct solids releases. The DRSPALL (Lord, 2004) code is used to calculate single intrusion direct solids releases via spallings, and the BRAGFLO code is used to calculate single intrusion direct brine release. MODFLOW 2000 (McKenna, 2005) and SECOTP2D (Gilkey, 2003) are used to calculate Culebra flow and transport, respectively. All of these calculations address the subjective uncertainty by producing results for the 300 separate vectors.

WIPP PA also addresses stochastic uncertainty, or the uncertainty in future events. Unlike subjective uncertainty, stochastic uncertainty cannot be reduced by further study. To deal with this type of uncertainty, WIPP PA employs a standard Monte Carlo method of sampling on random "futures." A future is defined as one possible sequence of events. The CCDFGF code (Vugrin, 2004d) uses the results from the other codes to construct individual futures and ultimately, CCDFs.

This section provides a summary of the actual PA calculations for the CRA-2004 PABC. For each of the processes discussed above, an individual analysis package has been produced. The analysis package gives details of the calculation, describes the changes that were made to produce the CRA-2004 PABC, and gives a comparison between CRA-2004 and CRA-2004 PABC results. A description of each analysis and references to the analysis packages are provided in the following sections.

Information Only
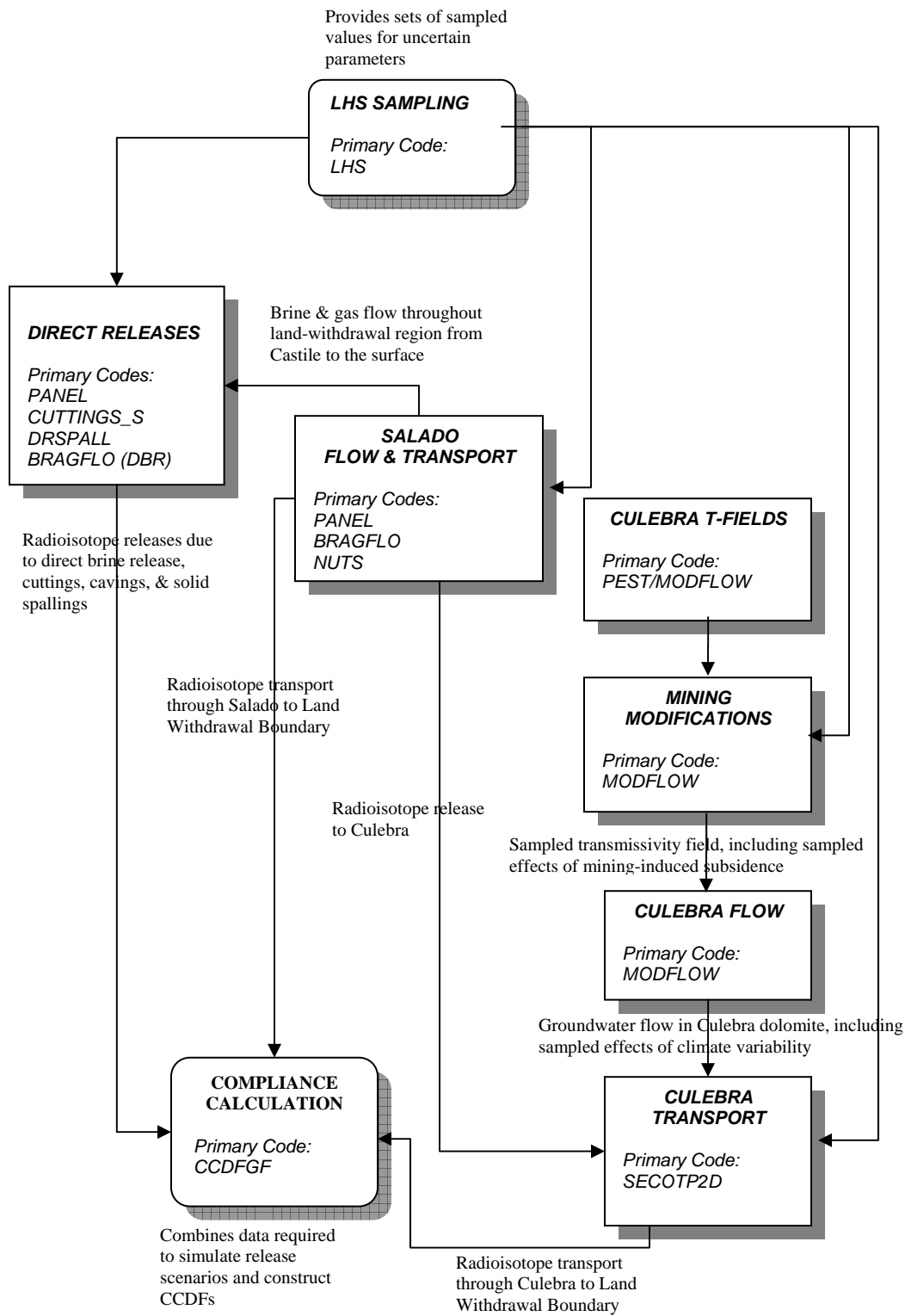
Figure 3-1. Primary Computational Models Used in the CRA-2004 PABC.

3.1   LHS SAMPLING

The primary role of the code LHS is to use Latin hypercube sampling to sample the subjectively uncertain parameters used in WIPP PA. Additionally, LHS uses these sampled parameters to create the 100 vectors per replicate that are input into the suite of codes used in WIPP PA. LHS was one of the first codes run for the CRA-2004 PABC, and an analysis of CRA-2004 PABC LHS calculations and a comparison of the CRA-2004 LHS calculations is provided in the LHS analysis package (Kirchner, 2005a).

The code LHS Version 2.41 was used for sampling in the CRA-2004. After completion of the CRA-2004, two errors were detected. The first error in LHS Version 2.41 affected the sampling of normal and lognormal distributions (Hansen, 2004b). The software is supposed to sample between the 1st and 99th quantiles, but because of the way the sampling technique was implemented in the code, it could return values outside of the specified sampling range. (It should be noted that since the CRA-2004 did not use any parameters modeled with normal or lognormal distributions, this error had no impact on the CRA-2004.)

The second error in LHS Version 2.41 affected the sampling of Student's t and Logstudent's t distributions (Vugrin, 2004e). Version 2.41 constrained sampled values to be within the range of data points supplied for the distribution by the PAPDB. As a result, multiple vectors could have the same value for a parameter. Additionally, constraining the sampled values by the data points could unnecessarily restrict the sampling range. LHS Version 2.42 corrected this error by sampling all Student's t and Logstudent's t distributions between the 1st and 99th quantiles. Additionally, all vectors are ensured to have distinct values for Student's t and Logstudent's t distributions.

These errors have been corrected, and a new version of the LHS software (Version 2.42) has been released (Vugrin, 2005e; Vugrin, 2005h). LHS Version 2.42 was used for the CRA-2004 PABC.

3.2   ACTINIDE MOBILIZATION

The code PANEL has four roles in the WIPP PA system. The first is to compute the potential for actinide mobilization due to dissolution and colloid mobilization. This is the amount of radionuclides mobilized for removal via a brine pathway. The second purpose is to calculate radionuclide decay, and the third is to calculate the amounts of radionuclides mobilized in a panel that contain a given volume of brine. The fourth is to compute the amounts of radionuclides removed by a volume of brine moving up the borehole to the Culebra. PANEL was run for the CRA-2004 PABC, and analysis of the CRA-2004 PABC PANEL calculations including a comparison to the CRA-2004 PA is provided in the PANEL analysis package (Garner and Leigh, 2005).

The code PANEL Version 4.02 was run for the CRA-2004. Prior to beginning CRA-2004 PABC calculations, PANEL was modified. In Version 4.02, the default panel brine volume was hardwired into the code itself. Version 4.03 which reads this volume from the input Compliance Assessment Methodology Database (CAMDAT) file (Garner, 2005) was used for CRA-2004 PABC calculations.

3.3   SALADO FLOW

The code BRAGFLO simulates brine and gas flow in and around the repository. BRAGFLO includes the effects of processes such as gas generation and creep closure. Outputs from the BRAGFLO simulations describe the conditions (pressure, brine saturation, porosity) and flow patterns (brine flow up an intrusion borehole and out anhydrite marker beds to the accessible environment) that are used by other software to predict radionuclide releases. Analysis of the CRA-2004 PABC BRAGFLO calculations including a comparison to the CRA-2004 PA is provided in the BRAGFLO analysis package (Nemer and Stein, 2005).

BRAGFLO Version 5.00 was run for the CRA-2004 PABC. The same version of the code was used for CRA-2004 calculations.

3.4   SALADO TRANSPORT

The WIPP PA radioisotope mobilization and decay code NUTS simulates the transport of radionuclides through the Salado Formation for Scenarios S1 through S5. Two types of NUTS runs are made for PA calculations. "Screening" runs use a conservative tracer to determine which vector/scenario combinations have potential for radionuclides to reach the accessible environment. These vector/scenario combinations are included in "non-screening" runs which calculate the transport of actual radionuclides. Analysis of the CRA-2004 PABC NUTS calculations including a comparison to the CRA-2004 is provided in the NUTS analysis package (Lowry, 2005).

NUTS Version 2.05b was used for CRA-2004 PABC Salado transport calculations. This is the same version that was used for the CRA-2004.

3.5   SINGLE INTRUSION DIRECT SOLIDS RELEASE VIA CUTTINGS/CAVINGS

Cuttings and cavings are the solid material removed from the repository and carried to the surface by the drilling fluid during the process of drilling a borehole. Cuttings are the materials removed directly by the drill bit, and cavings are the material eroded from the walls of the borehole by shear stresses from the circulating drill fluid. The CUTTINGS_S code calculates the quantity of material brought to the surface from a radioactive waste disposal repository as a consequence of an inadvertent human intrusion through drilling. WIPP PA utilizes the code CUTTINGS_S to calculate the amount of material removed from the repository by cuttings and cavings (Vugrin and Fox, 2005). CUTTINGS_S also uses the repository pressures calculated by BRAGFLO to interpolate spallings volumes from DRSPALL and calculate spallings volumes from an individual intrusion for the various drilling scenarios. Finally, CUTTINGS_S calculates the volume weighted averages of several different quantities, and the resulting averages are used as initial conditions for direct brine release (DBR) calculations by BRAGFLO. Analysis of the CRA-2004 PABC CUTTTING_S calculations including a comparison to the CRA-2004 PA is provided in the CUTTING_S analysis package (Vugrin, 2005a).

CUTTING_S Version 5.10 was run for the CRA-2004. After completion of the CRA-2004, several modifications were made to the software. The major modifications implemented in

subsequent versions of CUTTINGS_S are as follows (Gilkey, 2004; Vugrin, 2005d; Vugrin, 2005c) and (Vugrin, 2005i):

1) Unnecessary functionality was removed. Among other things, this includes the radionuclide release calculations, the calibration capability, the PreCuttings capability, and spall models 1 and 2.

2) CUTTINGS_S Version 6.00 processes multiple scenarios, vectors, cavities, and intrusions in a single execution. (Version 5.10 required 23,400 calculations for 3 replicates). This change necessitated a change to the format and content of input and output files.

3) CUTTINGS_S Version 6.00 produces a text output file with all the cuttings, cavings, and spallings information for all of the vector/time/scenario/location combinations. This modification eliminates the need for a SUMMARIZE step between CUTTINGS_S and PRECCDFGF.

4) If no value for the parameter RNDSPALL is specified in the input file, the code will map DRSPALL Vector 1 of Replicate R1 to PA Vector 1 of Replicate 1, DRSPALL Vector 2 of Replicate R1 to PA Vector 2 of Replicate R1, and so forth.

5) Parameters that were previously hardcoded into previous versions of the code are read from the input file (see Section 2.9).

6) When the flow is turbulent, the subroutine DRILL attempts to calculate the radius at which the flow becomes laminar. It is required, both physically and computationally, that ROUTER remains larger than the constant RINNER. An IF loop in the subroutine DRILL was modified to prevent the RINNER from being greater than ROUTER.

7) Extensive modifications were made to the code to make it easier to read and maintain.

CUTTINGS_S Version 6.02 (Vugrin and Fox, 2005) has all of the modifications and capabilities listed above, and this version was used for the CRA-2004 PABC calculations. Use of this version is a deviation from Analysis Plan (AP)-122 (Leigh and Kanney, 2005) since AP-122 indicated that Version 6.01 would be used for the CRA-2004 PABC. However, a combination of input parameters led to the need for the correction described above in 6), so the modified code Version 6.02 was used for CRA-2004 PABC calculations.

3.6   SINGLE INTRUSION DIRECT SOLIDS RELEASE (SPALLINGS)

A WIPP spallings event is a special case of drilling intrusion in which the repository contains gas at high pressure. This highly pressurized gas can cause localized mechanical failure and entrainment of solid WIPP waste into and up the borehole, resulting in transport to the land surface. Under the direction of the DOE, SNL developed a spallings model and the computer code DRSPALL to calculate the spallings volume from a single borehole intrusion (Lord, 2004). The first PA for which this model and code were utilized was the CRA- 2004. Analysis of the

CRA-2004 PABC DRSPALL calculations including a comparison to the CRA-2004 PA is provided in the DRSPALL analysis package (Vugrin, 2005b).

DRSPALL Version 1.10 was used in the CRA-2004 PABC (Version 1.00 was used in the CRA-2004 PA). The update to DRSPALL Version 1.10 comprised mainly cosmetic changes that had no effect on the results of the CRA-2004 calculations or any of the validation test cases. The cosmetic deficiencies in DRSPALL Version 1.00 are identified in Software Problem Report (SPR) 03-007 (Lord, 2003b) and the changes made to produce DRSPALL Version 1.10 are described in (Lord, 2003a).

3.7   SINGLE INTRUSION DIRECT BRINE RELEASE

DBRs are releases of contaminated brine originating in the repository and flowing up an intrusion borehole during the period of drilling. In order to have a significant DBR release, two criteria must be met (Stoelzel and O'Brien, 1996):

1. Volume averaged pressure in the vicinity of the repository encountered by drilling must exceed drilling fluid hydrostatic pressure (assumed to be 8 MPa).
2. Brine saturation in the repository must exceed the residual saturation of the waste material (Sampled from a uniform distribution ranging from 0.0 to 0.552).

DBRs are calculated using the code BRAGFLO with a two dimensional, oriented grid, which represents the vicinity of the waste panels.

BRAGFLO Version 5.00 was run for the CRA-2004 PABC DBR calculations. Analysis of the DBR results including a comparison to the CRA-2004 PA is provided in the BRAGFLO DBR analysis package (Stein et al., 2005). BRAGFLO Version 5.00 was also used for CRA-2004 DBR calculations.

3.8   CULEBRA FLOW AND TRANSPORT

Culebra flow is calculated by the code MODFLOW. MODFLOW 2000 Version 1.6 was used for both the CRA-2004 PABC and CRA-2004 Culebra flow calculations.

Transport of radionuclides through the Culebra is calculated by the code SECOTP2D. Analysis of the CRA-2004 PABC SECOTP2D calculations including a comparison to the CRA-2004 PA is provided in the SECOTP2D analysis package (Lowry and Kanney, 2005).

SECOTP2D Version 1.41A was used for both the CRA-2004 PABC and CRA-2004 Culebra transport calculations.

3.9   NORMALIZED RELEASES

WIPP PA uses the code CCDFGF to address stochastic uncertainty. CCDFGF employs a standard Monte Carlo method of sampling on random "futures". A future is defined as one possible sequence of events, and each future is based on sampled stochastic variables such as the time and location of a drilling event, plugging pattern used for a drilling event, and whether or

not waste was encountered. The CCDFGF code (Vugrin, 2004d) combines the sampled stochastic parameters with the release data calculated by the process model codes to calculate the cumulative normalized release for each future. Using these futures and ordered statistics, CCDFs are created, and these CCDFs are compared to regulatory limits to determine compliance with the EPA regulations. Analysis of the CRA-2004 PABC CCDFGF calculations including a comparison to the CRA-2004 PA is provided in the CCDFGF analysis package (Dunagan, 2005).

In order for CCDFGF to calculate the CCDFs, the release data from the various process model codes must be assembled. This is a multi-step process. Most of the release data from the process model codes is output in the form of binary CAMDAT files. In general, the code SUMMARIZE is run multiple times to extract and collate the release data from individual codes into text files. These files are then input into the code PRECCDFGF in order to assemble all of the release data for a single replicate into one release table (RELTAB) file. This file is input into CCDFGF.

In the past year, the process in which data is transferred from the process model codes to CCDFGF has been significantly improved. In response to several self-reported errors (Kirchner and Vugrin, 2004; Vugrin and Kirchner, 2004; Kirchner and Vugrin, 2005) and EPA queries (Cotsworth, 2005), the codes SUMMARIZE, PRECCDFGF, and CCDFGF have been modified to prevent errors in this data transfer process. The accuracy of the data transfer for the CRA-2004 PABC has been verified and documented in Kanney and Kirchner (2005). Summaries of the more significant modifications made to SUMMARIZE, PRECCDFGF, and CCDFGF are contained in Sections 3.9.1, 3.9.2, and 3.9.3, respectively.

3.9.1   SUMMARIZE Modifications

SUMMARIZE Version 2.20 was run for the CRA-2004 PA. After the CRA-2004 PA, several modifications were made to the code (Gilkey, 2005). The major modifications contained in SUMMARIZE Version 3.00 are listed below:

1) A new output driver for the PRECCDFGF code was added. This driver creates standardized headers at the top of the SUMMARIZE output files that indicate the CAMDAT parameter names to which the data in the columns correspond.

2) When SUMMARIZE is run, the user specifies the vectors to be processed. If Version 2.20 does not find the input CAMDAT file corresponding to a vector, the code writes a message to the error log and outputs zeroes for the data in the text output file. In Version 3.00 the SKIP command was added so that if a vector's CAMDAT file is not found and that vector number is specified to be skipped in the input file, the code outputs zeroes for that vector in the text output file and does not write an error message.

3) If Version 2.20 encounters unexpected conditions when reading a CAMDAT file, an error is written to the log file, and the code continues. Since the code runs to completion, these conditions could be overlooked if the error log file is not inspected. If Version 3.00 encounters unexpected conditions, the code aborts unless the IGNORE_WARNINGS command is specified.

SUMMARIZE Version 3.00 was used for CRA-2004 PABC calculations.

3.9.2   PRECCDFGF Modifications

PRECCDFGF Version 1.00B was run for the CRA-2004 PA. After the CRA-2004 PA, several modifications were made to the code (Hansen, 2004a; Kirchner, 2004a). Important changes to PRECCDFGF Version 1.01 are listed below:

1) In Version 1.00B, spallings volumes were multiplied by the parameter REFCON: FVRW, which has a value of 1. In Version 1.01, spallings volumes are not multiplied by this parameter. It should be noted that this multiplication had no impact on the performance of the code.

2) Version 1.01 reads release data for direct solids releases from a single output file created by CUTTINGS_S instead of a set of 78 files from SUMMARIZE.

3) Version 1.01 retrieves GLOBAL:PBRINE parameter values from a set of CAMDAT files instead of a text output file created by LHS.

4) Version 1.01 has automated error checking capabilities for reading the input files created by SUMMARIZE. PRECCDFGF reads the headers of the SUMMARIZE files, and if they do not match the format that PRECCDFGF expects, the code aborts after writing an error message to a log file.

PRECCDFGF Version 1.01 was used for the CRA-2004 PABC.

3.9.3   CCDFGF Modifications

CCDFGF Version 5.00A was originally run for the CRA-2004. After DOE submitted the CRA-2004 results (U. S. DOE, 2004) in March of 2004, an error was detected that affected how spallings releases were calculated. In Version 5.00A the spallings release from a single intrusion is erroneously calculated by multiplying the volume by the average repository activity. This error was corrected in subsequent versions of the code and its impact on CRA calculations were documented in (Vugrin, 2004a; Kirchner and Vugrin, 2005).

CCDFGF Version 5.02 was used for CRA-2004 PABC calculations. The major difference between Version 5.00A and 5.02 affects calculations of spallings releases.   Version 5.02 correctly calculates the spallings release from a single intrusion by multiplying the spallings volume by the average repository activity and the parameter REFCON:FVW, the fraction of the repository occupied by waste. Additional modifications were made to CCDFGF that yielded CCDFGF Version 5.02. For further discussion of these minor modifications affecting the development of CCDFGF see (Kirchner and Vugrin, 2005).

3.10   RUN CONTROL

Digital Command Language (DCL) scripts, referred to here as EVAL run scripts, are used to implement and document the running of all software. These scripts, which are the basis for the WIPP PA run control system, are stored in the CRA1BC_EVAL Code Management System (CMS) library. All inputs are fetched at run time by the scripts, and outputs and run logs are

automatically stored by the scripts in class CRA-2004 PABC-0 of the CMS libraries. Run control for the CRA-2004 PABC calculations is documented in Long and Kanney (2005).

4.   RESULTS FOR THE UNDISTURBED REPOSITORY

The PA tabulates releases from the repository for undisturbed conditions. Releases to the accessible environment from the undisturbed repository fall under two sets of protection requirements. The first, as set forth 40 CFR § 191.15, protects individuals from radiological exposure; the second, in 40 CFR Part 191, Subpart C, protects groundwater resources from contamination. This section shows how WIPP complies with these two requirements by presenting flow (BRAGFLO) and transport (NUTS) results from modeling the undisturbed repository.

4.1   SALADO FLOW

Flow in the Salado is computed by BRAGFLO (Stein, 2003a). This section summarizes the Salado flow calculation results for the undisturbed scenario (S1). Pressure in the repository, brine saturation in the waste, and brine flow out of the repository are presented, along with sensitivity analyses that identify the uncertain parameters to which these results are most sensitive. The analysis package for Salado Flow (Nemer and Stein, 2005) contains a detailed presentation on the BRAGFLO model, calculation results, and further sensitivity analyses.

4.1.1   Pressure in the Repository

In undisturbed conditions, pressure strongly influences the extent to which contaminated brine might migrate from the repository to the accessible environment. In addition, pressure developed under undisturbed conditions is an initial condition for the models for spallings and DBR (Sections 5.5.2 and Section 5.5.3 respectively).

The Salado flow model represents the repository as five regions in the numerical grid: three waste-filled regions (the Waste Panel, South Rest of Repository (RoR)**,** and North RoR in Figure 4-1) and two excavated regions with no waste (operations area and experimental area in Figure 4-1). Figure 4-2 shows pressure in the waste-filled regions for the 100 realizations in Replicate R1. Pressures within the three waste-filled areas are very similar because gas generation occurs in each region simultaneously.

During the first 1,000 years, repository pressure may increase rapidly due to several factors: rapid initial creep closure of rooms; initial inflow of brine causing gas generation due to corrosion; and availability of CPR material to produce gas by microbial degradation. Pressure generally approaches a steady-state value after 2,000 years as room closure ceases, brine inflow slows (thereby reducing gas generation by corrosion), and CPR materials are consumed.

CRA-2004 and CRA-2004 PABC BRAGFLO Grid

Col	ΔZ	ΔX	Δy
1	66177.07	12203.83	0.10
2	35515.71	3126.85	15.66
3	24949.10	2156.45	43.30
4	17661.78	1487.21	106.00
5	12636.05	1025.66	17.30
6	9170.02	707.35	8.50
7	6701.95	526.68	24.80
8	4922.12	363.23	7.70
9	3694.66	250.50	36.00
10	2848.13	172.76	54.73
11	2264.31	119.15	54.73
12	1861.68	82.17	54.73
13	1584.01	56.67	54.73
14	1392.51	39.08	54.73
15	1260.44	26.95	54.73
16	1169.36	18.59	54.73
17	1106.54	12.82	54.73
18	1063.22	8.84	0.18
19	1033.34	6.10	4.53
20	1012.74	4.20	4.53
21	998.53	2.90	0.27
22	988.73	2.00	2.62
23	126.20	43.80	1.32
24	28.80	10.00	1.32
25	4.80	2.00	1.32
26	0.27575	0.27575	1.32
27	4.80	2.00	0.89
28	28.80	10.00	0.69
29	126.20	43.80	0.85
30	20.00	32.10	1.00
31	20.00	7.90	65.72
32	156.904	140.20	66.72
33	156.904	140.20	66.72
34	40.00	32.10	52.27
35	40.00	7.90	125.83
36	196.13	140.20	
37	196.13	140.20	
38	40.00	32.10	
39	40.00	15.8	
40	32.18	98.7	
41	32.18	98.7	
42	32.18	98.7	
43	9.5	10	
44	30.61	361.65	
45	30.61	361.65	
46	2839.58	2.00	
47	2849.38	2.90	
48	2863.59	4.20	
49	2884.19	6.10	
50	2914.07	8.84	
51	2957.39	12.82	
52	3020.20	18.59	
53	3111.29	26.95	
54	3243.36	39.08	
55	3434.86	56.67	
56	3712.53	82.17	
57	4115.16	119.15	
58	4698.98	172.76	
59	5545.50	250.50	
60	6772.97	363.23	
61	8552.80	526.68	
62	11020.87	707.35	
63	14486.90	1025.66	
64	19512.63	1487.21	
65	26799.95	2156.45	
66	37366.56	3126.85	
67	52688.14	4533.94	
68	77095.80	7669.89	

Figure 4-1. CRA-2004 PABC BRAGFLO Grid .
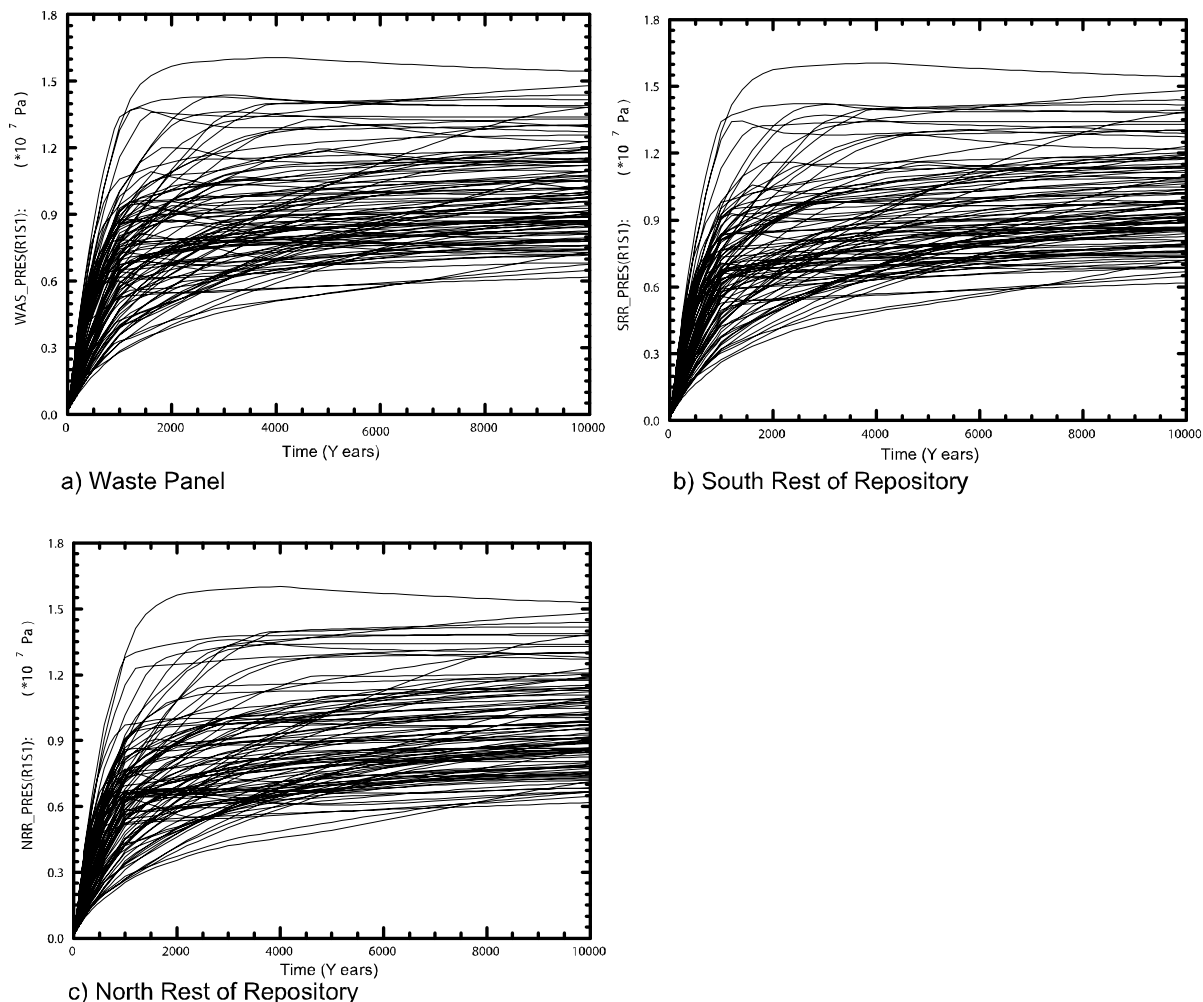
Figure 4-2. Pressure in the Waste-filled Areas, Replicate R1, Scenario S1, from the CRA-2004 PABC.

Figure 4-3 and Figure 4-4 show the mean and 90th percentile values for pressure in each region for the CRA-2004 and the CRA-2004 PABC. There is a consistent pattern of declining pressure from the waste panel through South RoR (SRR_PRES) and North RoR (NRR_PRES). The differences in pressure reflect the slow migration of gas from waste-filled regions to the non-waste regions where no gas is being produced. The 90th percentile pressures level off between 14 and 15 MPa indicating equilibrium between gas generation, which increases pressure, and pressure relief processes (e.g., fracturing, outward migration of fluids, and increased porosity of the excavated areas).

Sensitivity analyses are used to determine the importance of parameter uncertainty to the uncertainty in model results.   Figure 4-5 shows partial rank correlation coefficients (PRCCs), generated from code PCCSRC (Gilkey, 1995) resulting from regression between pressure in the waste panel (WAS_PRES) and the uncertain variables in the Latin hypercube sample (Section 3.1) for the CRA-2004 PABC. The figure shows that uncertainty in the pressure in the waste panel is primarily determined by the sampled input parameter, HALPOR, which is the halite porosity [see (Nemer and Stein, 2005)].
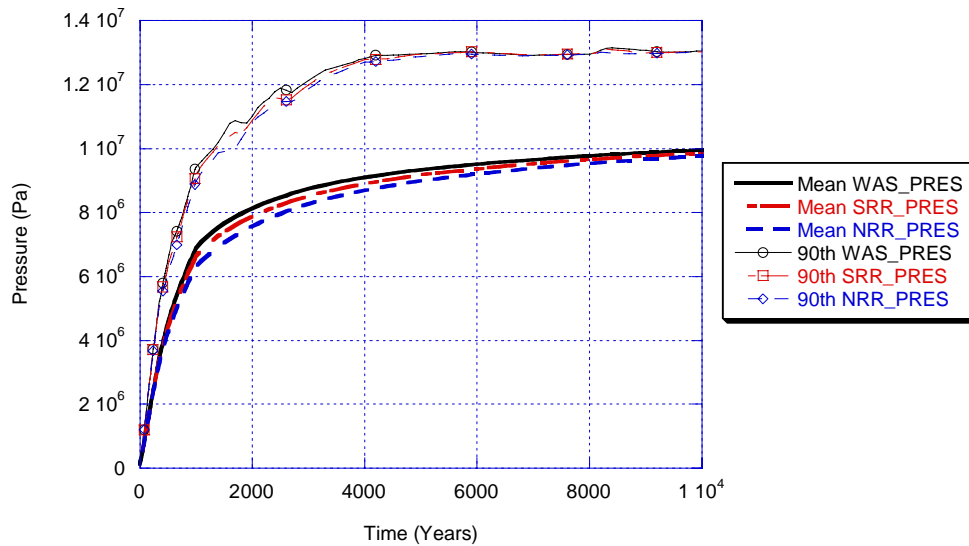
Figure 4-3. Mean and 90th Percentile Values for Pressure in Waste-filled Areas, Replicate R1, Scenario S1, from the CRA-2004 PABC.
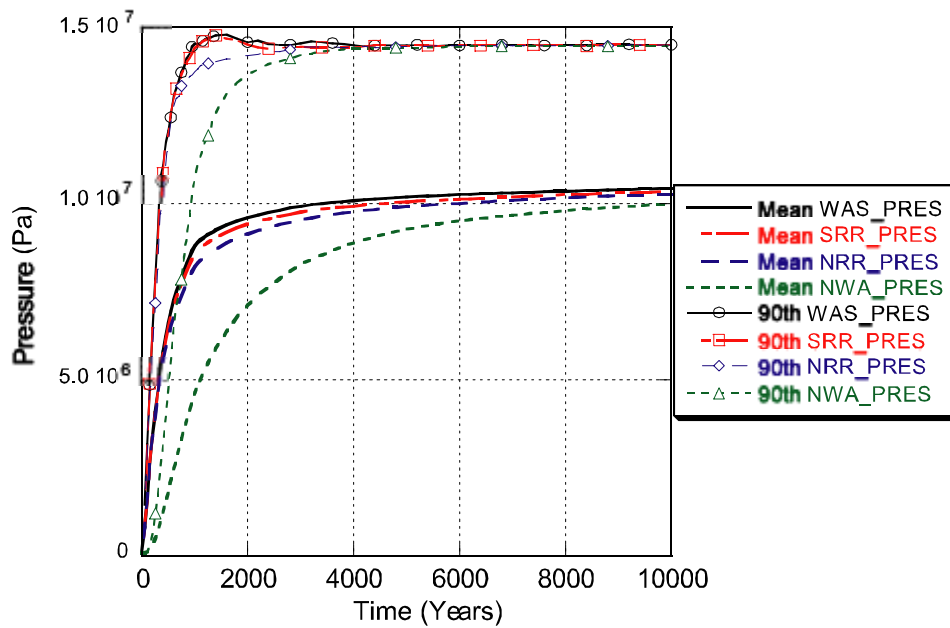
Figure 4-4. Mean and 90th Percentile Values for Pressure in Excavated Areas, Replicate R1, Scenario S1, from the CRA-2004.

The positive correlation indicates that higher pressures result from higher values of halite porosity (HALPOR). Consequently, uncertainties in other parameters are not very significant; the other PRCCs in Figure 4-5 indicate that the uncertainty factor for microbial gas generation (WBIOGENF), the corrosion rate for steel (WGRCOR), the waste wicking parameter (WASTWICK), and the disturbed rock zone (DRZ) permeability (DRZPRM) determine the remaining variability in waste panel pressure.

Figure 4-6 and Figure 4-7 compare statistics for pressure in the waste panel among the three replicates for the CRA-2004 and the CRA-2004 PABC and show that results for the three replicates are very similar. Mean pressures are nearly coincident; small differences between replicates are observable among the replicates at very high or very low pressures.
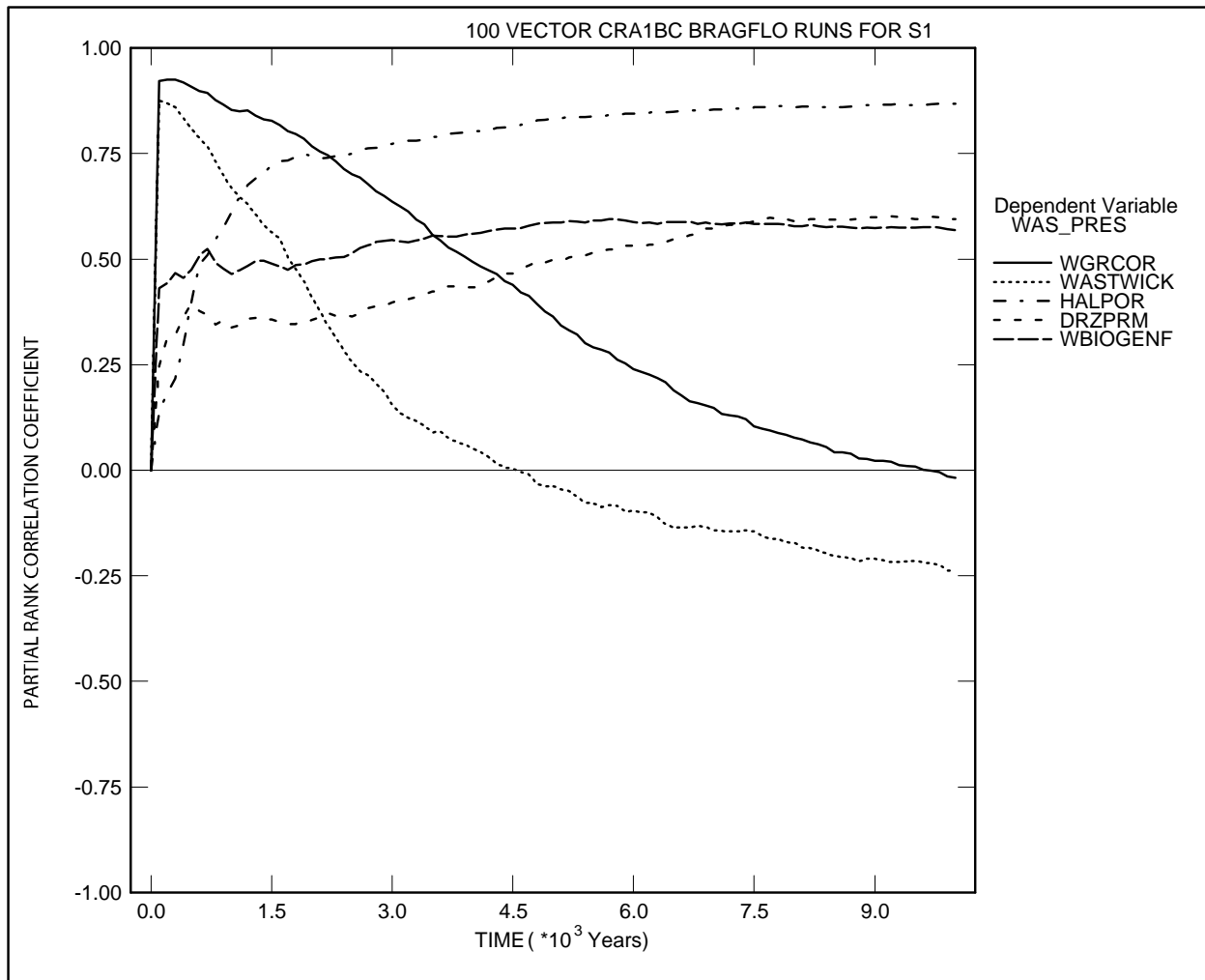
Figure 4-5. Primary Correlations of Pressure in the Waste Area with Uncertain Parameters, Replicate R1, Scenario S1, from the CRA-2004 PABC.
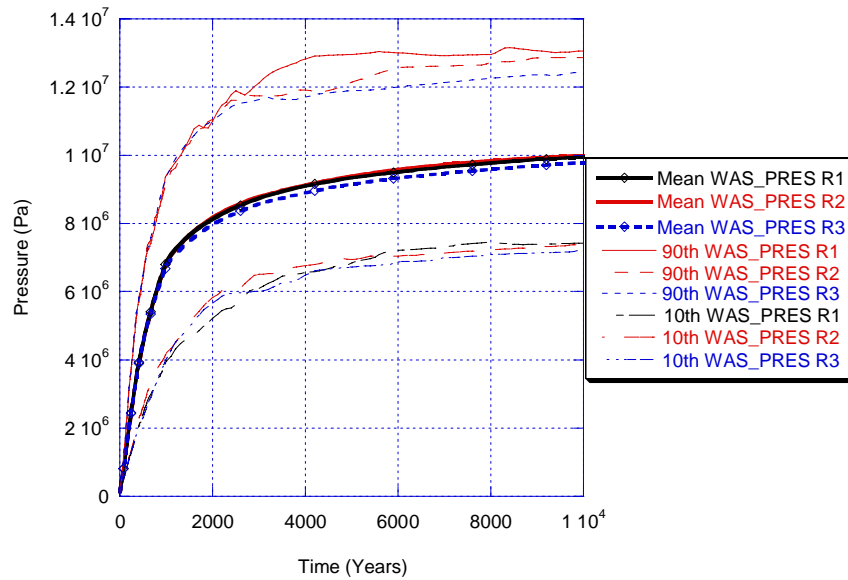
Figure 4-6. Comparison of Pressure in the Waste Panel Between All Replicates, Scenario S1, from the CRA-2004 PABC.
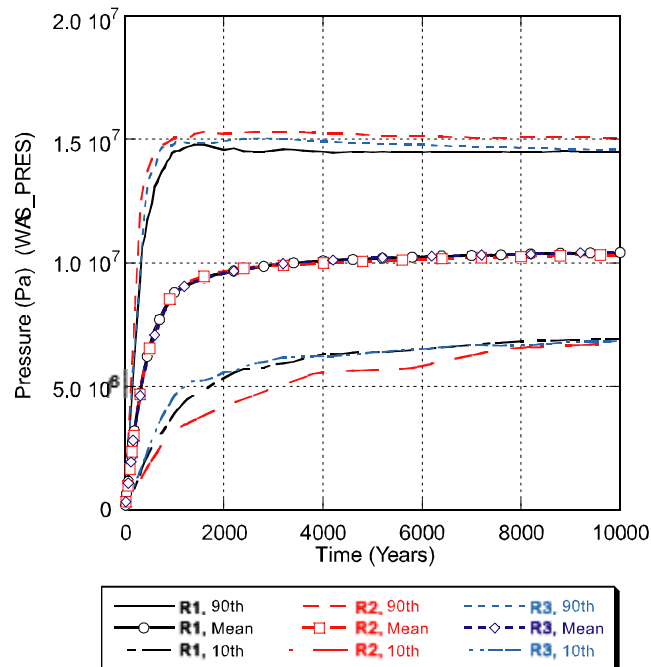
Figure 4-7. Comparison of Pressure in the Waste Panel Between All Replicates, Scenario S1, from the CRA-2004.

4.1.2   Brine Saturation in the Waste

Brine saturation is an important result of the model for Salado Flow because gas generation processes, which tend to increase pressure, require brine. Brine saturation is also an initial condition in the model for DBR (Section 5.5.3).

Figure 4-8 shows brine saturation in the various excavated areas of the repository for the 100 realizations of Replicate R1, Scenario S1. Brine saturation in the waste-filled areas is set initially to 0.015. Saturation increases very rapidly (in the first 100 years) in all excavated areas as brine flows toward the excavations, primarily from the DRZ above the excavation. Initially there is a large pressure differential between the DRZ and the excavated regions, and the relatively high permeability of the DRZ, compared to undisturbed halite, permits the rapid influx of brine. Brine inflow slows as the pressures equalize and as brine saturation in the DRZ decreases. Brine saturation in the waste areas decreases over time as brine is consumed by corrosion. Brine may also be driven out of the repository by high pressure.

a) Waste Panel

b) South Rest of Repository

c) North Rest of Repository
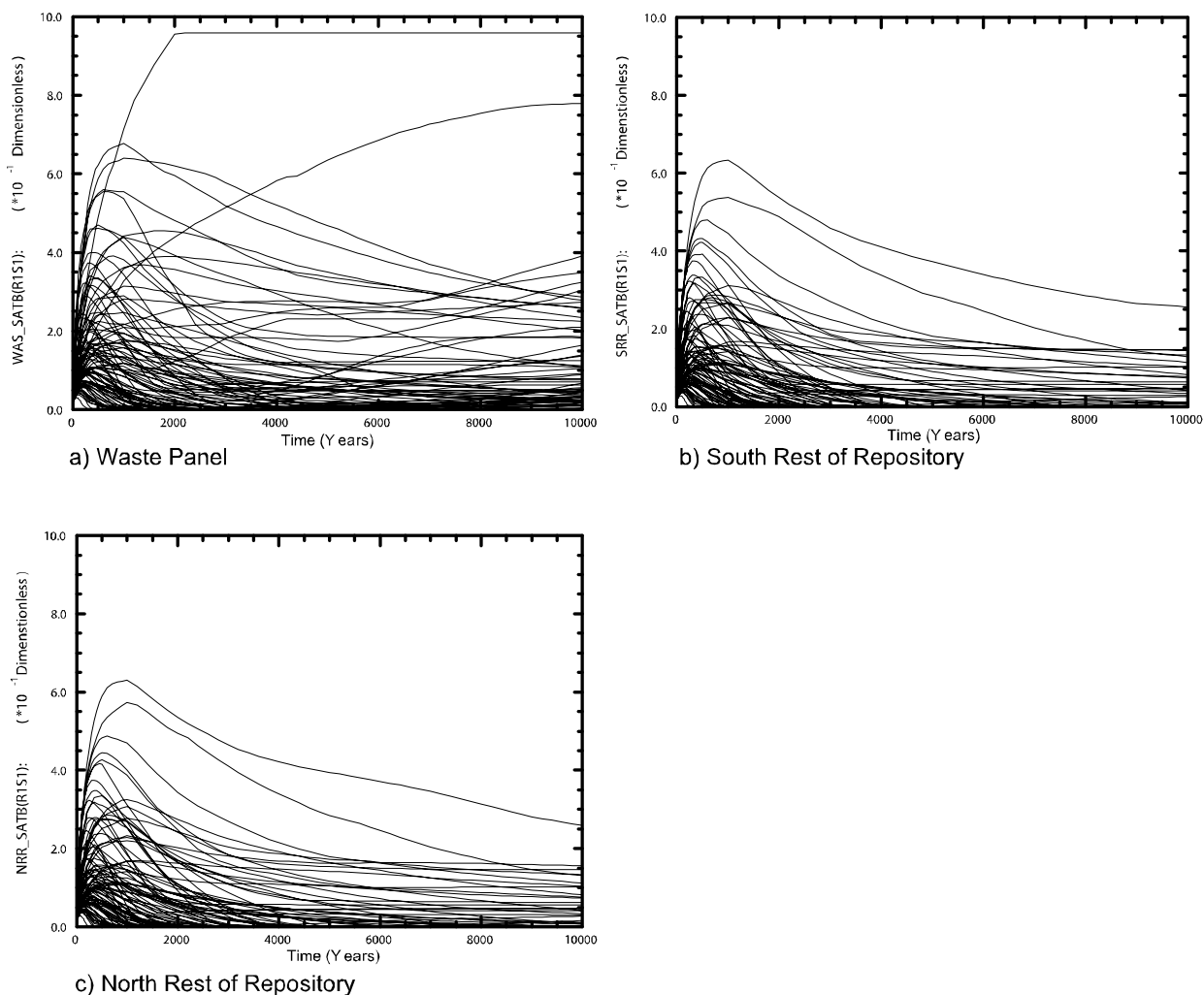
Figure 4-8. Brine Saturation in the Waste-filled Areas, Replicate R1, Scenario S1, from the CRA-2004 PABC.

Information Only

Figure 4-9 and Figure 4-10 compare statistics for brine saturation between the different regions of the repository from the CRA-2004 and the CRA-2004 PABC. Brine saturation in the waste panel (WAS_SATB) tends to be greater than in the rest of repository regions (SRR_SATB and NRR_SATB) due to the artificial two-dimensional modeling of the Salado; in the modeling grid (Figure 4-1), the waste panel has direct contact with the anhydrite marker beds (MBs) while the rest of repository regions do not. Brine saturation in the non-waste region (NWA_SATB) is higher than in the waste-filled regions due to brine consumption in the waste regions, but also due to the panel closures. Brine that enters the experimental area flows down the stratigraphic gradient into the operations area, then ponds up against the panel closure separating the operations area from the waste filled regions.

PRCC's between the brine saturation in the waste panel (WAS_SATB) and the uncertain parameters in the Latin hypercube sample identifies a number of parameters that contribute to the uncertainty in brine saturation. The relative importance of these parameters varies over the 10,000-year modeling period, and none of the parameters is clearly dominant. Figure 4-11 shows positive correlations with anhydrite permeability (ANHPRM), DRZ permeability (DRZPRM), and halite porosity (HALPOR). Increases in halite porosity increase the volume of brine available in the material overlying the waste; increases in DRZ permeability accelerate drainage into the waste. Negative correlations are found between brine saturation and the corrosion rate (WGRCOR) and the wicking factor (WASTWICK) because increases in these two variables increase the rate at which brine is consumed by corrosion, thus decreasing saturation.

Figure 4-12 and Figure 4-13 compare brine saturation statistics for the three replicates for the CRA-2004 and the CRA-2004 PABC. The plots of the mean brine saturation are nearly coincident. Significant differences between replicates are evident at the high end of the saturation scale because there are only a few vectors in each replicate with high saturations.
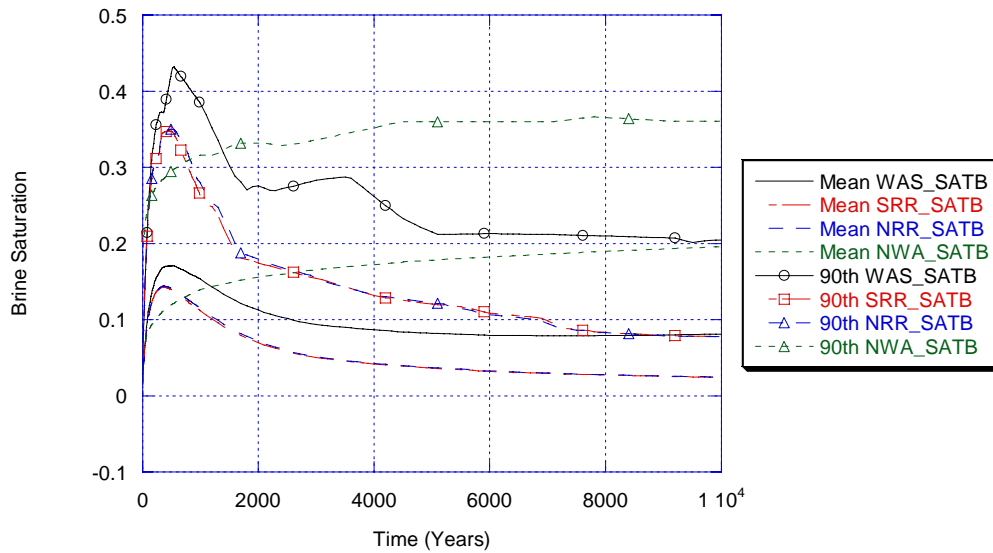
Figure 4-9. Mean and 90th Percentile Values for Brine Saturation in Excavated Areas, Replicate R1, Scenario S1, from the CRA-2004 PABC.
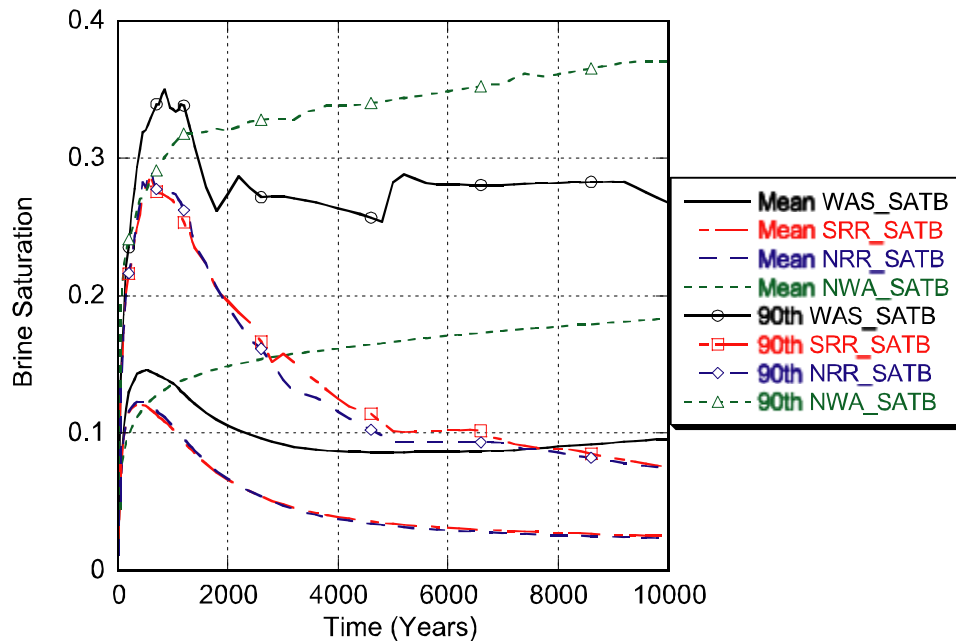
Figure 4-10. Mean and 90th Percentile Values for Brine Saturation in Excavated Areas, Replicate R1, Scenario S1, from the CRA-2004.

Information Only
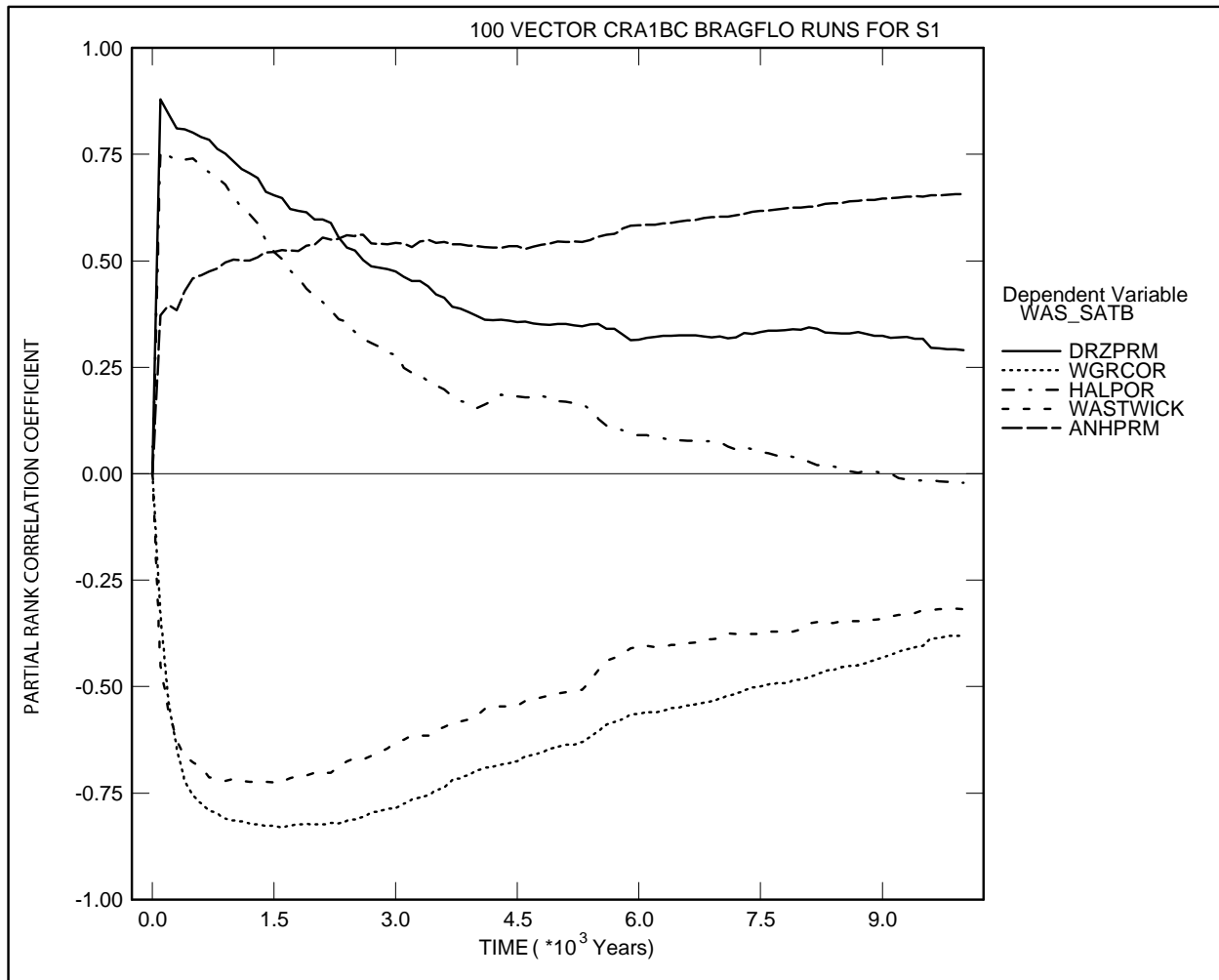
Figure 4-11. Primary Correlations of Brine Saturation in the Waste Panel with Uncertain Parameters, Replicate R1, Scenario S1, from the CRA-2004 PABC.

Information Only
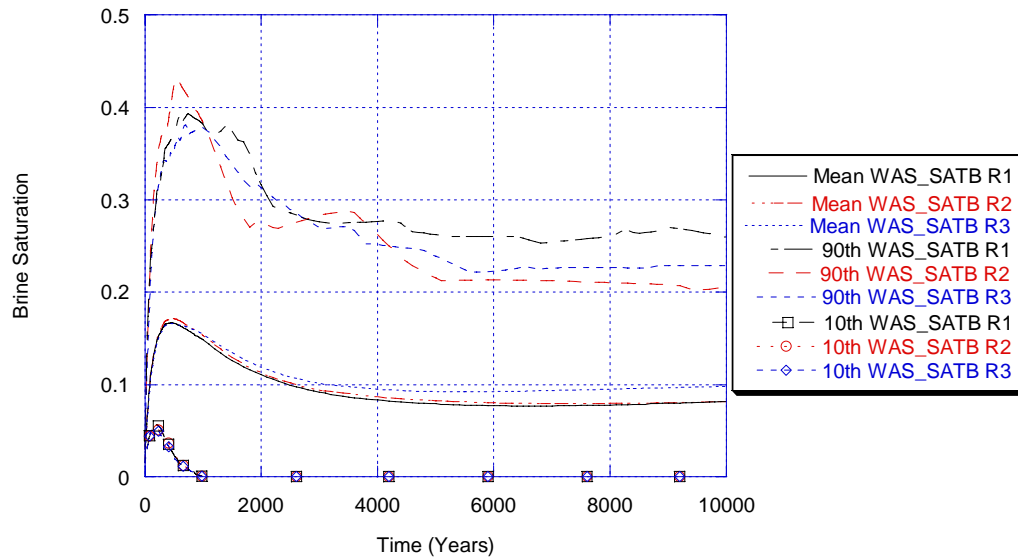
Figure 4-12. Comparison of Brine Saturation in the Waste Panel Between All Replicates, Scenario S1, from the CRA-2004 PABC.
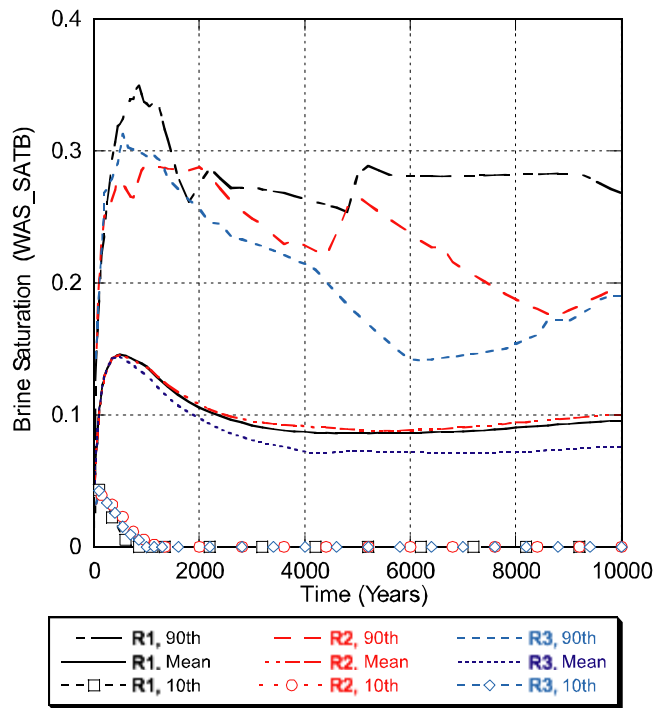
Figure 4-13. Comparison of Brine Saturation in the Waste Panel Between All Replicates, Scenario S1, from the CRA-2004.

4.1.3   Brine Flow Out of the Repository

The anhydrite MBs and the shafts provide possible pathways for brine flow away from the repository in the undisturbed scenario (S1). The Salado Flow model only tabulates the volume of brine crossing boundaries within the model grid; it does not identify whether the brine contains radionuclides from the waste. Transport is calculated separately from the flow and is discussed in Section 4.2.

Figure 4-14 shows cumulative brine outflow from the waste-filled regions of the repository (BRNREPOC). One vector has a cumulative brine outflow from the repository that is greater than the maximum brine outflows through the MBs or through the shafts; the extra brine outflow is going back into the DRZ. Brine flow out of the DRZ into the MBs is shown in Figure 4-15, and flow up the shaft to the bottom of the Culebra is shown in Figure 4-16.

Figure 4-17 shows the volumes of brine that cross the LWB through the MBs. The largest outflow across the LWB is 1,200 m^3. Brine crossing the LWB or moving up the shaft does not necessarily indicate releases from the repository, since the brine may not have been in contact with the waste; the brine may have been present in the MBs at the start of the regulatory period. Section 4.2 presents the results of the transport calculations that determine the amount of radionuclides that may be released by transport in brine.

Regression between total cumulative brine flow out of the waste-filled regions (BRNREPOC) and the uncertain parameters are shown in Figure 4-18. The permeability of the DRZ (DRZPRM) has the largest positive correlation, followed by the permeability of the concrete panel seal (CONPRM), and the porosity of undisturbed halite (HALPOR). The largest negative correlation is with the waste residual brine saturation (WRBRNSAT), which determines the immobile portion of the waste brine saturation.

Figure 4-19 and Figure 4-20 compare statistics of brine outflow from the repository for the three replicates from the CRA-2004 and the CRA-2004 PABC, and show that all three replicates produce similar results. The BRNREPOC provides a more valid basis for comparison among the replicates than the other outflow variables because it has fewer vectors with zero values.
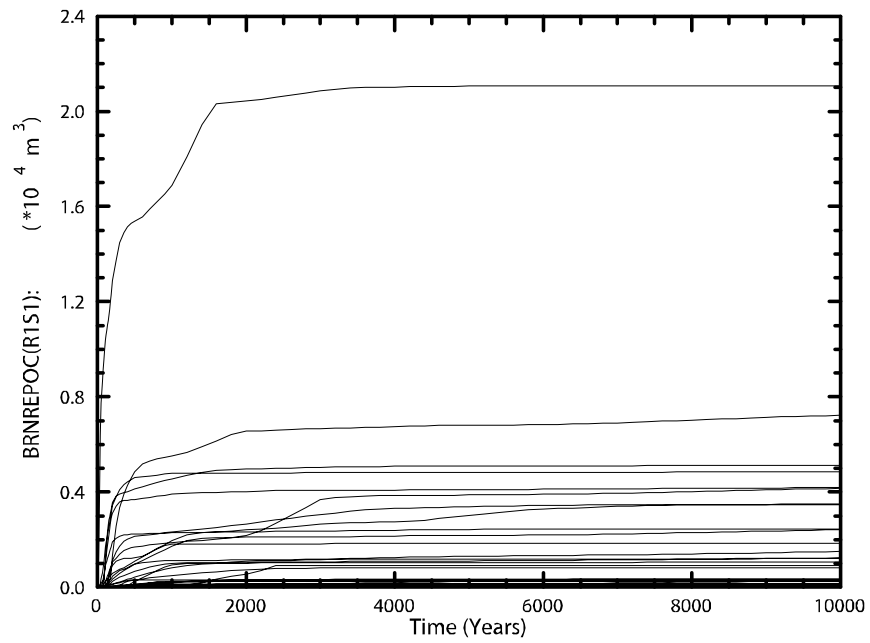
Figure 4-14. Brine Flow Away from the Repository, Replicate R1, Scenario S1, from the CRA-2004 PABC.
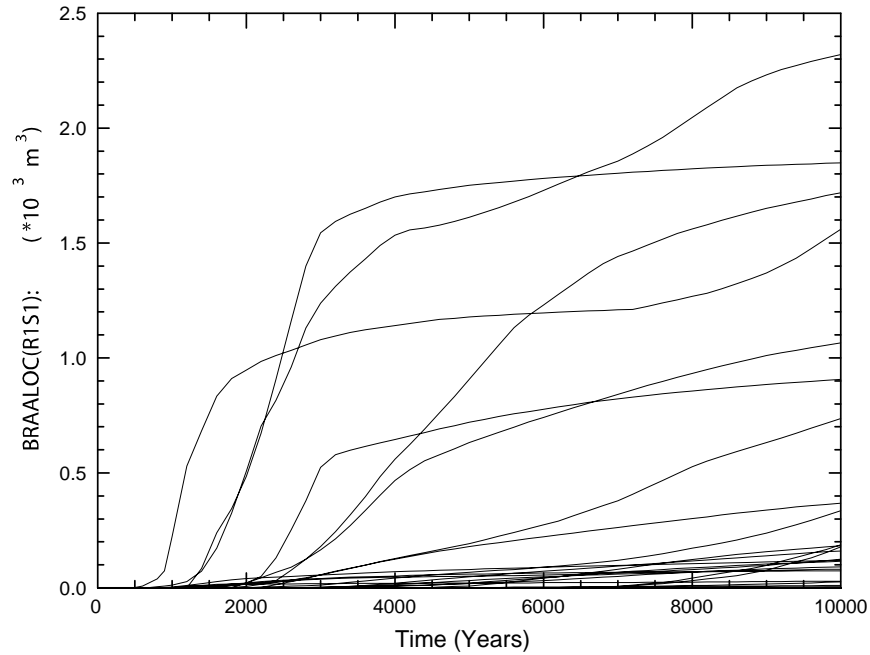
Figure 4-15. Brine Flow Away from the Repository via all MBs, Replicate R1, Scenario S1, from the CRA-2004 PABC.

Information Only
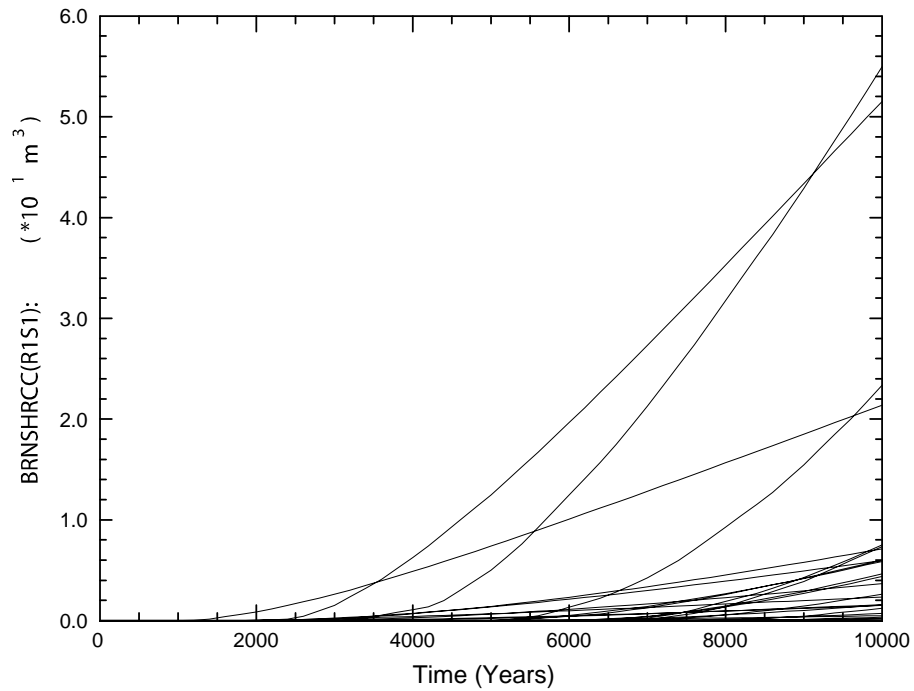
Figure 4-16. Brine Outflow Up the Shaft, Replicate R1, Scenario S1, from the CRA-2004 PABC.
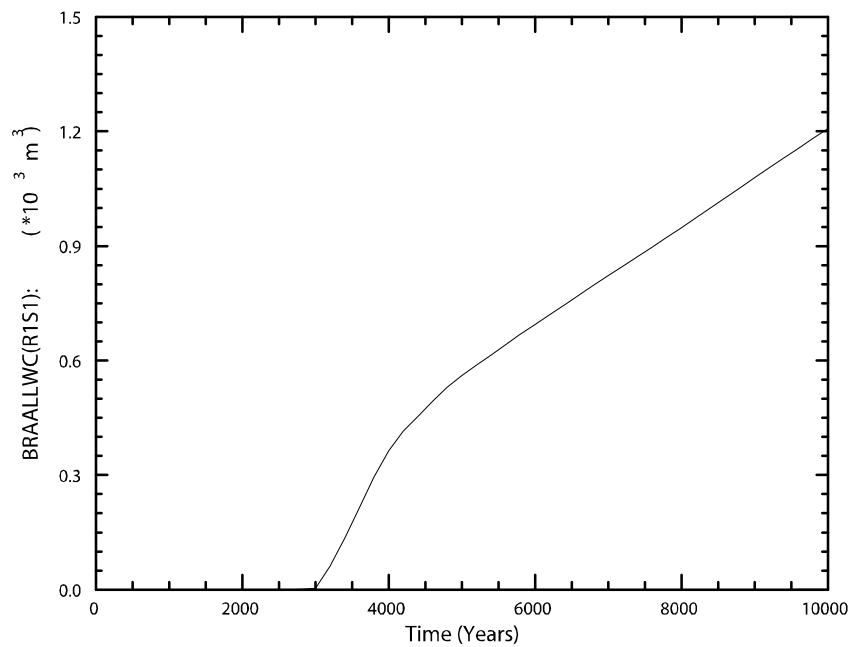
Figure 4-17. Brine Flow via All MBs across the LWB, Replicate R1, Scenario S1, from the CRA-2004 PABC.
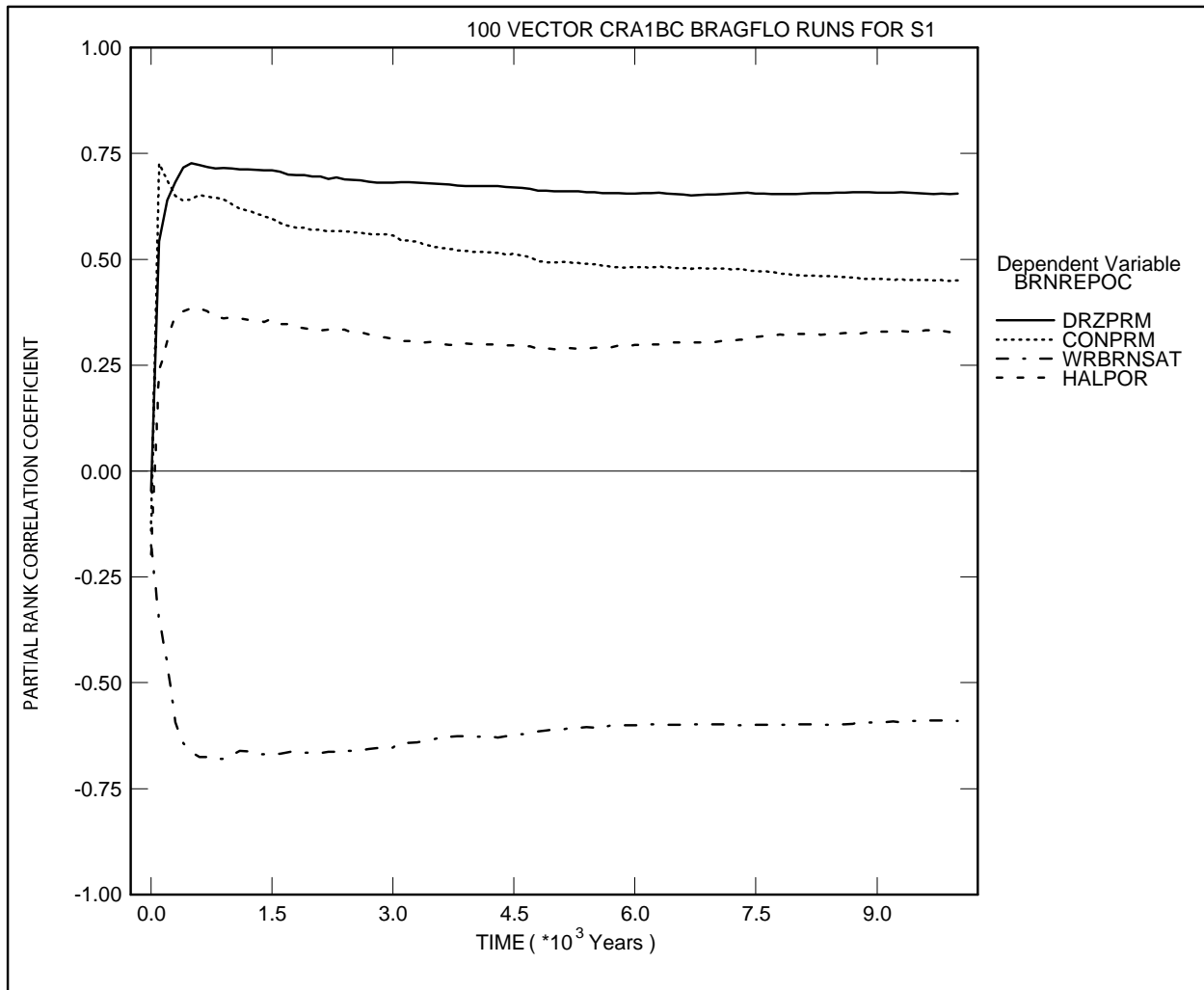
Figure 4-18. Primary Correlations of Total Cumulative Brine Flow Away from the Repository Through All MBs with Uncertain Parameters, Replicate R1, Scenario S1, from the CRA-2004 PABC.
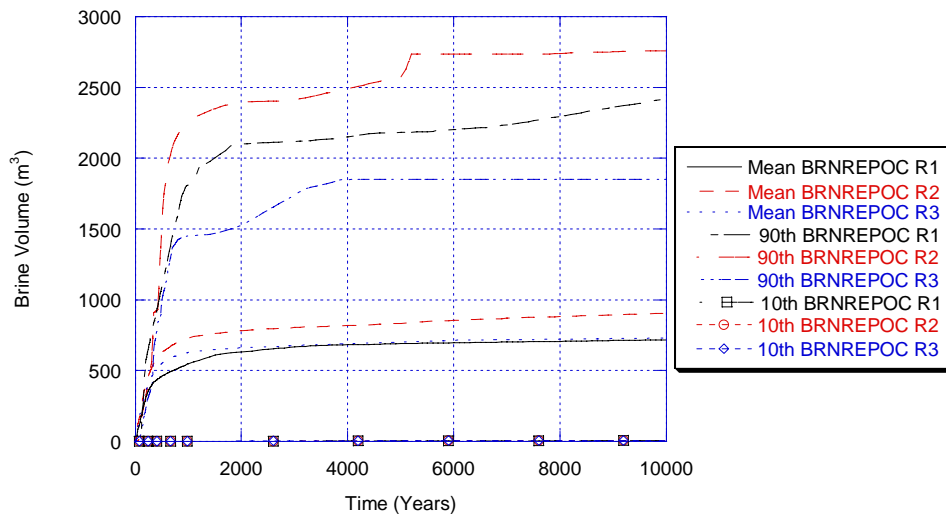
Figure 4-19. Comparison of Brine Flow Away from the Repository between All Replicates, Scenario S1, from the CRA-2004 PABC.
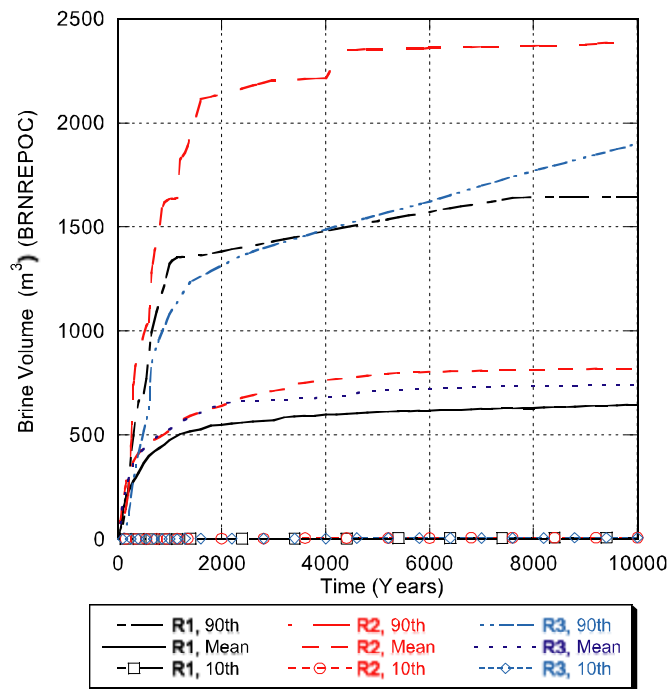
Figure 4-20. Comparison of Brine Flow Away from the Repository between All Replicates, Scenario S1, from the CRA-2004.

4.2   RADIONUCLIDE TRANSPORT (UNDISTURBED CASE)

This section summarizes the radionuclide transport results for the undisturbed repository, both up the shaft to the Culebra, and through the Salado to the LWB. Lowry (2005) presents a detailed analysis of NUTS results for the CRA-2004 PABC.

Radionuclide transport in the undisturbed scenario is calculated by the code NUTS. Screening runs using a conservative tracer are conducted to determine which vectors have the potential to transport radionuclides to the accessible environment. Full transport simulations are then performed for all vectors that are screened in. Based upon results of the screening exercise, full radionuclide transport simulations were performed for only one vector in the undisturbed case, Replicate R1, vector 53.

4.2.1   Radionuclide Transport to the Culebra (undisturbed case)

For the undisturbed repository, no vectors showed radionuclide transport through the shafts to the Culebra. Consequently, no radionuclides could be transported through the Culebra to the accessible environment under undisturbed conditions

4.2.2   Radionuclide Transport to the LWB (undisturbed case)

Radionuclides can potentially also be transported through the Salado marker beds to the LWB. For the undisturbed case, only one vector was screened in. The maximum total integrated activity across the LWB at the Salado marker beds for Replicate R1, vector 53 was 1.3169×10^{-12} EPA units. This is comparable to the CRA-2004 PA results for Replicate R1, Scenario S1, vector 82 (the only screened in vector) which had 2.89×10^{-15} EPA units at the boundary. One should note that this magnitude is smaller than the effective numerical precision of the transport calculations. As explained in Lowry (2005), this value is most likely due to numerical dispersion as a result of the NUTS finite-difference solution method. The magnitude of the non-zero release is indicative of numerical dispersion resulting from the coarse grid spacing between the repository and the LWB, rather than a probable transport of radionuclides.

Regardless of the significance attached to the numerical values reported above, the releases from the undisturbed scenario are insignificant when compared to releases from drilling intrusions (see Sections 5.5 and 6). Consequently, releases in the undisturbed scenario are omitted from the calculation of total releases from the repository.

5.   RESULTS FOR A DISTURBED REPOSITORY

The WIPP repository might be disturbed by exploratory drilling for natural resources during the 10,000-year regulatory period.   Drilling could create additional pathways for radionuclide transport, especially in the Culebra, and could release material directly to the surface.   In addition, mining for potash within the LWB might alter flow in the overlying geologic units and may locally accelerate transport through the Culebra.   The disturbed scenarios used in PA modeling capture the range of possible releases resulting from drilling and mining.

Total releases are computed by the code CCDFGF.   Total releases comprise transport releases and direct releases.   Transport releases generally involve movement of radionuclides up an abandoned borehole into the Culebra, then through the Culebra to the LWB.   Transport of radionuclides to the Culebra is computed using the codes NUTS and PANEL (see Section 3.4 and Section 3.2, respectively) using the brine flows computed by BRAGFLO.   Transport through the Culebra is computed by the code SECOTP2D (see Section 3.8) using flow fields calculated by MODFLOW (see Section 3.8).

Direct releases occur at the time of a drilling intrusion and include releases of solids (cuttings, cavings, and spallings) computed using the code CUTTINGS_S (see Section 3.5 and Section 3.6) and direct releases of brine computed using BRAGFLO (see Section 3.7).   Pressure and brine saturation within the waste are initial conditions to the models for direct releases.   Results from the undisturbed repository (see Section 4) are used as the initial conditions for the first intrusion.   To calculate initial conditions for subsequent intrusions, and to compute the source of radionuclides for transport in the Culebra, a set of drilling scenarios are used to calculate conditions within the repository after an intrusion, using BRAGFLO (Section 3.3).

This section first summarizes the scenarios used to represent drilling intrusions and the resulting repository conditions calculated by BRAGFLO.   Next, transport releases are presented, followed by cuttings and cavings, spallings, and DBRs.   Finally, total releases from the repository are summarized.

5.1   DRILLING SCENARIOS

As shown in Table 5-1, the PA considers two types of drilling intrusions, E1 and E2.   The E1 scenario represents the possibility that a borehole connects the repository with a pressurized brine reservoir located within the underlying Castile formation.   The E2 scenario represents a borehole that does not connect the repository with an underlying brine reservoir.   Repository conditions are calculated for the E1 scenario at 350 and 1,000 years, referred to as the BRAGFLO S2 and S3 scenarios, respectively.   The BRAGFLO Scenarios S4 and S5 represent E2 drilling events that occur at 350 and 1,000 years, respectively.   An additional BRAGFLO scenario, S6, simulates the effects of an E2 intrusion at 1,000 years followed by an E1 intrusion 1,000 years later into the same panel.

Table 5-1. WIPP PA Modeling Scenarios

Scenario	Description
S1	Undisturbed Repository
S2	E1 intrusion at 350 years
S3	E1 intrusion at 1000 years
S4	E2 intrusion at 350 years
S5	E2 intrusion at 1000 years
S6	E2 intrusion at 1000 years; E1 intrusion at 1200 years.

E1: Borehole penetrates through the repository and into a hypothetical pressurized brine reservoir in the Castile Formation.
E2: Borehole penetrates the repository, but does not encounter brine in the Castile. (Nemer and Stein, 2005)

5.2 MINING SCENARIOS

Long-term releases within the Culebra could be influenced by future mining activities that remove all the known potash reserves within the LWB and cause the transmissivity within the overlying Culebra to change. Full mining of known potash reserves within the LWB in the absence of active and passive controls occurs with a probability specified as a Poisson process with a rate of 10^{-4} yr^{-1}. For any particular future, this rate is used to define a time at which full mining has occurred. Flow fields are calculated for the Culebra for two conditions: partial mining, which assumes that all potash as been mined from reserves outside the LWB; and full mining, which assumes all reserves have been mined both inside and outside the LWB. Transport through the Culebra uses the partial mining flow fields prior to the time at which full mining has occurred and the full mining flow fields after that time.

5.3 SALADO FLOW

This section summarizes the results of the Salado flow calculations for the disturbed scenarios. (Nemer and Stein, 2005) provide a detailed presentation on the BRAGFLO model, calculation results, and further sensitivity analyses.

5.3.1 Pressure in the Repository

Figure 5-1 shows pressure in the waste panel (WAS_PRES for area of Waste Panel in Figure 4-1) for the 100 vectors of Replicate R1 for each BRAGFLO scenario. Scenario S1 represents undisturbed repository conditions; before the drilling intrusions at 350 or 1,000 years, repository pressure follows that of the undisturbed scenario. After the intrusion, pressure exhibits patterns that vary depending on the type of intrusion and the timing of that intrusion.

Scenarios S2 and S3 represent E1 intrusions at 350 and 1,000 years, respectively. At the time of the intrusion, brine flow from the Castile brine reservoir leads to an increase in pressure (Figure 5-1b and c). However, pressure drops sharply 200 years after the intrusion when the borehole plugs above the repository are assumed to fail and the permeability of the borehole generally increases. In vectors with low borehole permeability, pressure does not change noticeably as a result of the borehole plug failure. Twelve hundred years after the drilling intrusion, the permeability of the borehole connecting the repository to the Castile is assumed to be reduced by

an order of magnitude because of creep closure. This material change reduces pressure slightly in some vectors, but does not appear to have a significant effect on the pressure in most vectors.

Scenarios S4 and S5 represent E2 intrusions at 350 years and 1,000 years, respectively. The borehole plugs effectively prevent any change in repository pressure from the time of the intrusion until the borehole plugs fail (Figure 5-1d and e). As in the scenarios for E1 intrusions, pressure generally drops sharply when the plugs fail, except for vectors with low borehole permeability after plug failure.

Scenario S6 represents two intrusions into the same panel: an E2 intrusion at 1,000 years followed by an E1 intrusion at 2,000 years. Figure 5-1f shows pressure in the panel for the S6 scenario. The changes in pressure after the first intrusion are nearly identical to that observed in Scenario S5. In most vectors, the pressure decreases so much that there is a sharp increase in pressure at the time of the second intrusion, which connects the waste panel to the Castile brine reservoir. The changes in pressure after the second intrusion are very similar to those predicted after an E1 intrusion.

Information Only
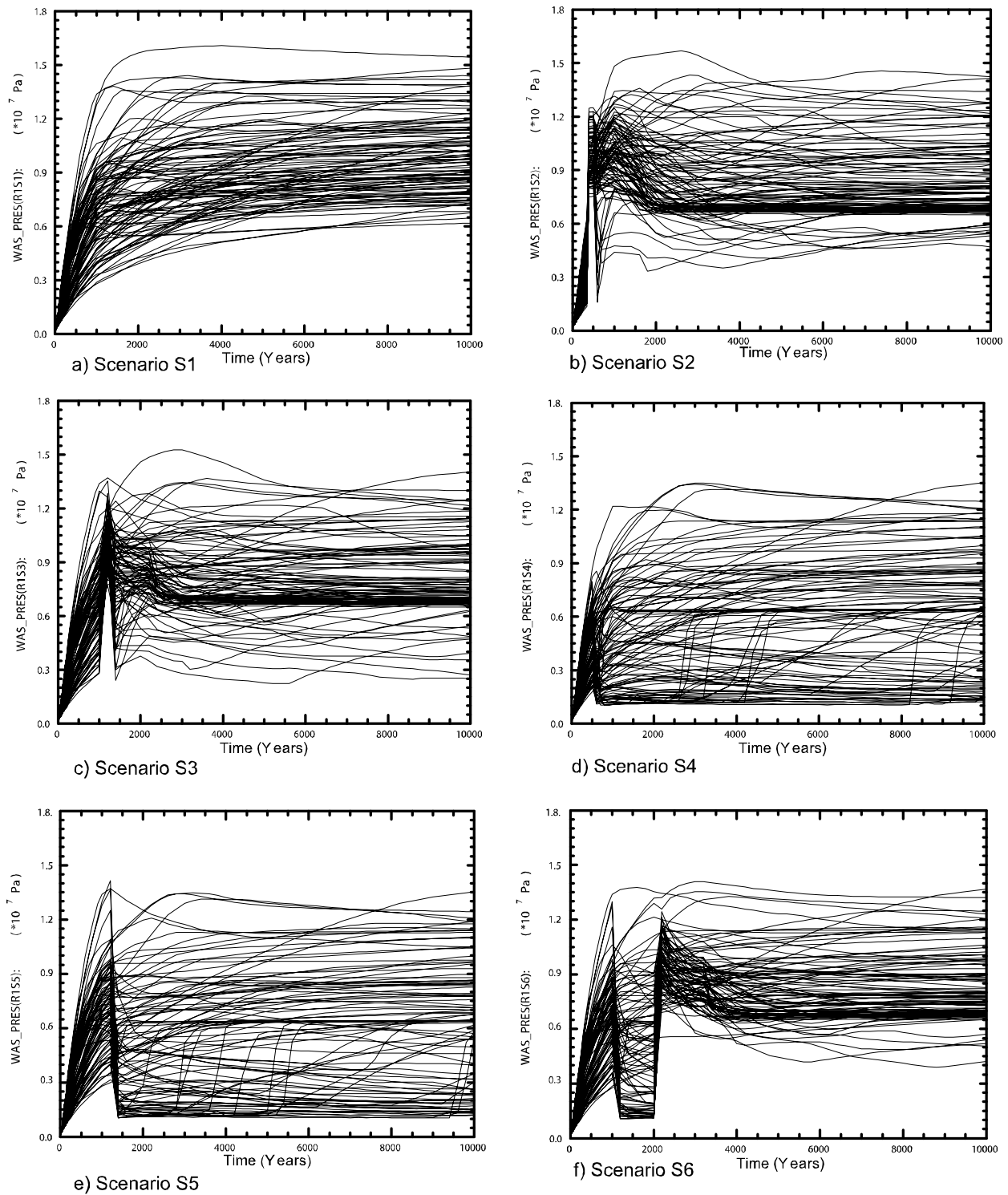
Figure 5-1. Pressure in the Waste Panel for All Scenarios, Replicate R1, from the CRA-2004 PABC.

Figure 5-2 shows pressure in the rest of repository areas (SRR_PRES for area South RoR and NRR_PRES for area North RoR in Figure 4-1) for Scenarios S2 and S5, which represent E1 and E2 drilling intrusions into the waste panel at 350 and 1,000 years, respectively. In general,

pressure in the rest of repository is not immediately affected by the intrusion. The low permiability Option D panel closures inhibit flow of gas and brine between the intruded panel and adjoining areas, moderating the effects of the intrusion.

Figure 5-3 and Figure 5-4 compare mean pressure in the waste panel among the scenarios for the CRA-2004 and the CRA-2004 PABC. Pressure in the disturbed scenarios tends to be lower after the intrusion than pressure in the undisturbed scenario due to the borehole connection to the surface. By 10,000 years, the mean pressure after an E1 intrusion (Scenarios S2, S3, and S6) is about 80 percent of the mean pressure in undisturbed conditions (Scenario S1), and the mean pressure after an E2 intrusion (Scenarios S4 and S5) is 60 percent of the mean pressure in undisturbed conditions.

Figure 5-5 and Figure 5-6 illustrate the differences in pressure among the various waste-filled regions after an E1 intrusion at 350 years (Scenario S2). Following the intrusion, mean pressure in the waste panel (WAS_PRES) is temporarily higher than in the other repository regions. About 1,500 years after the intrusion, mean pressure in the South RoR (SRR_PRES) and North RoR (NRR_PRES) is approximately equal to mean pressure in the waste panel. The delay in pressure equalization between different repository regions is due to the panel closures, which tend to prevent rapid exchange of brine and gas between regions (Hansen et al., 2002) unless pressure exceeds the fracture initiation pressure (approximately 12-14 MPa) after which pressure can rapidly equalize among the regions.

Regression between pressure in the waste panel for an E1 intrusion at 350 years (Scenario S2) and the uncertain parameters in the analysis is shown in Figure 5-7. The initial Castile brine pocket pressure (BPINTPRS) has the largest positive correlation. Borehole permeability has the largest negative correlation with pressure as this is the main flow route in the disturbed scenarios.

a) Scenario S2 - South Rest of Repository

b) Scenario S5 - South Rest of Repository

c) Scenario S2 - North Rest of Repository

d) Scenario S5 - North Rest of Repository
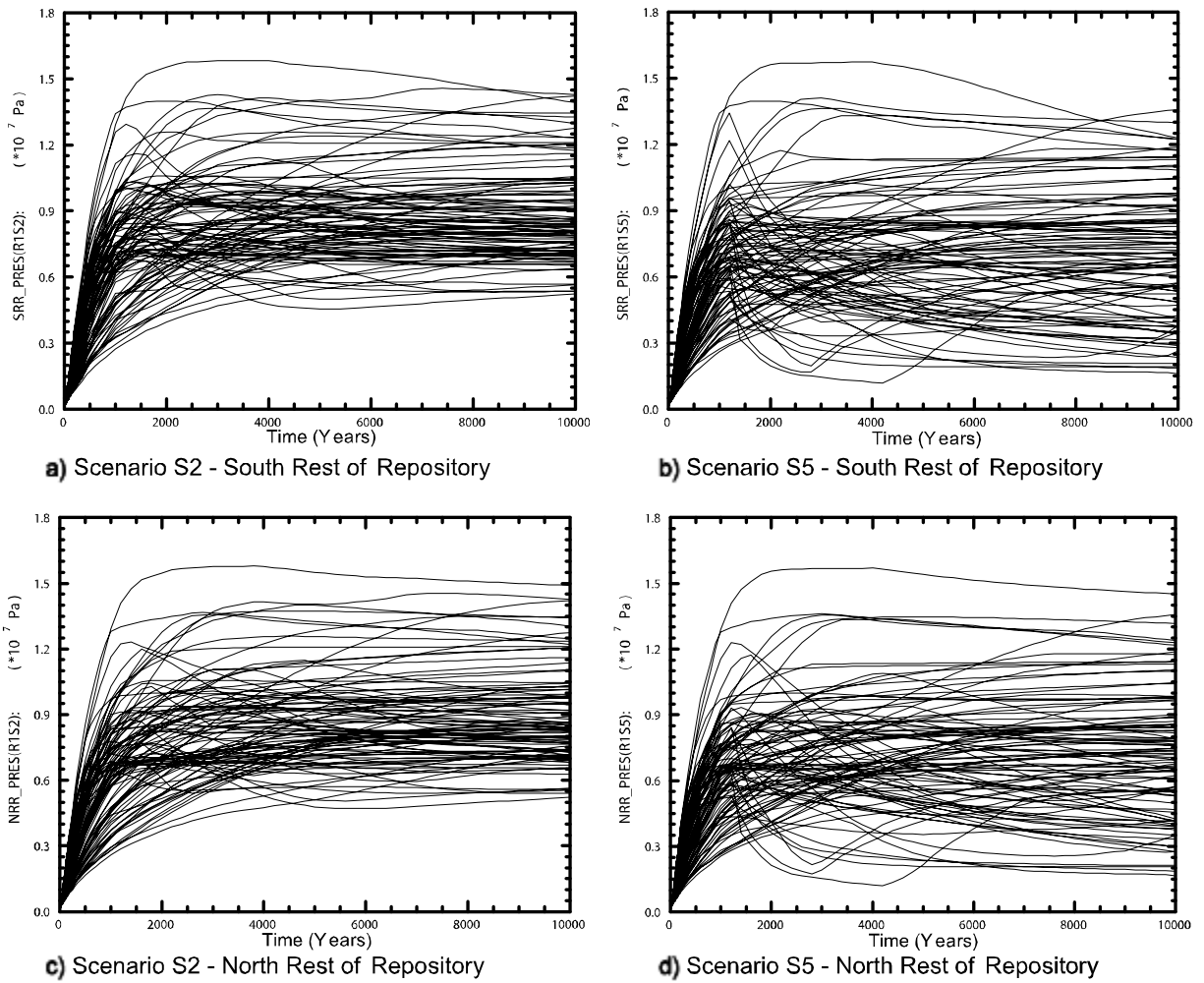
Figure 5-2. Pressure in Various Regions, Replicate R1, Scenarios S2 and S5, from the CRA-2004 PABC.
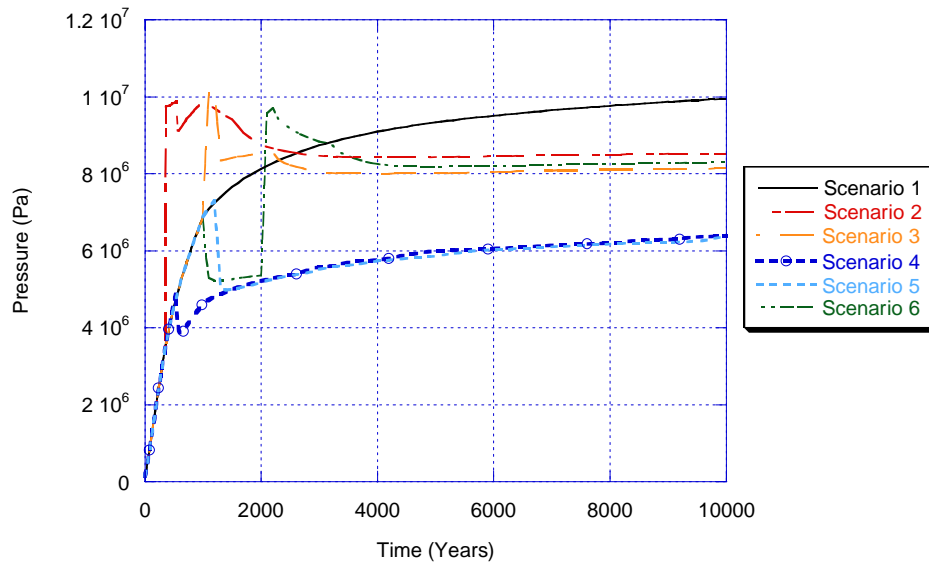
Figure 5-3. Mean Pressure in the Waste Panel for All Scenarios, Replicate R1, from the CRA-2004 PABC.
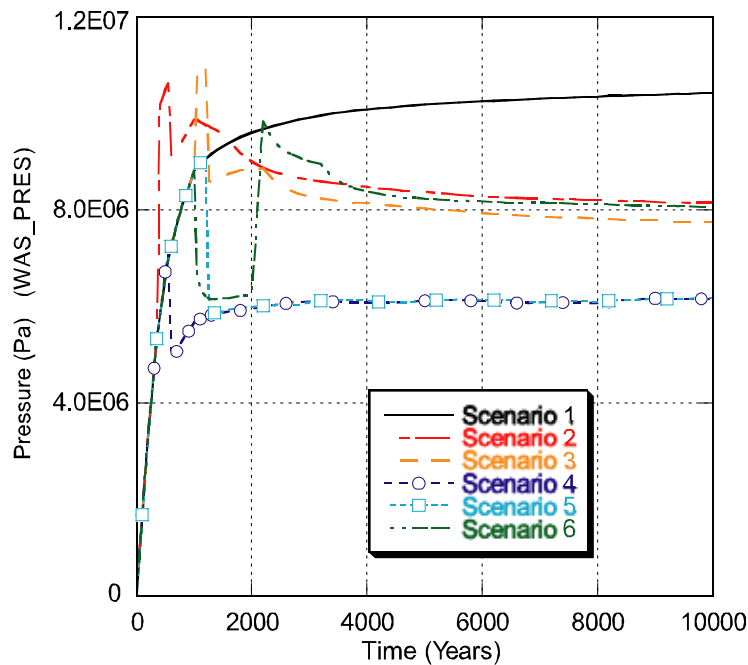
Figure 5-4. Mean Pressure in the Waste Panel for All Scenarios, Replicate R1, from the CRA-2004.
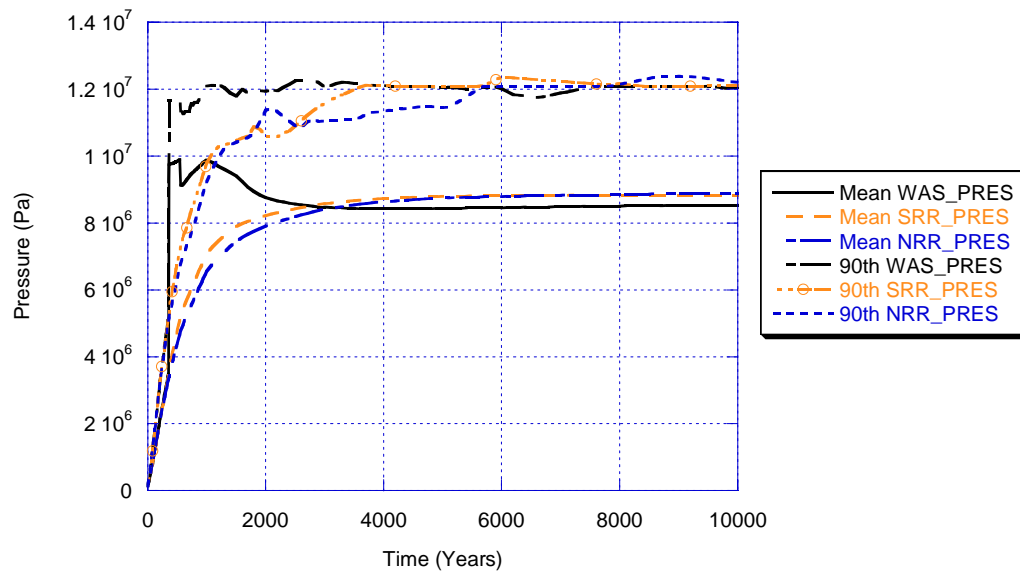
Figure 5-5. Mean And 90th Percentile Values for Pressure in the Waste Areas Regions of the Repository, Replicate R1, Scenario S2, from the CRA-2004 PABC.
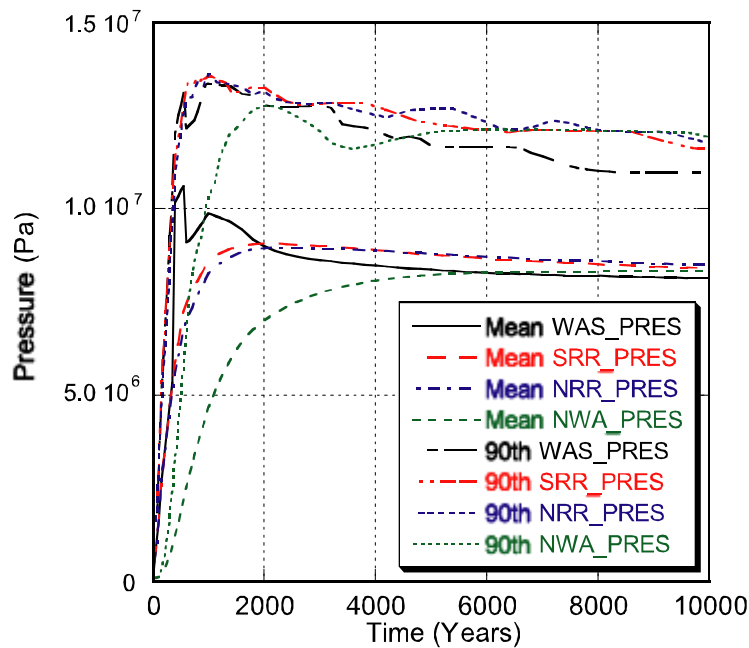
Figure 5-6. Mean and 90th Percentile Values for Pressure in the Excavated Regions of the Repository, Replicate R1, Scenario S2, from the CRA-2004.
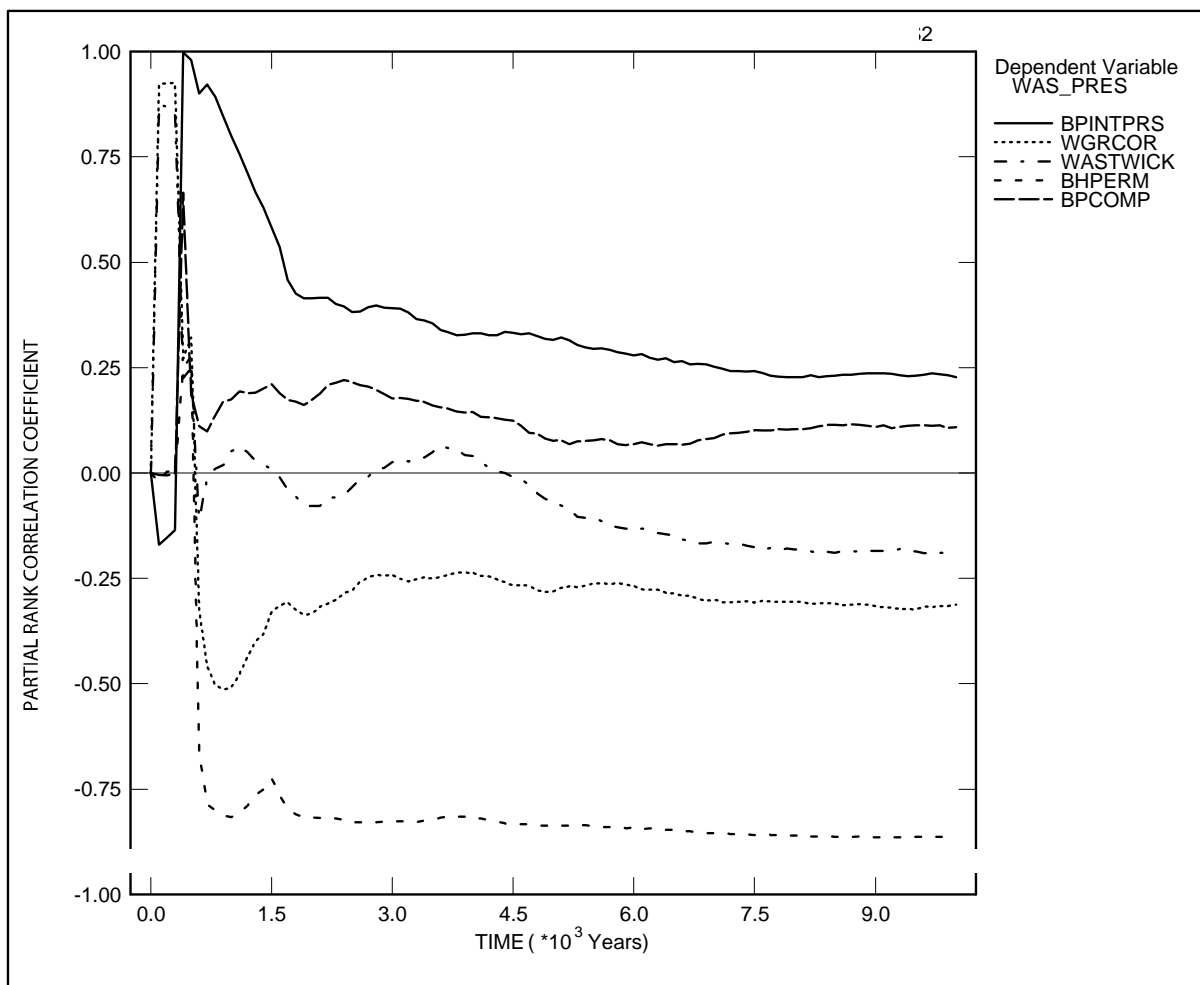
Figure 5-7. Primary Correlations for Pressure in the Waste Panel with Uncertain Parameters, Replicate R1, Scenario S2, from the CRA-2004 PABC.

Figure 5-8 and Figure 5-9 show the regression analysis results for pressure in the Waste Panel with uncertain parameters versus time for Scenario S5, Replicate R1 from the CRA-2004 PABC and the CRA-2004.   Before the intrusion the iron corrosion rate has the largest positive correlation in the CRA-2004 PABC. In the CRA-2004 it was the indicator for microbial gas generation (WMICDFLG). After the intrusion the strongest correlation is with the permeability of the borehole fill (BHPERM) and is negative for both the CRA-2004 PABC and the CRA-2004.

Figure 5-10 and Figure 5-11 compare statistics for pressure in the waste panel for Scenario S2 among the three replicates, for the CRA-2004 and the CRA-2004 PABC. The figures show that the three replicates produced statistically similar results.
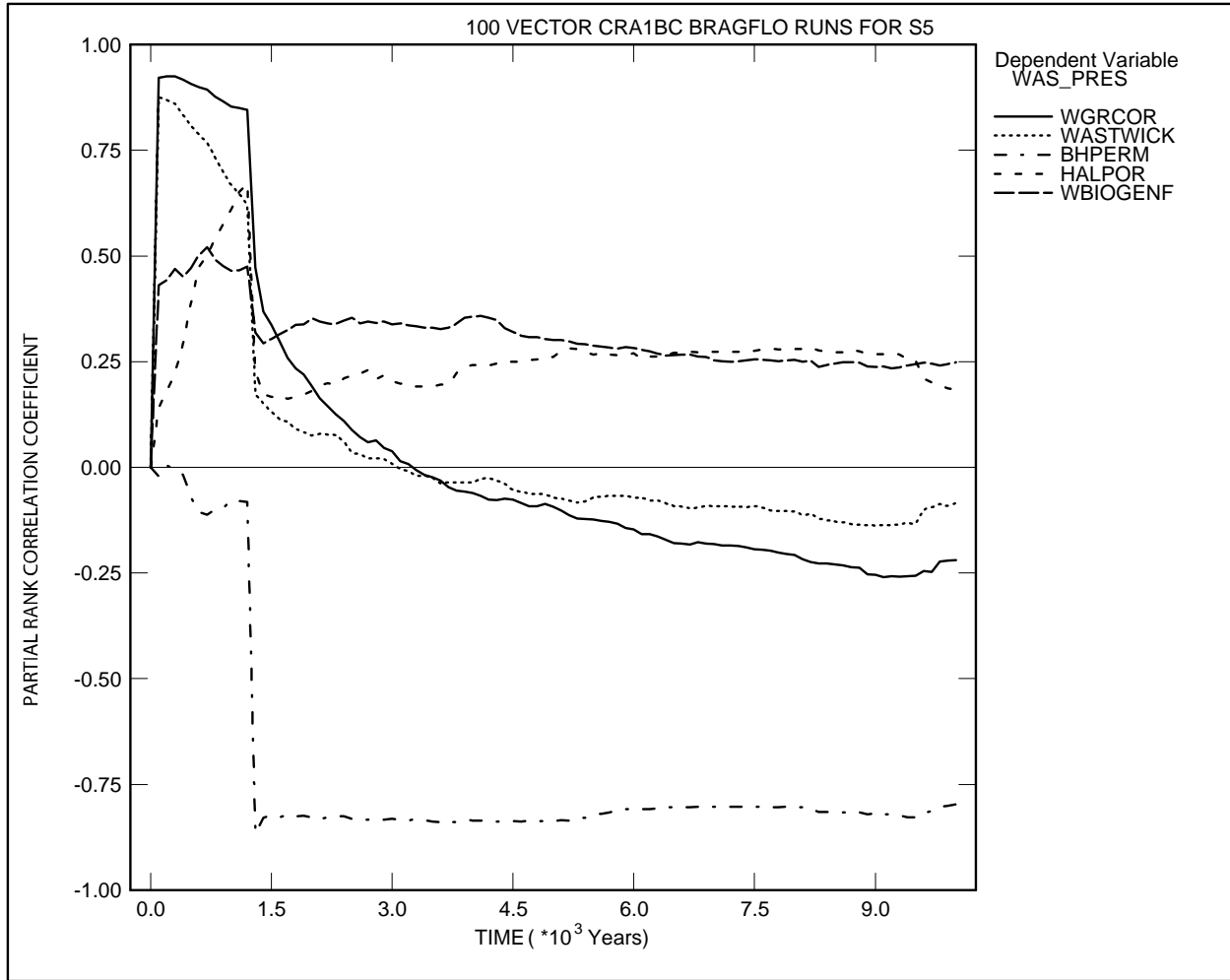
Figure 5-8. Primary Correlations for Pressure in the Waste Panel with Uncertain Parameters, Replicate R1, Scenario S5, from the CRA-2004 PABC.
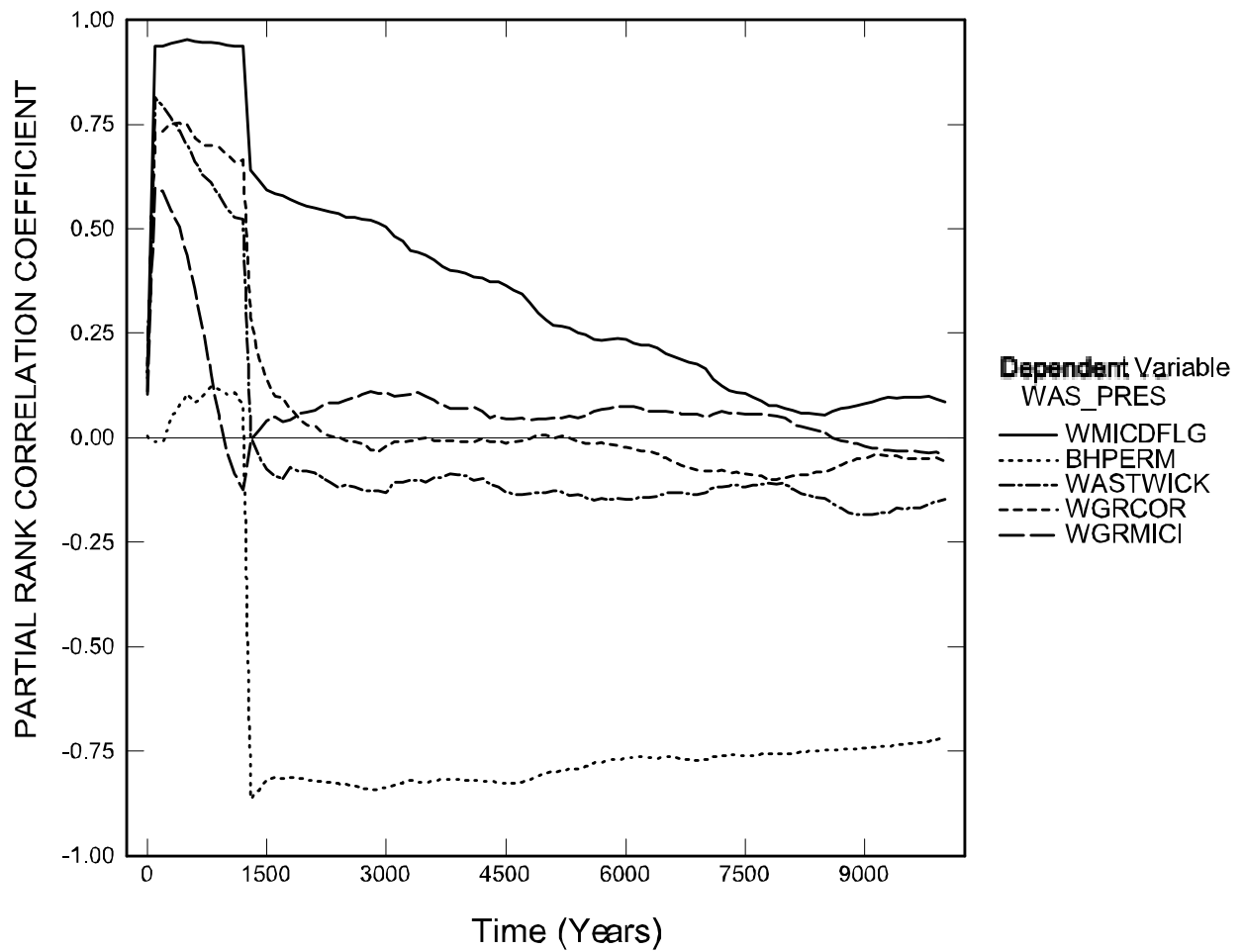
Figure 5-9. Primary Correlations for Pressure in the Waste Panel with Uncertain Parameters, Replicate R1, Scenario S5, from the CRA-2004.
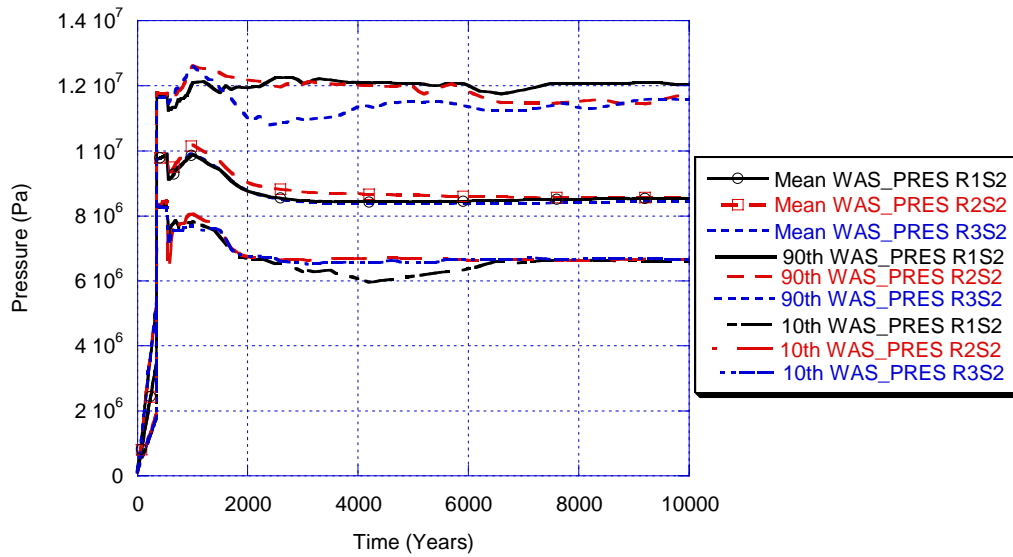
Figure 5-10. Mean and 90th Percentile for Pressure in the Waste Panel for All Replicates, Scenario S2, from the CRA-2004 PABC.

Figure 5-11. Mean and 90th Percentile for Pressure in the Waste Panel for All Replicates, Scenario S2, from the CRA-2004.

5.3.2 Brine Saturation

Brine saturation tends to increase after a drilling intrusion. Figure 5-12 shows brine saturation in the waste panel (WAS_SATB for area Waste Panel in Figure 4-1) for Replicate R1 of each BRAGFLO scenario. Saturation typically increases after an intrusion.

Figure 5-13 and Figure 5-14 compare the mean values for brine saturation in the waste panel (WAS_SATB) for each scenario from the CRA-2004 PABC and the CRA-2004. Brine saturation is highest after E1 intrusions (Scenarios S2, S3 and S6) but also increases somewhat after an E2 intrusion (Scenarios S4 and S5).

Figure 5-15 shows brine saturation in the rest of repository (SRR_SATB for area South RoR and NRR_SATB for area North RoR, as shown in Figure 4-1) for the Scenarios S2 and S5. Comparison of Figure 5-12 with Figure 5-15 shows that brine saturation in un-intruded regions is generally unaffected by the intrusion. The lack of intrusion of brine into the rest of the repository is due to the low permeability of the panel closures. The panel closures separating the intruded panel from these regions effectively prevent brine flow between excavated areas.

Information Only
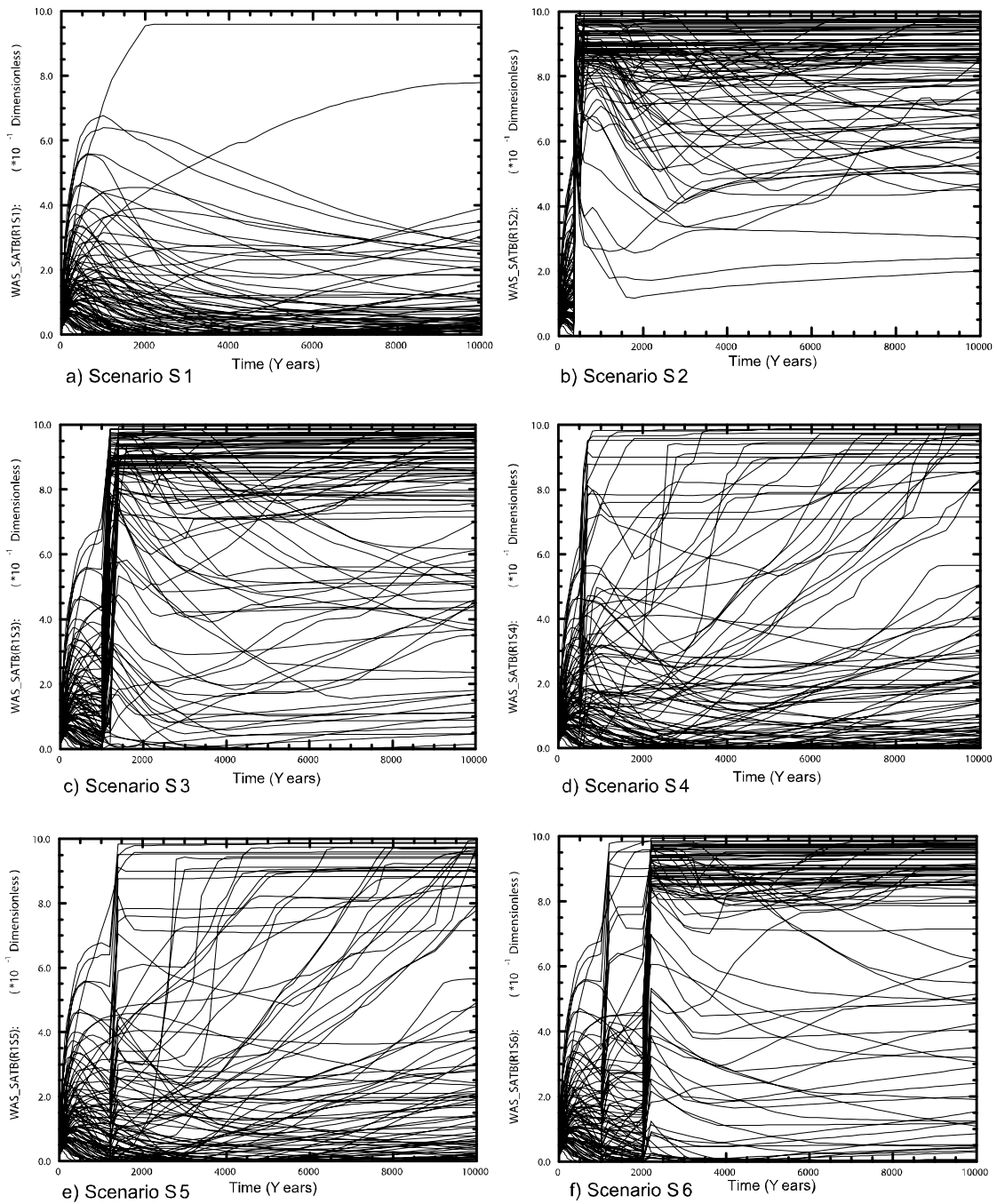
Figure 5-12. Brine Saturation in the Waste Panel for All Scenarios, Replicate R1 from the CRA-2004 PABC.
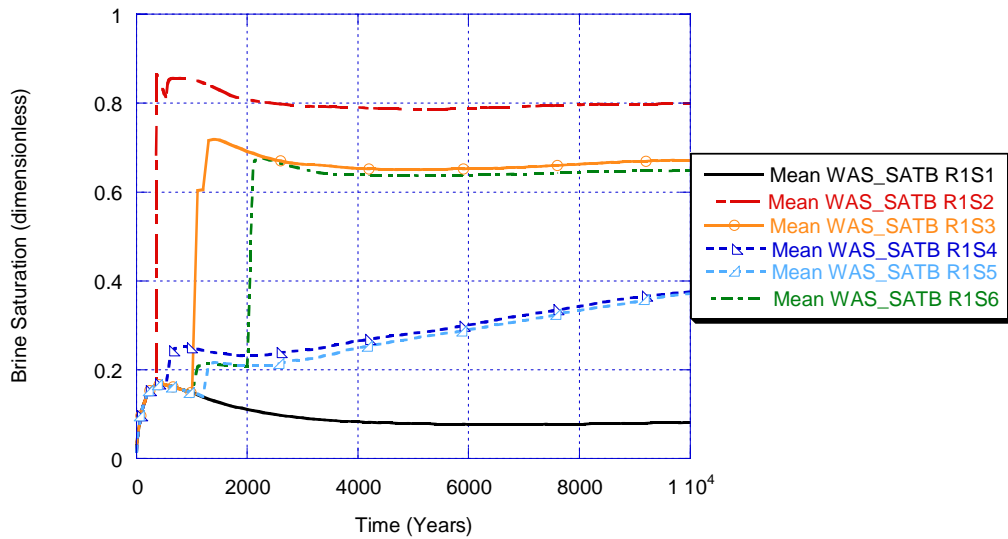
Figure 5-13. Mean Values for Brine Saturation in the Waste Panel for All Scenarios, Replicate R1, from the CRA-2004 PABC.
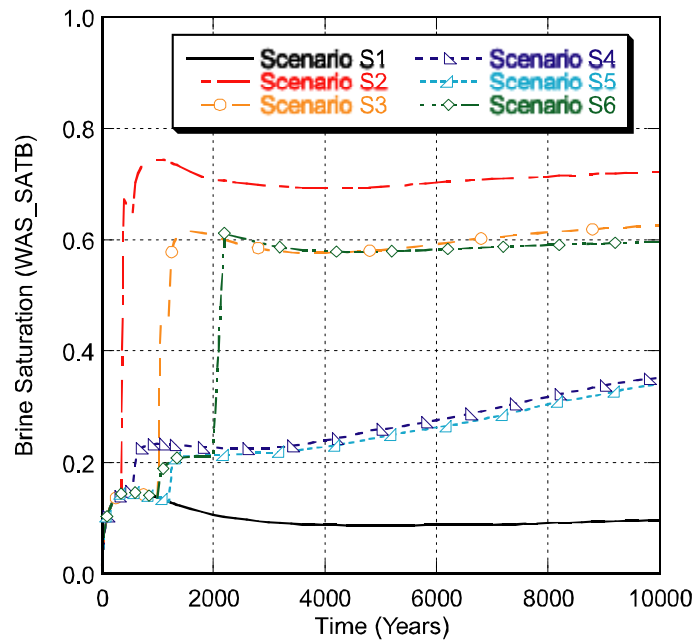
Figure 5-14. Mean Values for Brine Saturation in the Waste Panel for All Scenarios, Replicate R1, from the CRA-2004.

70 of 153

a) Scenario S2 - South Rest of Repository

b) Scenario S5 - South Rest of Repository

c) Scenario S2 - North Rest of Repository

d) Scenario S5 - North Rest of Repository
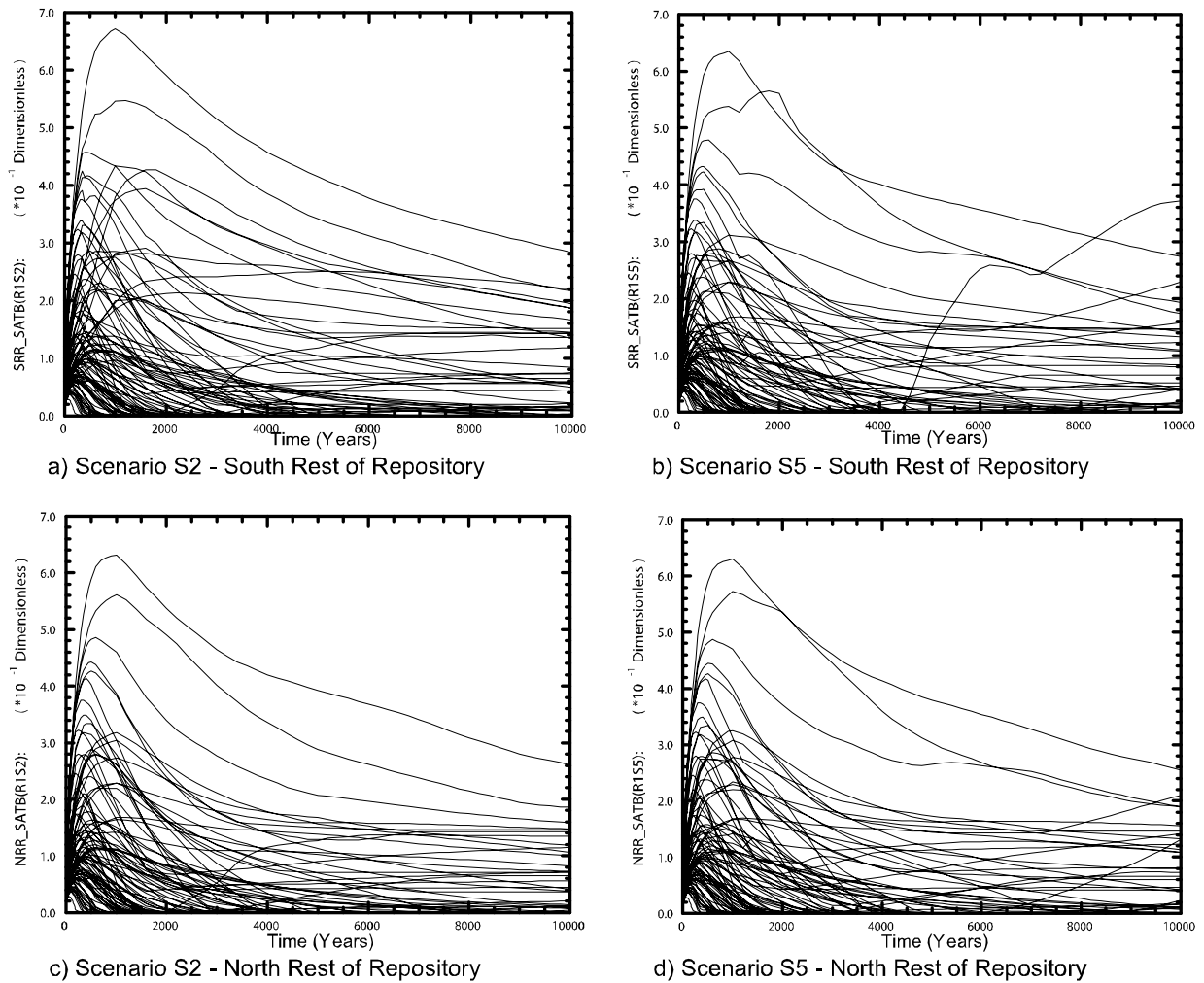
Figure 5-15. Brine Saturation in Excavated Areas, Replicate R1, Scenarios S2 and S5 from CRA-2004 PABC.

Figure 5-16 and Figure 5-17 compare mean and 90th percentile brine saturations among the excavated areas for an E1 intrusion at 350 years (Scenario S2), from the CRA-2004 and the CRA-2004 PABC. Brine saturations in the waste panel (WAS_SATB) are the highest among the repository regions due to the connection with the brine reservoir. Comparison of Figure 5-17 and Figure 5-16 to Figure 4-9 and Figure 4-10 shows that brine saturation outside of the waste panel is very similar to the undisturbed Scenario S1.
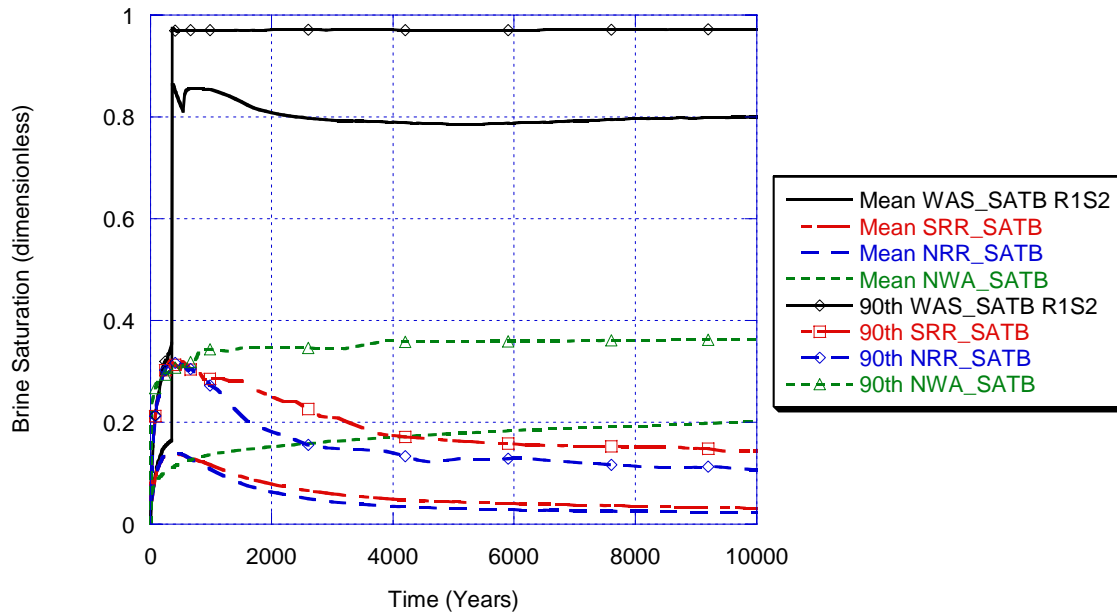
Figure 5-16. Mean and 90th Percentile for Brine Saturation in Excavated Areas, Replicate R1, Scenario S2, from the CRA-2004 PABC.
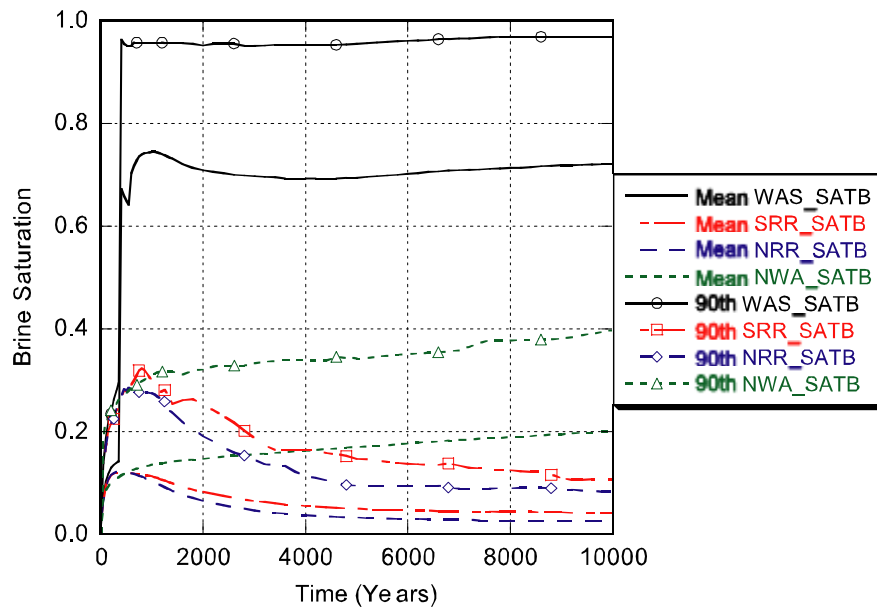
Figure 5-17. Mean and 90th Percentile for Brine Saturation in Excavated Areas, Replicate R1, Scenario S2, from the CRA-2004.

Information Only

Figure 5-18 shows the results of the regression analysis between brine saturation in the waste panel (WAS_SATB) for the S2 scenario and the uncertain parameters in the analysis. The permeability of the DRZ (DRZPRM) and borehole permeability (BHPERM) have the largest positive correlations, as these are means by which brine can enter the repository. The wicking factor (WASTWICK) and the iron corrosion rate (WGRCOR) have a strong negative correlation around the time of the intrusion, owing to the iron corrosion consumption of brine.

Figure 5-19 and Figure 5-20 show the results of the regression analysis between brine saturation in the waste panel (WAS_SATB) for the S5 scenario and the uncertain parameters in the analysis, for the CRA-2004 PABC and the CRA-2004. As with the S2 scenario, borehole permeability (BHPERM) and DRZ permeability (DRZPRM) have strong positive correlations, while the wicking factor (WASTWICK) and the iron corrosion rate (WGRCOR) have negative correlations.
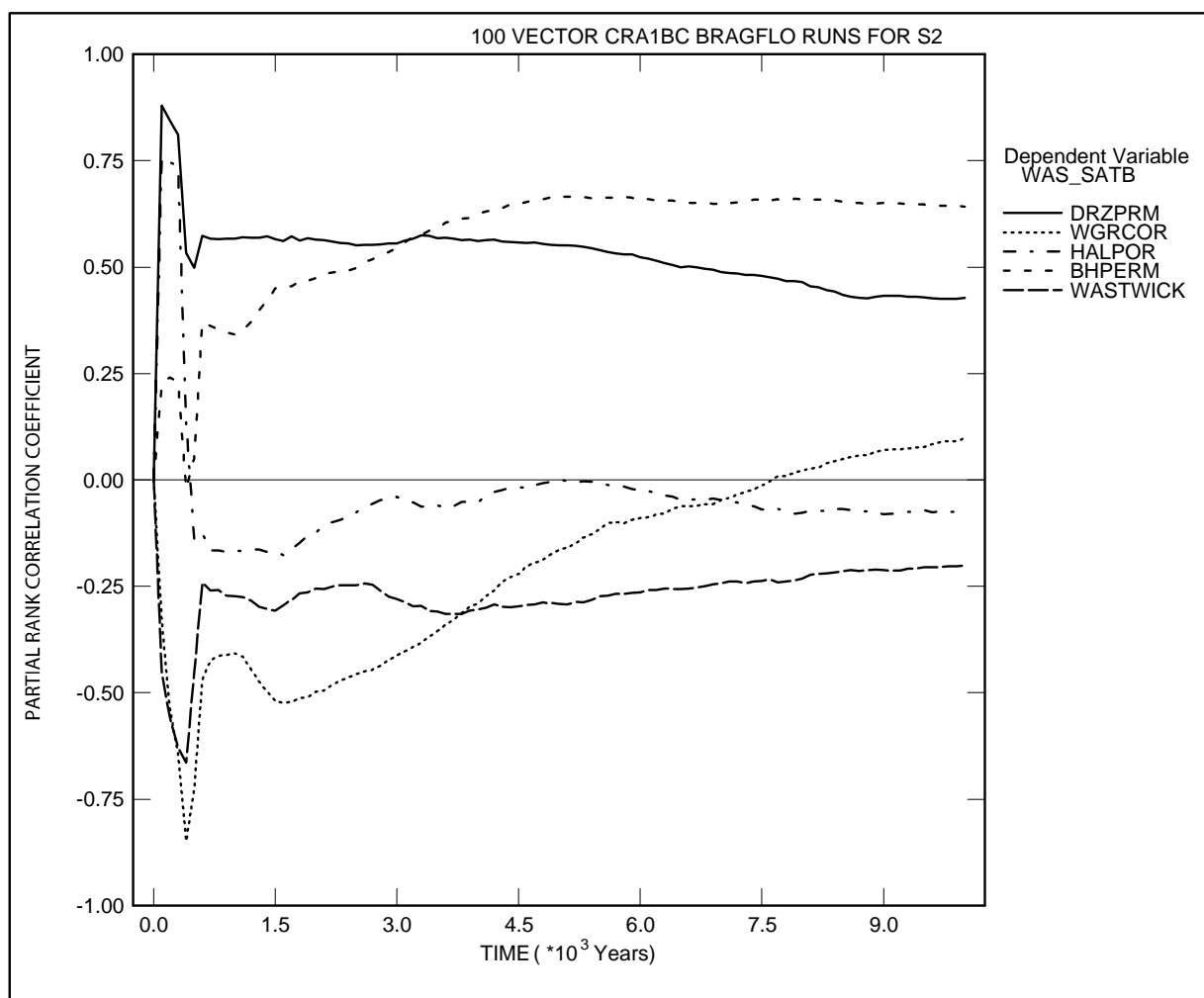
Figure 5-18. Primary Correlations for Brine Saturation in the Waste Panel with Uncertain Parameters, Replicate R1, Scenario S2, from the CRA-2004 PABC.
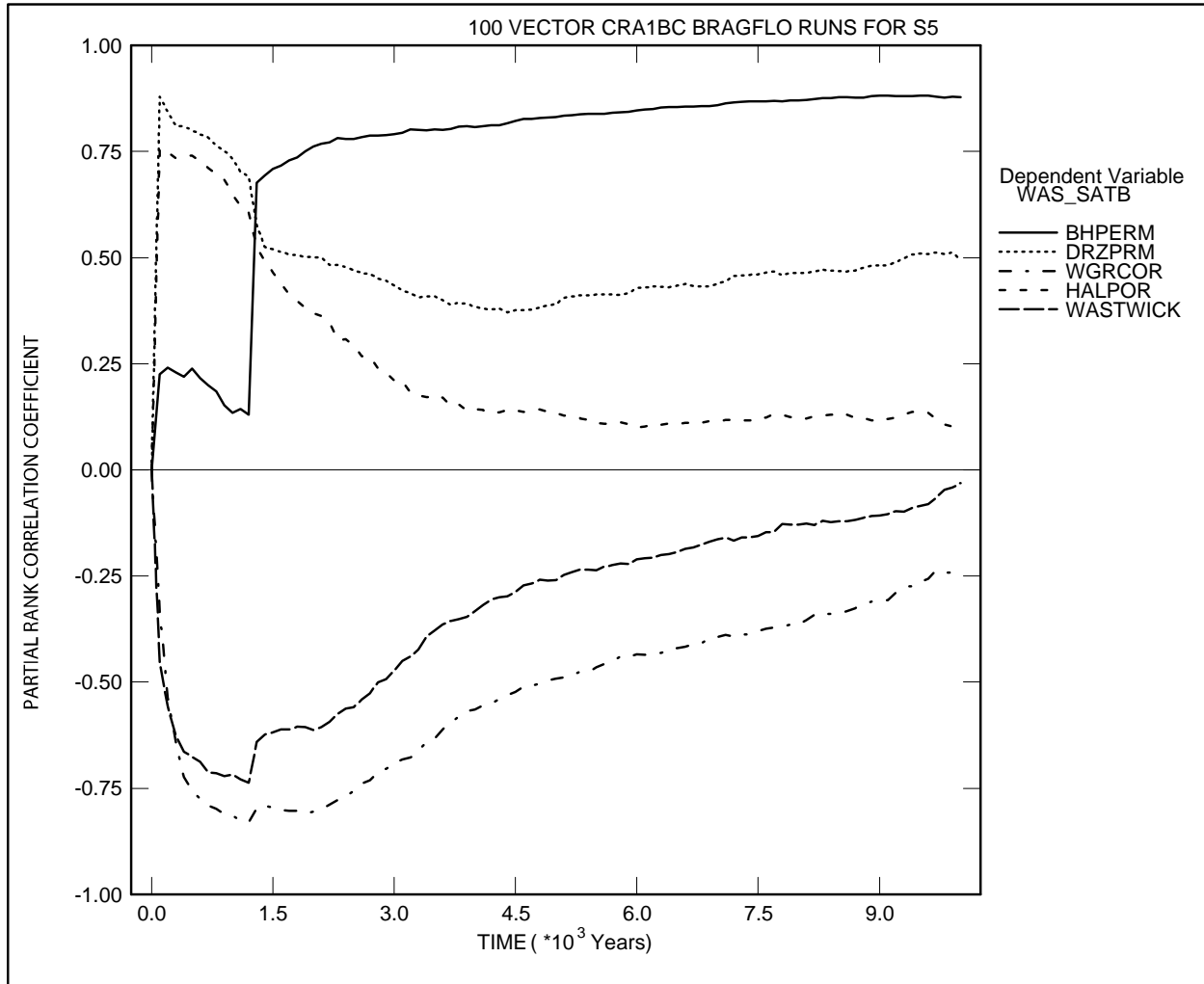
Figure 5-19. Primary Correlations of Brine Saturation in the Waste Panel with Uncertain Parameters, Replicate R1, Scenario S5, from the CRA-2004 PABC.

Information Only
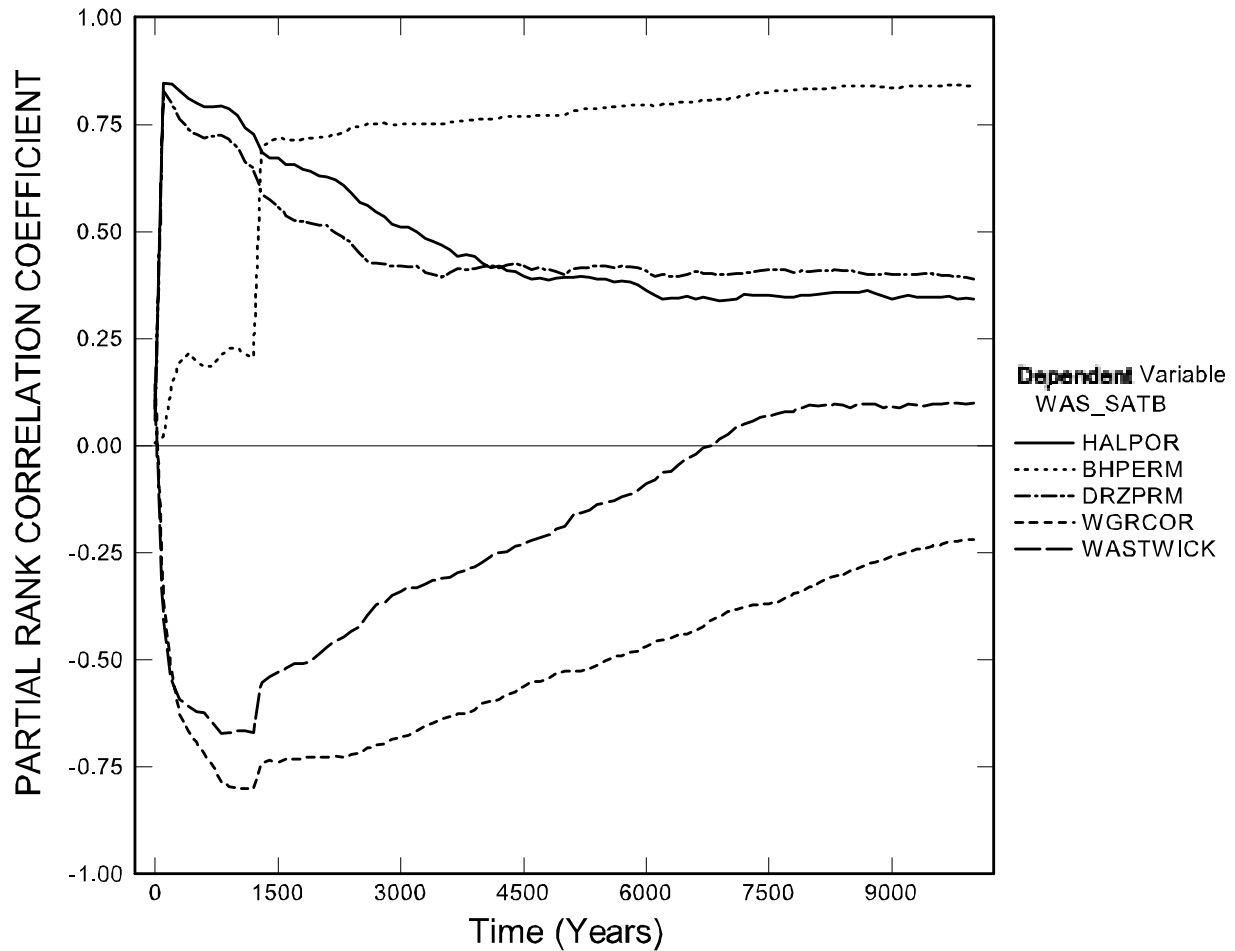
Figure 5-20. Primary Correlations of Brine Saturation in the Waste Panel with Uncertain Parameters, Replicate R1, Scenario S5, from the CRA-2004.

Figure 5-21 and Figure 5-22 compare statistics for brine saturation for the three replicates of the S2 scenario, for the CRA-2004 PABC and the CRA-2004. The plots show that the three replicates produced similar results.

Information Only
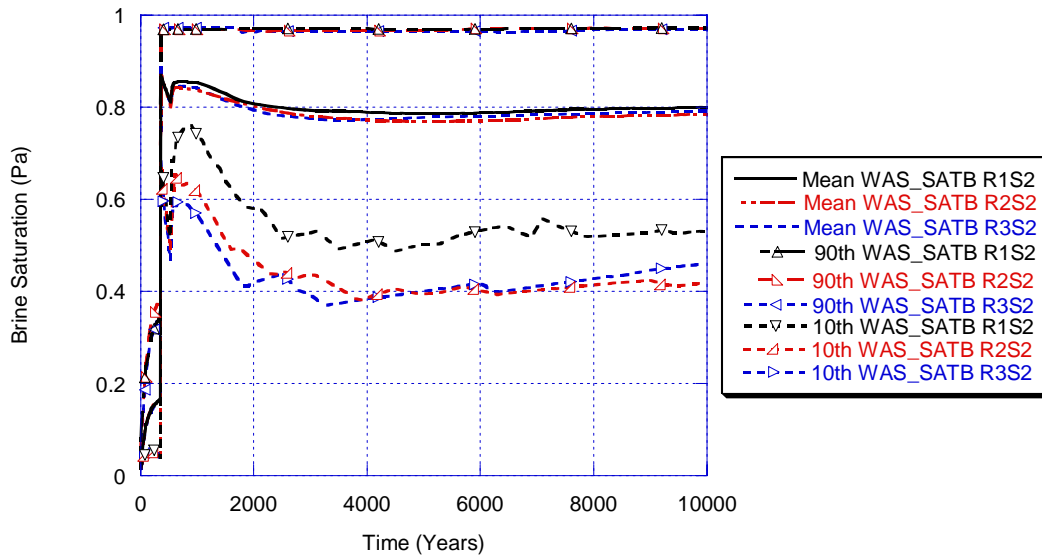
Figure 5-21. Mean and 90th Percentile for Brine Saturation in the Waste Panel for All Replicates, Scenario S2, from the CRA-2004 PABC.
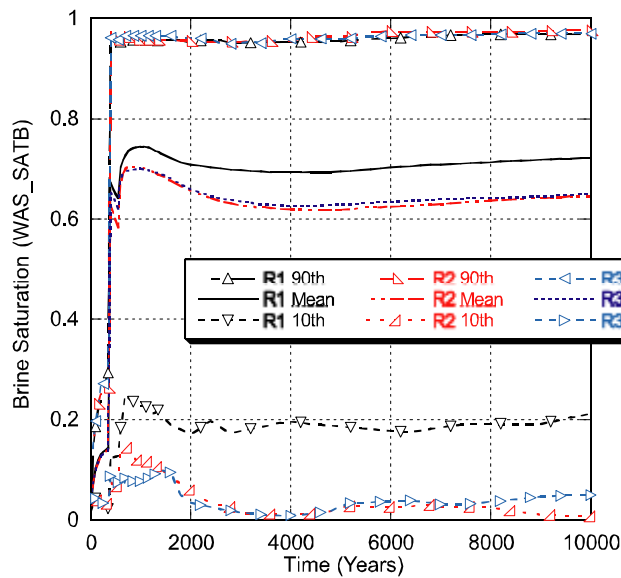
Figure 5-22. Mean and 90th Percentile for Brine Saturation in the Waste Panel for All Replicates, Scenario S2, from the CRA-2004.

5.3.3   Brine Flow Out of the Repository

This section describes the flow of brine up a borehole to the Culebra. Brine flow to the Culebra is important in calculating long-term releases to the Culebra. Direct brine flow up the borehole to the surface at the time of drilling is modeled separately in the DBR calculations, presented in Section 5.5.3.

Figure 5-23 shows cumulative brine flow out of the repository (BRNREPOC) and brine flow up a borehole to the Culebra (BRNBHRCC) for the five BRAGFLO scenarios that model drilling intrusions. The largest volumes of brine flow from the repository after E1 intrusions (Scenarios S2, S3 and S6) are consistent with the higher brine saturation in the intruded panel (Figure 5-23b, Figure 5-23d, and Figure 5-23j, respectively). For Scenarios S2, S3 and S6, 200 years after an E1 intrusion, the borehole plugs fail allowing flow to the Culebra. The similarity between the plots of BRNREPOC and BRNBHRCC in Figure 5-23 (for Scenarios S2, S3 and S6) indicates that after the borehole plugs fail, most of the brine leaving the repository flows up the borehole to the Culebra. At 1,200 years after an E1 intrusion, the permeability of the borehole between the repository and the Castile is reduced by an order of magnitude because of creep closure, reducing brine flow into the repository and causing a corresponding decrease in brine out of the repository.
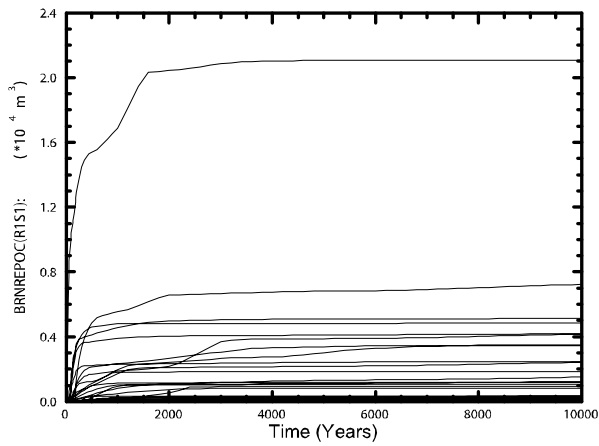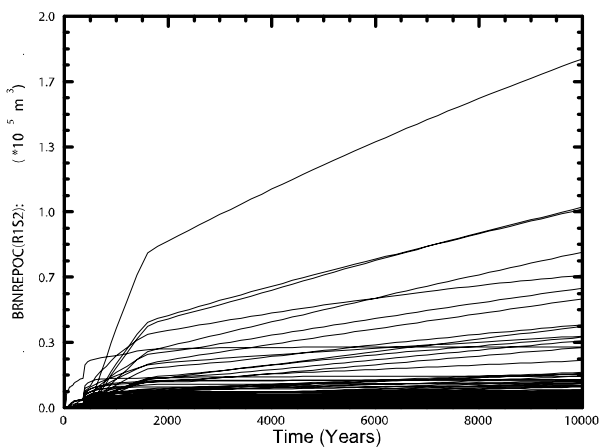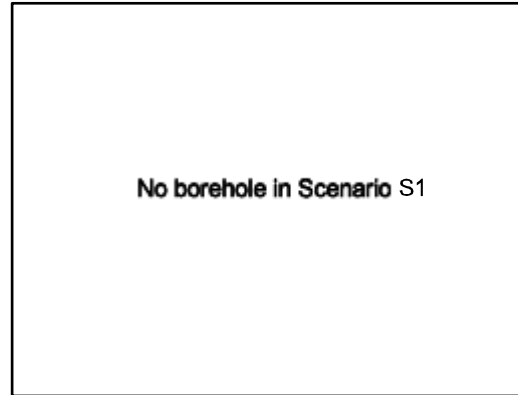
Information Only
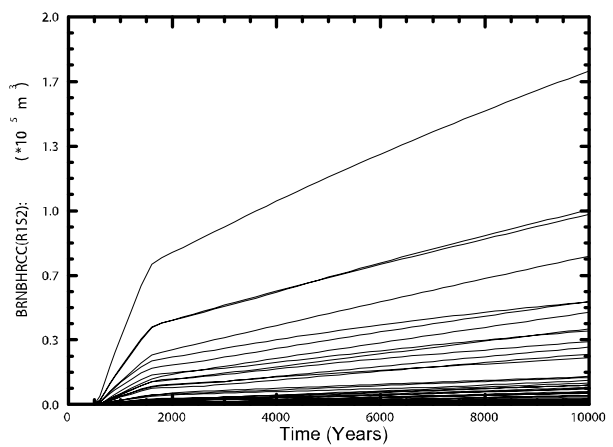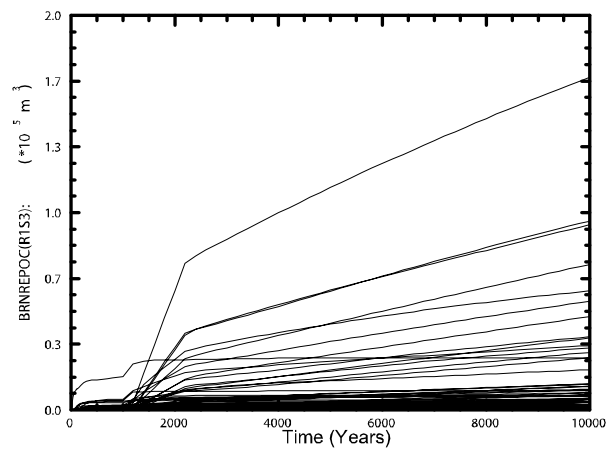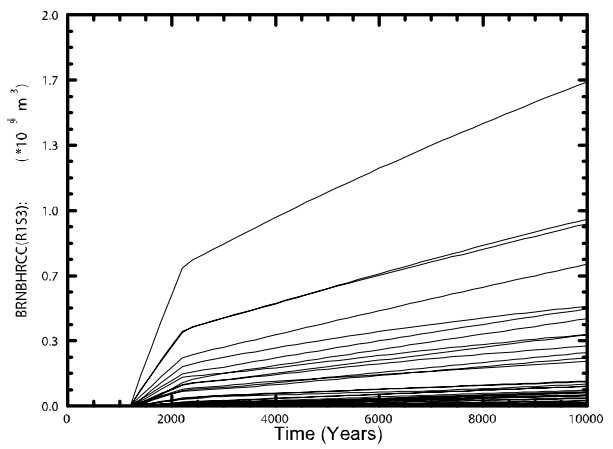
Figure 5-23. Total Cumulative Brine Outflow and Brine Flow Up the Borehole in All Scenarios, Replicate R1, CRA-2004 PABC.
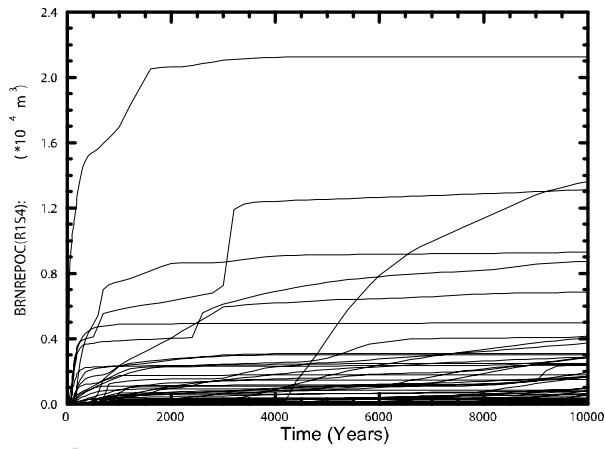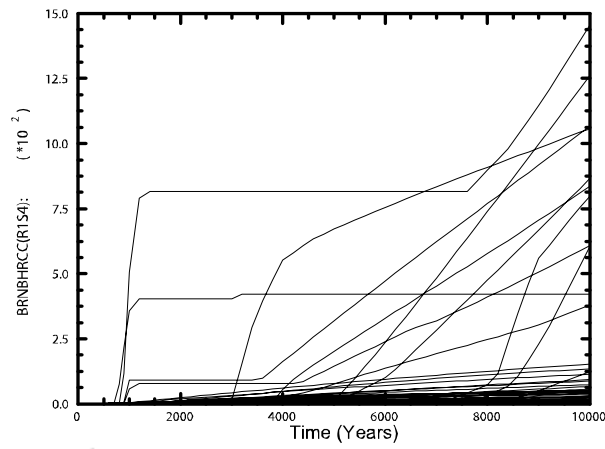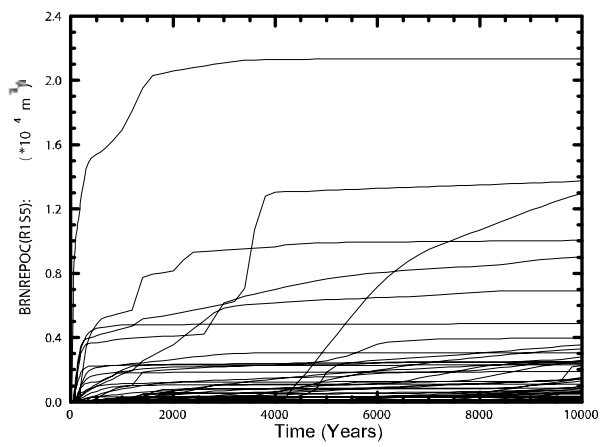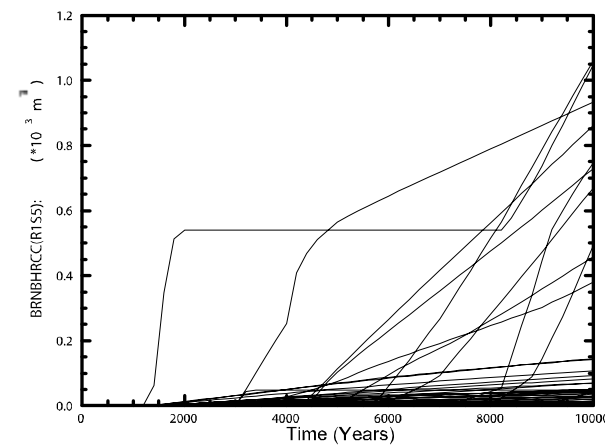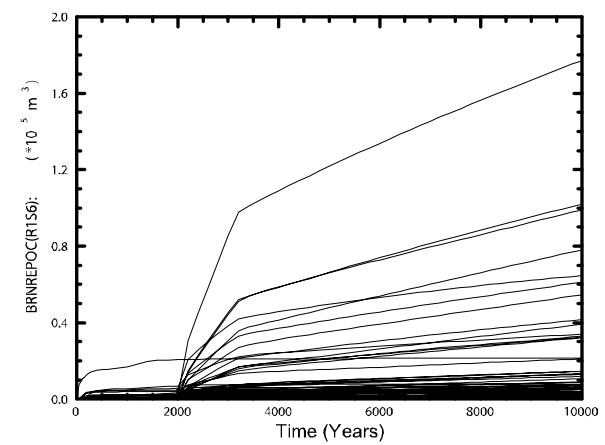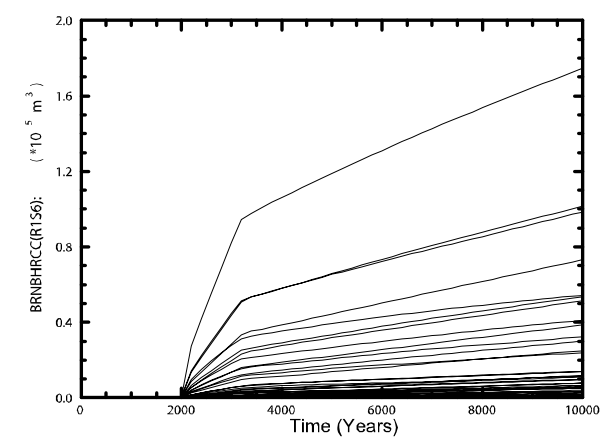
Figure 5-23 (cont). Total Cumulative Brine Outflow and Brine Flow Up the Borehole in All Scenarios, Replicate R1, CRA-2004 PABC.

Information Only

Figure 5-24 and Figure 5-25 show the results of regression analysis between the brine flow up the borehole to the Culebra (BRNBHRCC) and the uncertain parameters in the analysis, for the CRA-2004 and the CRA-2004 PABC. Before the intrusion, non-zero values of BRNBHRCC result from numerical dispersion in the calculation; these values do not exceed 10^{-18} m^3 and thus the correlation to uncertainty in shaft permeability (SHUPRM) is not meaningful. Immediately after the intrusion, uncertainty in the permeability of the un-degraded borehole plugs (PLGPRM) contributes most of the uncertainty in brine flow volumes. After the borehole plugs degrade (200 years after the intrusion), uncertainty in the permeability of the borehole (BHPERM) almost exclusively determines the uncertainty in brine volumes reaching the Culebra.

Figure 5-26 and Figure 5-27 compare statistics for brine flow out of the repository for the three replicates of Scenario S2. The figure shows that brine flow results are very similar among replicates.
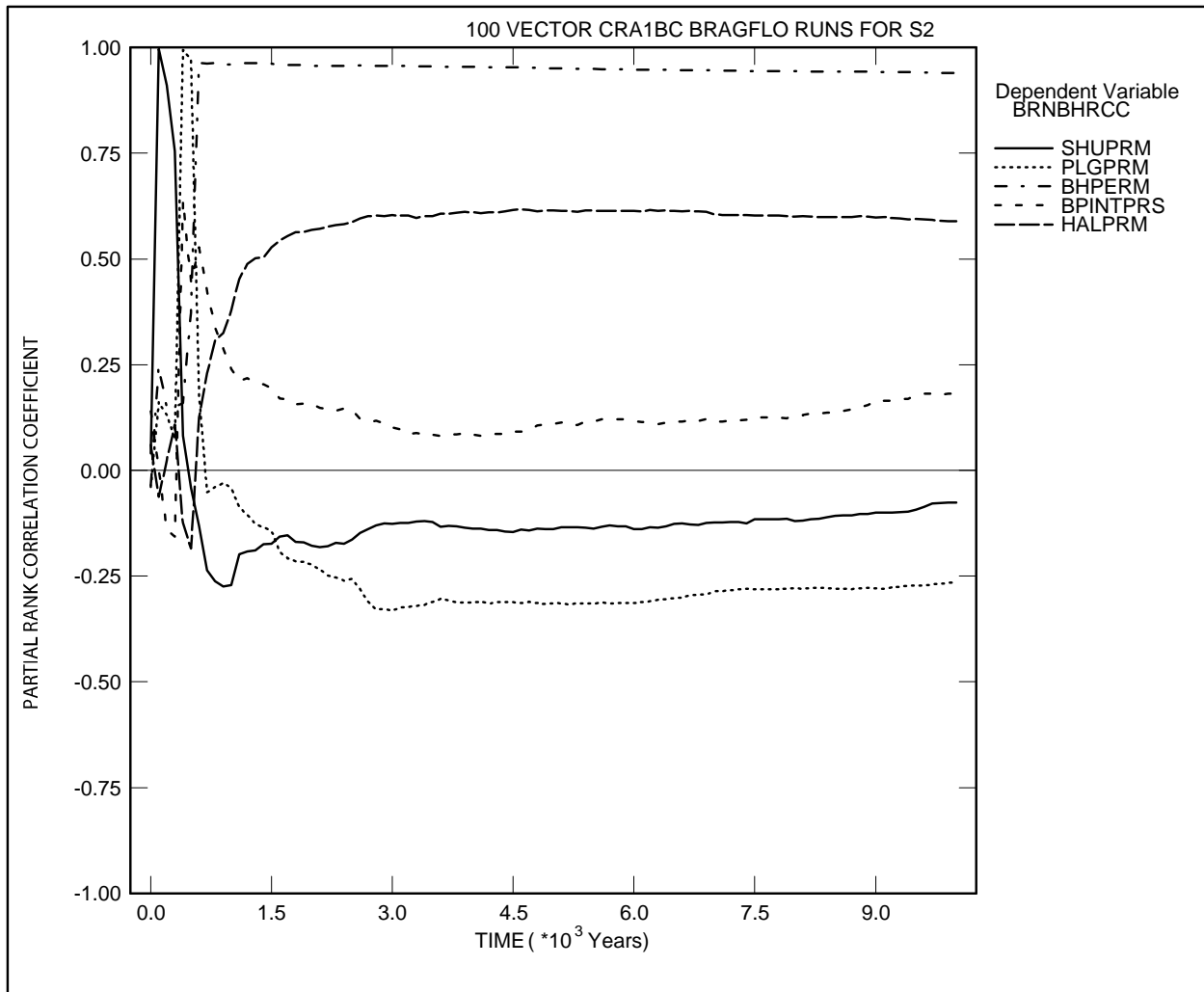
Figure 5-24. Primary Correlations for Cumulative Brine Flow Up the Borehole with Uncertain Parameters, Replicate R1, Scenario S2, from the CRA-2004 PABC.

Information Only
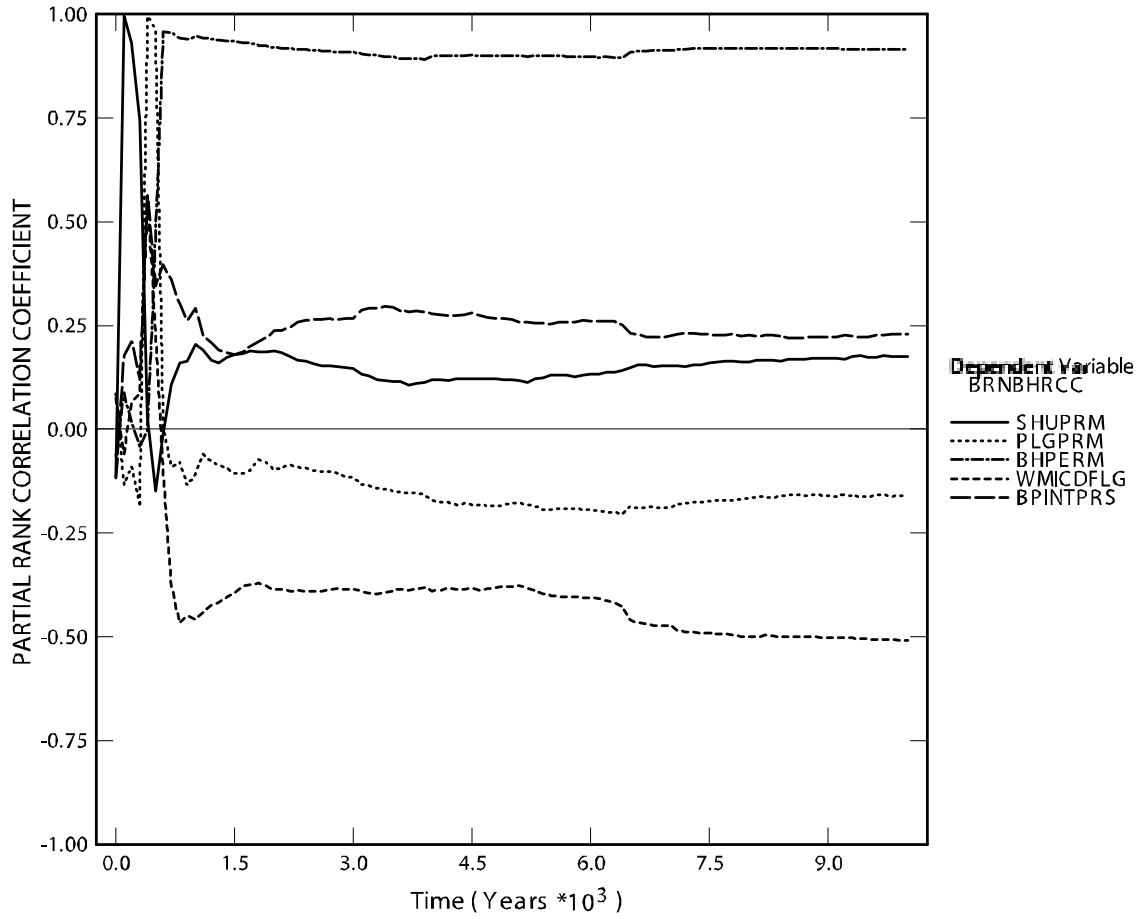
Figure 5-25. Primary Correlations for Cumulative Brine Flow Up the Borehole with Uncertain Parameters, Replicate R1, Scenario S2, from the CRA-2004.
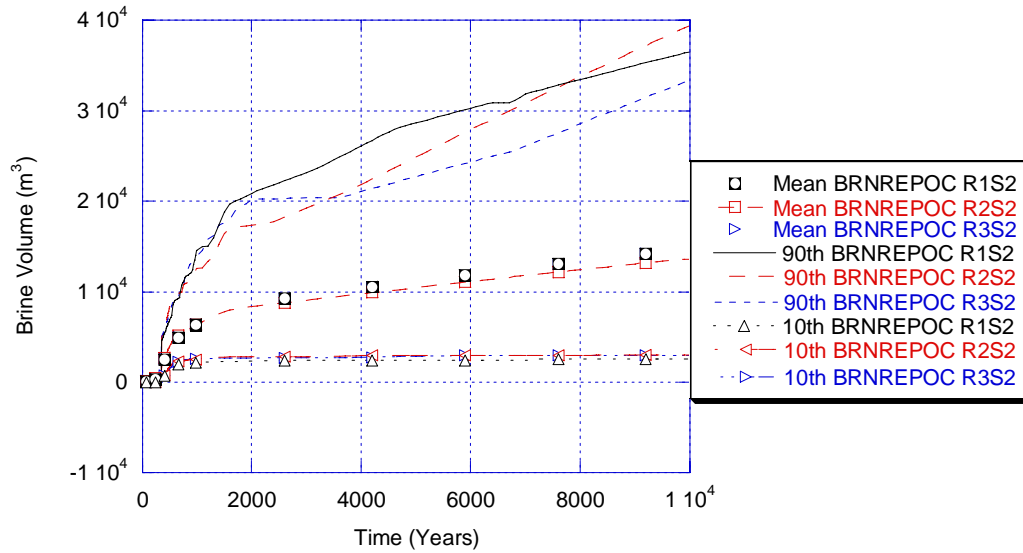
Figure 5-26. Mean and 90th Percentile for Cumulative Brine Outflow in All Replicates, Scenario S2, from the CRA-2004 PABC.
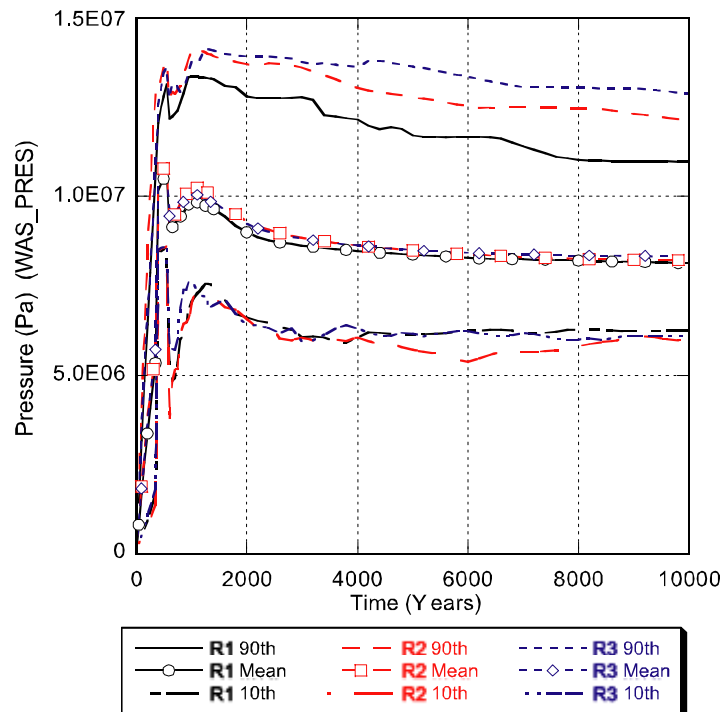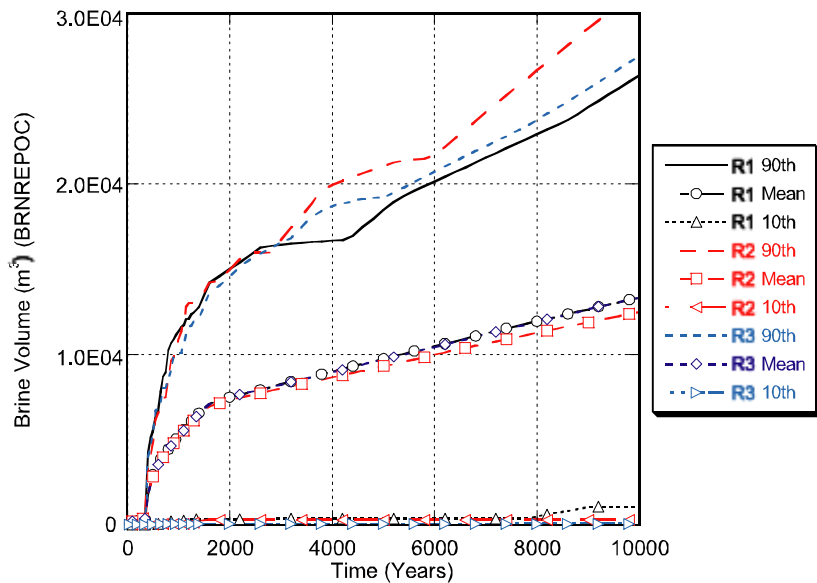

Figure 5-27. Mean and 90th Percentile for Cumulative Brine Outflow in All Replicates, Scenario S2, from the CRA-2004.

5.4   RADIONUCLIDE TRANSPORT

In the disturbed scenarios, radionuclide transport in the Salado is calculated by the code NUTS (see Section 3.4). Transport from the Salado to the Culebra is calculated by NUTS and PANEL (see Section 3.4 and Section 3.2). Transport within the Culebra is calculated by SECOTP2D (see Section 3.8). For all transport calculations, mobilized concentrations of radionuclides in Salado and Castile brines are computed by the code PANEL (see Section 3.2).

This section summarizes the transport results for the disturbed scenarios. Detailed analysis of the NUTS results is presented in Lowry (2005). Garner and Leigh (2005) provides analysis of the PANEL results; Lowry and Kanney (2005) presents analysis of the SECOPT2D results.

5.4.1   Radionuclide Source Term

The code PANEL calculates the time-varying concentration of radioactivity mobilized in brine, either as dissolved isotopes or as isotopes sorbed to mobile colloids. Two different brines are considered: the interstitial brine present in the Salado Formation, which is magnesium rich; and the brine in the Castile Formation, which is sodium rich. Radionuclide solubility in the two brines can be considerably different. Before an E1 intrusion, performance assessment assumes that the brine in the repository is Salado brine. After an E1 intrusion, brine in the repository is assumed to be from the Castile.

Figure 5-28 and Figure 5-30 show the concentration of radioactivity mobilized in Salado and Castile brines, respectively, as a function of time for all vectors in Replicate R1 for the CRA-2004 PABC. Concentrations are expressed as EPA units/m^3 to combine the radioactivity in different isotopes. Short-lived radionuclides, such as ^{238}Pu, decay rapidly in the first few years. After this initial decay, the mobilized concentration is dominated by Am (Garner and Leigh, 2005); the concentration of Am is limited by its solubility until all the inventory of Am is in solution. After all Am is in solution, the total radionuclide concentration generally decreases as the Am decays, until the mobilized concentration becomes dominated by Pu (Garner and Leigh, 2005). The horizontal lines in the figures indicate periods of time when the total radionuclide concentration is limited by the solubility of Am (before about 3,000 years) or Pu (after about 6,000 years). Thus, the uncertainty in total radionuclide concentration is determined by the uncertainty factors used in the calculation of solubilities for Am and Pu (see Table 2-1).

Figure 5-29 and Figure 5-31 show the concentration of radioactivity mobilized in Salado and Castile brines, respectively, as a function of time for all vectors in Replicate R1 for CRA-2004. When compared to Figure 5-28 and Figure 5-30, there is a noticeable difference in the mobilized concentration in Salado and Castile brines between CRA-2004 and CRA-2004 PABC. High values (which occur at time = 0) are between 0.1 and 1 EPA units per m^3 in the CRA-2004 PABC while the high values at time zero were between 0.01 and 0.1 EPA units per m^3 in CRA-2004. The lowest values (at 10,000 years) are also higher in the CRA-2004 PABC (between 10^{-5} and 10^{-4} EPA units per m^3) than they were in CRA-2004 (between 10^{-6} and 10^{-5} EPA units per m^3).

Not only are the mobilized concentration curves shifted toward higher values in CRA-2004 PABC when compared to CRA-2004, there is more spread in the distribution of values for the
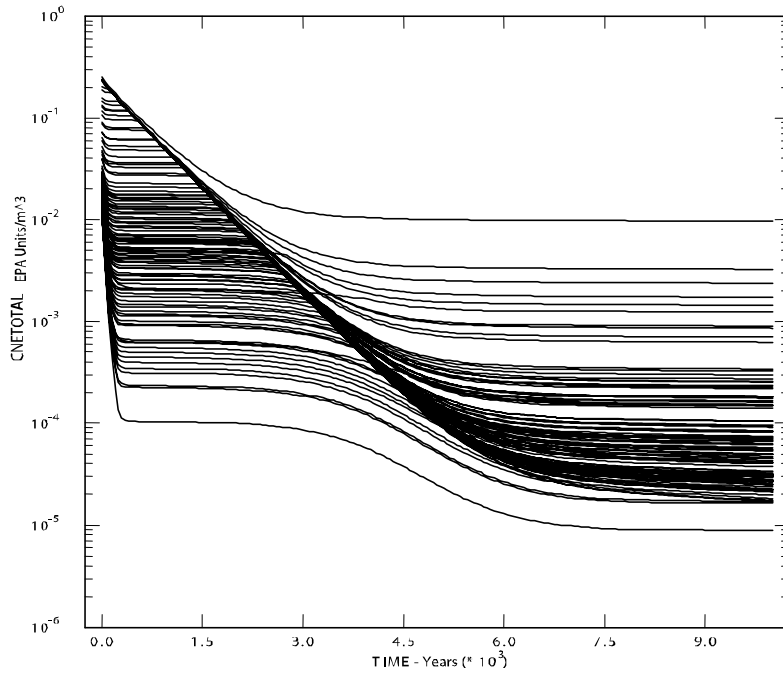
Figure 5-28. Total Mobilized Concentrations in Salado Brine from the CRA-2004 PABC.
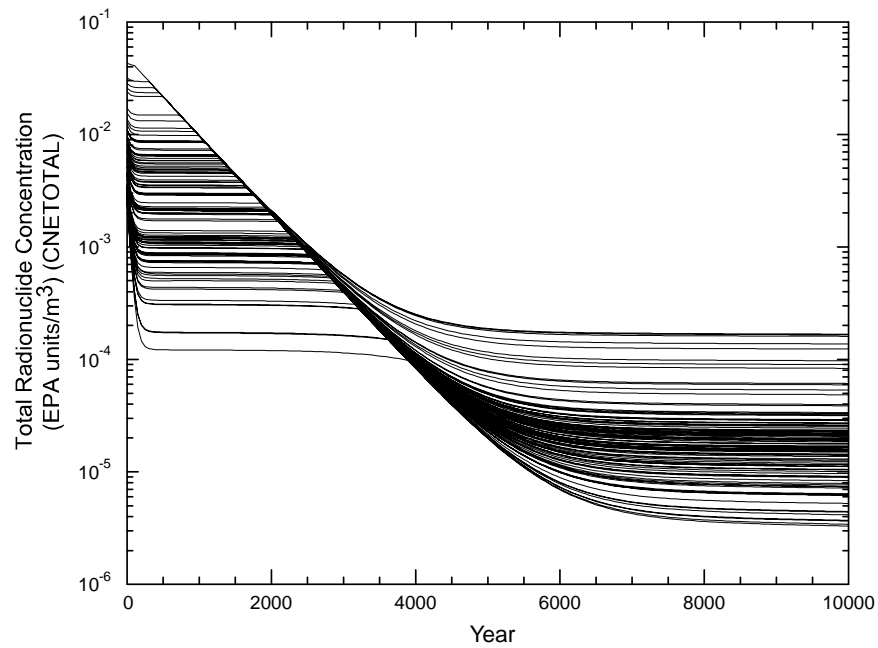
Figure 5-29. Total Mobilized Concentrations in Salado Brine from the CRA-2004.

Information Only
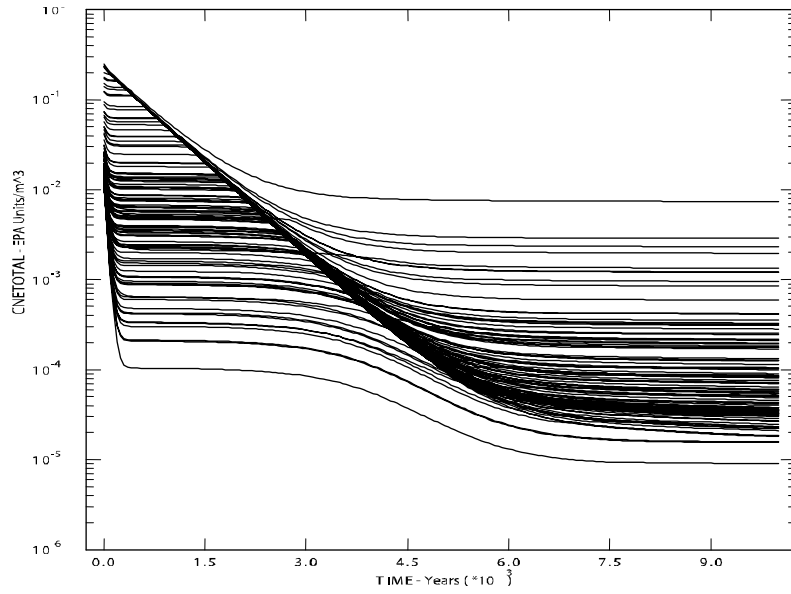
Figure 5-30. Total Mobilized Concentrations in Castile Brine from the CRA-2004 PABC.
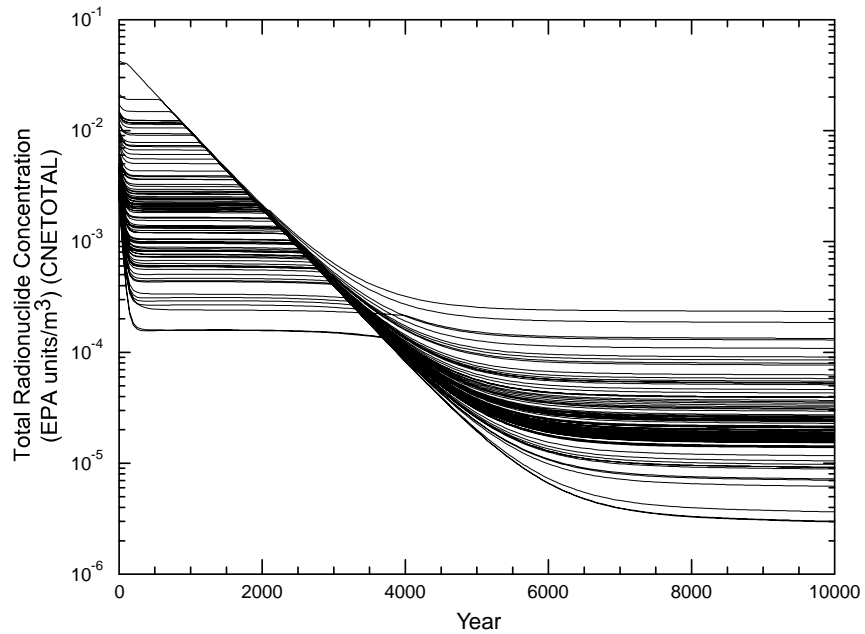
Figure 5-31. Total Mobilized Concentrations in Castile Brine from the CRA-2004.

86 of 153   Information Only

CRA-2004 PABC. Differences in mobilized concentrations between CRA-2004 and CRA-2004 PABC are the result of changes in actinide solubilities and actinide solubility uncertainty ranges.

5.4.2   Transport through Marker Beds and Shaft

In the disturbed scenarios, none of the 300 realizations resulted in transport of radionuclides through the MBs and across the LWB (Lowry, 2005). In addition, no realization showed transport of radionuclides through the shaft to the Culebra.

5.4.3   Transport to the Culebra

Radionuclide transport to the Culebra via a single intrusion borehole (disturbed Scenarios S2, S3, S4, and S5) is modeled with the code NUTS. Transport to the Culebra in the multiple intrusion scenario (S6), is modeled with the code NUTS. Detailed discussion of the NUTS calculations and the PANEL calculations can be found in Lowry (2005), and Garner and Leigh (2005), respectively.

5.4.3.1   Single Intrusion Scenarios

Figure 5-32 through Figure 5-35 show cumulative radioactivity transported up the borehole to the Culebra in the single intrusion scenarios. These results are for Replicate R1. Results from the other replicates are similar and can be found in Lowry (2005) and Garner and Leigh (2005). Transport to the Culebra is larger and occurs for more vectors in the S2 and S3 scenarios (E1 intrusions) than in the S4 or S5 scenarios (E2 intrusions). For most vectors that show significant transport, most of the transport occurs over a relatively short period of time, immediately after the borehole plugs fail.

Figure 5-36 compares mean values among all three replicates for cumulative normalized releases up the borehole to the Culebra for a representative single intrusion case (Scenario S3). The results from each replicate are very similar.

These results are similar to CRA-2004 in extent, but show about an order of magnitude increase in the release flux. As an example, comparing the equivalent of Figure 5-36 to that of CRA-2004 shows a mean value for all three replicates at 10,000 years for CRA-2004 of ~0.2 EPA units. For the CRA-2004 PABC results presented here, the mean value for all three replicates is ~1.5 EPA units.
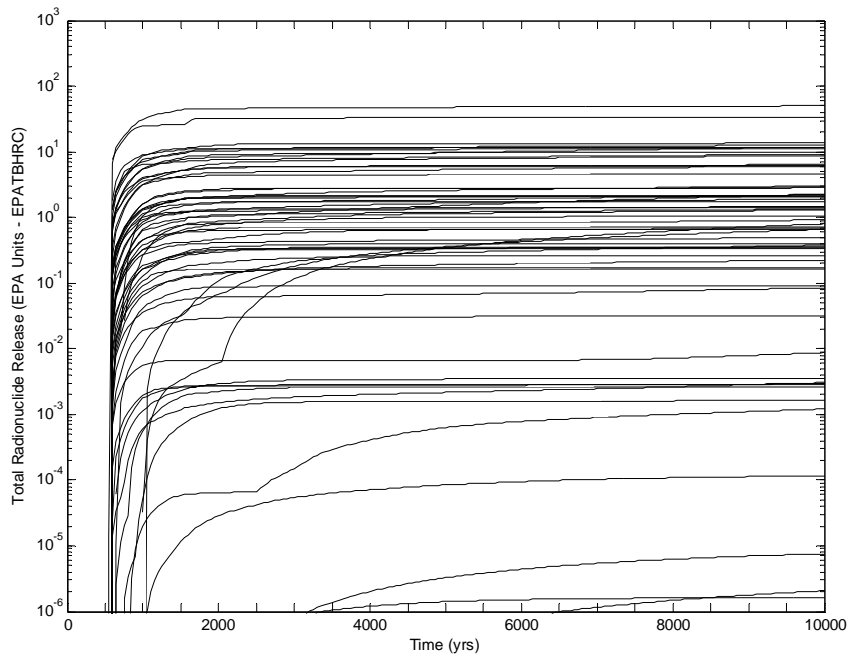
Figure 5-32. Cumulative Normalized Release Up the Borehole, Replicate R1, Scenario S2 for CRA-2004 PABC.
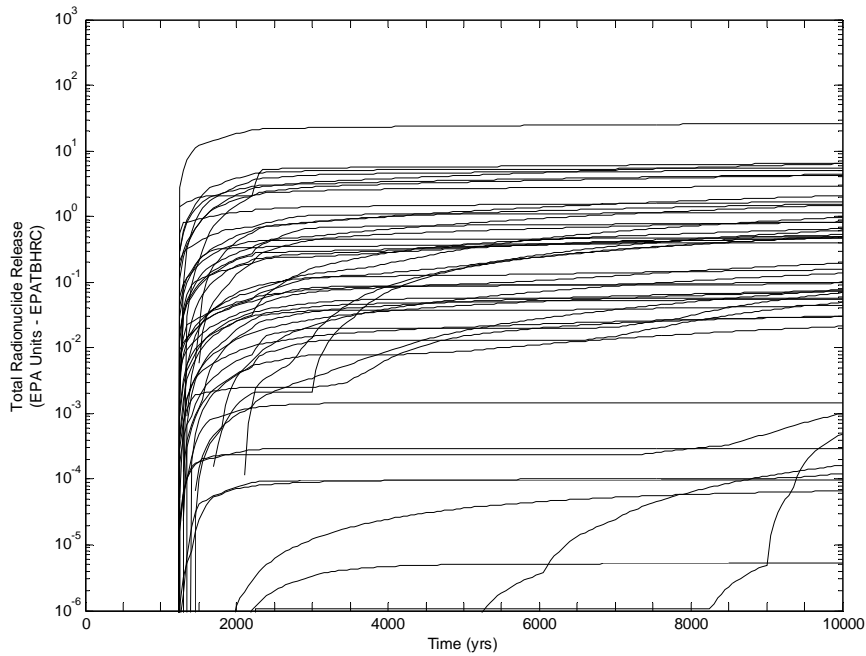
Figure 5-33. Cumulative Normalized Release Up the Borehole, Replicate R1, Scenario S3 for CRA-2004 PABC.
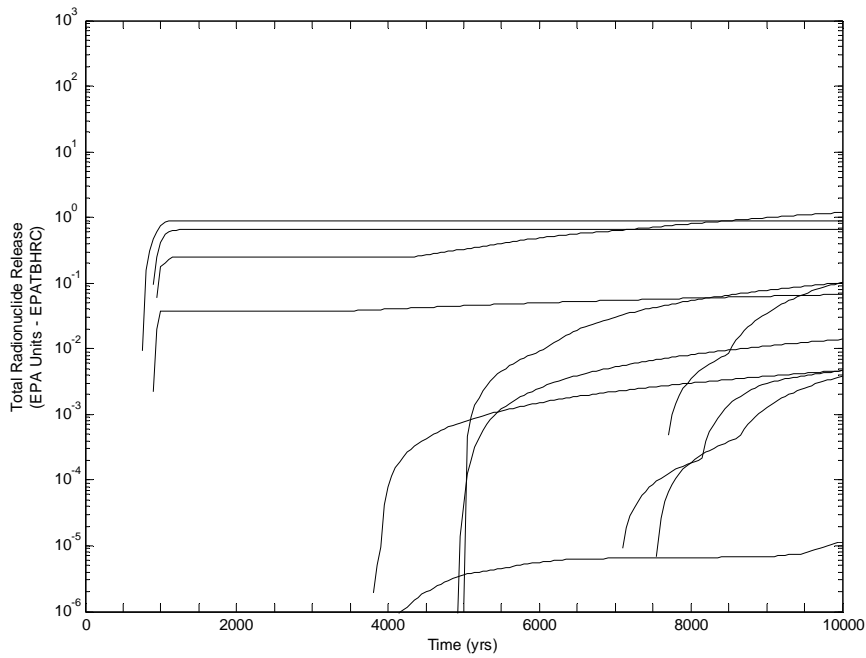
Figure 5-34. Cumulative Normalized Release Up the Borehole, Replicate R1, Scenario S4 for CRA-2004 PABC.
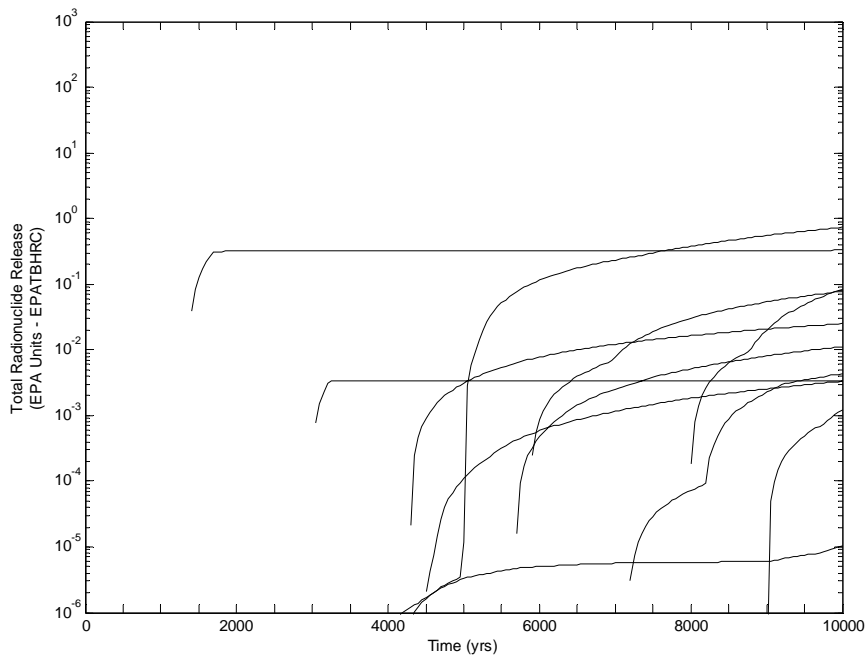
Figure 5-35. Cumulative Normalized Release Up the Borehole, Replicate R1, Scenario S5 for CRA-2004 PABC.

Information Only
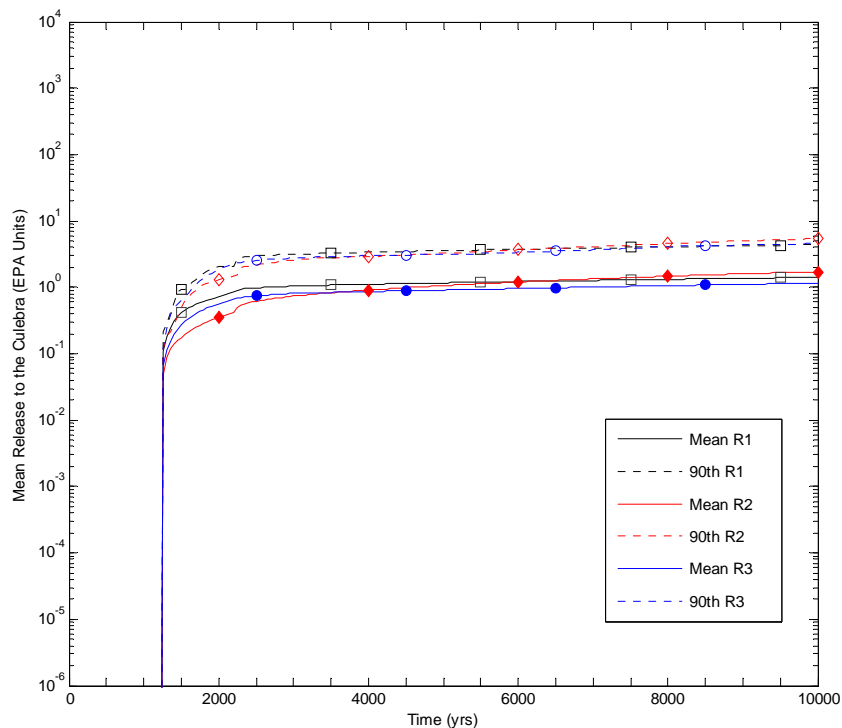
Figure 5-36. Mean Values for Cumulative Normalized Release Up the Borehole for All Replicates, Scenario S3 for CRA-2004 PABC.

5.4.3.2   Multiple Intrusion Scenario

Figure 5-37 shows total EPA units transported to the Culebra via the borehole in the S6 scenario. Almost no radionuclides are released after the E2 intrusion at 800 years; most transport occurs immediately following the E1 intrusion at 2,000 years.

Figure 5-38 compares mean values among all three replicates for cumulative normalized releases up the borehole to the Culebra in the multiple intrusion scenario (S6). The results from each replicate are very similar.

Information Only
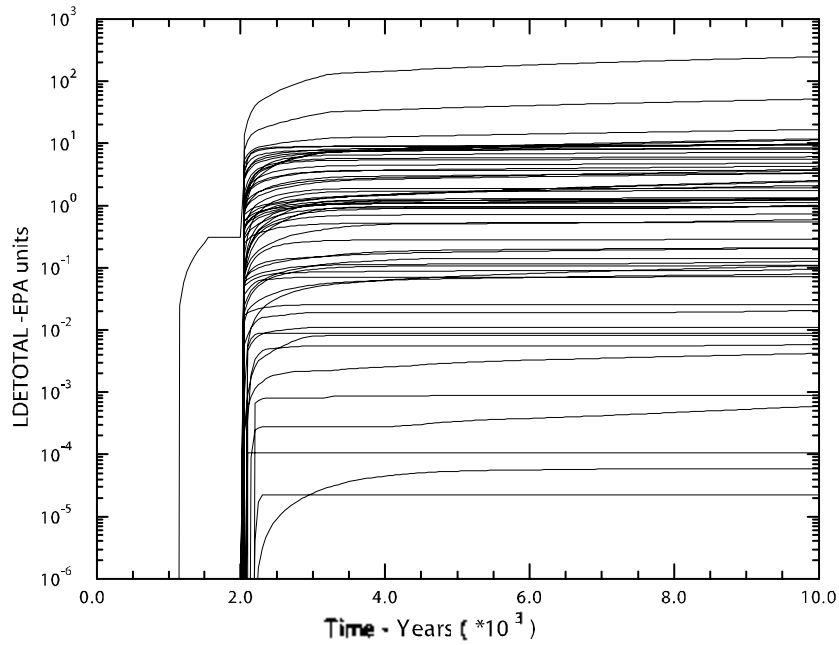
Figure 5-37. Cumulative Normalized Release Up the Borehole, Replicate R1, Scenario S6 for CRA-2004 PABC.
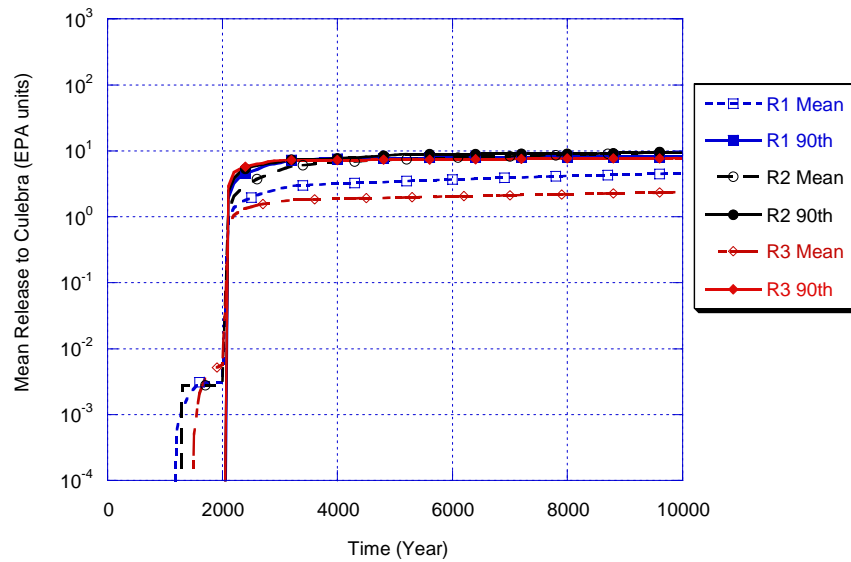
Figure 5-38. Mean Values for Cumulative Normalized Release Up Borehole for All Replicates, Scenario S6 for CRA-2004 PABC.

     Information Only

5.4.3.3 Sensitivity

For both single intrusion and multiple intrusion scenarios, there is a strong correlation relationship between the uncertainty in the total release to the Culebra and the uncertainty in the brine flow up the borehole (calculated by BRAGFLO; see Section 5.3.3). Figure 5-39 shows the relationship between total releases to the Culebra at 10,000 years calculated by NUTS and brine flow up the borehole calculated by BRAGFLO for the S3 scenario (an E1 intrusion at 1,000 years). Figure 5-40 shows a similar relationship for the S6 scenario (combination of an E2 intrusion at 1000 years followed by an E1 intrusion in the same panel at 2,000 years) wherein the total releases to the Culebra have been calculated by PANEL. These results are very similar to those calculated in the CRA-2004 PABC

Previous sensitivity studies (Lowry, 2003) have identified the borehole permeability as the most important parameter contributing to the uncertainty in flow up the borehole and observed a corresponding influence on releases to the Culebra (Garner, 2003a; Lowry, 2003). These analyses also identified the initial pressure in the brine pocket, the indicator flag for microbial activity, and the steel corrosion rate as contributing to uncertainty in releases to the Culebra although the importance of these parameters is much less than that of borehole permeability. The CRA-2004 PABC results show similar correlations.
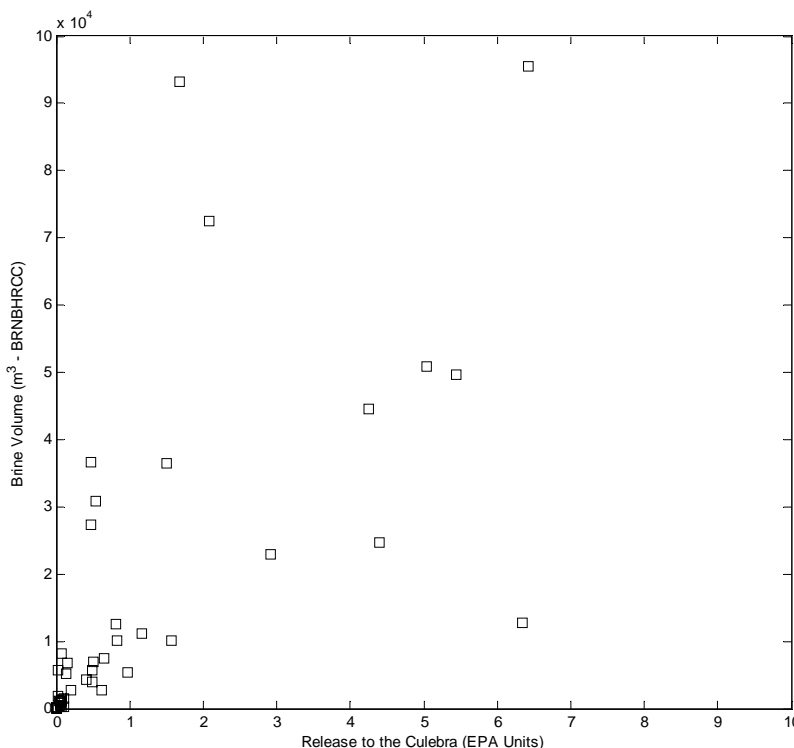
Figure 5-39. Comparison of Total Release to Culebra with Flow Up Borehole, Replicate R1 Scenario S3 for CRA-2004 PABC.
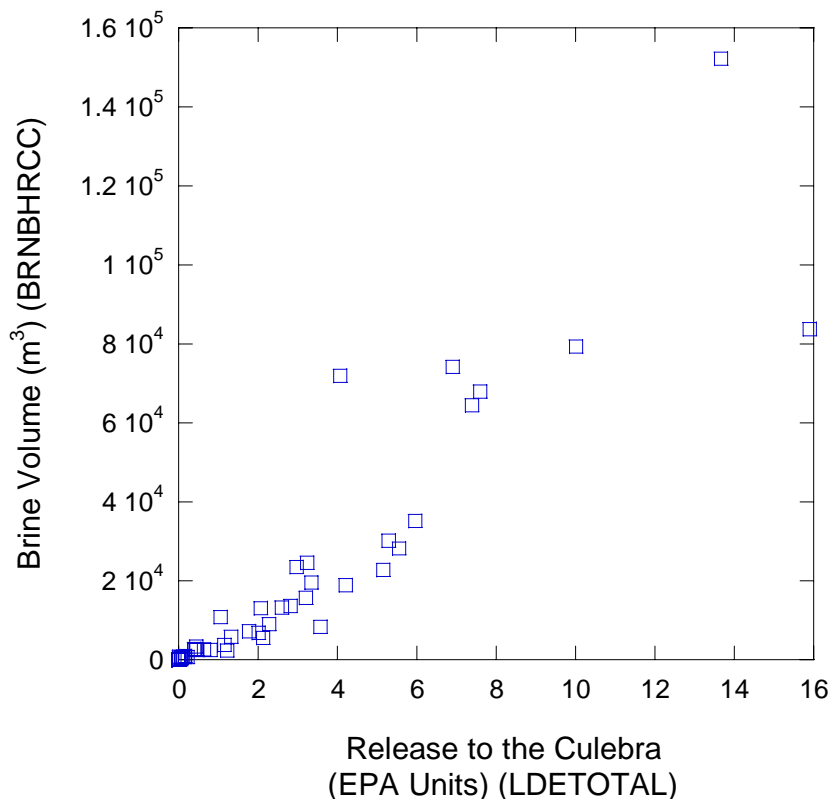
Figure 5-40. Comparison of Total Release to Culebra with Flow Up Borehole, Replicate R1 Scenario S6 for CRA-2004 PABC.

5.4.4   Transport through the Culebra

Radionuclide transport through the Culebra for a given set of uncertain parameters is calculated with the code SECOTP2D (see Section 3.8). Note that the total release of radionuclides across the LWB at the Culebra for given futures is calculated with the code CCDFGF by convolving the SECOTP2D results with the transport to the Culebra calculated by NUTS and PANEL. This section discusses the SECOTP2D results; total releases through the Culebra are presented in Section 6.5.

Culebra transport calculations were performed for three replicates of 100 vectors each for both partial-mining and full-mining scenarios (600 total transport simulations). Each of the 600 transport simulations used a unique flow field computed separately with the code MODFLOW [see Section 3.8 and (Lowry and Kanney, 2005)]. The partial-mining scenario assumes the extraction of all potash reserves outside the LWB while full mining assumes that all potash reserves both inside and outside the LWB are exploited.

In each transport simulation, 1 kg of each of four radionuclides (^{241}Am, ^{234}U, ^{230}Th, and ^{239}Pu) are released at the center of the waste panel area. Transport of the ^{230}Th daughter product of ^{234}U decay is calculated and tracked as a separate species. In the following discussion, ^{230}Th will refer to the ^{234}U daughter product and ^{230}ThA will refer to that released at the waste panel area.

The effect of oxidation state on radionuclide transport is explicitly included in the simulations through the use of oxidation-state specific distribution coefficients (Kds). Am is present as Am(III) and Th as Th(IV). Uranium may be present as either U(IV) or U(VI); plutonium may be present as Pu(III) or Pu(IV). The oxidation state of uranium and plutonium is an uncertain parameter (see WOXSTAT).

All SECOTP2D results, regardless of magnitude, are included in the calculation of releases through the Culebra. In practice, most non-zero releases computed by SECOTP2D are vanishingly small and result from numerical error Lowry and Kanney (2005). Consequently, the analysis of SECOTP2D results focused on realizations in which at least one billionth (10^{-9}) of the 1 kg source was transported to the LWB

5.4.4.1 Partial Mining Results

Under partial-mining conditions, only the ^{234}U species and its ^{230}Th decay product were transported to the LWB in any significant amount during the course of the 10,000-year simulation (Lowry and Kanney, 2005). Table 5-2 shows that no releases greater than one billionth of the 1 kg source were calculated for Replicates R1 and R3. For replicate R2, three vectors produced ^{234}U releases greater than 10^{-9} kg. One of these vectors also resulted in a ^{230}Th release greater 10^{-9} kg.

Table 5-2. Radionuclide Transport to the LWB under Partial Mining Conditions[1,2]

Replicate	^{241}Am	^{239}Pu	^{234}U	^{230}Th	^{230}ThA
1	0	0	0	0	0
2	0	0	3	1	0
3	0	0	0	0	0

1. Number of vectors for which release (transported to LWB) is greater than 1 billionth of the 1 kg source released at center of waste panel area.
2. ^{230}ThA refers to thorium released at waste panel area. ^{230}Th refers to thorium resulting from ^{234}U decay.

5.4.4.2 Full Mining Results

Under full-mining conditions, only the ^{234}U species and its ^{230}Th decay product were transported to the LWB in any significant amount during the course of the 10,000-year simulation. More vectors resulted in releases greater than 10^{-9} kg for the full-mining scenario than were seen under partial mining conditions. In addition, releases greater than 10^{-9} kg were calculated for all three replicates. Table 5-3 shows that three vectors in replicate R1, six vectors in replicate R2, and three vectors in replicate R3 had ^{234}U releases greater than 10^{-9} kg. None of the three vectors in replicate R1 that showed a ^{234}U release greater than 10^{-9} kg showed a release of ^{230}Th daughter product greater than 10^{-9} kg. In replicate R2, three vectors of the six vectors that showed a ^{234}U release grater than 10^{-9} kg showed a release of ^{230}Th daughter greater than 10^{-9} kg. In replicate R2, three vectors of the six vectors that showed a ^{234}U release grater than 10^{-9} kg showed a release of ^{230}Th daughter greater than 10^{-9} kg.

Table 5-3. Radionuclide Transport to the LWB under Full Mining Conditions[1,2]

Replicate	^{241}Am	^{239}Pu	^{234}U	230Th	^{230}ThA
1	0	0	3	0	0
2	0	0	6	3	0
3	0	0	3	1	0

1. Number of vectors for which release (transported to LWB) is greater than 1 billionth of the 1 kg source released at
    center of waste panel area.
2. ^{230}ThA refers to thorium released at waste panel area. ^{230}Th refers to thorium resulting from ^{234}U decay.

5.4.4.3 **Summary and Additional Information**

In summary, very few vectors showed significant transport of radionuclides to the LWB during the 10,000-year simulation under partial or full mining conditions. Only ^{234}U and its ^{230}Th daughter product were transported in any noticeable amount.

Comparing these results to those for the CRA-2004 PA, one observes the same general trends: 1) the ^{234}U species dominates the releases; and 2) there are more releases under full-mining conditions than under partial-mining conditions. There are also some noticeable differences: 1) there are generally fewer vectors that show transport of radionuclides to the LWB in the CRA-2004 PABC results; and 2) no releases of ^{239}Pu are calculated in the CRA-2004 PABC PA while two such vectors were observed in the CRA-2004 results.

Sensitivity analysis indicates that releases of ^{234}U in both the full and partial mining conditions is associated with the U(VI) oxidation state. This result is reasonable because the matrix distribution coefficients for uranium in the (IV) state are much lower than for the (VI) state. This sensitivity was also observed and reported in the CRA-2004 PA.

More detailed information on the results of the Culebra transport calculations can be found in the Analysis Package for the Culebra Flow and Transport Calculations: Compliance Recertification Application Performance Assessment Baseline Calculations (Lowry and Kanney, 2005).

5.5 **DIRECT RELEASES**

Direct releases occur at the time of a drilling intrusion, and include cuttings and cavings; spallings; and DBRs. This section presents analysis of the volume released by each mechanism.

Vugrin (2005a) provides additional information about the cuttings and cavings releases calculated for the CRA-2004 PABC. Additional information about the spallings releases is found in Vugrin (2005b). Stein et al. (2005) provides detailed analysis of direct brine releases in the CRA-2004 PABC.

5.5.1 Cuttings and Cavings

Cuttings and cavings are the solid waste material removed from the repository and carried to the surface by the drilling fluid during the process of drilling a borehole. Cuttings are the materials removed directly by the drill bit, and cavings are the material eroded from the walls of the borehole by shear stresses from the circulating drill fluid. The volume of cuttings and cavings material removed from a single drilling intrusion into the repository is in the shape of a cylinder. The code CUTTINGS_S calculates the area of the base of this cylinder, and cuttings and cavings results in this section are reported in terms of these areas. The volumes of cuttings and cavings removed can be calculated by multiplying these areas with the initial repository height, 3.96 m (BLOWOUT:HREPO).

Cuttings and cavings areas calculated for the CRA-2004 PABC range between 0.0760 m^2 and 0.861 m^2, with a mean area of approximately 0.253 m^2 in Replicate R1 (Table 5-4). These results are similar to the cuttings and cavings calculations from the CRA-2004 (Table 5-5).

Table 5-4. CRA-2004 PABC Cuttings & Cavings Area Statistics

Replicate	Min (m^2)	Max (m^2)	Mean (m^2)	Vectors w/o Cavings
R1	0.0760	0.824	0.253	9
R2	0.0760	0.861	0.251	10
R3	0.0760	0.829	0.254	11

Table 5-5. CRA-2004 Cuttings & Cavings Area Statistics

Replicate	Min (m^2)	Max (m^2)	Mean (m^2)	Vectors w/o Cavings
R1	0.0760	0.909	0.253	11
R2	0.0760	0.790	0.253	11
R3	0.0760	0.994	0.253	8
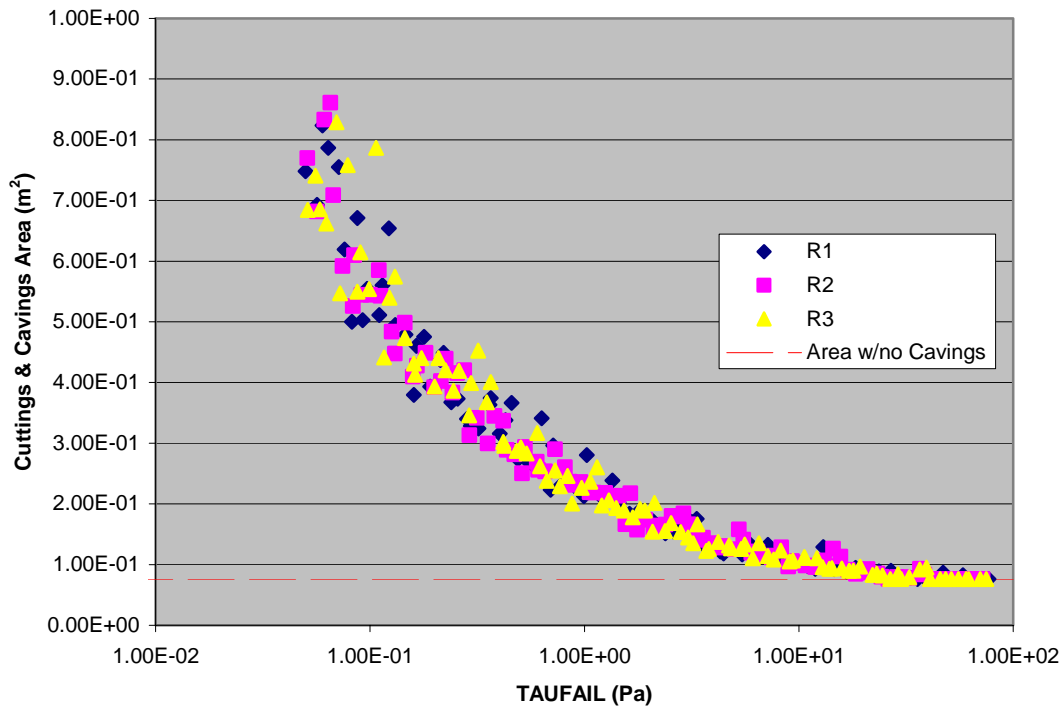
Figure 5-41. Scatterplot of Cuttings & Cavings Areas versus Shear Strength from CRA-2004 PABC.
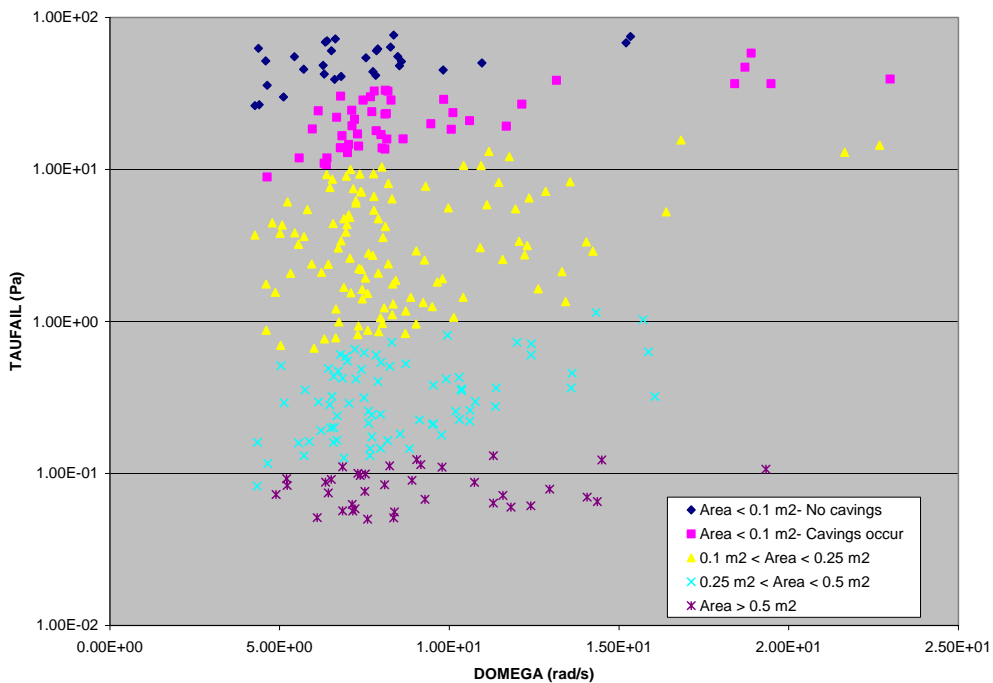
Figure 5-42. Scatter Plot of Drill String Angular Velocity versus Shear Strength from CRA-2004 PABC.
Symbols indicate the range of cuttings and cavings areas in square meters.

97 of 153   Information Only

Two uncertain sampled parameters affect the cavings calculations. The uncertainty in cavings areas arises primarily from the uncertainty in the shear strength of the waste (BOREHOLE:TAUFAIL). Lower shear strengths tend to result in larger cavings, and the converse is true as well (Figure 5-41). The uncertainty in the drill string angular velocity (BOREHOLE:DOMEGA) has a smaller impact on the cavings results, but the combination of a low angular velocity and a high shear strength can prohibit cavings from occurring (Figure 5-42). In fact, cavings did not occur in ten percent of all vectors (Table 5-4).

5.5.2   Spall Volumes

Calculation of the volume of solid waste material released to the surface from a single drilling intrusion into the repository due to spallings is a two part procedure. The code DRSPALL calculates the spallings volumes from a single drilling intrusion at four values of repository pressure (10, 12, 14, and 14.8 MPa). The second step in calculating spall volumes from a single intrusion consists of using the code CUTTINGS_S to interpolate the DRSPALL volumes. The repository pressures calculated by BRAGFLO are used to interpolate the spallings volumes to calculate spall volumes in the scenarios for drilling intrusions. Results from both of these calculations are documented in this section.

5.5.2.1   DRSPALL Results

The code DRSPALL was run for each of 100 vectors in three replicates and for four values of repository pressure (10, 12, 14, and 14.8 MPa) for the CRA-2004 PABC. This change was mandated for CRA-2004 PABC by the EPA (Cotsworth, 2005). In contrast, DRSPALL was run for only one replicate of fifty vectors at the four pressures for the CRA-2004.

No spallings occurred at 10 MPa for either analysis. In general, the mean spallings volumes calculated by DRSPALL for the CRA-2004 PABC were slightly smaller than the spallings volumes from the CRA-2004 (see Table 5-6). It is hypothesized that it was simply the stochastic nature of sampling that lead to mean spall volumes for the CRA-2004 that were larger than those of the CRA-2004 PABC.

The maximum CRA-2004 PABC spallings volumes for all pressures were larger than the respective CRA-2004 maximum spallings volumes (Table 5-6). Since the CRA-2004 PABC had a larger sample size, there is an increased probability of observing large spallings volumes. That is, the likelihood of coupling parameters that lead to material failure, fluidization, and, ultimately, large spall volumes increased for the CRA-2004 PABC because of the larger set of vectors and a greater number of extreme parameter values. Despite these differences in extreme values, the shape of the spallings volume distributions remains similar (Figure 5-43, Figure 5-44, and Figure 5-45).

Table 5-6. Pooled Summary Spallings Statistics for CRA-2004 PABC and CRA-2004.

DRSPALL Pressure Scenario (DPS)	CRA-2004 PABC		CRA-2004	
	Mean Spall Volume (m^3)	Max. Spall Volume (m^3)	Mean Spall Volume (m^3)	Max. Spall Volume (m^3)
DPS 2- 12 MPa	0.172	7.71	0.244	7.00
DPS 3- 14 MPa	0.665	11.8	0.793	9.45
DPS 4- 14.8 MPa	0.978	14.5	1.09	12.1
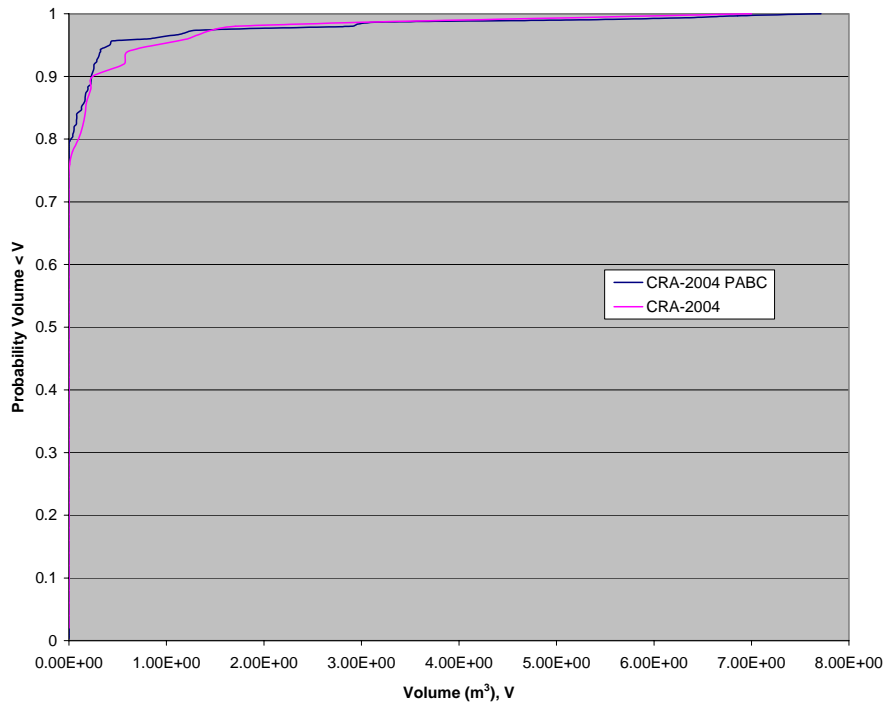
Figure 5-43. Observed Probability Distribution for CRA-2004 PABC and CRA-2004 Spall Volumes: 12 MPa
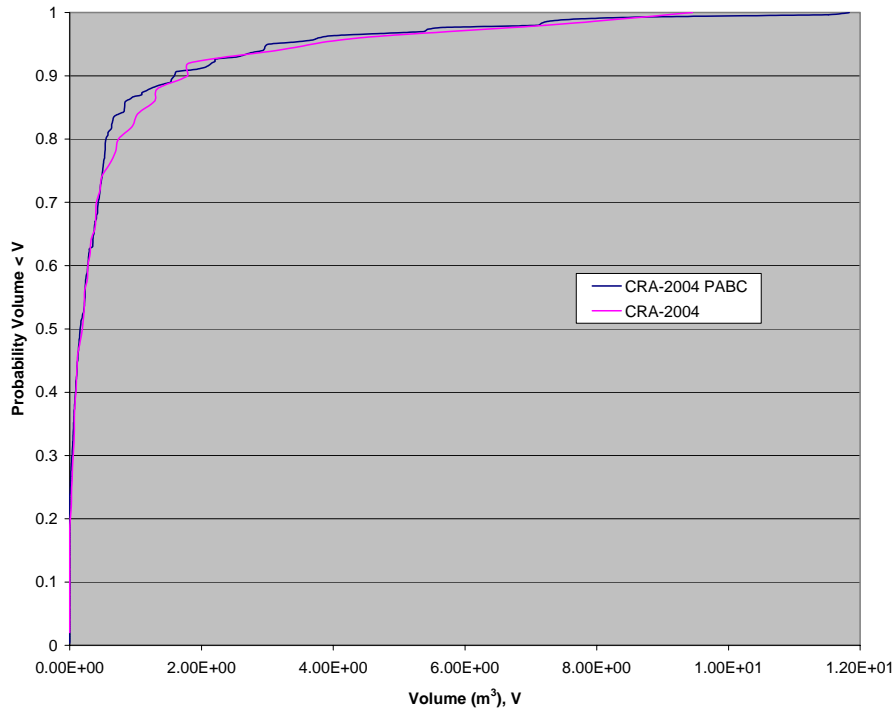
Figure 5-44. Observed Probability Distribution for CRA-2004 PABC and CRA-2004 Spall Volumes: 14 MPa
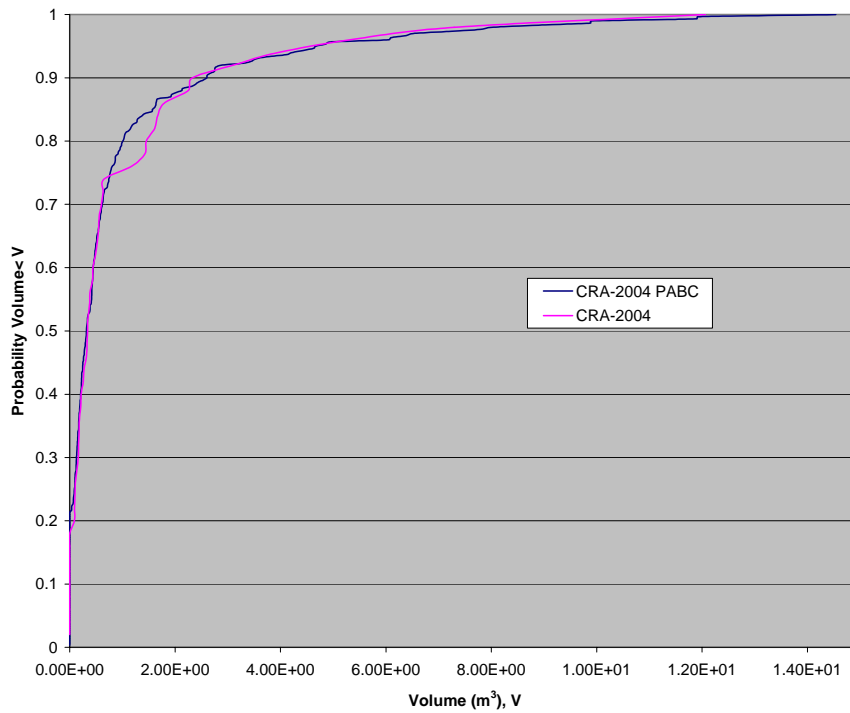
Figure 5-45. Observed Probability Distribution for CRA-2004 PABC and CRA-2004 Spall Volumes: 14.8 MPa

The uncertainty in these volumes arises from four variables that are uncertain in the DRSPALL calculations: waste permeability, waste porosity, waste tensile strength, and waste particle diameter after tensile failure. Figure 5-46 indicates that the largest spall volumes occur when waste permeability is less than 1.00E-13 m^2, but larger permeability values result in a higher frequency of nonzero spall volumes. This observation can be explained as follows: the higher permeability values that were sampled result in less tensile stresses and less tensile failure but promote fluidization. Lower permeability leads to greater tensile stresses and tensile failure, but failed material may not be able to fluidize at this low permeability. Smaller particle diameter values (see Figure 5-47) tend to result in larger spall volumes and higher frequency of nonzero spall volumes. The uncertainty in the spall volumes from a single intrusion is largely determined by the uncertainty in these two parameters. Obvious correlations between spall volumes and the two other parameters could not be established.
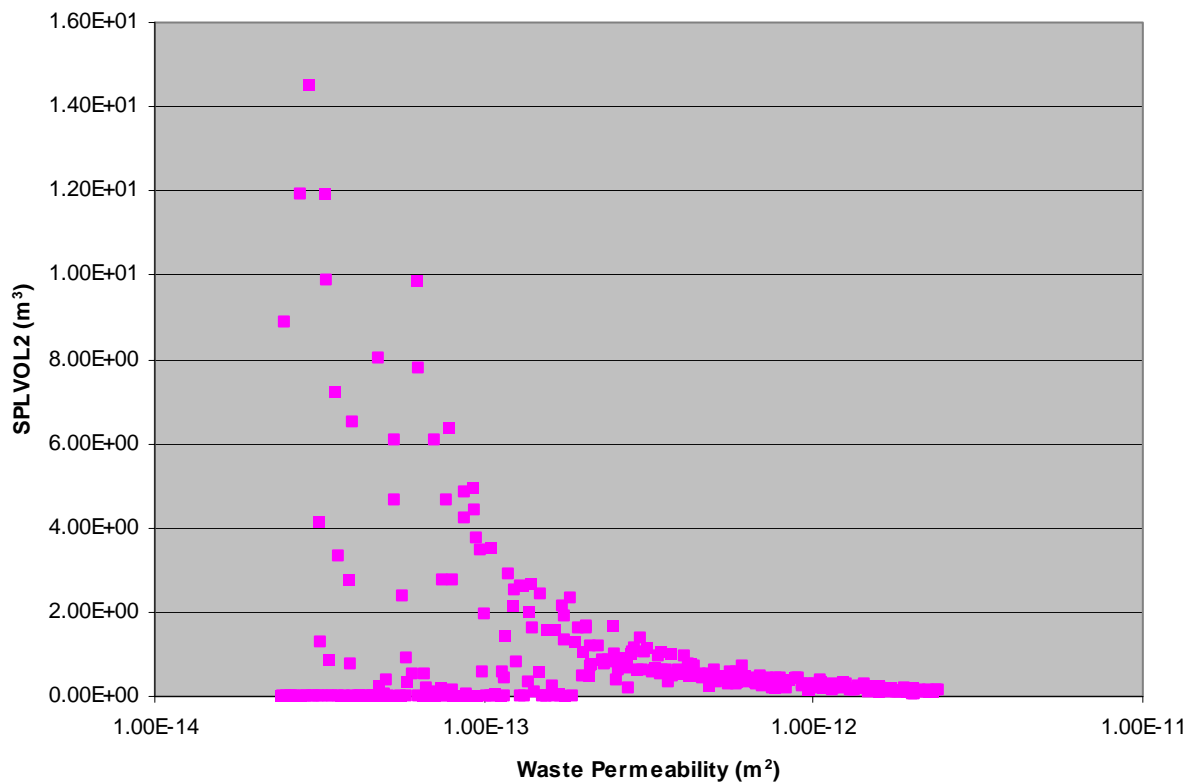
Figure 5-46. Scatter Plot of Pooled Vectors: Waste Permeability vs SPLVOL2 for CRA-2004 PABC.
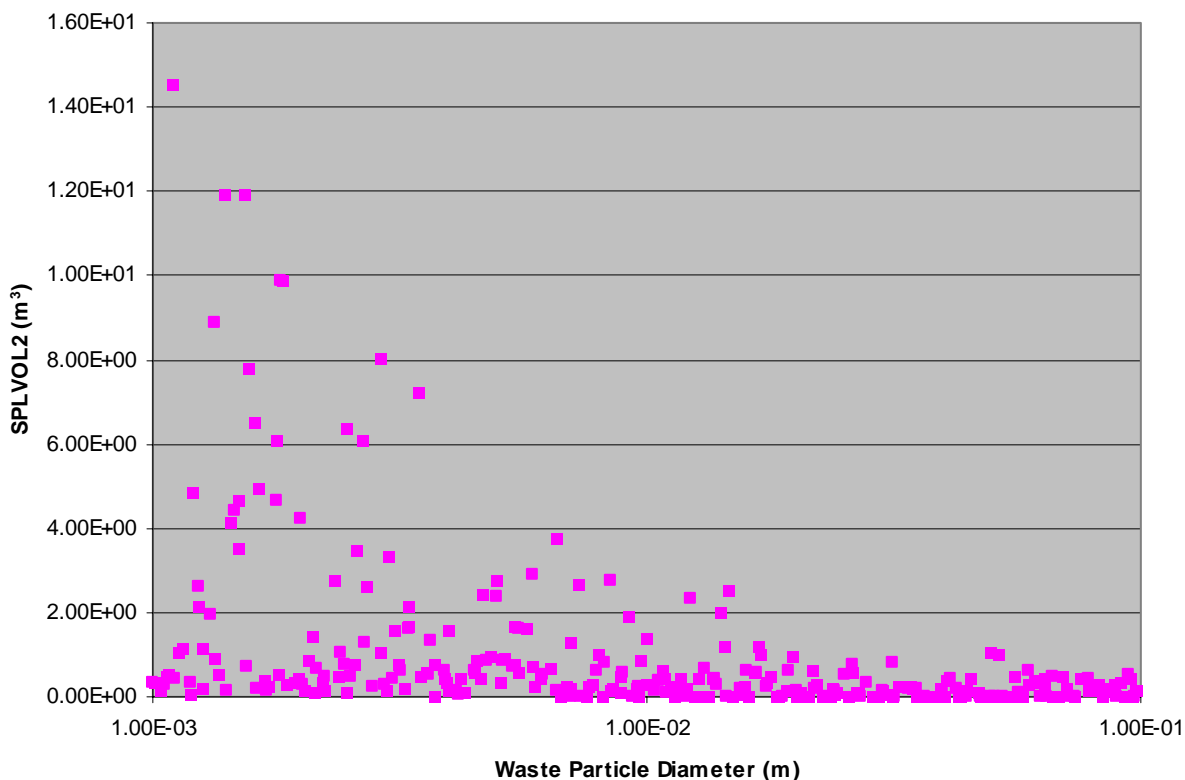
Figure 5-47. Scatter Plot of Pooled Vectors: Waste Particle Diameter vs. SPLVOL2 for CRA-2004 PABC.

5.5.2.2 CUTTINGS_S Results

Two factors directly affect the CUTTINGS_S calculation of spallings volumes for the drilling scenarios: the volumes calculated by DRSPALL and the repository pressures calculated by BRAGFLO.

Of the 7,800 spallings volumes calculated per replicate, more than 94% of each replicate's calculations resulted in no spallings. Only about a third of the vectors in each replicate had spallings occur in at least one of the scenarios, and therefore spallings will not contribute to the total releases calculated for the other vectors. For each replicate, Scenarios S2 and S3 resulted in the largest maximum spallings volume and largest number of nonzero spallings volumes per time intrusion. (Spallings calculations were done at six S1 times as opposed to five S2 and S3 times.) For the CRA-2004 PABC, Scenarios S2 and S3 have the highest pressures in general because, in these scenarios, the drillbit intrudes into a pressurized brine pocket (Nemer and Stein, 2005). These high pressures lead to more spallings events and larger spallings volumes.

Table 5-7. CRA-2004 PABC and CRA-2004 Spallings Summary Statistics by Scenario

Scenario		CRA-2004	CRA-2004 PABC		
		Replicate R1	Replicate R1	Replicate R2	Replicate R3
S1	Maximum [m^3]	9.77	1.67	1.04	3.14
	# of nonzero volumes	355	115	109	125
S2	Maximum [m^3]	8.55	8.33	3.81	6.30
	# of nonzero volumes	235	117	107	89
S3	Maximum [m^3]	8.51	8.04	2.14	2.68
	# of nonzero volumes	258	103	100	75
S4	Maximum [m^3]	8.25	1.67	0.854	1.11
	# of nonzero volumes	198	52	43	31
S5	Maximum [m^3]	8.76	1.67	0.798	2.27
	# of nonzero volumes	240	68	62	47
All Scenarios	Maximum [m^3]	9.77	8.33	3.81	6.30
	# of nonzero volumes	1286	455	421	367

The CRA-2004 Replicate R1 maximum volumes are larger than the maximum volumes calculated for the CRA-2004 PABC volumes for each scenario, and Replicate R1 of the CRA-2004 had almost three times as many nonzero volumes as each of the CRA-2004 PABC (Table 5-7). This is largely due to the new gas generation model that was implemented for the CRA-2004 PABC (Nemer and Stein, 2005). In general, CRA-2004 PABC pressures calculated by BRAGFLO are significantly lower than pressures calculated for the CRA-2004 (Nemer and Stein, 2005). These reduced gas generation rates lead to lower pressures at the times calculated for intrusions and are the major factor that led to a decrease in maximum spallings volumes and frequency of spallings. An additional factor is the slight decrease in the magnitude of spallings volumes calculated by DRSPALL for the CRA-2004 PABC (Vugrin, 2005b).

5.5.3   Direct Brine Release Volumes

DBRs to the surface can occur during or shortly after a drilling intrusion. For each element of the Latin hypercube sample, the code BRAGFLO calculates volumes of brine released for a total of 78 combinations of intrusion time, intrusion location, and initial conditions. Initial conditions for the DBR calculations are obtained from the BRAGFLO Salado Flow modeling results from Scenarios S1 through S5. Salado modeling results from the S1 scenario (Section 4.1) are used as initial conditions for DBR for a first intrusion into the repository which may have a direct brine release. Salado modeling results from the S2 through S5 scenarios (Section 5.3) are used as initial conditions for DBR for second or subsequent drilling intrusions that may have a direct brine release.

For Replicate R1, only 721 of the 7,800 DBR calculations (100 vectors × 78 combinations) resulted in direct brine flow to the surface. The maximum DBR release is approximately 69 m^3. Only intrusions into a lower panel [see Section 6.1 of (Stein et al., 2005)] resulted in significant

brine volume releases. In the S1 scenario, the lower panel represents an undisturbed panel at the south end of the repository. In the S2 and S3 scenarios, the lower panel represents any panel that has a previous E1 intrusion; in the S4 and S5 scenarios, the lower panel has a previous E2 intrusion.

Figure 5-48 through Figure 5-52 show probability plots of CRA-2004 PABC DBR volumes for Scenarios S1 through S5, lower intrusion, at the discrete times for which DBR is calculated. A probability plot displays the percentage of the vectors on the x‑axis where release volumes are less than the value on the y-axis. Figure 5-48 shows DBR volumes for Scenario S1 representing the initial intrusion at various times. Figure 5-49 and Figure 5-50 show DBR volumes for Scenarios S2 and S3, which represents a subsequent intrusion (at various times) into a panel that had an E1 intrusion at 350 years and 1,000 years, respectively. Figure 5-51 and Figure 5-52 show DBR volumes for Scenarios S4 and S5, which represent a subsequent intrusion (at various times) into a panel that had an E2 intrusion at 350 years and 1,000 years, respectively. Release volumes are larger and occur more frequently in the S2 and S3 scenarios, because the lower panel has much higher saturations after an E1 intrusion.

Previous sensitivity analysis has determined that a DBR volume from a single intrusion is most sensitive to the initial pressure and brine saturation in the intruded panel (Stein 2003). This analysis is repeated below for Scenario S2, for the CRA-2004 PABC. The initial pressure and brine saturation in the DBR calculations are transferred from the Salado Flow calculations as described above. Thus, the uncertain parameters that are most influential to the uncertainty in pressure and brine saturation in the Salado Flow calculations (see Sections 4.1 and 5.3) are also most influential in the uncertainty in DBR volumes.

The combination of relatively high pressure and brine saturation in the intruded panel is required for direct brine release to the surface. Figure 5-53 shows a scatter plot of pressure in the waste panel versus DBR volumes for Scenario S2, lower intrusion, with symbols indicating the value of the mobile brine saturation [defined as brine saturation S_b minus residual brine saturation S_{br} in the waste, see (Stein, 2003b)]. The figure clearly shows that there are no releases until pressures exceed about 8 MPa as indicated by the vertical line. Above 8 MPa, a significant number of vectors have zero releases, but these vectors have mobile brine saturations less than zero and thus no brine is available to be released. When mobile brine saturation approaches 1, relative permeability to gas becomes small enough that no gas flows into the well, and in these circumstances DBR releases end after three days. Thus, in vectors with high mobile brine saturations, DBR releases increase proportionally with increases in pressure, as evidenced by the linear relationship between DBR volume and pressure for mobile brine saturation between 0.8 and 1.0. For vectors with mobile saturations between 0.2 and 0.8, both gas and brine can flow in the well, and the rate of gas flow can be high enough that the ending time of DBR releases may be as long as 11 days. Although brine may be flowing at slower rates in these vectors than in vectors with high mobile saturations, brine flow may continue longer and thus result in larger DBR volumes.

CRA-2004 PABC DBR R1S1 Lower
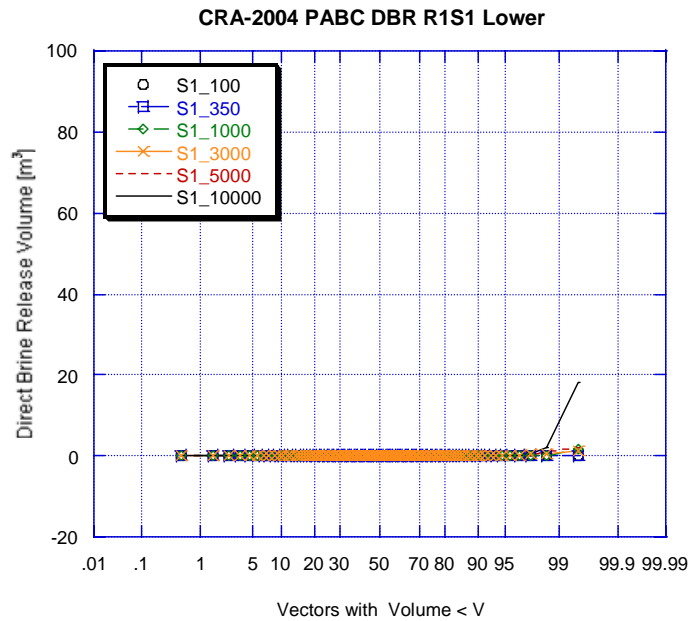
Figure 5-48. DBRs for Initial Intrusions into Lower Panel, Replicate R1,
Scenario S1 from CRA-2004 PABC.
(Note: Legend gives scenario number and intrusion time)

CRA-2004 PABC DBR R1S2 Lower
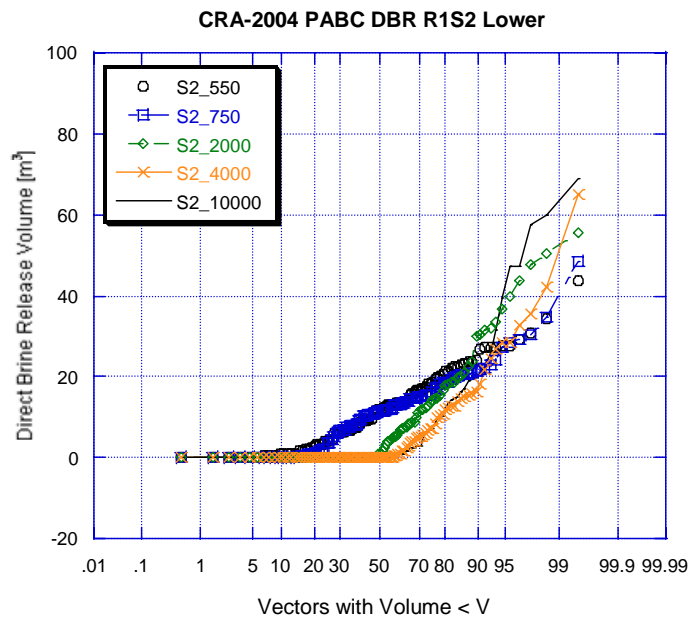
Figure 5-49. DBRs for Second Intrusions into Lower Panel, After an Initial E1 Intrusion at 350 Years
Replicate R1, Scenario S2 from CRA-2004 PABC.
(Note: Legend gives scenario number and intrusion time)

Information Only

CRA-2004 PABC DBR R1S3 Lower
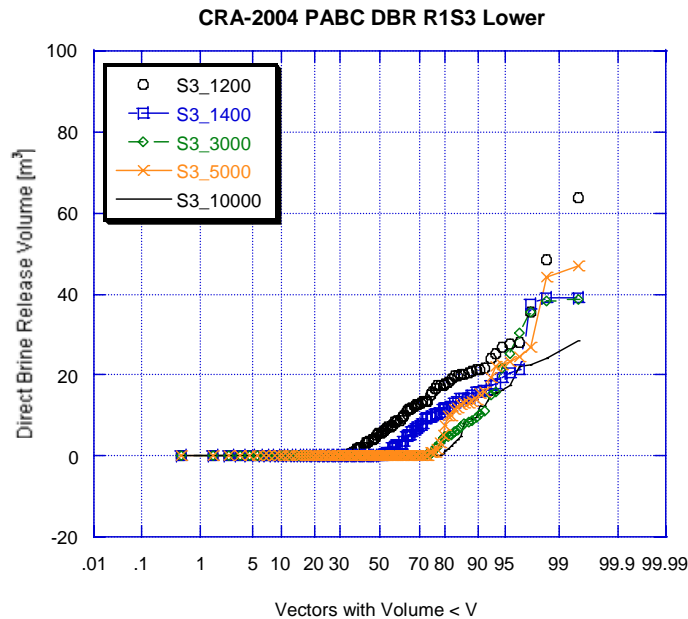
Figure 5-50. DBRs for Second Intrusions into Lower Panel, After an Initial E1 Intrusion at 1,000 Years
Replicate R1, Scenario S3 from CRA-2004 PABC.
(Note: Legend gives scenario number and intrusion time)

CRA-2004 PABC DBR R1S4 Lower
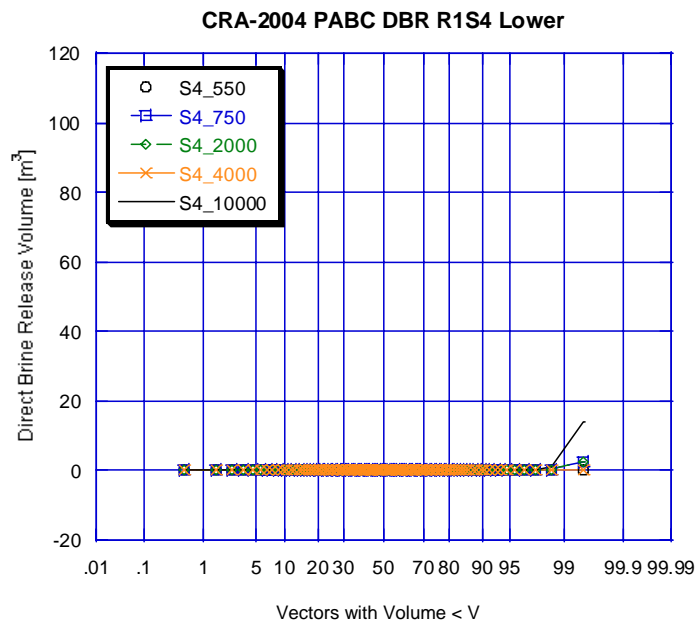
Figure 5-51. DBRs for Second Intrusions into Lower Panel, After an Initial E2 Intrusion at 350 Years
Replicate R1, Scenario S4 from CRA-2004 PABC.
(Note: Legend gives scenario number and intrusion time)

Information Only
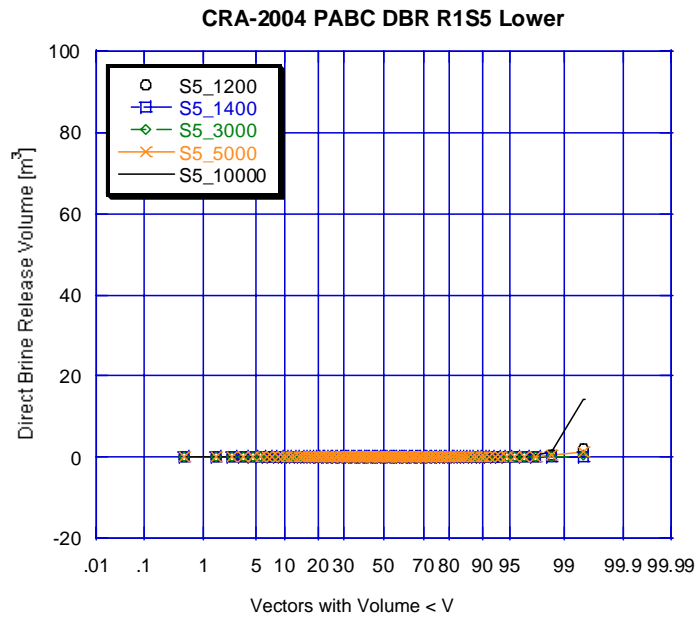
Figure 5-52. DBRs for Second Intrusions into Lower Panel, After an Initial E2 Intrusion at 1,000 Years
Replicate R1, Scenario S5 from CRA-2004 PABC.
(Note: Legend gives scenario number and intrusion time)
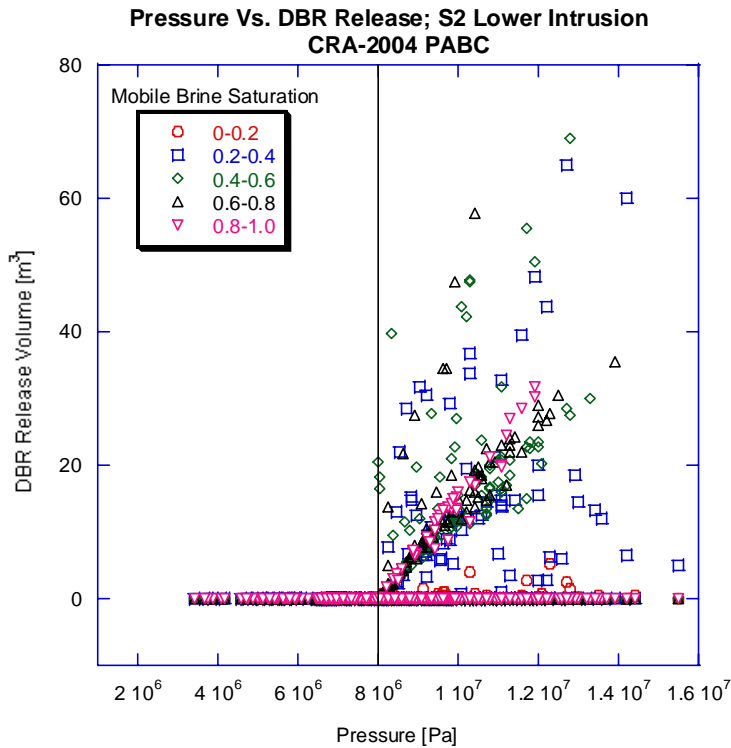
Figure 5-53. Sensitivity of DBR Volumes to Pressure and Mobile Brine Saturation, Replicate R1,
Scenario S2, Lower Panel from CRA-2004 PABC.
(Note: Symbols indicate the range of mobile brine saturation given in the legend.)

Information Only

Figure 5-54 plots mobile saturation versus pressure for the S2 scenario for all intrusion times with symbols indicating the range of DBR volumes.

Borehole permeability may be an important parameter in controlling the volume of direct brine releases. Borehole permeability is not a direct input to the DBR calculations, but this parameter affects conditions in the repository as modeled in the 10,000-year BRAGFLO calculations, which are used as initial conditions of the DBR model. Figure 5-55 shows a scatter plot of the log of borehole permeability against DBR volume for Scenario S2, lower intrusion with symbols indicating intrusion times. As borehole permeability decreases, direct brine releases tend to increase, especially at late intrusion times (4,000 and 10,000 years). Helton et al. (Helton et al., 1998) identified this same relationship in analysis of the CCA PA. Low values of borehole permeability tend to result in higher pressures following an E1 intrusion (Figure 5-55), which in turn lead to higher DBRs from subsequent intrusions.

Information Only
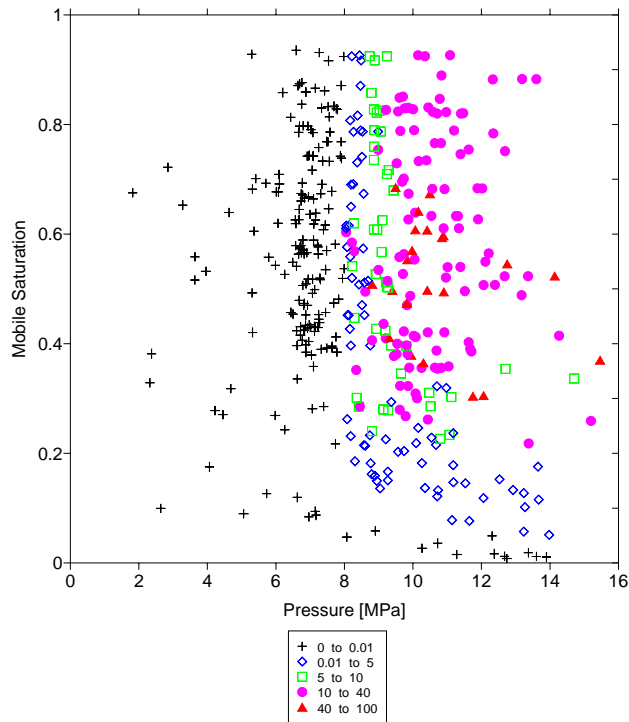
Figure 5-54. Sensitivity of DBR Volumes to Pressure and Mobile Brine Saturation, Replicate R1, Scenario S2, Lower Panel, from CRA-2004 PABC.
Here symbols in the plot and the legend represent the bin of DBR volumes (m^3) obtained.
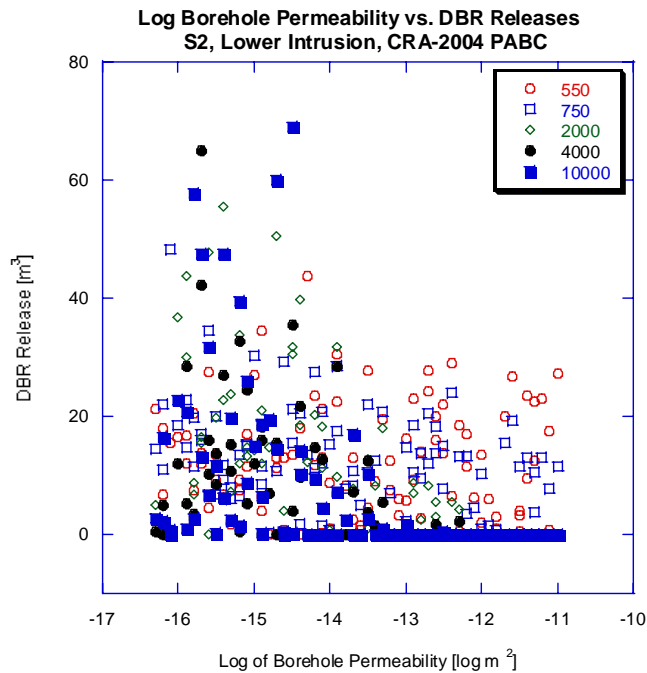
Figure 5-55. Sensitivity of DBR Volumes to Borehole Permeability, Replicate R1, Scenario S2, Lower Panel, from the CRA-2004 PABC.
(Note: Legend gives intrusion time)

109 of 153   Information Only

6. NORMALIZED RELEASES

This section presents total normalized releases for the CRA-2004 PABC, followed by discussion of each of the four categories of releases that constitute the total release: cuttings and cavings; spallings; DBRs; and transport releases. Within each following section, CRA-2004 PABC results are compared with CRA-2004 results.

6.1 TOTAL NORMALIZED RELEASES

Figure 6-1, Figure 6-2, and Figure 6-3 show the CCDFs for total releases for Replicates R1, R2, and R3 of the CRA-2004 PABC. Total releases are calculated by totaling the releases from each release pathway: cuttings and cavings releases, spallings releases, DBRs, and transport releases (there were no undisturbed releases to contribute to total release). Each CCDF lies below and to the left of the limits specified in 40 CFR § 191.13(a). Thus, the WIPP continues to comply with the containment requirements of 40 CFR Part 191.

To compare the distributions of CCDFs among replicates and to demonstrate sufficiency of the sample size, mean and quantile CCDFs are calculated. At each value for normalized release R on the abscissa, the CCDFs for a single replicate define 100 values for probability. The arithmetic mean of these 100 probabilities is the mean probability that release exceeds R; the curve defined by the mean probabilities for each value of R is the mean CCDF. The quantile CCDFs are defined analogously.

Figure 6-4 compares the mean, median, 90th, 50th, and 10th quantiles for each replicate's distribution of CCDFs for total releases. Figure 6-4 shows that each replicate's distribution is quite similar, and shows qualitatively that the sample size of 100 in each replicate is sufficient to generate a stable distribution of outcomes.

The overall mean CCDF in Figure 6-4 is computed as the arithmetic mean of the three mean CCDFs from each replicate. To quantitatively determine the sufficiency of the sample size, a confidence interval is computed about the overall mean CCDF using the Student's t-distribution and the mean CCDFs from each replicate. Figure 6-5 shows 95 percent confidence intervals about the overall mean.

Figure 6-6, Figure 6-8, and Figure 6-10 show the mean CCDFs for each component of total releases, for Replicates R1, R2, and R3 of the CRA-2004 PABC, respectively. For comparison, the mean CCDFs for each component of total releases for Replicates R1, R2, and R3 from the CRA-2004 are shown in Figure 6-7, Figure 6-9, and Figure 6-11, respectively.

Two significant differences between the mean CCDFs are observed. The first is that DBRs make a larger contribution to total releases in the CRA-2004 PABC than in the CRA-2004. For probabilities exceeding 0.01, cuttings and cavings are still the release mechanism that has the greatest impact on total releases. In fact, for probabilities larger than 0.02, the CRA-2004 PABC cuttings and cavings mean CCDF exceeds the other mean CCDFs by at least an order of magnitude. However, at low probabilities (<0.002), mean CRA-2004 PABC DBR releases exceed all other mean releases. In general, the mean DBR CCDF was at least an order of

magnitude less than the mean cuttings and cavings CCDF for all probabilities of the CRA-2004. Further discussion of normalized DBRs follows in Section 6.4.

The second major difference between the two analyses concerns the mean spallings CCDFs. The mean spallings releases for the CRA-2004 were larger than the mean spallings releases from the CRA-2004 PABC at all probabilities. In fact, at a probability of 0.1, the mean spallings CCDFs from the CRA-2004 exceed those from the CRA-2004 PABC by approximately two orders of magnitude (10^{-2} EPA units versus 10^{-4} EPA Units). Additionally, mean DBR releases are larger than mean spallings releases at all probabilities for the CRA-2004 PABC, whereas the opposite was true for almost all probabilities in the CRA-2004. Further discussion of spallings releases follows in Section 6.3.

Figure 6-12 provides an additional comparison between the CRA-2004 and CRA-2004 PABC. At probabilities exceeding 0.001, the overall mean CCDFs for total normalized releases from the two analyses are very similar. Mean total releases differ by less than 10^{-2} at a probability of 0.1 and by less than 10^{-1} at a probability of 0.001 (Table 6-1). The same trend holds true for the 90th quantile CCDFs for total releases. For lower probabilities, the CRA-2004 PABC mean CCDF slightly exceeds the CRA-2004 mean CCDF. This is attributed to the increased DBRs at these probabilities. Additionally, the CRA-2004 PABC confidence intervals on the overall means are narrower than the CRA-2004 confidence intervals at probabilities of 0.1 and 0.001. Explanation of this narrowing follows in Section 6.3.

There are some definite similarities between the CCDFs for the two analyses. First, for most probabilities, cuttings and cavings are the most significant pathways for release of radioactive material to the land surface. Second, release by subsurface transport in the Salado or Culebra make essentially no contribution to total releases. Finally, the resulting CCDFs of both analyses are within regulatory limits.

Table 6-1. CCA PAVT[a], CRA-2004, and CRA-2004 PABC Statistics on the Overall Mean for Total Normalized Releases at Probabilities of 0.1 and 0.001, All Replicates Pooled.

Probability	Analysis	Mean Total Release	90th Quantile Total Release	Lower 95% CL	Upper 95% CL
0.1	CCA PAVT	1.237E-1	1.916E-1	1.231E-1	1.373E-1
	CRA-2004	9.565E-2	1.571E-1	8.070E-2	1.104E-1
	CRA-2004 PABC	8.770E-2	1.480E-1	8.471E-2	9.072E-2
0.001	CCA PAVT	3.819E-1	3.907E-1	2.809E-1	4.357E-1
	CRA-2004	5.070E-1	8.582E-1	2.778E-1	5.518E-1
	CRA-2004 PABC	6.006E-1	8.092E-1	5.175E-1	6.807E-1

[a] CCA PAVT and CRA-2004 data was initially reported in (Vugrin, 2004b; Vugrin, 2004c)
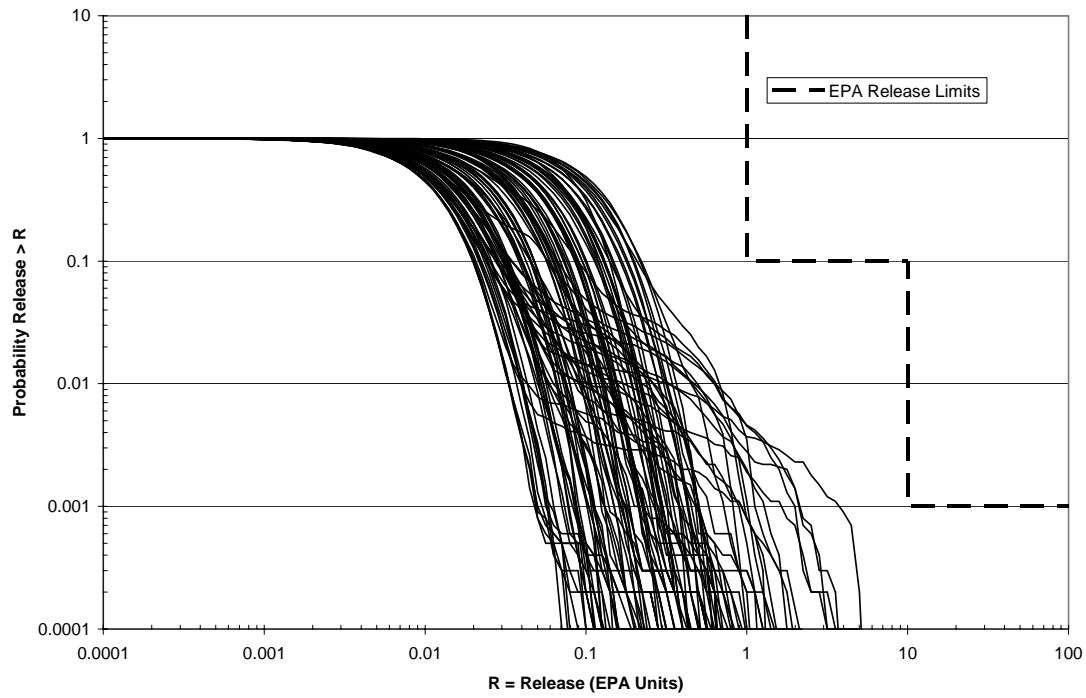
Figure 6-1. Total Normalized Releases: Replicate R1 of the CRA-2004 PABC
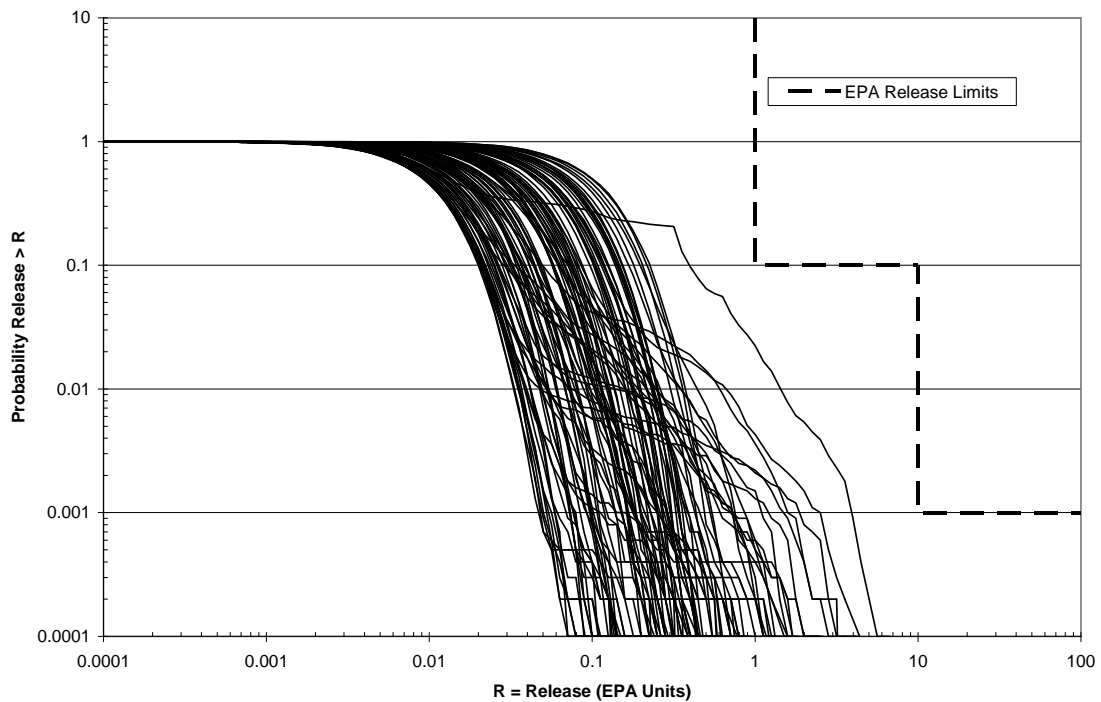
Figure 6-2. Total Normalized Releases: Replicate R2 of the CRA-2004 PABC
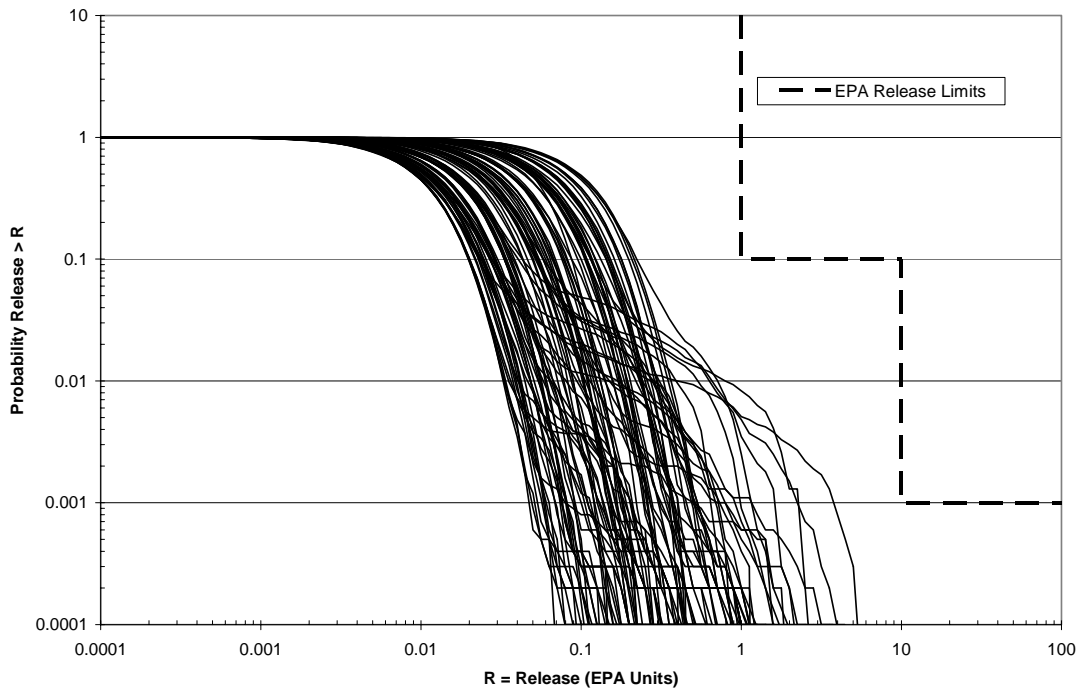
Figure 6-3. Total Normalized Releases: Replicate R3 of the CRA-2004 PABC
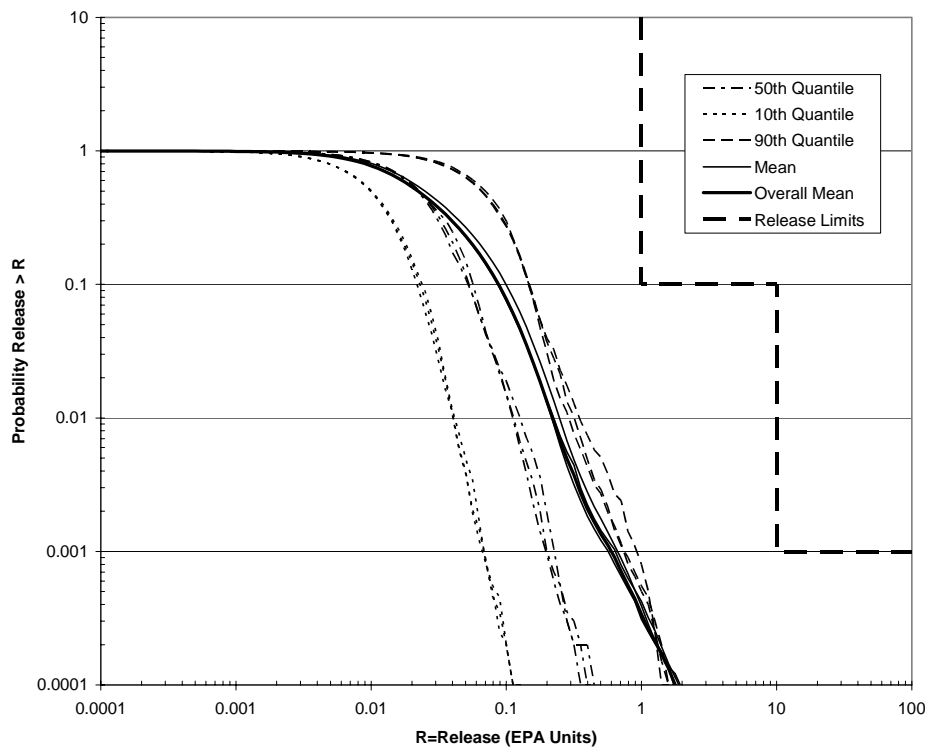
Figure 6-4. Mean and Quantile CCDFs for Total Normalized Releases: All Replicates of the CRA-2004
PABC
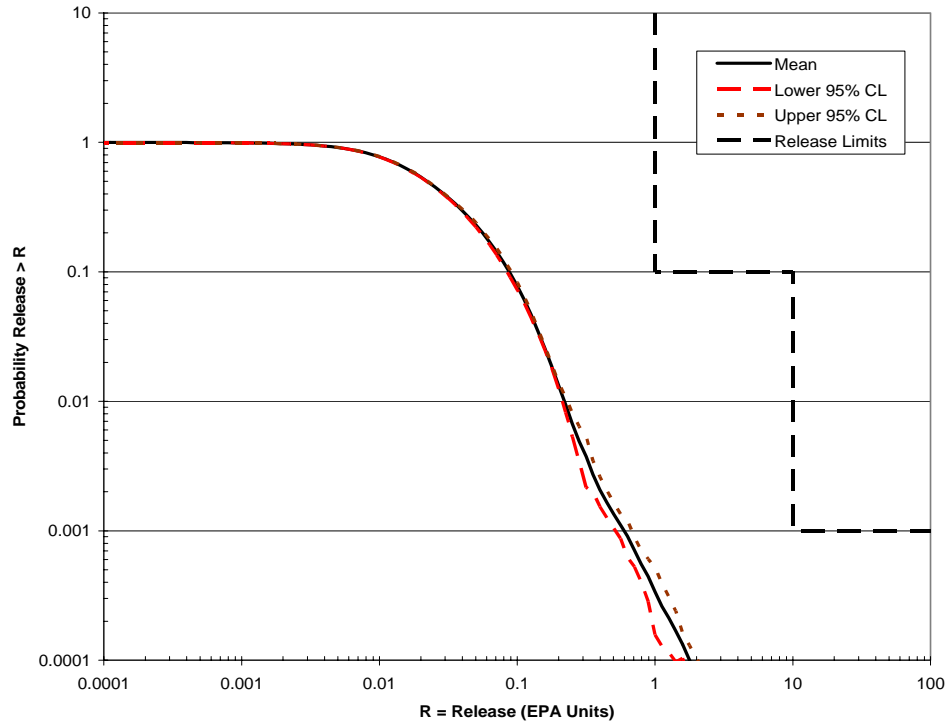
Figure 6-5. Confidence Interval on Overall Mean CCDF for Total Normalized Releases: CRA-2004 PABC
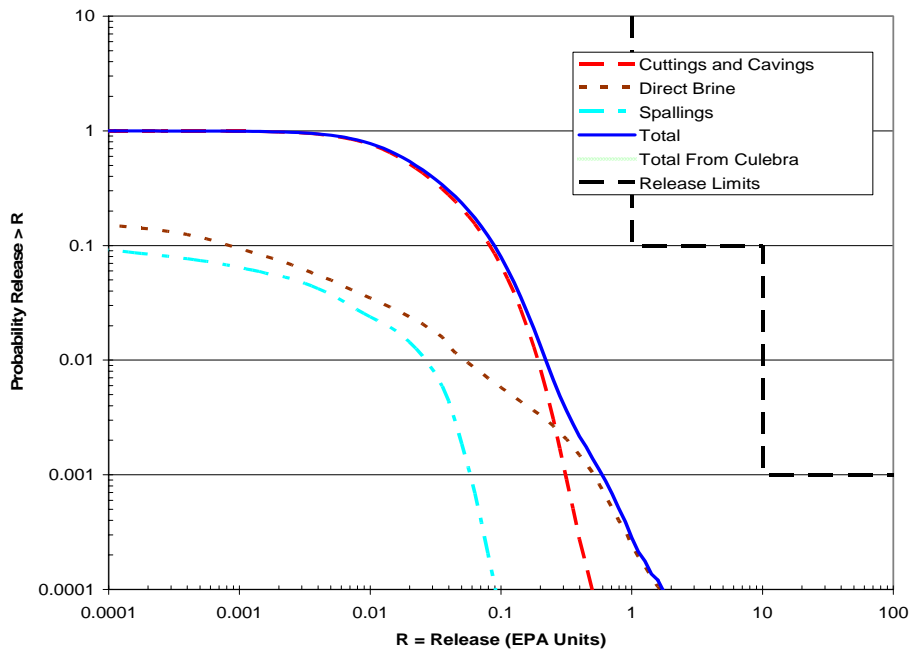
Figure 6-6. Mean CCDFs for Components of Total Normalized Releases: Replicate R1 of CRA-2004 PABC
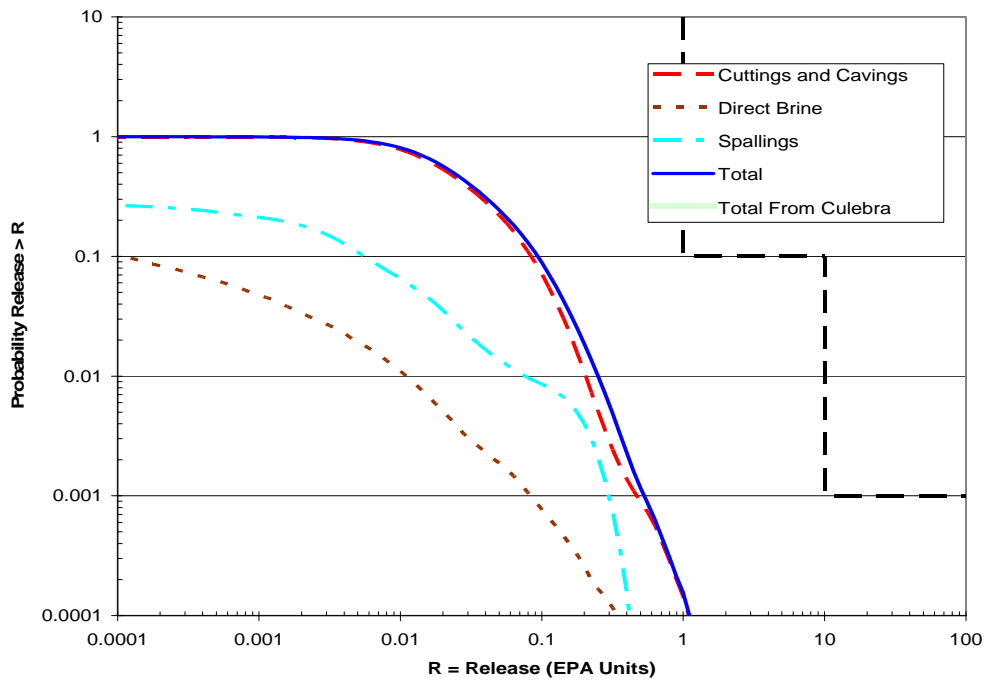
Figure 6-7. Mean CCDFs for Components of Total Normalized Releases: Replicate R1 of CRA-2004

Information Only
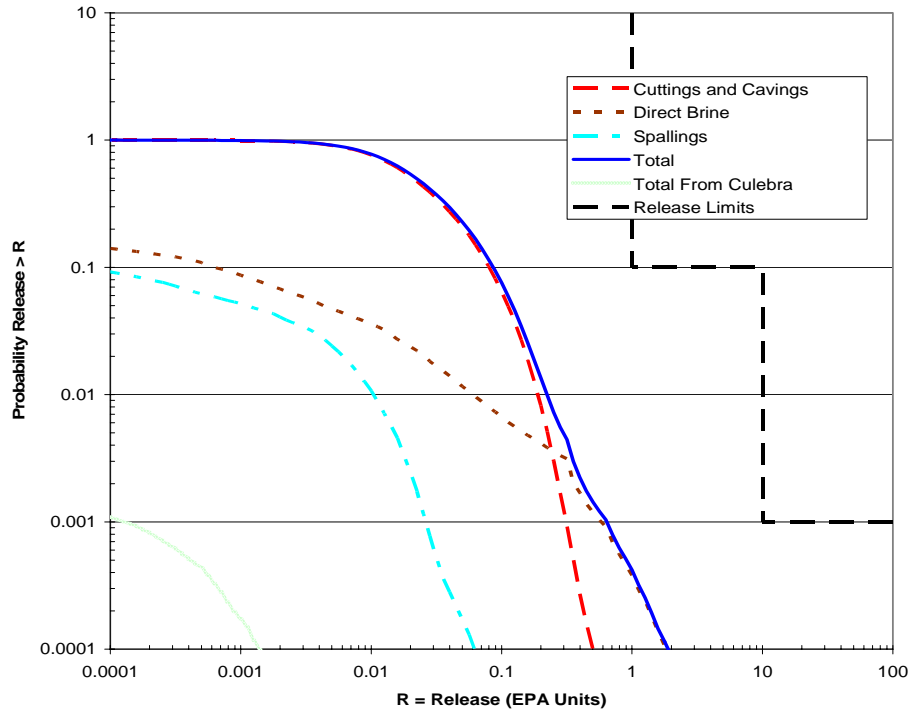
Figure 6-8. Mean CCDFs for Components of Total Normalized Releases: Replicate R2 of CRA-2004 PABC
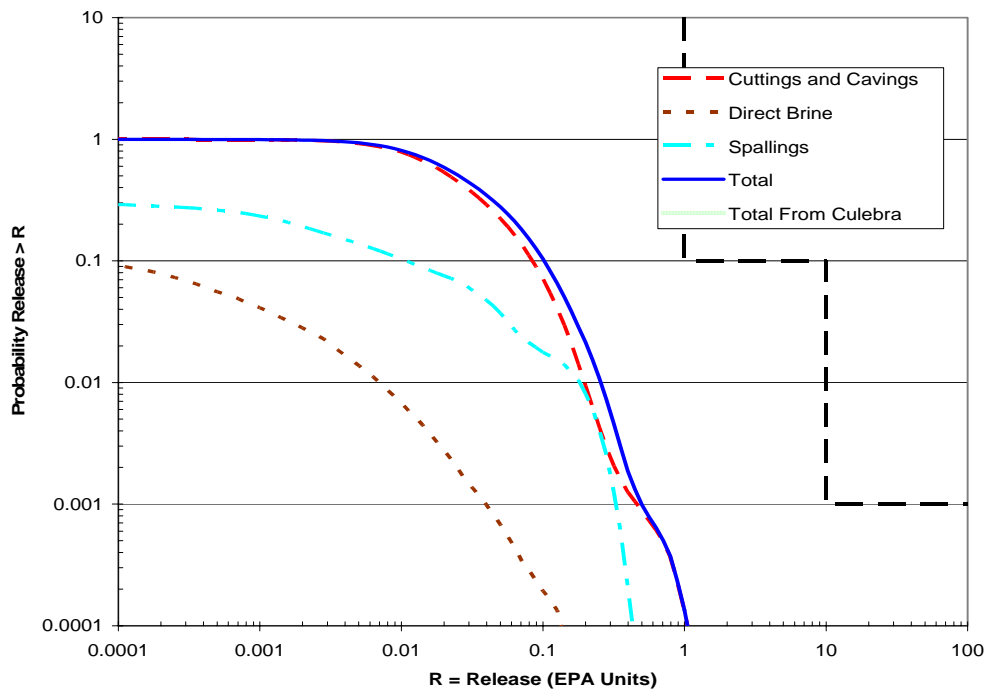
Figure 6-9. Mean CCDFs for Components of Total Normalized Releases: Replicate R2 of CRA-2004
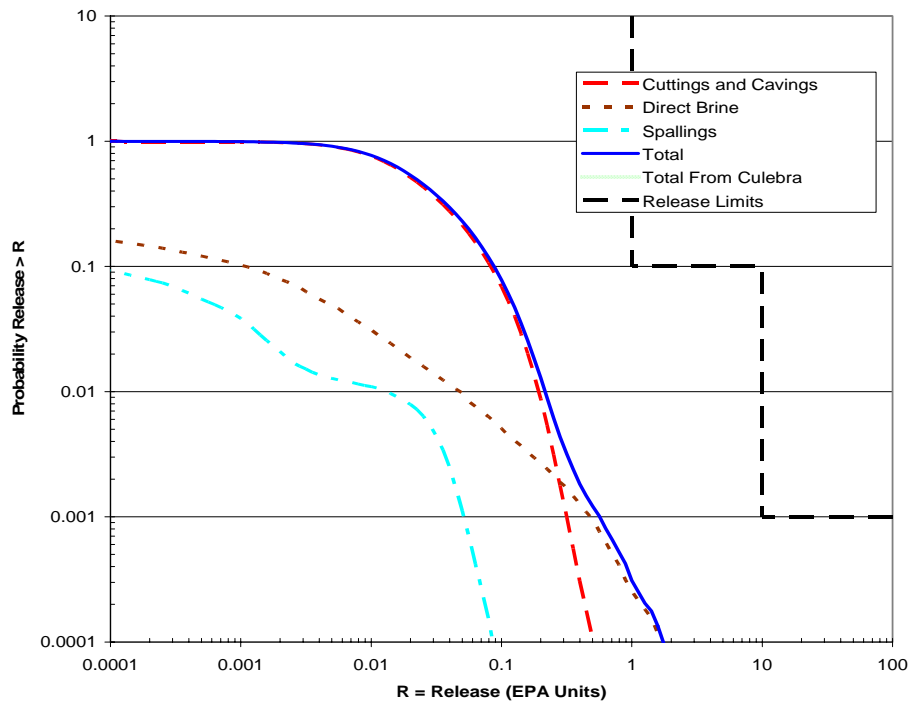
Figure 6-10. Mean CCDFs for Components of Total Normalized Releases: Replicate R3 of CRA-2004 PABC
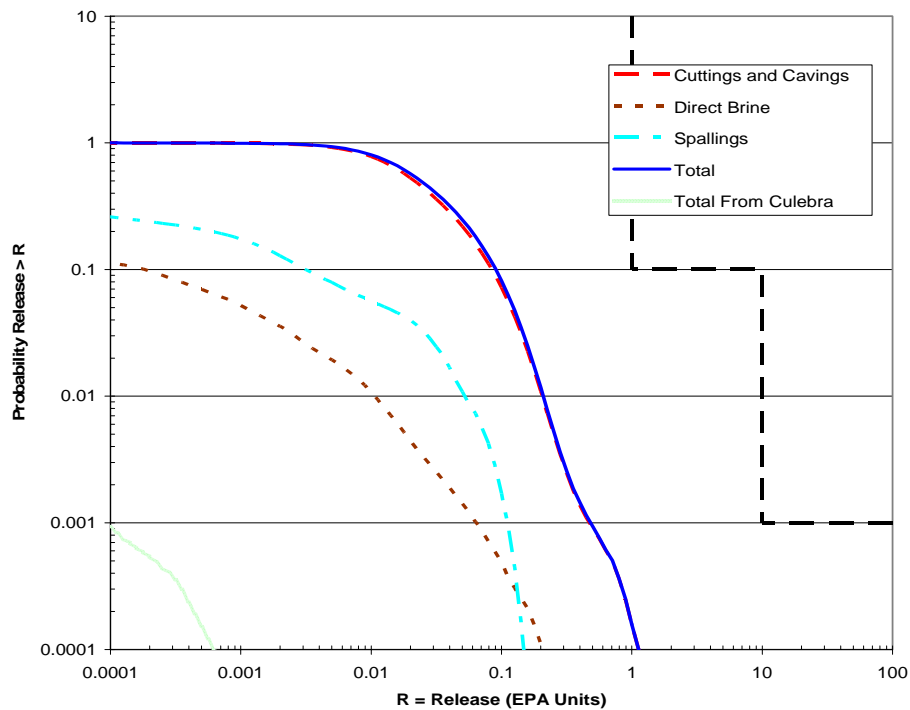
Figure 6-11. Mean CCDFs for Components of Total Normalized Releases: Replicate R3 of CRA-2004

Information Only
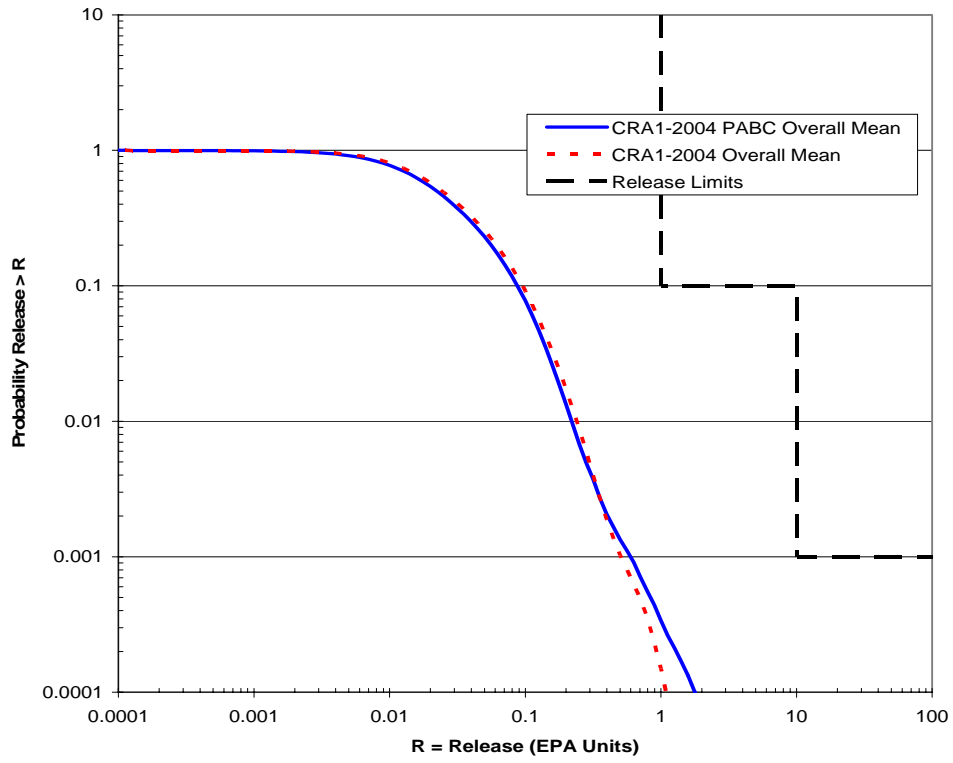
Figure 6-12. Overall Mean CCDFs for Total Normalized Releases: CRA-2004 PABC and CRA-2004

Information Only

6.2   CUTTINGS AND CAVINGS NORMALIZED RELEASES

Figure 6-13 shows the mean CCDFs for cuttings and cavings releases for Replicates R1, R2, and R3 of the CRA-2004 PABC. The releases in each replicate are very similar.

Figure 6-14 shows the mean CCDFs for cuttings and cavings releases for all replicates of the CRA-2004. For further comparison, the overall mean CCDFs for cuttings and cavings releases from both analyses are shown in Figure 6-15. These resulting overall mean CCDFs are very similar, with the only significant differences occurring at probabilities less than approximately 0.003. These differences are due to modifications of the inventory implemented in the CRA-2004 PABC since the overall mean CCDFs for cuttings and cavings volumes from the two analyses are nearly identical (Figure 6-16), and releases are calculated by multiplying the cuttings and cavings volume by the average activity of three randomly sampled waste streams.

The increase in CRA-2004 cuttings and cavings releases at a probability of 0.003 in each replicate was due to a single waste stream, LA-TA-55-48, with very high radioactivity that was present in the CRA-2004 inventory. This waste stream maintains significant radioactivity during the 10,000-year period. The volume of the LA-TA-55-48 waste stream in the CRA-2004 inventory (31 m^3) implies a probability of $31/168,500 = 0.00018$ that this waste stream is selected as one of the three waste streams contributing to the cuttings and cavings release for a single intrusion. However, in any future of the repository, roughly six intrusions are expected (Dunagan, 2003), implying that 18 waste streams are selected for cuttings and cavings releases. The mean probability that the LA-TA-55-48 waste stream was selected at least once for cuttings and cavings releases in the CRA-2004 is estimated to be

$$1 - \left(1 - 0.00018\right)^{18} = 0.0033 \, .$$

LA-TA-55-48 was updated for the CRA-2004 PABC (See Section 2.1). The volume did not change significantly (23 m^3 in the CRA-2004 PABC), but the radionuclide activities for this waste stream are significantly smaller in the CRA-2004 PABC than they were in CRA-2004. The result is that the CRA-2004 PABC cuttings and cavings releases at a probability of about 0.003 are less than those from CRA-2004.
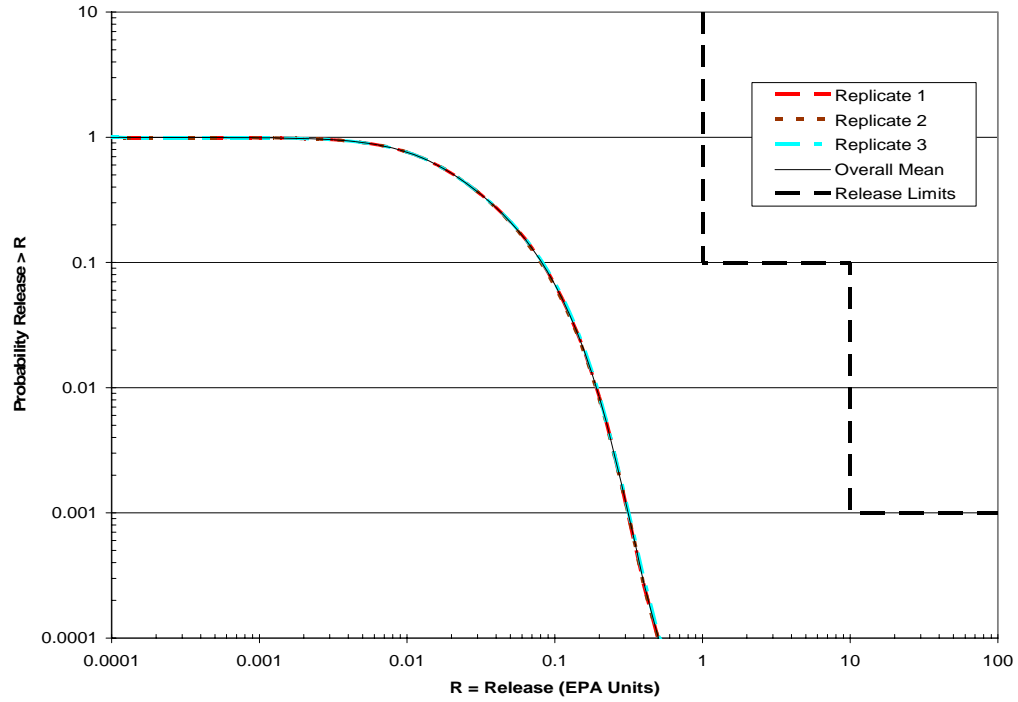
Figure 6-13. Mean CCDFs for Cuttings and Cavings Releases: All Replicates of the CRA-2004 PABC
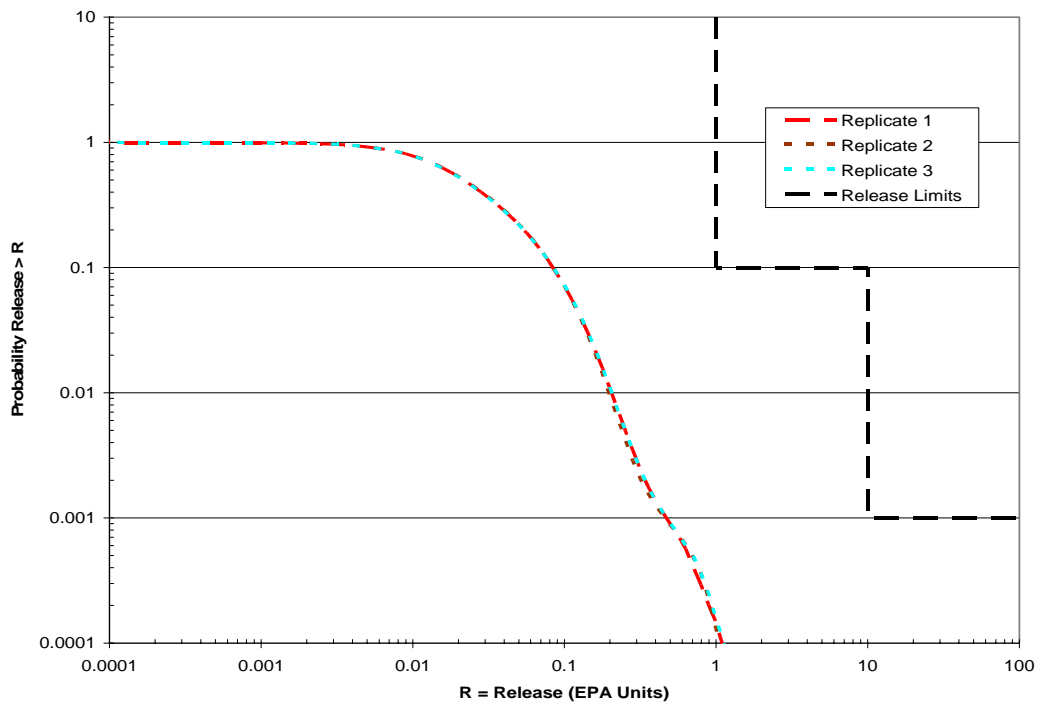
Figure 6-14. Mean CCDFs for Cuttings and Cavings Releases: All Replicates of the CRA-2004
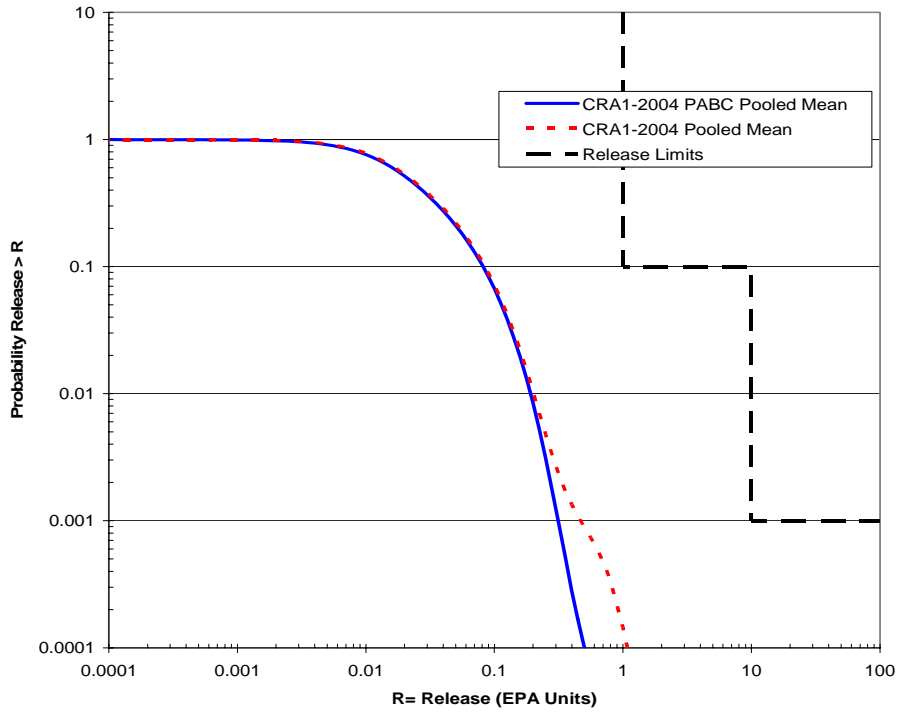
Figure 6-15. Overall Mean CCDFs for Cuttings and Cavings Releases: CRA-2004 PABC and CRA-2004
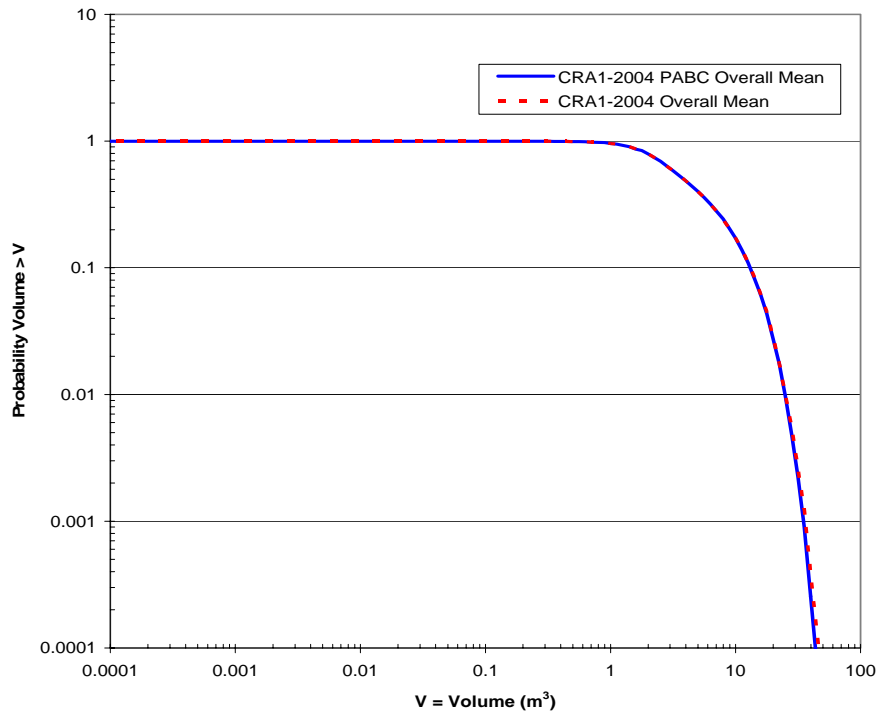
Figure 6-16. Overall Mean CCDFs for Cuttings and Cavings Volumes: CRA-2004 PABC and CRA-2004

6.3   SPALLINGS NORMALIZED RELEASES

Figure 6-17 shows the mean spallings release CCDFs for all replicates of the CRA-2004 PABC. For comparison, the mean spallings release CCDFs from the CRA-2004 are shown in Figure 6-18, and Figure 6-19 shows the overall mean spallings release CCDFs for both analyses.

At all probabilities, CRA-2004 PABC overall mean spallings releases are significantly smaller than overall mean spallings releases from the CRA-2004. At a probability of 0.1, CRA-2004 PABC releases are approximately two orders of magnitude smaller (approximately 10^{-4} versus 10^{-2}), and at a probability of 0.001, CRA-2004 PABC releases are one order of magnitude smaller (approximately 10^{-2} versus 10^{-1}).

This decrease in overall mean spallings release values can be directly attributed to a decrease in overall mean spallings volumes (Figure 6-20). Spallings releases are calculated by multiplying spallings volume by the average repository activity at the time of the release. For any given probability shown in Figure 6-19 and Figure 6-20, the overall mean spallings release decreased by approximately the same order of magnitude as the overall mean spallings volume.

As indicated in Figure 5-43, Figure 5-44, and, Figure 5-45 the distributions of spallings volumes from a single intrusion calculated by DRSPALL from the CRA-2004 PABC and CRA-2004 were similar. CUTTINGS_S interpolates the DRSPALL volumes using repository pressures calculated by BRAGFLO to calculate the spallings volume released from a single intrusion for the WIPP PA intrusion scenarios. As shown in Section 5.5.1, the frequency of nonzero spallings intrusions calculated by CUTTINGS_S decreased significantly when compared with CUTTINGS_S calculations for the CRA-2004. This reduction is directly attributed to the lower pressures resulting from reduced gas generation rates implemented in BRAGFLO for the CRA-2004 PABC. In fact, about two thirds of all CRA-2004 PABC vectors did not have CCDFs that predicted a release of 10^{-4} EPA units at any probability. This compares with approximately one half of all CRA-2004 vectors.

The decreased mean spallings releases for the CRA-2004 PABC had a direct impact on the confidence intervals for the overall mean CCDF for total releases. Of cuttings and cavings, spallings, and DBRs, the mean CCDFs for spallings releases showed the greatest variability in the CRA-2004. This variability directly contributed to the variability of the mean CCDFs for total releases which affects the size of the confidence intervals on the overall mean CCDF. Since the CRA-2004 PABC mean spallings CCDFs decreased in magnitude, the spallings mean variability has less of an impact on the variability of total releases. Little variability is observed between replicates of DBR mean CCDFs and cuttings and cavings mean CCDFs for the CRA-2004 PABC, and the result was narrower confidence intervals on the overall mean for total releases.
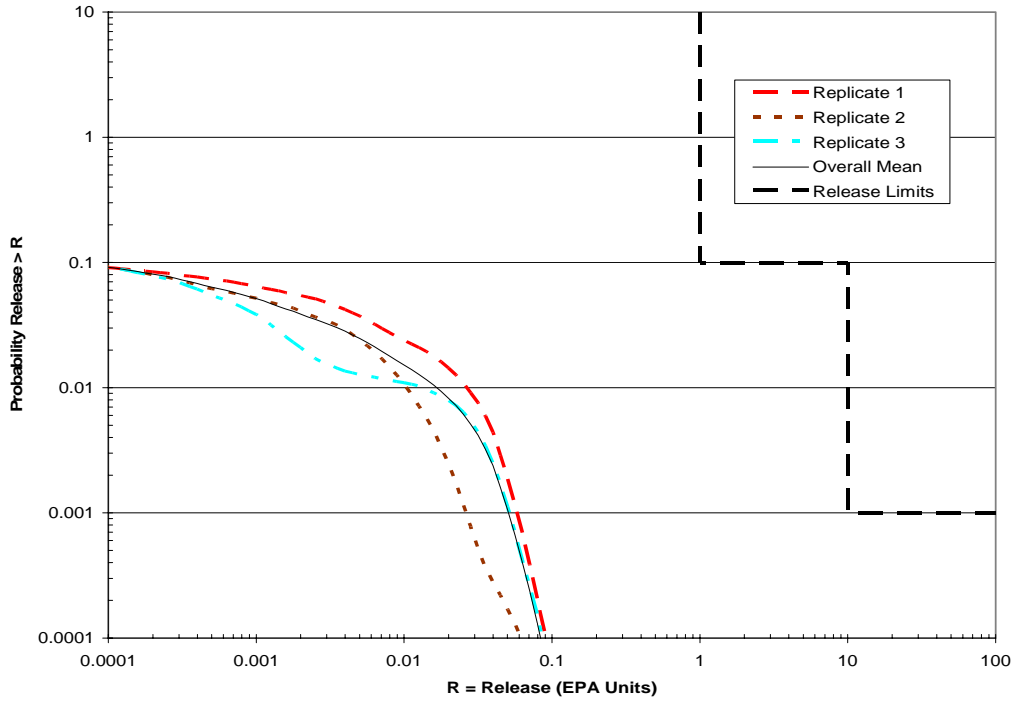
Figure 6-17. Mean CCDFs for Spallings Releases: All Replicates of the CRA-2004 PABC
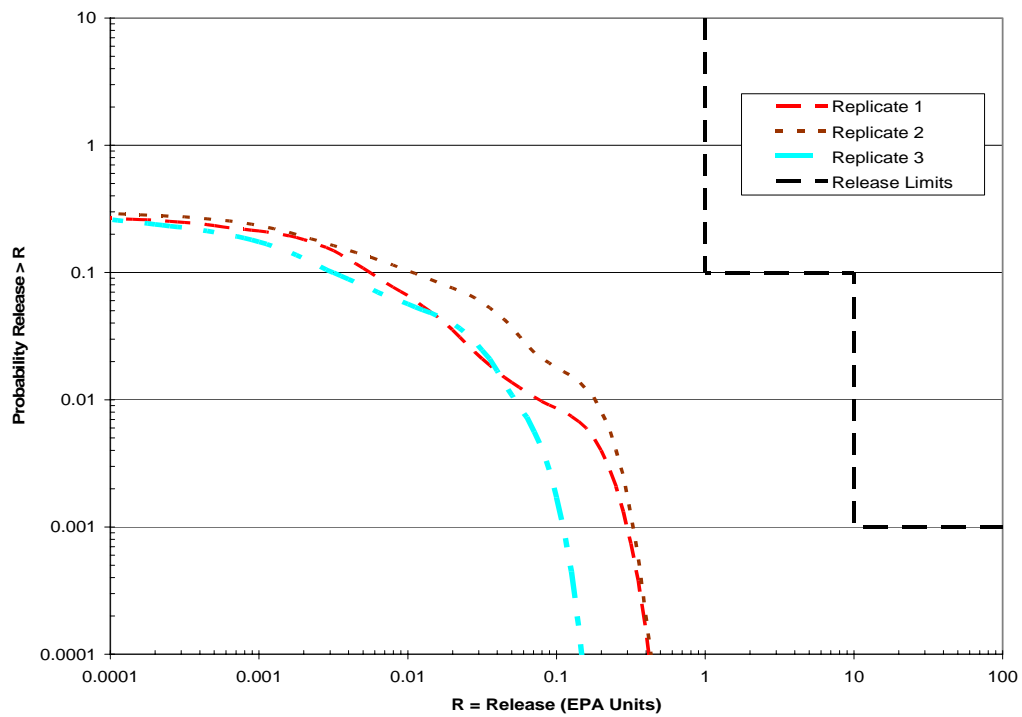
Figure 6-18. Mean CCDFs for Spallings Releases: All Replicates of the CRA-2004
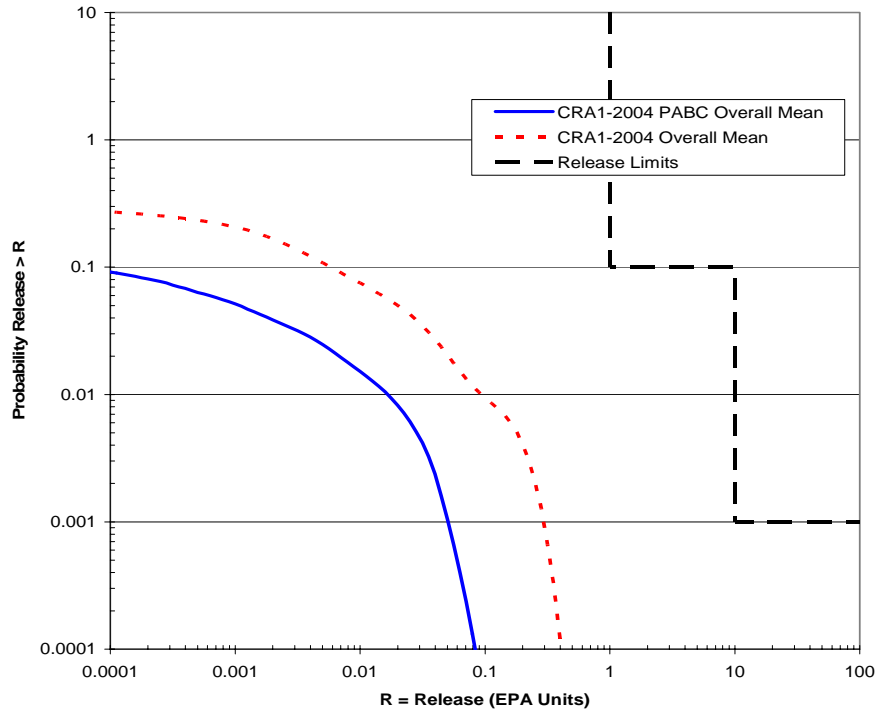
Figure 6-19. Overall Mean CCDFs for Spallings Releases: CRA-2004 PABC and CRA-2004
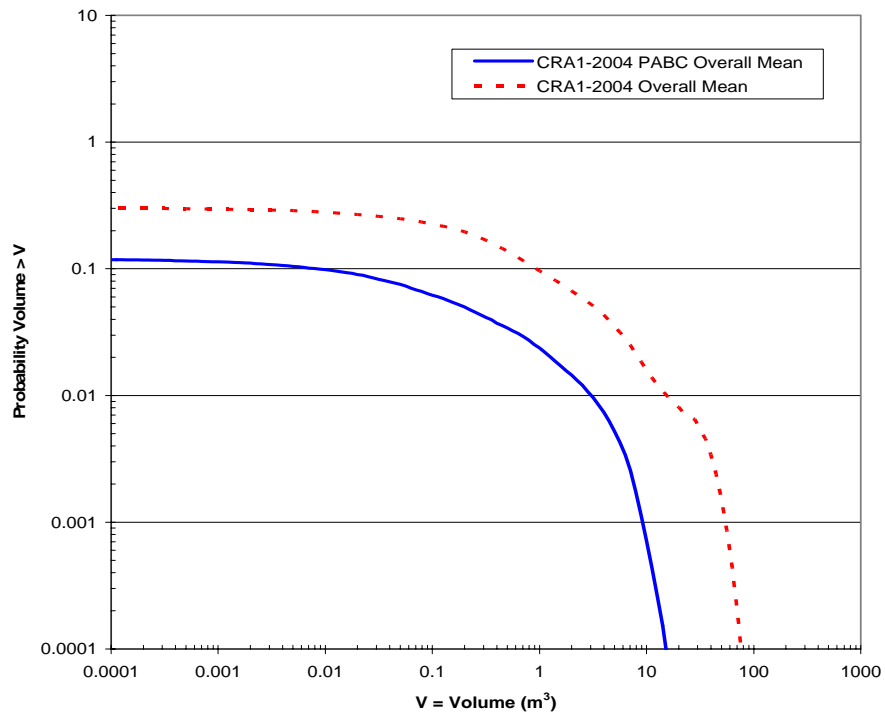
Figure 6-20. Overall Mean CCDFs for Spallings Volumes: CRA-2004 PABC and CRA-2004

6.4   NORMALIZED DIRECT BRINE RELEASES

Figure 6-21 shows the mean DBR CCDFs for all replicates of the CRA-2004 PABC. For comparison, the mean DBR CCDFs are shown in Figure 6-22, and Figure 6-23 shows the overall mean DBR CCDFs from both analyses. At all probabilities, CRA-2004 PABC mean DBRs increased from the CRA-2004 values. In fact, DBRs are now the second largest contributor to total releases at most probabilities, and the dominant contributor at very low probabilities (Figure 6-6, Figure 6-8, and Figure 6-10).

Calculation of DBRs can be primarily affected by two sources: the volume of the DBR and the solubility of actinides in the brine. The overall mean CCDFs for DBR volumes from the two analyses are shown in Figure 6-24. The overall mean CCDF for CRA-2004 PABC volumes exceeds that of the CRA-2004 for probabilities greater than 0.02, and for smaller probabilities, the CRA-2004 overall mean CCDF for DBR volumes predicts slightly larger volumes. Implementation of the reduced gas generation rates may have had a small impact on mean DBR volumes or mean DBRs, but, the larger CRA-2004 PABC mean DBR releases must be attributed primarily to the changes implemented in the CRA-2004 PABC that affect actinide solubilities (see Sections 2.5 and 2.6) since the differences in overall mean DBR volumes are not as large as the differences in overall mean DBRs.
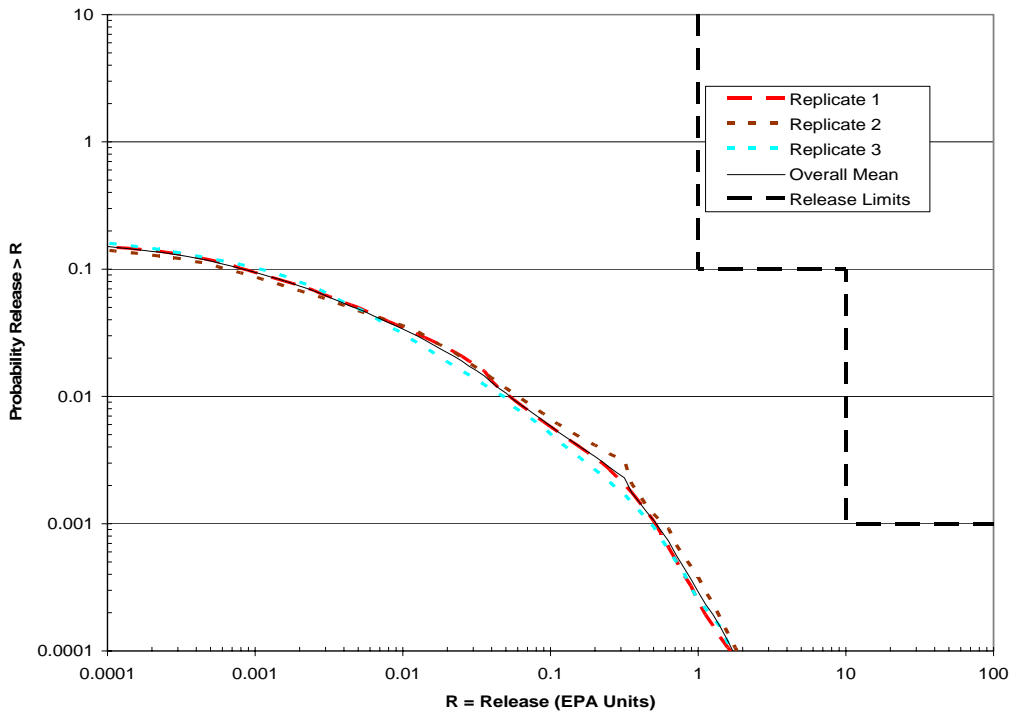
Figure 6-21. Mean CCDFs for DBRs: All Replicates of the CRA-2004 PABC
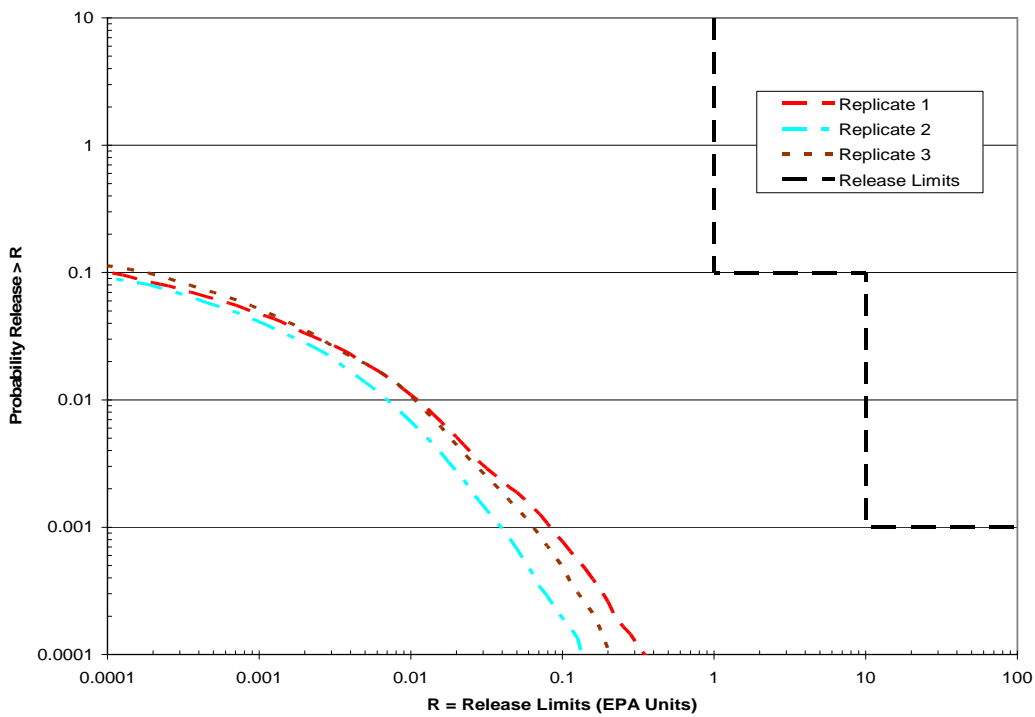
Figure 6-22. Mean CCDFs for DBRs: All Replicates of the CRA-2004
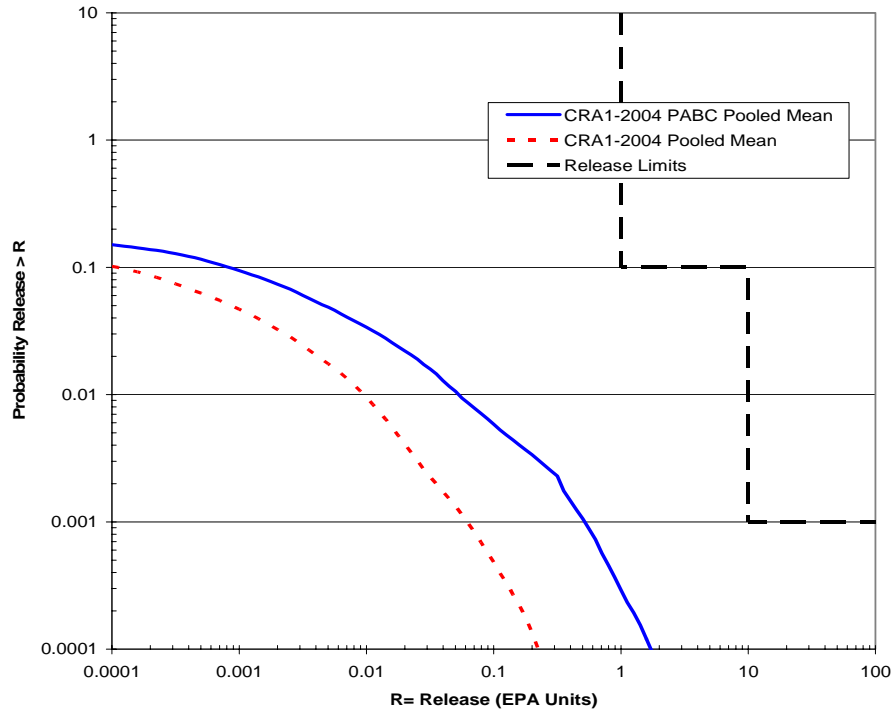
Figure 6-23. Overall Mean CCDFs for DBRs: CRA-2004 PABC and CRA-2004
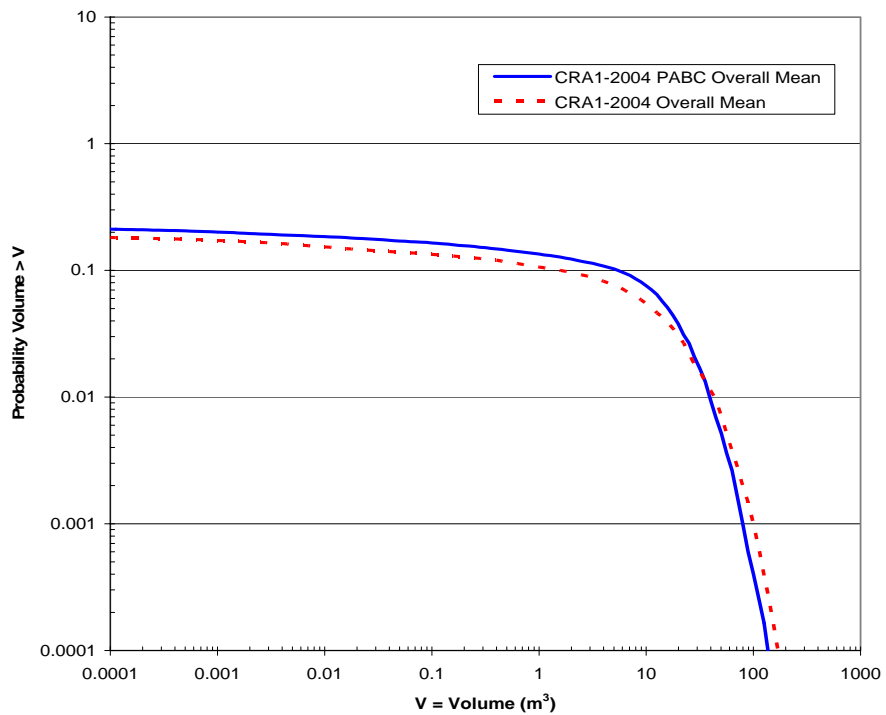
Figure 6-24. Overall Mean CCDFs for DBR Volumes: CRA-2004 PABC and CRA-2004

127 of 153

Information Only

6.5   NORMALIZED TRANSPORT RELEASES

Figure 6-25 shows the mean CCDF for normalized releases due to transport through the Culebra for replicate R2 (no transport releases larger than 10^{-6} EPA units occurred in Replicates R1 and R3).

Normalized transport releases for the CRA-2004 PABC are qualitatively similar to the CRA-2004 results in that only one replicate exhibits releases that are significantly larger than the numerical error inherent in the transport calculations. Overall, fewer vectors had releases in the CRA-2004 PABC than were observed in the CRA-2004. This decrease is attributed to the increase in mean advective travel times that occurred when the exclusion zone around oil and gas boreholes was removed from the mining-modified Culebra T-fields.
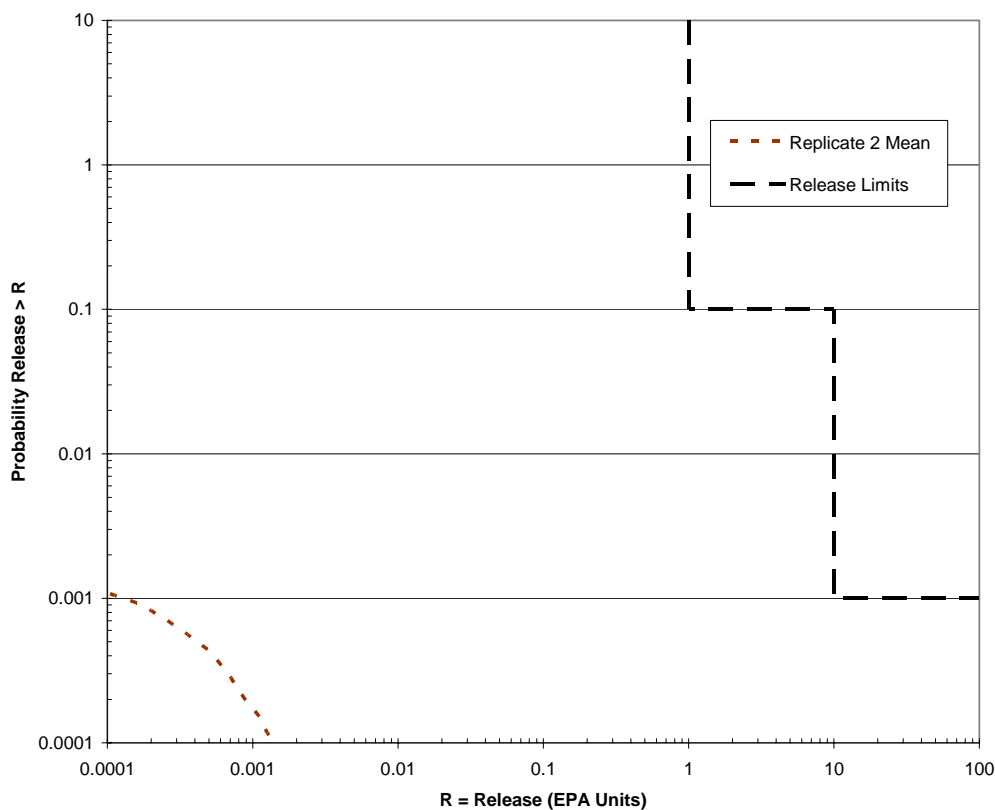
Figure 6-25. Mean CCDF for Releases from the Culebra for Replicate R2 of the CRA-2004 PABC

7. SENSITIVITY ANALYSIS FOR NORMALIZED RELEASES

Regression was used to evaluate the sensitivity of the output variables to the sampled parameters. The rank regression analyses were conducted using STEPWISE version 2.21. STEPWISE receives sampled input parameter values and calculated release data that correspond to those input data. STEPWISE relates the sampled input parameter values to the calculated release data by performing a multiple regression analysis and reporting the results tabularly. Scatter plots of the dependent versus independent rank transformed variables resulting from the analysis were examined to determine if there were any obvious non-monotonic relationships. Obvious non-monotonic relationships were not found although there are cases involving inputs that are categorized as discrete variables (e.g. OXSTAT) and cases where there are large proportions of the vectors showing no release (e.g. CULREL). Application of linear regression to such cases is somewhat problematic in terms of the assumptions of normally-distributed residuals and homogeneous variance among the residuals. However, in terms of ranking the relative importance of the parameters these issues are probably not significant. Additional analyses were performed on selected subsets of the data using Microsoft® Excel. Details of the analysis can be found in Kirchner (2005b).

Most of the regression models produced by STEPWISE do not include all of the variables, even after rank transforming the data. This simply indicates that the uncertainties in many of the parameters have statistically insignificant effects on the output variable. Statistical insignificance can arise because the output variable has a low functional response to the input variable, because the magnitude of uncertainty in the input variable is small relative to the other inputs, or from a combination of both conditions. This is not to say that these non-significant variables have no influence on the releases. Their exclusion from the tables reflects the inability of this statistical technique to rank their importance with an acceptable degree of confidence. For example, if the response of the output variable to an input variable was non-monotonic then the regression analysis might fail to properly identify that variable's importance. This possibility is unlikely for total releases and cuttings and cavings releases because the R^2 value indicates that nearly all the variability in the output variables has been accounted for by the listed input variables.

Several of the parameters that appear in the model often contribute very little to the R^2 value and, therefore, explain very little of the variability in the output variable. Parameters that have minor contributions can appear by chance, simply due to random correlations. Many of the parameters that account for only a few percent to the variability in an output from one replicate may show different rankings, or can even be absent, in another replicate. Thus, it is difficult to assess the importance of the parameters that improve the regression model very little and, in reality, they may have no importance at all. Therefore, only the parameters that appear to have significant impacts on the regression model will be explained in detail.

In the following discussion the results of the CRA-2004 PABC sensitivity analysis are discussed and compared to the results obtained for the CRA-2004 sensitivity analysis prepared in response to EPA's comment C-23-18 (Kirchner, 2004b). Although STEPWISE was run on the results for all three replicates, only the results for replicate one are discussed herein. The results from the

other two replicates were examined to verify that results of the analysis of replicate one were representative of the other two replicates. The tables that appear in the following sections list the variable names of the parameters as assigned in the input file to STEPWISE. These short names are required because of a limitation in the length of variable names in STEPWISE. Table 7-1 associates these names with the material and property names.

Table 7-1. Material and Property Values Associated with the Variable Names Used in the CRA-2004 PABC Sensitivity Analysis.

Variable Name	Material Name	Property Name	Description
ANHBCEXP	S_MB139	PORE_DIS	Brooks-Corey pore distribution parameter for anhydrite (dimensionless). Defines λ for regions MB 138, Anhydrite AB, and MB 139 for use with Brooks-Corey model; defines λ in m= λ /(1+ λ) for use with van Genuchten-Parker model in the same regions. Units: NONE Distribution: Student Minimum: 0.49053 Maximum: 0.84178 Mean: 0.6436 Median: 0.6436 Standard Deviation: 0.1086
ANHBCVGP	S_MB139	RELP_MOD	Indicator for relative permeability model (dimensionless) for regions MB 138, Anhydrite AB and MB 139. Units: NONE Distribution: Delta Minimum: 1 Maximum: 4 Mean: 4 Median: 4
ANHPRM	S_MB139	PRMX_LOG	Logarithm of intrinsic anhydrite permeability (m^2). Used in regions MB 138, Anhydrite AB, and MB 139. Units: $\log(m^2)$ Distribution: Student Minimum: -21 Maximum: -17.1 Mean: -18.89 Median: -18.89 Standard Deviation: 1.196
ANRBRSAT	S_MB139	SAT_RBRN	Residual brine saturation in anhydrite (dimensionless). Defines S_{br} in regions MB 138, Anhydrite AB, and MB 139. Units: NONE Distribution: Student Minimum: 0.0077846 Maximum: 0.17401 Mean: 0.08362 Median: 0.08362 Standard Deviation: 0.05012
BHPERM	BH_SAND	PRMX_LOG	Logarithm of intrinsic permeability (m^2) of the silty sand-filled borehole. Used in regions Upper Borehole and Lower Borehole. Units: $\log(m^2)$ Distribution: Uniform Minimum: -16.3 Maximum: -11 Mean: -13.65 Median: -13.65 Standard Deviation: 1.53
BPCOMP	CASTILER	COMP_RCK	Bulk compressibility (Pa^{-1}) of Castile brine reservoir. Units: Pa^{-1} Distribution: Triangular Minimum: 0.00000000002 Maximum: 0.0000000001 Mean: 0.000000000053 Median: 0.00000000004 Standard Deviation: 0.000000000017
BPINTPRS	CASTILER	PRESSURE	Initial brine pore pressure in the Castile brine reservoir. Defines $P_b(x,y,-5)$ for region CASTILER. Units: Pa Distribution: Triangular Minimum: 11100000 Maximum: 17000000 Mean: 13600000 Median: 12700000 Standard Deviation: 1245700
BPPRM	CASTILER	PRMX_LOG	Logarithm of intrinsic permeability (m^2) of the Castile brine reservoir. Used in region CASTILER. Units: $\log(m^2)$ Distribution: Triangular Minimum: -14.7 Maximum: -9.8 Mean: -12.1 Median: -11.8 Standard Deviation: 1.01
CCLIMSF	GLOBAL	CLIMTIDX	Climate scale factor (dimensionless) for Culebra flow field. Defines SFC. Units: NONE Distribution: Cumulative Minimum: 1 Maximum: 2.25 Mean: 1.31 Median: 1.17 Standard Deviation: 0.348
CCLIMSF	GLOBAL	CLIMTIDX	Climate index Units: NONE Distribution: Cumulative Minimum: 1 Maximum: 2.25 Mean: 1.31 Median: 1.17 Standard Deviation: 0.348
CFRACPOR	CULEBRA	APOROS	Culebra fracture (i.e., advective) porosity (dimensionless). Units: NONE Distribution: Loguniform Minimum: 0.0001 Maximum: 0.01 Mean: 0.0021 Median: 0.001 Standard Deviation: 0.0025

Variable Name	Material Name	Property Name	Description
CFRACSP	CULEBRA	HMBLKLT	Culebra fracture spacing (m). Equal to half the distance between fractures (i.e., the Culebra half matrix block length). Units: m Distribution: Uniform Minimum: 0.05 Maximum: 0.5 Mean: 0.275 Median: 0.275 Standard Deviation: 0.13
CMKDAM3	AM+3	MKD_AM	Matrix distribution coefficient (m^3/kg) for Am in +3 oxidation state. Units: m^3/kg Distribution: Loguniform Minimum: 0.02 Maximum: 0.4 Mean: 0.13 Median: 0.09 Standard Deviation: 0.1
CMKDPU3	PU+3	MKD_PU	Matrix distribution coefficient (m^3/kg) for Pu in +3 oxidation state. Units: m^3/kg Distribution: Loguniform Minimum: 0.02 Maximum: 0.4 Mean: 0.13 Median: 0.09 Standard Deviation: 0.1
CMKDPU4	PU+4	MKD_PU	Matrix distribution coefficient (m^3/kg) for Pu in +4 oxidation state. Units: m^3/kg Distribution: Loguniform Minimum: 0.7 Maximum: 10 Mean: 3.5 Median: 2.6 Standard Deviation: 2.5
CMKDTH4	TH+4	MKD_TH	Matrix distribution coefficient (m^3/kg) for Th in +4 oxidation state. Units: m^3/kg Distribution: Loguniform Minimum: 0.7 Maximum: 10 Mean: 3.5 Median: 2.6 Standard Deviation: 2.5
CMKDU4	U+4	MKD_U	Matrix distribution coefficient (m^3/kg) for U in +4 oxidation state. Units: m^3/kg Distribution: Loguniform Minimum: 0.7 Maximum: 10 Mean: 3.5 Median: 2.6 Standard Deviation: 2.5
CMKDU6	U+6	MKD_U	Matrix distribution coefficient (m^3/kg) for U in +6 oxidation state. Units: m^3/kg Distribution: Loguniform Minimum: 0.00003 Maximum: 0.02 Mean: 0.0031 Median: 0.00077 Standard Deviation: 0.0046
CMTRXPOR	CULEBRA	DPOROS	Culebra matrix (i.e., diffusive) porosity (dimensionless). Units: NONE Distribution: Cumulative Minimum: 0.1 Maximum: 0.25 Mean: 0.16 Median: 0.16 Standard Deviation: 0.035
CONBCEXP	CONC_PCS	PORE_DIS	Brooks-Corey pore distribution parameter (dimensionless) for panel closure concrete. Defines λ for region CONC_PCS for use with Brooks-Corey model; defines λ in m= λ /(1+ λ) for use with van Genuchten-Parker model in region CONC_PCS. Units: NONE Distribution: Cumulative Minimum: 0.11 Maximum: 8.1 Mean: 2.52 Median: 0.94 Standard Deviation: 2.48
CONBRSAT	CONC_PCS	SAT_RBRN	Residual brine saturation (dimensionless) in panel closure concrete. Defines S_{br} for use in region CONC_PCS. Units: NONE Distribution: Cumulative Minimum: 0 Maximum: 0.6 Mean: 0.25 Median: 0.2 Standard Deviation: 0.176
CONGSSAT	CONC_PCS	SAT_RGAS	Residual gas saturation (dimensionless) in panel closure concrete. Defines S_{gr} area CONC_PCS. Units: NONE Distribution: Uniform Minimum: 0 Maximum: 0.4 Mean: 0.2 Median: 0.2 Standard Deviation: 0.1155
CONPRM	CONC_PCS	PRMX_LOG	Logarithm of intrinsic permeability (m^2) for the concrete portion of the panel closure. Used in region CONC_PCS. Units: $\log(m^2)$ Distribution: Triangular Minimum: -20.699 Maximum: -17 Mean: -18.816 Median: -18.7496 Standard Deviation: 0.755
CTRAN	GLOBAL	TRANSIDX	Indicator variable for selecting transmissivity field. Units: NONE Distribution: Uniform Minimum: 0 Maximum: 1 Mean: 0.5 Median: 0.5 Standard Deviation: 0.289
CTRAN	GLOBAL	TRANSIDX	Index for selecting realizations of the transmissivity field Units: NONE Distribution: Uniform Minimum: 0 Maximum: 1 Mean: 0.5 Median: 0.5 Standard Deviation: 0.289

Information Only

Variable Name	Material Name	Property Name	Description
CTRANSFM	CULEBRA	MINP_FAC	Multiplier (dimensionless) applied to transmissivity of the Culebra within the land withdrawal boundary after mining of potash reserves. Defines MF. Units: NONE Distribution: Uniform Minimum: 1 Maximum: 1000 Mean: 500.5 Median: 500.5 Standard Deviation: 288.4
CTRANSFM	CULEBRA	MINP_FAC	Mining transmissivity multiplier Units: NONE Distribution: Uniform Minimum: 1 Maximum: 1000 Mean: 500.5 Median: 500.5 Standard Deviation: 288.4
DOMEGA	BOREHOLE	DOMEGA	Drill string angular velocity (rad/s). Units: rad/s Distribution: Cumulative Minimum: 4.2 Maximum: 23 Mean: 8.63 Median: 7.8 Standard Deviation: 3.16
DRZPCPRM	DRZ_PCS	PRMX_LOG	Logarithm of intrinsic permeability (m^2) of the DRZ immediately above the panel closure concrete. Used in region DRZ_PCS. Units: $\log(m^2)$ Distribution: Triangular Minimum: -20.699 Maximum: -17 Mean: -18.816 Median: -18.7496 Standard Deviation: 0.755
DRZPRM	DRZ_1	PRMX_LOG	Logarithm of intrinsic permeability (m^2) of the DRZ. Used in regions Upper DRZ and Lower DRZ. Units: $\log(m^2)$ Distribution: Uniform Minimum: -19.4 Maximum: -12.5 Mean: -16 Median: -16 Standard Deviation: 2
HALCROCK	S_HALITE	COMP_RCK	Bulk compressibility of halite (Pa^{-1}). Units: Pa^{-1} Distribution: Uniform Minimum: 0.00000000000294 Maximum: 0.000000000192 Mean: 0.0000000000975 Median: 0.0000000000975 Standard Deviation: 0.0000000000546
HALPOR	S_HALITE	POROSITY	Halite porosity (dimensionless). Units: NONE Distribution: Cumulative Minimum: 0.001 Maximum: 0.03 Mean: 0.0128 Median: 0.01 Standard Deviation: 0.00852
HALPRM	S_HALITE	PRMX_LOG	Logarithm of intrinsic halite permeability (m^2). Used in region Salado. Units: $\log(m^2)$ Distribution: Uniform Minimum: -24 Maximum: -21 Mean: -22.5 Median: -22.5 Standard Deviation: 0.866025
PBRINE	GLOBAL	PBRINE	Probability that a drilling intrusion penetrates pressurized brine in the Castile Formation. Units: NONE Distribution: Uniform Minimum: 0.01 Maximum: 0.6 Mean: 0.305 Median: 0.305 Standard Deviation: 0.17
PLGPRM	CONC_PLG	PRMX_LOG	Logarithm of intrinsic permeability (m^2) of the concrete borehole plugs. Used in region Borehole Plugs. Units: $\log(m^2)$ Distribution: Uniform Minimum: -19 Maximum: -17 Mean: -18 Median: -18 Standard Deviation: 0.58
REPIPERM	SPALLMOD	REPIPERM	Waste permeability of gas local to intrusion borehole. Units: m^2 Distribution: Loguniform Minimum: 0.000000000000024 Maximum: 0.0000000000024 Mean: 0.000000000000516 Median: 0.00000000000024 Standard Deviation: 0.0000000000006
SALPRES	S_HALITE	PRESSURE	Initial brine pore pressure (Pa) in the Salado halite, applied at an elevation consistent with the intersection of MB 139. Units: Pa Distribution: Uniform Minimum: 11040000 Maximum: 13890000 Mean: 12470000 Median: 12470000 Standard Deviation: 823000
SHLPRM2	SHFTL_T1	PRMX_LOG	Logarithm of intrinsic permeability (m^2) of lower shaft seal materials for the first 200 years after closure. Used in region Lower Shaft. Units: $\log(m^2)$ Distribution: Cumulative Minimum: -20 Maximum: -16.5 Mean: -18 Median: -18.2 Standard Deviation: 0.597

Information Only

Variable Name	Material Name	Property Name	Description
SHLPRM3	SHFTL_T2	PRMX_LOG	Logarithm of intrinsic permeability (m^2) of lower shaft seal materials from 200 years to 10,000 years after closure. Used in region Lower Shaft. Units: log(m^2) Distribution: Cumulative Minimum: -22.5 Maximum: -18 Mean: -19.8 Median: -20.1 Standard Deviation: 0.937
SHUPRM	SHFTU	PRMX_LOG	Logarithm of intrinsic permeability (m^2) of upper shaft seal materials. Used in region Upper Shaft. Units: log(m^2) Distribution: Cumulative Minimum: -20.5 Maximum: -16.5 Mean: -18.2 Median: -18.3 Standard Deviation: 0.794
SHURBRN	SHFTU	SAT_RBRN	Residual brine saturation in upper shaft seal materials (dimensionless). Units: NONE Distribution: Cumulative Minimum: 0 Maximum: 0.6 Mean: 0.25 Median: 0.2 Standard Deviation: 0.176
SHURGAS	SHFTU	SAT_RGAS	Residual gas saturation in upper shaft seal materials (dimensionless). Units: NONE Distribution: Uniform Minimum: 0 Maximum: 0.4 Mean: 0.2 Median: 0.2 Standard Deviation: 0.116
SPLPTDIA	SPALLMOD	PARTDIAM	Particle diameter of disaggregated waste. Units: m Distribution: Loguniform Minimum: 0.001 Maximum: 0.1 Mean: 0.0215 Median: 0.01 Standard Deviation: 0.025
SPLRPOR	SPALLMOD	REPIPOR	Waste porosity at time of drilling intrusion Units: NONE Distribution: Uniform Minimum: 0.35 Maximum: 0.66 Mean: 0.505 Median: 0.505 Standard Deviation: 0.0895
TENSLSTR	SPALLMOD	TENSLSTR	Tensile strength of waste. Units: Pa Distribution: Uniform Minimum: 120000 Maximum: 170000 Mean: 145000 Median: 145000 Standard Deviation: 14400
WASTWICK	WAS_AREA	SAT_WICK	Increase in brine saturation of waste due to capillary forces (dimensionless). Defines S_{wick} for areas Waste Panel, South RoR, and North RoR. Units: NONE Distribution: Uniform Minimum: 0 Maximum: 1 Mean: 0.5 Median: 0.5 Standard Deviation: 0.289
WBIOGENF	WAS_AREA	BIOGENFC	Probability of obtaining sampled microbial gas generation rates. Units: NONE Distribution: Uniform Minimum: 0 Maximum: 1 Mean: 0.5 Median: 0.5 Standard Deviation: 0.288675
WFBETCEL	CELLULS	FBETA	Scale factor used in definition of stoichiometric coefficient for microbial gas generation (dimensionless). Units: NONE Distribution: Uniform Minimum: 0 Maximum: 1 Mean: 0.5 Median: 0.5 Standard Deviation: 0.28868
WGRCOR	STEEL	CORRMCO2	Rate of anoxic steel corrosion (m/s) under brine inundated conditions and with no CO2 present. Defines Rci for areas Waste Panel, South RoR, and North RoR. Units: m/s Distribution: Uniform Minimum: 0 Maximum: 3.17E-14 Mean: 1.585E-14 Median: 1.585E-14 Standard Deviation: 9.151E-15
WGRMICH	WAS_AREA	GRATMICH	Rate of CPR biodegradation (mol C6H10O5 / kg C6H10O5 / s) under anaerobic, humid conditions. Defines Rmh for areas Waste Panel, South RoR, and North RoR. Units: moles/(kg-s) Distribution: Uniform Minimum: 0 Maximum: 0.00000000102717 Mean: 0.000000000513585 Median: 0.000000000513585 Standard Deviation: 0.000000000296518
WGRMICH	WAS_AREA	GRATMICH	Rate of CPR biodegradation (mol C6H10O5 / kg C6H10O5 / s) under anaerobic, humid conditions. Defines Rmh for areas Waste Panel, South RoR, and North RoR. Units: moles/(kg-s) Distribution: Uniform Minimum: 0 Maximum: 0.0000000012684 Mean: 0.0000000006342 Median: 0.0000000006342 Standard Deviation: 0.00000000036616

Information Only

Variable Name	Material Name	Property Name	Description
WGRMICI	WAS_AREA	GRATMICI	Rate of CPR biodegradation (mol C6H10O5 / kg C6H10O5 / s) under anaerobic, brine-inundated conditions. Units: moles/(kg-s) Distribution: Uniform Minimum: 3.08269E-11 Maximum: 0.000000000556921 Mean: 0.000000000293874 Median: 0.000000000293874 Standard Deviation: 0.00000000015187
WMICDFLG	WAS_AREA	PROBDEG	Index for model of microbial degradation of CPR materials (dimensionless). Used in areas Waste Panel, South RoR, and North RoR. Units: NONE Distribution: Delta Minimum: 1 Maximum: 2 Mean: 1.25 Median: 1.25
WOXSTAT	GLOBAL	OXSTAT	Indicator variable for elemental oxidation states (dimensionless). WOXSTAT = 0 indicates use of CMKDPU3, CMKDU4, WSOLPU3C, WSOLPUS, WSOLU4C, and WSOLU4S. WOXSTAT = 1 implies use of CMKDPU4, CMKDU6, WSOLPU4C, WSOLPU4S, WSOLU6C, and WSOLU6S. Units: NONE Distribution: Uniform Minimum: 0 Maximum: 1 Mean: 0.5 Median: 0.5 Standard Deviation: 0.289
WPHUMOX3	PHUMOX3	PHUMCIM	Ratio (dimensionless) of concentration of actinides attached to humic colloids to dissolved concentration of actinides for oxidation state +III in Castile brine. Defines SFHum(Castile, +3, Am) and SFHum(Castile, +3, Pu). Units: NONE Distribution: Cumulative Minimum: 0.065 Maximum: 1.6 Mean: 1.1 Median: 1.37 Standard Deviation: 0.469
WRBRNSAT	WAS_AREA	SAT_RBRN	Residual brine saturation in waste (dimensionless). Units: NONE Distribution: Uniform Minimum: 0 Maximum: 0.552 Mean: 0.276 Median: 0.276 Standard Deviation: 0.1593
WRGSSAT	WAS_AREA	SAT_RGAS	Residual gas saturation in waste (dimensionless). Units: NONE Distribution: Uniform Minimum: 0 Maximum: 0.15 Mean: 0.075 Median: 0.075 Standard Deviation: 0.0433
WSOLTH4C	SOLTH4	SOLCIM	Uncertainty factor (dimensionless) for solubility of Th in the +IV oxidation state in Castile brine. Units: moles/liter Distribution: Cumulative Minimum: -2 Maximum: 1.4 Mean: 0.18 Median: -0.09 Standard Deviation: 0.368
WSOLU4C	SOLU4	SOLCIM	Uncertainty factor (dimensionless) for solubility of U in the +IV oxidation state in Castile brine. Units: moles/liter Distribution: Cumulative Minimum: -2 Maximum: 1.4 Mean: 0.18 Median: -0.09 Standard Deviation: 0.368
WSOLVAR3	SOLMOD3	SOLVAR	Solubility multiplier for +III oxidation states Units: NONE Distribution: Cumulative Minimum: -3 Maximum: 2.85 Mean: 0.034877 Median: -0.030682 Standard Deviation: 0.9002
WSOLVAR4	SOLMOD4	SOLVAR	Solubility multiplier for +IV oxidation states Units: NONE Distribution: Cumulative Minimum: -1.8 Maximum: 2.4 Mean: 0.108333 Median: 0.075 Standard Deviation: 0.837116
WTAUFAIL	BOREHOLE	TAUFAIL	Shear strength of waste (Pa). Units: Pa Distribution: Loguniform Minimum: 0.05 Maximum: 77 Mean: 10.5 Median: 1.96 Standard Deviation: 17.1

In addition, three variables are created in STEPWISE through transformation of the variable WOXSTAT (material GLOBAL, property OXSTAT), the indicator variable for oxidation states of uranium and plutonium. WOXSTAT is sampled as a (0,1) uniform distribution but is treated in the code as a Bernoulli distribution (a distribution having only two discrete states). The

variable OXSTAT is assigned 0 if WOXSTAT is less than 0.5 and is assigned 1 otherwise. If OXSTAT is 0 then CMKDU is assigned CMKDU6 and CMKDPU is assigned CMKDPU4. These are the K_ds for the +VI and +IV oxidation states of uranium and plutonium, respectively. If OXSTAT is 1 then CMKDU is assigned CMKDU4 and CMKDPU is assigned CMKDPU3, i.e. the K_ds for the +IV and +III oxidation states of uranium and plutonium, respectively.

7.1   THE METHODS USED BY STEPWISE

The sampling design used to propagate uncertainty in the CRA-2004 PABC starts with the generation of three replicates of 100 samples of the uncertain (epistemic) parameters using a Latin Hypercube sampling design. Each sample of the parameters, or "LHS element", represents a vector in parameter space. For each of these elements, 10,000 simulations are run in which the stochastic (aleatory) variables, such as drilling location, are sampled. Thus a distribution of releases is produced for every LHS element. In the STEPWISE analysis, it is the expected values (means) of these distributions that are correlated with parameter values.

STEPWISE uses a forward stepwise approach. In this approach, a sequence of regression models is constructed starting with the input parameter that has the strongest simple correlation with the output variable. Partial correlations between the residuals of the output and the remaining variables are then computed. The partial correlations remove the linear effects of variables already included in the model. The variable having the largest significant partial correlation coefficient is added next, and the partial correlations for the remaining input variables are recomputed. Significance is determined using an F-test, and the significance level for adding an input variable to the model is $1-\alpha_{in}$, where α_{in} is a parameter set by the analyst. The F-test compares the variability contributed by the variable to the variability not accounted for by the regression, i.e. the variability of the residuals. By default STEPWISE sets $\alpha_{in} = 0.05$, so that one is 95% confident that there is a partial correlation between the input and output variables. This process is repeated until there are no variables remaining having significant correlations with the output variable. Variables excluded from the regression model contribute no significant information in relation to the unexplained variability and hence the results are judged to be relatively insensitive to those parameters.

Input variables that are added to the regression model are not necessarily retained. For an input variable to be retained, its regression coefficient, i.e. the linear contribution of an input to the prediction of the output variable, must be statistically distinguishable from zero. A t-test is used to determine whether a regression coefficient is significantly different than zero. The t-test evaluates the null hypothesis that the regression coefficient is zero. The hypothesis is not rejected when random effects can give rise to the observed regression coefficient with probability α_{out}. The random effects are caused by the stochastic variability contributed by the input variables not in the regression model. In other words, the hypothesis is rejected, and the variable is included in the model when the $1-\alpha_{out}$ confidence interval of the regression coefficient does not encompass zero. By default the STEPWISE α_{out} -value for allowing a variable to enter the regression model is 0.05. Thus, in the default case, one is 95% confident that the input variables make a linear contribution to the response of the output variable. The user may specify different α-values in the input control file. However, the value allowing a variable to enter the

model, α_{in}, must be less than or equal to the value by which a variable is allowed to leave the model, α_{out}, to avoid looping. In the following analyses, α_{in} was 0.05, and α_{out} was 0.05.

7.2 TOTAL RELEASES

As shown in the CRA-2004, cuttings, cavings and spallings releases account for an overwhelming majority of the total releases (DOE 2004). In both analyses, uncertainty in total normalized releases is largely due to uncertainty in waste shear strength (WTAUFAIL). The volumes of cuttings and cavings are primarily controlled by shear strength, and the negative correlation found in the analysis is expected. In the CRA-2004, the first five parameters added to the regression model for mean total releases are associated with the production of cuttings, cavings and spallings (Table 7-2). However, in the CRA-2004 PABC direct brine releases supplant spallings as the second-most important contributor to total releases, and even surpass cuttings and cavings at low probabilities (Figure 7-1). In the CRA-2004 the second most important variable was the index for microbial degradation (WMICDFLG), although it explained less than an additional 2% of the variability. In the CRA-2004 PABC the second most important variable is WSOLVAR3, a "solubility multiplier" added to the CRA-2004 PABC analysis to represent uncertainty in solubilities for all actinides in the +III oxidation state (Xiong et al., 2005). The drill string angular velocity (DOMEGA), also used in computing cuttings and cavings, appears third in the list of both analyses. Each of the remaining parameters explain less than 1% of the variability in the total releases.

Table 7-2. Stepwise Rank Regression Analysis For Expected Normalized Total Releases

	Expected Normalized Release					
	CRA-2004 PABC			**CRA-2004**		
Step[a]	**Variable[b]**	**SRRC[c]**	**$R^{2\,[d]}$**	**Variable**	**SRRC**	**R^2**
1	WTAUFAIL	-0.94	0.88	WTAUFAIL	-0.95	0.91
2	WSOLVAR3	0.14	0.91	WMICDFLG	0.12	0.93
3	DOMEGA	0.10	0.92	DOMEGA	0.11	0.94
4	WFBETCEL	-0.09	0.93	SPALLVOL	0.08	0.94
5	BPINTPRS	0.08	0.93	BPINTPRS	0.06	0.94
6	PBRINE	0.07	0.94	PLGPRM	0.06	0.95
7	SHURGAS	-0.06	0.94	SHLPRM3	-0.05	0.95
8	SHLPRM2	0.06	0.95	----	----	----

[a] Steps in stepwise regression analysis; [b] Variables listed in order of selection in regression analysis; [c] Standardized Rank Regression Coefficient in final regression model; [d] Cumulative R^2 value with entry of each variable into regression model

7.3 CUTTINGS AND CAVING RELEASES

Table 7-3 lists the parameters that showed significant correlations to cuttings and cavings releases based on a stepwise regression using rank transformed data. The uncertainty in mean cuttings and cavings releases is primarily due to the uncertainty in the cuttings and cavings volume, as described in CRA-2004 Appendix PA [(U. S. DOE, 2004) Figure PA-105]. Thus,

waste shear strength (WTAUFAIL) controls much of the variability in mean cuttings and cavings releases. The drill string angular velocity (DOMEGA) has a very minor contribution as well, as is discussed in Dunagan (2004). The remaining parameters in Table 7-3 explain less than 0.2% of the variability in cuttings and cavings. Thus the differences in Table 7-4 between the lists of variables associated with for the CRA-2004 and CRA-2004 PABC analyses are of no real significance.

Table 7-3. Stepwise Rank Regression Analysis for Expected Normalized Cuttings and Cavings Releases

| | Expected Normalized Release | | | | | |
| | CRA-2004 PABC | | | CRA-2004 | | |
Step[a]	Variable[b]	SRRC[c]	$R^{2\,[d]}$	Variable	SRRC	R^2
1	WTAUFAIL	-0.99	0.98	WTAUFAIL	-0.98	0.98
2	DOMEGA	0.11	0.99	DOMEGA	0.11	0.99
3	OXSTAT	-0.02	0.99	BPINTPRS	0.02	0.99
4	SHLPRM2	0.02	0.99	ANHBCEXP	0.02	0.99
5	CFRACSP	0.02	0.99	CTRANSFM	-0.02	0.99
6	DRZPCPRM	0.02	0.99	WASTWICK	-0.02	0.99

[a] Steps in stepwise regression analysis; [b] Variables listed in order of selection in regression analysis; [c] Standardized Rank Regression Coefficient in final regression model; [d] Cumulative R^2 value with entry of each variable into regression model

7.4   DIRECT BRINE RELEASES

A stepwise regression analysis based on results from the CRA-2004 (Table 7-4) determined that the uncertainty in mean DBR is dominated by the parameters that influence the DBR volumes (WMICDFLG, the indicator for microbial action; BPINTPRS, the pressure in the Castile brine reservoir; PBRINE, the probability of an intrusion hitting the Castile brine reservoir; and WRBRNSAT, the residual brine saturation in the waste). The uncertainty in radionuclide concentration appears to have a relatively small influence on mean direct brine release, as only a single related parameter entered the analysis (WSOLAM3C, the uncertainty in the solubility of Am(III) in Castile brine). In contrast, the analysis of the CRA-2004 PABC results shows that DBR is most sensitive to SOLVAR3, a "solubility multiplier" added to the CRA-2004 PABC analysis to represent uncertainty in solubilities for all actinides in the +III oxidation state (Xiong et al., 2005) and shows no sensitivity to WMICDFLG. The lack of sensitivity to WMICDFLG is undoubtedly due to changing the probability of microbial degradation from 0.5 to 1.0, as required by EPA (Leigh and Kanney, 2005). WGRCOR is the inundated corrosion rate for steel in the absence of CO_2. The corrosion of iron is expected to produce hydrogen but at the same time it consumes water. The net effect is a negative correlation with DBR. BHPERM is the intrinsic permeability of a silt sand-filled borehole and its negative correlation with DBR is probably due to the reduction of pressure in the repository as permeability increases. WASTWICK is the increase in brine saturation due to capillary forces and thus the negative

correlation reflects an increase in iron consumption leading to a reduction of brine at higher values of WASTWICK. DRZPCPRM is the intrinsic permeability of the DRZ immediately above the concrete of the panel closure. The positive correlation of DBR with DRZPCPRM is likely due to an increase in water flow from the DRZ to the repository as permeability increases.

Table 7-4. Stepwise Rank Regression Analysis for Expected Normalized Direct Brine Releases

				Expected Normalized Release		
	CRA-2004 PABC			CRA-2004		
Step[a]	Variable[b]	SRRC[c]	R^{2} [d]	Variable	SRRC	R^2
1	WSOLVAR3	0.47	0.24	WMICDFLG	-0.47	0.16
2	BPINTPRS	0.40	0.40	BPINTPRS	0.488	0.34
3	PBRINE	0.32	0.51	PBRINE	0.36	0.47
4	WGRCOR	-0.29	0.60	WSOLAM3C	0.29	0.52
5	BHPERM	-0.18	0.63	WRBRNSAT	-0.15	0.55
6	WASTWICK	-0.17	0.67	CONGSSAT	-0.22	0.58
7	DRZPCPRM	0.15	0.69	REPIPERM	-0.21	0.61
8	ANHBCVGP	-0.17	0.71	WGRCOR	-0.16	0.63
9	ANHPRM	0.12	0.73	TENSLSTR	-0.15	0.65
10	HALCROCK	-0.11	0.74	---	---	---
11	CONGSSAT	-0.11	0.75	---	---	---
12	WPHUMOX3	0.11	0.76	---	---	---

[a] Steps in stepwise regression analysis; [b] Variables listed in order of selection in regression analysis; [c] Standardized Rank Regression Coefficient in final regression model; [d] Cumulative R^2 value with entry of each variable into regression model

7.5 CULEBRA RELEASES

A Culebra release represents the potential release of radioactivity from the Culebra at the LWB over 10,000 years. The analysis of the sensitivity of Culebra releases to the input parameters using linear regression is problematic. In the CRA-2004, sixty-six percent of the distributions of Culebra releases consisted only of values of zero while in the CRA-2004 PABC eighty-four percent of the distributions of Culebra releases had only values of zero. The releases of 0 are found across the entire range of every parameter. This is undoubtedly due, for the most part, to transport rates frequently being too small to enable contaminants to reach the LWB boundary within the simulation period, 10,000 years. Removal of the potash mining exclusion zone around existing oil and gas wells in the CRA-2004 PABC analysis appears to have changed the transmissivity fields in such a way that travel times were increased, thus reducing the number of non-zero mean releases. The times of the intrusions giving rise to flows to the Culebra are also likely to influence whether or not such releases occur. These times are not represented in the "sampled" input parameters and thus cannot be associated with the releases. In addition, the preponderance of 0 values tends to negate the assumption of linear regression that errors

Information Only

(residuals) are normally distributed. In many cases it appears that it is the distribution of zeros along the independent axis that determines whether a positive or negative correlation is observed (e.g. Figure 7-1). Because of these issues, the linear rank regression analysis is unlikely to yield a definitive identification of the sensitivity of Culebra releases to the sampled parameters. Most of the variability in Culebra releases remains unexplained by the regression model (Table 7-5).
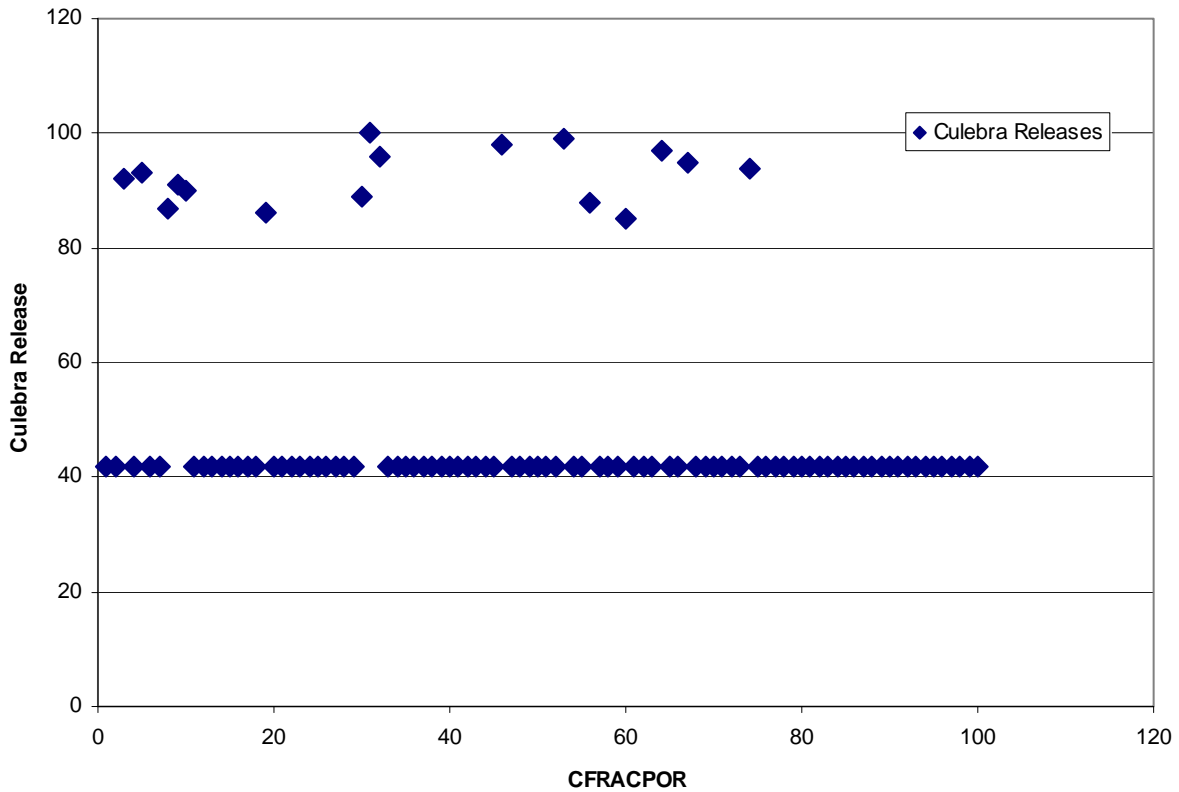
Figure 7-1. The Preponderance and Distribution of 0 Releases Can Control the Regression.

Information Only

The dominant parameter in the CRA-2004 analysis, BHPERM, is the logarithm of intrinsic permeability in the X-direction for a sand-filled borehole (Table 7-5). Conceptually, the flow of brine up the borehole (and thus to the Culebra) should be positively influenced by increasing values for BHPERM (Stein and Zelinski, 2003). CMKDPU is the matrix partition coefficient, K_d, for plutonium (Pu+4). The positive correlation seen here is counterintuitive because larger values of K_d generally result in greater sorption and thus lower releases. This positive correlation may be spurious and reflect the impact of the many zeros on the analysis. WSOLU4S is the solubility uncertainty factor for uranium in the +IV oxidation state in Salado brines, and CFRACPOR is the Culebra advective porosity, i.e. the fracture volume per unit volume of porous media. Positive correlations are expected for these variables, thus the negative correlation between Culebra releases and CFRACPOR is also counterintuitive. CONBRSAT is the residual gas saturation in the concrete panel closure system. When CONBRSAT is low, gas can flow through the concrete panel closure system under very wet conditions. The negative correlation seen here could be caused by higher values for CONBRSAT leading to lower brine saturations and thus lower brine volumes going up the borehole to the Culebra.

In the CRA-2004 PABC the Culebra releases appear to be most sensitive to the K_ds for uranium, thorium and plutonium, to CFRACPOR, and to CCLIMSF, the climate scale factor for the Culebra flow field. The climate scale factor accounts for uncertainty in the climate that could result in increased precipitation. Culebra releases once again showed a negative correlation with CFRACPOR. It appears that this negative correlation is due to a slight preponderance of releases of 0 at high values of CFRACPOR. A ranked-regression analysis conducted with Microsoft® Excel using only the non-zero release data showed a non-significant positive slope ($R^2 = 0.075$). The positive correlation between Culebra releases and CMKDU4, the matrix K_d for uranium in the +IV oxidation state, was also unexpected. A ranked-regression using only non-zero releases also showed a non-significant, positive correlation.

Table 7-5. Stepwise Regression Analysis for Expected Normalized Culebra Releases

	Expected Normalized Release					
	CRA-2004 PABC			**CRA-2004**		
Step[a]	**Variable[b]**	**SRRC[c]**	**R[2] [d]**	**Variable**	**SRRC**	**R[2]**
1	CMKDU	-0.67	0.12	BHPERM	0.32	0.11
2	CFRACPOR	-0.24	0.16	CMKDPU	0.24	0.15
3	CCLIMSF	0.19	0.21	WSOLU4S	0.20	0.19
4	CMKDTH4	-0.26	0.25	CFRACPOR	-0.19	0.22
5	CMKDPU	-0.36	0.28	CONBRSAT	-0.18	0.26
6	CMKDU4	0.22	0.33	---	---	---
7	WGRCOR	-0.19	0.36	---	---	---
8	SHURGAS	-0.18	0.40	---	---	---
9	WTAUFAIL	0.19	0.43	---	---	---
10	BHPERM	0.17	0.45	---	---	---
11	WGRMICI	0.17	0.48	---	---	---

[a] Steps in stepwise regression analysis; [b] Variables listed in order of selection in regression analysis; [c] Standardized Rank Regression Coefficient in final regression model; [d] Cumulative R^2 value with entry of each variable into regression model

7.6 SPALLINGS RELEASE

Table 7-6 lists the parameters that showed correlation to mean spallings releases after a stepwise rank regression. Fifty-seven percent of the mean releases in the CRA-2004 and sixty-six percent of the mean releases in the CRA-2004 PABC showed no spallings release, thus reducing the effectiveness of the regression analysis in the same manner as that described for Culebra releases. One major difference between the two analyses is that the variable SPALLVOL is not present in the CRA-2004 PABC analyses. SPALLVOL was not a parameter but instead was a computed value representing the spall volume. It was added to the CRA-2004 analysis in order to help verify that resampling of fifty realizations of spallings releases did not greatly influence the results. Spall releases are computed by multiplying the volume released by the repository wide average concentration of radioactivity in the CH-TRU waste at the time of intrusion. Thus the positive correlation between SPALLVOL and spallings release was expected. The resampling of spallings samples was eliminated from the CRA-2004 PABC analysis, as required by EPA (Leigh and Kanney, 2005). Instead, spallings releases for three hundred LHS samples were generated for the CRA-2004 PABC analysis. SPALLVOL was eliminated as a dependent variable because it was no longer needed.

The dominant parameter in the CRA-2004 analysis, WMICDFLG, was not found to be an important contributor to the variability of spallings releases in the CRA-2004 PABC. Previously there was a probability of 0.50 that there would be no microbial degredation occurring, a

probability of 0.25 that only cellulose-type would materials would decompose, and a probability of 0.25 that cellulose, plastic and rubber would decompose. In the CRA-2004 PABC these probabilities were changed to 0.75 for the decomposition of the cellulose-type materials and 0.25 for the decomposition of cellulose, plastic and rubber, as specified by the EPA (Leigh and Kanney, 2005). The lack of sensitivity of WMICDFLG is undoubtedly due to this change. The dominant parameter in the CRA-2004 PABC analysis is SPLPTDIA, the particle diameter for disaggregated waste. The negative correlation with SPLPTDIA is due to the tendency to have greater fluidization at smaller particle diameters. The remaining variables, with the exception of CMKDPU3, impact the gas pressures within the repository. HALPOR is the effective porosity in intact halite. The positive correlation is likely to be due to having greater gas pressures under higher porosities due to greater brine flow into the repository. CMTRXPOR is the diffusive porosity of the Culebra dolomite and the correlation shown is most likely spurious. ANHPRM is the intrinsic permeability of the Salado marker bed. BPINTPRS is the far-field pore pressure in the Castile brine reserve. WBIOGENF is the probability of obtaining the sampled microbial gas generation rates. BHPERM is the intrinsic permeability of the silt sand-filled borehole. The correlations between spallings and CMKDPU3, the K_d for plutonium in oxidation state +III is likely to be spurious. The K_d of plutonium should have no impact on spallings releases. This variable is not included in the STEPWISE results for the other two replicates.

Table 7-6. Stepwise Rank Regression Analysis for Expected Normalized Spallings Releases

	Expected Normalized Release					
	CRA-2004 PABC			CRA-2004		
Step[a]	Variable[b]	SRRC[c]	R^{2} [d]	Variable	SRRC	R^2
1	SPLPTDIA	-0.31	0.11	WMICDFLG	0.64	0.37
2	HALPOR	0.22	0.17	SPALLVOL	0.35	0.50
3	CMTRXPOR	-0.23	0.21	ANHBCVGP	-0.19	0.54
4	ANHPRM	0.21	0.26	REPIPERM	0.17	0.57
5	BPINTPRS	0.20	0.29	WRBRNSAT	0.13	0.59
6	WBIOGENF	0.18	0.32	WSOLPU3C	-0.14	0.61
7	CMKDPU3	0.17	0.35	SHLPRM2	0.13	0.63
8	BHPERM	-0.17	0.38	HALPOR	0.13	0.65

[a] Steps in stepwise regression analysis; [b] Variables listed in order of selection in regression analysis; [c] Standardized Rank Regression Coefficient in final regression model; [d] Cumulative R^2 value with entry of each variable into regression model

7.7   SUMMARY

In general, the parameters to which releases are sensitive were the same for the CRA-2004 PABC as those in the CRA-2004. The change in the assumptions about microbial degradation had the greatest impact on the differences between the sensitivities exhibited in the CRA-2004 analysis as compared to those of the CRA-2004 PABC analysis. On the one hand, the sensitivities of direct brine releases and mean total releases to WMICDFLG were eliminated, undoubtedly due to the elimination of the "no microbial degradation", previously assigned a probability of 0.5, and the expansion of the probability of microbial decomposition of cellulose-type materials from 0.25 to 0.75. On the other hand, WMICDFLG became the dominant contributor to the uncertainty in spallings releases. The only other significant change was that BHPERM replaced CMKDU as the parameter contributing most to the uncertainty in Culebra releases. The majority of the variability in Culebra releases could not be accounted for by the parameters. This was probably caused by the low frequency of non-zero releases and the failure of linear regression to model the data. All of the regression models include parameters that contribute only a few percent to the uncertainty in the releases. Comparing the models by release across replicates showed that these minor contributors were not consistently present. In general, these parameters cannot be distinguished from spurious correlations and should be disregarded.

8.   REFEERENCES

Babb, S. C. and C. F. Novak (1997). User's Manual for FMT Version 2.3: A Computer Code Employing the Pitzer Activity Coefficient Formalism for Calculating Thermodynamic Equilibrium in Geochemical Systems to High Electrolyte Concentrations. Sandia National Laboratories, Albuquerque, NM. ERMS 243037.

Brush, L. H. (2005). Results of Calculations of Actinide Solubilities for the WIPP Performance Assessment Baseline Calculations. Sandia National Laboratories, Carlsbad, NM. ERMS 539800.

Brush, L. H. and Y. Xiong (2005). Calculation of Organic Ligand Concentrations for the WIPP Performance Assessment Baseline Calculations. Sandia National Laboratories, Carlsbad, NM. ERMS 539635.

Bynum, R. V. (1996a). Estimation of Uncertainty for Predicted Actinide Uncertainties, Analysis Plan, AP-024, Rev. 0. Sandia National Laboratories, Albuquerque, NM. ERMS 410354.

Bynum, R. V. (1996b). Implementation of Analysis Plan AP-024, Rev. 0, Analysis to Estimate the Uncertainty for Predicted Actinide Solubilities. Sandia National Laboratories, Albuquerque, NM. ERMS 241374.

Bynum, R. V. (1996c). Update of Uncertainty Range and Distribution for Actinide Solubilities to Be Used in CCA NUTS Calculation. Sandia National Laboratories, Albuquerque, NM. ERMS 238268.

Chavez, M. J. (2002). NWMP Procedure NP 9-2, Parameters. Revision 0. Sandia National Laboratories, Carlsbad, NM. ERMS 520473.

Chavez, M. J. (2005). Document Review and Comment (DRC), QA Review by Mario Chavez for Analysis Package for CUTTINGS_S, CRA-2004 Performance Assessment Baseline Calculation. Sandia National Laboratories, Carlsbad, NM. ERMS 540469.

Cotsworth, E. (2004a). EPA's CRA Completeness Comments, 1st set. U.S. Environmental Protection Agency., Washington, DC. ERMS 535554.

Cotsworth, E. (2004b). EPA's CRA Completeness Comments, 2nd set. U.S. Environmental Protection Agency, Washington, DC. ERMS 537187.

Cotsworth, E. (2004c). EPA's CRA Completeness Comments, 3rd set. U.S. Environmental Protection Agency, Washington, DC. ERMS 536771.

Cotsworth, E. (2004d). EPA's CRA Completeness Comments, 4th set. U.S. Environmental Protection Agency, Washington, DC. ERMS 540236.

Cotsworth, E. (2005). EPA Letter on Conducting the Performance Assessment Baseline Change (PABC) Verification Test. U.S. EPA, Office of Radiation and Indoor Air, Washington, D.C. ERMS 538858.

Crawford, B. A. (2005). Waste Material Densities In TRU Waste Streams From TWBID Revision 2.1 Version 3.13, Data Version D.4.15. Los Alamos National Laboratory, Carlsbad, NM. ERMS 539323.

Detwiler, P. (2004a). Initial Response to Environmental Protection Agency (EPA) September 2, 2004, Letter on Compliance Recertification Application [DOE Letter #6]. U.S. Department of Energy, Carlsbad, NM. ERMS 540239.

Detwiler, P. (2004b). MgO Emplacement [DOE Letter #5]. U.S. Department of Energy, Carlsbad, NM. ERMS 540238.

Detwiler, P. (2004c). Partial response to Environmental Protection Agency (EPA) May 20, 2004 letter on CRA. U.S. Department of Energy, Carlsbad, NM. ERMS 537372.

Detwiler, P. (2004d). Partial response to Environmental Protection Agency (EPA) May 20, 2004 letter on CRA, [1st response submittal to EPA]. U.S. Department of Energy, Carlsbad, NM. ERMS 537430.

Detwiler, P. (2004e). Response to Environmental Protection Agency (EPA) July 12, 2004 letter on CRA. U.S. Department of Energy, Carlsbad, NM. ERMS 537369.

Detwiler, P. (2004f). Response to EPA May 20, 2004 Letter on CRA [DOE Letter #4]. U.S. Department of Energy, Carlsbad, NM. ERMS 540237.

Dunagan, S. (2003). Estimated Number of Boreholes into CH Waste in 10,000 Years. Sandia National Laboratories, Carlsbad, NM. ERMS 532277.

Dunagan, S. (2004). Analysis Package for Cuttings and Cavings: Compliance Recertification Application. Revision 1.0. Sandia National Laboratories, Carlsbad, NM. ERMS 533541.

Dunagan, S. (2005). Analysis Package for CCDFGF, Compliance Recertification Application, Revision 1.0. Sandia National Laboratories, Carlsbad, NM. ERMS 538354.

Fox, B. (2005). Analysis Package For EPA Unit Loading Calculations, Performance Assessment Baseline Calculation, Revision 0. Sandia National Laboratories, Carlsbad, NM. ERMS 540378.

Francis, A. J., J. B. Gillow and M. R. Giles (1997). Microbial Gas Generation Under Expected Waste Isolation Pilot Plant Repository Conditions. Sandia National Laboratories, Albuquerque, NM. SAND96-2582. ERMS 244883.

Information Only

Garner, J. W. (2003a). Analysis Package for PANEL: Compliance Recertification Application, Revision 1. Sandia National Laboratories, Carlsbad, NM. ERMS 532349.

Garner, J. W. (2003b). Software Installation and Checkout Form for PANEL, Version 4.00. Sandia National Laboratories, Carlsbad, NM. ERMS 526221.

Garner, J. W. (2005). Change Control Form for PANEL, Version 4.02. Sandia National Laboratories, Carlsbad, NM. ERMS 539537.

Garner, J. W. and C. D. Leigh (2005). Analysis Package for PANEL, CRA-2004 Performance Assessment Baseline Calculation, Revision 0. Sandia National Laboratories, Carlsbad, NM. ERMS 540572.

Gilkey, A. P. (1995). PCCSRC, Version 2.21, Software Installation And Checkout Form. Sandia National Laboratories, Carlsbad, NM. ERMS 227771.

Gilkey, A. P. (2003). Software Installation And Checkout Form For SECOTP2D, Version 1.41. Sandia National Laboratories, Carlsbad, NM. ERMS 525384.

Gilkey, A. P. (2004). Change Control Form for CUTTING_S, Version 5.10. Sandia National Laboratories, Carlsbad, NM. ERMS 537036.

Gilkey, A. P. (2005). Change Control Form for SUMMARIZE, Version 2.20, [Proposed 3.00]. Sandia National Laboratories, Carlsbad, NM. ERMS 540117.

Gilkey, A. P. and E. D. Vugrin (2005). Software Installation and Checkout and Installation and Checkout for CUTTINGS_S Version 6.00 Regression Testing for the Compaq ES45 Platform. Sandia National Laboratories, Carlsbad, NM. ERMS 537042.

Gitlin, B. C. (2005). Fifth Set of CRA Comments. U.S. Environmental Protection Agency, Washington, DC. ERMS 540240.

Hansen, C. W. (2003). Software Installation and Checkout Form for CUTTINGS_S, Version 5.10, [8400]. Sandia National Laboratories, Carlsbad, NM. ERMS 532519.

Hansen, C. W. (2004a). Change Control Form for PRECCDFGF Version 1.00B. Sandia National Laboratories, Carlsbad, NM. ERMS 535669.

Hansen, C. W. (2004b). Software Problem Report (SPR) form 04-006 for LHS Version 2.41. Sandia National Laboratories, Carlsbad, NM. ERMS 536209.

Hansen, C. W., C. D. Leigh, D. L. Lord and J. S. Stein (2002). BRAGFLO Results for the Technical Baseline Migration. Sandia National Laboratories, Carlsbad, NM. ERMS 523209.

Helton, J. C., J. E. Bean, F. W. Berglund, F. Davis, K. Economy, J. W. Garner, J. D. Johnson, R. J. MacKinnon, J. Miller, D. G. O'Brien, J. L. Ramsey, J. D. Schreiber, A. Shinta, L. N. Smith, D.

M. Stoelzel, C. Stockman and P. Vaughn (1998). Uncertainty and Sensitivity Analysis Results Obtained in the 1996 Performance Assessment for the Waste Isolation Pilot Plant. Sandia National Laboratories, Albuquerque, NM. SAND98-0365 ERMS 252619.

Hobart, D. E. and R. C. Moore (1996). Analysis of Uranium(VI) Solubility Data for WIPP Performance Assessment: Implementation of Analysis Plan AP-028. Sandia National Laboratories, Albuquerque, NM. ERMS 236488.

Kanney, J. F. and T. B. Kirchner (2005). Verification of the SUMMARIZE Interface in the CRA-2004 Performance Assessment Baseline Calculation. Sandia National Laboratories, Carlsbad, NM. ERMS 540977.

Kirchner, T. B. (2004a). Change Control Form for PRECCDFGF Version 1.00B. Sandia National Laboratories, Carlsbad, NM. ERMS 536658.

Kirchner, T. B. (2004b). Stepwise Regression Analysis of the Final Release for Each Release Mechanism in Response to C-23-18, Revision 1. Sandia National Laboratories, Carlsbad, NM. ERMS 537872.

Kirchner, T. B. (2005a). Generation of the LHS Samples for the CRA 2004 PA Baseline Calculations, Revision 0. Sandia National Laboratories, Carlsbad, NM. ERMS 540279.

Kirchner, T. B. (2005b). Sensitivity of Performance Assessment Baseline Calculation Releases to Parameters. Sandia National Laboratories, Carlsbad, NM. ERMS 540767.

Kirchner, T. B. and E. D. Vugrin (2004). Errors Affecting Spallings Releases. Sandia National Laboratories, Carlsbad, NM. ERMS 537852.

Kirchner, T. B. and E. D. Vugrin (2005). A Summary of Changes Made to PRECCDFGF and CCDFGF, the Reason for these Changes, and their Impacts on the CRA Results. Sandia National Laboratories, Carlsbad, NM. ERMS 538863.

Kirkes, G. R. (2005a). Baseline Features, Events, and Processes List for the Waste Isolation Pilot Plant, Revision 1. Sandia National Laboratories, Carlsbad, NM. ERMS 539356.

Kirkes, G. R. (2005b). Features Events and Processes Assessment for the Performance Assessment Baseline Calculation. Sandia National Laboratories, Carlsbad, NM. ERMS 540366.

Kirkes, G. R. (2005c). SP 9-4, Performing FEPS Baseline Impact Assessment for Planned or Unplanned Changes. Revision 0. Sandia National Laboratories, Carlsbad, NM. ERMS 539468.

Leigh, C. D. (2003). Software Installation and Checkout Form for NUTS, Version 2.05A. Sandia National Laboratories, Carlsbad, NM. ERMS 526220.

Leigh, C. D. (2005a). Calculation of Moles of Sulfate and Nitrate for Performance Assessment Baseline Calculation. Sandia National Laboratories, Carlsbad, NM. ERMS 539331.

Leigh, C. D. (2005b). Unit Conversion and Data Transfer for Decay to 2033 Using Origen2, Version 2.2, Post CRA Performance Assessment Baseline Calculation, Revision 0. Sandia National Laboratories, Carlsbad, NM. ERMS 539329.

Leigh, C. D. and J. F. Kanney (2005). SNL WIPP Analysis Plan AP-122, Revision 0, Analysis Plan for Post CRA PA Baseline Calculation. Sandia National Laboratories, Carlsbad, NM. ERMS 539624.

Leigh, C. D. and J. R. Trone (2005a). Calculation of Radionuclide Inventories for Use in NUTS in the Performance Assessment Baseline Calculation, Revision 0. Sandia National Laboratories, Carlsbad, NM. ERMS 539644.

Leigh, C. D. and J. R. Trone (2005b). Calculation of the Waste Unit Factor for the Performance Assessment Baseline Calculation, Revision 0. Sandia National Laboratories, Carlsbad, NM. ERMS 539613.

Leigh, C. D., J. R. Trone and B. Fox (2005). TRU Waste Inventory for the 2004 Compliance Recertification Application Performance Assessment Baseline Calculation. Sandia National Laboratories, Carlsbad, NM. ERMS 541118.

Long, J. J. and J. F. Kanney (2005). Execution of Performance Assessment Codes for the CRA 2004 Performance Assessment Baseline Calculation, Revision 0. Sandia National Laboratories, Carlsbad, NM. ERMS 541394.

Lord, D. L. (2002). Analysis Plan for Completion of the Spallings Model for WIPP Recertification AP-096. Sandia National Laboratories, Carlsbad, NM. ERMS 524993.

Lord, D. L. (2003a). Software Change Control Form for DRSPALL Version 1.10. Sandia National Laboratories, Carlsbad, NM. ERMS 533161.

Lord, D. L. (2003b). Software Problem Report (SPR) 03-007 for DRSPALL, Version 1.00. Sandia National Laboratories, Carlsbad, NM. ERMS 533921.

Lord, D. L. (2004). Software Installation and Checkout Form for DRSPALL, Version 1.10. Sandia National Laboratories, Carlsbad, NM. ERMS 533957.

Lord, D. L., D. Rudeen and C. W. Hansen (2005). Analysis Package for DRSPALL, Compliance Recertification Application, Part II (Rev 1), CCDF Analysis. Sandia National Laboratories, Carlsbad, NM. ERMS 538467.

Lowry, T. S. (2003). Analysis Package for Salado Transport Calculations, Compliance Recertification Application, Revision 0. Sandia National Laboratories, Carlsbad, NM. ERMS 530164.

Lowry, T. S. (2004). Analysis Report for Inclusion of Omitted Areas in Mining Transmissivity Calculations in Response to EPA Comment G-11. Sandia National Laboratories, Carlsbad, NM. ERMS 538218.

Lowry, T. S. (2005). Analysis Package for Salado Transport Calculations: CRA-2004 PA Baseline Calculation, Revison 0. Sandia National Laboratories, Carlsbad, NM. ERMS 541084.

Lowry, T. S. and J. F. Kanney (2005). Analysis Report for the CRA-2004 PABC Culebra Flow and Transport Calculations. Sandia National Laboratories, Carlsbad, NM. ERMS 541508.

McKenna, S. A. (2005). Software Installation and Checkout for Modflow 2000, Version 1.6. Sandia National Laboratories, Carlsbad, NM. ERMS 540470.

Monod, J. (1949). "The growth of bacterial cultures." Annual Review of Microbiology **3**: 371-394.

Nemer, M. B. (2005). Updated Value of WAS_AREA:PROBDEG. Sandia National Laboratories, Carlsbad, NM. ERMS 539441.

Nemer, M. B. and J. S. Stein (2005). Analysis Package for BRAGFLO, 2004 Compliance Recertification Application Performance Assessment Baseline Calculation. Sandia National Laboratories, Carlsbad, NM. ERMS 540527.

Nemer, M. B., J. S. Stein and W. P. Zelinski (2005). Analysis Report for BRAGFLO Preliminary Modeling Results with New Gas Generation Rates Based upon Recent Experimental Results. Sandia National Laboratory, Carlsbad, NM. ERMS 539437.

Nowak, E. J. and Y. Xiong (2005). Recommended Change in the FMT Thermodynamic Data Base. Sandia National Laboratories, Carlsbad, NM. ERMS 539227.

Patterson, R. (2005). Hanford Tank and K-Basin Wastes [DOE Letter #9: Response to CRA Comments]. U.S. Department of Energy, Carlsbad, NM. ERMS 540241.

Piper, L. (2004). Partial Response to Environmental Protection Agency (EPA) September 2, 2004 Letter on Compliance Recertifiation Application [DOE Letter #7: Response to CRA Comments]. U.S. Department of Energy, Carlsbad, NM. ERMS 540242.

Popielak, R. S., R. L. Beauheim, S. R. Black, W. E. Coons, C. T. Ellingson and R. L. Olsen (1983). Brine Reservoirs in the Castile Formation, Waste Isolation Pilot Plant (WIPP) Project, Southeastern New Mexico. U.S. Department of Energy Waste Isolation Pilot Plant, Albuquerque, NM. TME-3153.

Sandia National Laboratories (1997). Final, Supplemental Summary of EPA-Mandated Performance Assessment Verification Test (All Replicates) and Comparison with the Compliance Certification Application Calculations.   ERMS 414879.

Snider, A. C. (2003). Verification of the Definition of Generic Weep Brine and the Development of a Recipe for This Brine. Sandia National Laboratories, Carlsbad, NM. ERMS 527505.

Stein, J. S. (2003a). Software Installation and Checkout Form for BRAGFLO, Version 5.0. Sandia National Laboratories, Carlsbad, NM. ERMS 525704.

Stein, J. S. (2003b). User's Manual for BRAGFLO Version 5.00, Document Version 5.00. Sandia National Laboratories, Carlsbad, NM. ERMS 525702.

Stein, J. S., M. B. Nemer and J. R. Trone (2005). Analysis Package for Direct Brine Releases, Compliance Recertification Application, 2004 PABC, Revision 0. Sandia National Laboratory, Carlsbad, NM. ERMS 540633.

Stein, J. S. and W. P. Zelinski (2003). Analysis Package for BRAGFLO: Compliance Recertification Application. Sandia National Laboratories, Carlsbad, NM. ERMS 530163.

Stoelzel, D. M. and D. G. O'Brien (1996). Conceptual Model Description of BRAGFLO Direct Brine Release Calculations to Support the Compliance Certification Application (CCA MASS Attachment 16-2). U.S. Department of Energy, Carlsbad, NM. ERMS 239090.

Triay, I. R. (2005). Partial Response to Environmental Protection Agency (EPA) September 2, 2004, Letter on Compliance Recertification Application [DOE Letter #8: Response to CRA Comments]. U.S. Department of Energy, Carlsbad Field Office, Carlsbad, NM. ERMS 540243.

Trone, J. R. (2005). Record Correction to Memorandum to Records, Calculation of Moles of Sulfate and Nitrate for Performance Assessment Baseline Calculation (ERMS Number 539331). Sandia National Laboratories, Carlsbad, NM. ERMS 539376.

U. S. DOE (1980). Final Environmental Impact Statement: Waste Isolation Pilot Plant. U.S. Department of Energy, Assistant Secretary for Defense Programs, Vols. 1-2., Washington, D.C. DOE/EIS-0026, ERMS 238839.

U. S. DOE (1990). Final Supplement: Environmental Impact Statement, Waste Isolation Pilot Plant. U.S. Department of Energy, Office of Environmental Resoration and Waste Management. Vols. 1-13, Washington, D.C. DOE/EIS-0026-FS, ERMS 247955 and 243022.

U. S. DOE (1993). Waste Isolation Pilot Plant Strategic Plan. U.S. Department of Energy, Washington, D.C. ERMS 251353.

U. S. DOE (1996). Title 40 CFR Part 191 Compliance Certification Application for the Waste Isolation Pilot Plant. U.S. Department of Energy, Waste Isolation Pilot Plant Carlsbad Area Office, Carlsbad, NM. DOE/CAO-1996-2184.

Information Only

U. S. DOE (2002). January 31'st, 2002 Technical baseline Report: Compliance Monitoring and Repository Investigations, Milestone RI110. U.S. Department of Energy Waste Isolation Pilot Plant, Carlsbad, NM. ERMS 520467.

U. S. DOE (2004). Title 40 CFR Part 191 Compliance Recertification Application for the Waste Isolation Pilot. U.S. Department of Energy Waste Isolation Pilot Plant, Carlsbad Field Office, Carlsbad, NM. DOE/WIPP 2004-3231.

U. S. EPA (1996). 40 CFR 194: Criteria for the Certification and Recertification of the Waste Isolation Pilot Plant's Compliance with the 40 CFR Part 191 Disposal Regulations; Final Rule. Federal Register, Vol. 61, No. 28, pp. 5224 - 5245. U.S. Environmental Protection Agency, Washington, DC. ERMS 241579.

U. S. EPA (1998). 40 CFR 194: Criteria for the Certification and Recertification of the Waste Isolation Pilot Plant's Compliance with the 40 CFR Part 191 Disposal Regulations: Certification Decision; Final Rule. Federal Register, Vol. 63, No. 95, pp. 27353-27406. U.S. Environmental Protection Agency, Office of Radiation and Indoor Air, Washington, D.C.

Vugrin, E. D. (2004a). Corrected CRA Figures. Sandia National Laboratories, Carlsbad, NM. ERMS 538260.

Vugrin, E. D. (2004b). CRA Response Activitiy, Tracking Number 09/02/04J, Response to EPA C-23-11, Revision 1. Sandia National Laboratories, Carlsbad, NM. ERMS 538113.

Vugrin, E. D. (2004c). CRA Response Activity, Tracking Number 05/20/04P, Response to EPA Question C-23-1, Revision 1. Sandia National Laboratories, Carlsbad, NM. ERMS 538111.

Vugrin, E. D. (2004d). Software Installation and Checkout and Regression Testing for CCDFGF Version 5.02 on the ES40 and ES45. Sandia National Laboratories, Carlsbad, NM. ERMS 538169.

Vugrin, E. D. (2004e). Software Problem Report (SPR) 2004-09 for LHS Version 2.41. Sandia National Laboratories, Carlsbad, NM. ERMS 538239.

Vugrin, E. D. (2005a). Analysis Package for CUTTINGS_S, CRA 2004 Performance Assessment Baseline Calculation. Sandia National Laboratories, Carlsbad, NM. ERMS 540468.

Vugrin, E. D. (2005b). Analysis Package for DRSPALL, CRA 2004 Performance Assessment Baseline Calculation. Sandia National Laboratories, Carlsbad, NM. ERMS 540415.

Vugrin, E. D. (2005c). Change Control Form for CUTTING_S, Version 6.01. Sandia National Laboratories, Carlsbad, NM. ERMS 540159.

Vugrin, E. D. (2005d). Change Control Form for CUTTINGS_S, Version 6.00. Sandia National Laboratories, Carlsbad, NM. ERMS 539215.

Vugrin, E. D. (2005e). Change Control Form for LHS Version 2.41 to 2.42. Sandia National Laboratories, Carlsbad, NM. ERMS 538375.

Vugrin, E. D. (2005f). Design Document for LHS Version 2.42 Document Version 2.42. Sandia National Laboratories, Carlsbad, NM. ERMS 538371.

Vugrin, E. D. (2005g). Justification of Parameter Values for DRILLMUD:SHEARRT and DRILLMUD:MUDFLWRT for CUTTINGS_S. Sandia National Laboratories, Carlsbad, NM. ERMS 540643.

Vugrin, E. D. (2005h). Software Installation and Checkout and Analysis Report for the ES45 Regression Test of LHS, Version 2.42. Sandia National Laboratories, Carlsbad, NM. ERMS 538376.

Vugrin, E. D. (2005i). Software Problem Report (SPR) 05-001 for CUTTINGS_S Version 6.01. Sandia National Laboratories, Carlsbad, NM. ERMS 540158.

Vugrin, E. D. (2005j). User's Manual for LHS Version 2.42 Document Version 2.42. Sandia National Laboratories, Carlsbad, NM. ERMS 538374.

Vugrin, E. D. (2005k). User's Manual for CUTTINGS_S Version 6.00. Sandia National Laboratories, Carlsbad, NM. ERMS 537039.

Vugrin, E. D. and B. Fox (2005). Software Installation and Checkout and Regression Testing for CUTTINGS_S Version 6.02 on the ES40 and ES45, Revision 0. Sandia National Laboratories, Carlsbad, NM. ERMS 540155.

Vugrin, E. D. and T. B. Kirchner (2004). Incorrect LHS and SUMMARIZE Input Files for PRECCDFGF. Sandia National Laboratories, Carlsbad, NM. ERMS 537965.

Vugrin, E. D., T. B. Kirchner, J. S. Stein and W. P. Zelinski (2005). Analysis Report for Modifying Parameter Distributions for S_MB139:COMP_RCK and S_MB139:SAT_RGAS. Sandia National Laboratories, Carlsbad, NM. ERMS 539301.

Wang, Y. (1998). WIPP PA Validation Document for FMT (Version 2.4), Document Version 2.4. Sandia National Laboratories, Carlsbad, NM. ERMS 251587.

Wang, Y. and L. H. Brush (1996). Estimates of Gas-Generation Parameters for the Long-Term WIPP Performance Assessment. Sandia National Laboratory, Albuquerque, NM. ERMS 231943.

Xiong, Y. (2005). Release of FMT_050405.CHEMAT. Sandia National Laboratories, Carlsbad, NM. ERMS 539304.

Xiong, Y., E. J. Nowak and L. H. Brush (2004). Updated Uncertainty Analysis of Actinide Uncertainties for the Response to EPA Comment C-23-16. Sandia National Laboratories, Carlsbad, NM. ERMS 538219.

Xiong, Y., E. J. Nowak and L. H. Brush (2005). Updated Uncertainty Analysis to Actinide Solubilities for the Response to EPA Comment C-23-16, Rev 1. Sandia National Laboratories, Carlsbad, NM. ERMS 539595.

Information Only